Technische Universität München
TUM School of Natural Sciences

Development of Rapid Automated Chemiluminescence Microarray Immunoassays for SARS-CoV-2 Serological Assessments

Julia Teresa Klüpfel

Die vorliegende Arbeit wurde am Lehrstuhl für Analytische Chemie und Wasserchemie der Technischen Universität München in der Gruppe für Bioanalytik und Mikroanalytische Systeme im Zeitraum von Januar 2020 bis Januar 2023 angefertigt.

Das Leben muss nicht einfach sein,
vorausgesetzt, es ist nicht leer.

Lise Meitner (1878 - 1968)

Danksagung

Mein besonderer Dank gilt meinem Doktorvater

Herrn Privatdozent Dr. Michael Seidel

für die freundliche Aufnahme in seine Arbeitsgruppe, für seine große Unterstützung bei Fragen und Problemen und insbesondere für sein Vertrauen in meine Arbeit und die Möglichkeit, mich innerhalb meines Forschungsthemas frei entfalten zu können.

Weiterhin möchte ich meinem Mentor

Herrn Prof. Dr. Martin Elsner

für seine große Unterstützung, sein offenes Ohr, seinen fachlichen Input und seine äußerst hilfreichen Ratschläge, sowohl zum wissenschaftlichen Schreiben als auch zum Projekt- und Zeitmanagement danken.

Großer Dank gilt weiterhin

Herrn Prof. Dr. Oliver Hayden

für die großzügige und bereitwillige Aufnahme in sein Labor und seine kreativen und hilfreichen Ratschläge und Visionen zu meiner Forschung.

Besonderen Dank hat außerdem die

ISAR Bioscience GmbH

verdient, insbesondere an **Herrn Prof. Dr. Martin Lohse**, **Herrn Prof. Dr. Martin Ungerer** sowie **Herrn Dr. Hans-Peter Holthoff**. Danke für das Vertrauen in mich und die Gelegenheit, in den Laboren von ISAR Bioscience zu arbeiten.

Schließlich möchte ich mich herzlich bei

Frau Prof. Dr. Ulrike Protzer

bedanken für die Unterstützung bei virologischen Fragestellungen, ihre Impulse zu neuen spannenden Forschungsfeldern und für die Durchführung zahlreicher Vergleichsmessungen.

Aber natürlich gibt es zahlreiche weitere Personen, ohne die diese Arbeit nicht möglich gewesen wäre und dank derer die Zeit meiner Promotion zu einer bereichernden und unvergesslichen Erfahrung wurde.

Liebe **IWCler**, danke für die Zeit, die ich mit euch am Institut verbringen durfte, sowohl in Großhadern als auch in Garching. Danke für viele gemeinsame unterhaltsame Stunden im und außerhalb des Labors. Danke an alle **Mit-Doktoranden und -Doktorandinnen** für den Zusammenhalt und Austausch, danke an **Christine, Conny und Sonja** für alles, was ihr sichtbar und unsichtbar für das Institut tut, danke an **Rani** und **Christoph** für viele inspirierende Gespräche, an **Natascha** für die Chance, Studierende für Laborroboter zu begeistern und danke an **Roland und Sebastian**: es war purer Luxus, euch in der Werkstatt zu haben.

Liebe **Biopritschler*innen**, es war mir eine Freude, Teil eurer Gruppe zu sein. Danke, dass ihr mich nicht vergessen habt, auch wenn ich meistens in anderen Laboren war. Ganz besonderer Dank gebührt **Lisa**: danke, dass du mich in die Gruppe geholt hast und **Sandra**: danke, dass du geblieben bist und weitermachst, was ich angefangen habe.

Vielen Dank auch an alle Studierenden, die mich auf Abschnitten meiner Promotion begleitet haben: **Charlotte, Rosalie, Luis, Nina, Melina und Sandra** - ohne euch wäre ich in diesen drei Jahren sicher nicht so weit gekommen.

Beim **Lehrstuhl für Biomedizinische Elektronik** möchte ich mich für die schöne Zeit am TranslaTUM bedanken. Besonderen Dank verdient **Martin**: du hast Probleme gelöst, an denen ich verzweifelt wäre und Gespräche mit dir waren immer eine große Bereicherung.

Herzlichen Dank auch an meine weiteren Projektpartner am Klinikum Rechts der Isar: an **Prof. Dr. Percy Knolle** für die Unterstützung mit Proben, ohne die meine Arbeit nicht möglich gewesen wäre sowie an **Silvia**: danke für deine Unterstützung in Ethikfragen und deine herzliche Art!

Liebe **Birgit**, danke, dass du mich in Planegg unter deine Fittiche genommen hast und dafür gesorgt hast, dass ich mich gut einleben konnte!

Liebe **Oksana**, danke, dass ich in den letzten Jahren für dich arbeiten und abseits der Chemie in einem nicht weniger wichtigen Feld lernen durfte.

Danke auch an meine Freunde, die mir in den letzten Jahren den Rücken gestärkt haben und dafür gesorgt haben, dass ich nicht völlig im Laborwahnsinn verschwunden bin. Ganz besonders an **Daniel, Jo und Sandra**, aber auch an das Team der **Studentischen Vertretung**, das mir gezeigt hat, dass man gemeinsam Großes schaffen kann.

Florian, danke! Für alles.

Und zu guter Letzt der wichtigste Dank an diejenigen, die mir all das ermöglicht haben: meine **Familie**. Mama, Papa, danke, dass ihr hinter mir steht und mich seit jeher immer unterstützt! Ohne euch hätte ich es nicht bis hierhin geschafft.

Zusammenfassung

Die SARS-CoV-2-Pandemie hat seit 2020 für weitreichende, weltweite Einschränkungen und massiven Forschungseinsatz gesorgt. Durch die Entwicklung serologischer Diagnostikassays und unter Verwendung der Analyseplattform MCR, die nie zuvor in der Humanserodiagnostik eingesetzt worden war, hat diese Arbeit zu folgenden Entwicklungen in diesem Gebiet beigetragen.

Zunächst wurde ein automatisierter, flussbasierter Chemilumineszenz-Mikroarray-Immunoassay (CL-MIA) für den Nachweis von IgG-Antikörpern gegen verschiedene SARS-CoV-2-Antigene - Rezeptorbindedomäne (RBD), Spike- und Nukleokapsid-Protein - entwickelt. Er ermöglichte die Multiplex-Messung von Antikörpern innerhalb von acht Minuten und damit deutlich schneller als von kommerziellen Plattformen bekannt. Für diesen Test auf aminomodifizierten Glas-Microarray-Chips mit kovalent gebundenen rekombinanten Antigenen wurde eine im Vergleich zu anderen Tests herausragende Sensitivität und Spezifität von 100 % ermittelt.

Der nächste Entwicklungsschritt war die Optimierung hin zu Point-of-Care-Anwendungen, um etwa die Effizienz der neu entwickelten Impfstoffe kontrollieren zu können. Hierzu wurden Polycarbonat-Microarray-Chips mit einer carboxymodifizierten Oberfläche und kürzerer Herstellungszeit eingesetzt. Weiterhin wurde der Injektionsprozess optimiert, sodass die Messzeit um 50 % und das Probenvolumen um 90 % reduziert werden konnte. Dieser Assay erwies sich als nützlich bei der retrospektiven Erkennung von asymptomatischen, unbemerkten Infektionen, aber auch für das Seromonitoring nach Impfungen. Zusätzlich wurde ein Assay zum sequentiellen Nachweis von IgM- und IgG-Antikörpern entwickelt, der zur Untersuchung des zeitlichen Verlaufs der Immunantwort einsetzbar war.

Im Verlauf der Pandemie wurde deutlich, dass neutralisierende Antikörper eine wichtige Rolle für die klinische Bewertung der Immunität gegen SARS-CoV-2 spielen werden. Diese Antikörper verhindern den Zelleintritt des Virus über den ACE2-Rezeptor, jedoch werden für ihre Bestimmung üblicherweise aktive Viren verwendet, was Labore der Sicherheitsstufe 3 notwendig macht. Deshalb wurde in dieser Dissertation ein kompetitiver Surrogat-Neutralisationsassay entwickelt, der mit einer Messdauer von etwa fünf Minuten deutlich schneller als andere Neutralisationstests ist. Dieser ermöglicht die Messung der Interaktion zwischen RBD und ACE2 sowie die Hemmung derselben durch neutralisierende Antikörper. Im Vergleich mit alternativen Neutralisationstests zeigte sich sehr gute Übereinstimmung für den kompetitiven CL-MIA.

Damit trägt diese Dissertation zum hochaktuellen Thema der serologischen Schnelltests für SARS-CoV-2 bei. Die entwickelten Assays zeichnen sich durch die Verwendung rekombinanter Antigene auf optimierten Microarray-Chips mit äußerst geringer unspezifischer Bindung aus. Die mikrofluidische Plattform MCR ermöglicht automatisierte Testverfahren, die in Zukunft breite Anwendung finden können. Durch ihre flexible Anpassbarkeit bieten sich vielfältige Optionen zur raschen Entwicklung von Antikörperschnelltests für zahlreiche Erkrankungen.

Abstract

The SARS-CoV-2 pandemic has not only caused global restrictions but also massive research effort since its outbreak in 2020. By developing serological diagnostic tools using the MCR analytical platform that had never previously been used for diagnostic assessments in humans, this work contributed to the following developments in this area.

First, an automated flow-based chemiluminescence microarray immunoassay (CL-MIA) was developed for the detection of IgG antibodies against different SARS-CoV-2 antigens - receptor binding domain (RBD), spike (S1) and nucleocapsid (N) protein. It enabled the multiplex determination of antibodies within eight minutes. For this assay, performed on amino-modified glass microarray chips with covalently bound recombinant antigens, a sensitivity and specificity of 100% was achieved, keeping pace with the best commercial assays.

The next development step was an optimization towards point-of-care applications, e.g. to control the efficiency of the newly developed vaccines. For this purpose, polycarbonate microarray chips with a carboxy-modified surface were used, which enabled significantly shorter production times. Moreover, the injection process was optimized so that the measurement time could be reduced by 50% and the sample volume by 90%. This assay proved to be effective for retrospective detection of asymptomatic, unnoticed infections, but also for seromonitoring after vaccinations. In addition, a novel assay for the sequential detection of IgM and IgG antibodies was developed that could be used to study the time course of the immune response.

During the course of the pandemic, it became clear that neutralizing antibodies will play an important role in the clinical evaluation of immunity to SARS-CoV-2. These antibodies prevent the virus from entering the cell via the ACE2 receptor but for their determination usually active virus is necessary, thus the requirement for biosafety level 3 laboratories. The use of recombinant proteins allows the design of surrogate neutralization assays that do without active virus. Therefore, a competitive surrogate neutralization assay was developed in this dissertation, enabling results notably faster than commonly used neutralization assays with a measurement time of about five minutes. This allowed measurement of the interaction between RBD and ACE2 and inhibition of the same by neutralizing antibodies. Comparison of patient cohort measurements with several alternative neutralization assays showed very good agreement for the competitive CL-MIA.

Thus, this dissertation contributes to the highly topical issue of rapid serological tests for SARS-CoV-2. The developed assays stand out by the use of native recombinant antigens on optimized microarray chips enabling low unspecific binding. The microfluidic analysis platform MCR allows for rapid and automated assay procedures that can find widespread application for a variety of serological assays in the future. Their flexible adaptability offers countless opportunities for rapid development of fast antibody tests for various diseases.

List of Abbreviations

°C	Degree celsius
a.u.	Arbitrary unit
ACE2	Angiotensin converting enzyme 2
APC	Antigen presenting cell
ARDS	Acute respiratory distress syndrome
AUC	Area under the curve
BCR	B cell receptor
BSA	Bovine serum albumin
BSL	Biosafety level
CCD	Charge-coupled device
CHO cells	Chinese hamster ovary cells
CL	Chemiluminescence
CLIA	Chemiluminescence immunoassay
CLP	Common lymphoid progenitor
CMV	Cytomegalovirus
CoV	Coronavirus
COVID-19	Coronavirus disease 2019
CoVRapid	Title of research project
Da	Dalton
DSC	Disuccinimidyl-carbonate
diepoxy PEG	Poly(ethylene glycol) diglycidyl ether
E protein	Envelope protein
EC50	Half maximal effective concentration
ECLIA	Electrochemiluminescence immunoassay
EDC	1-Ethyl-3-(3-dimethylaminopropyl)carbodiimide
ELISA	Enzyme-linked immunosorbent assay
Fab	Fragment antigen binding
Fc	Fragment crystallizable
g	Gram
gRNA	Genomic RNA
GOPTS	(3-Glycidyloxypropyl)-trimethoxysilane
h	Hour
HAMA	Human anti-mouse antibodies
H chain	Heavy chain
HEK cells	Human embryonic kidney cells

HIV	Human immunodeficiency virus
HRP	Horseradish peroxidase
IFA	Immunofluorescence assay
Ig	Immunoglobulin
ITC	Isothermal titration calorimetry
ISC	Intersystem crossing
IWC	Institute of Water Chemistry
K_D	Dissociation constant
L	Liter
L chain	Light chain
LFA	Lateral flow assay
m	Meter
m	Milli
MHC	Major histocompatibility complex
μ	Micro
m	Molar
M protein	Membrane protein
Mb	Megabases
MCR 3	Microarray Chip Reader 3
MCR-R	Microarray Chip Reader-Research
MERS-CoV	Middle East respiratory syndrome-related coronavirus
MIA	Microarray immunoassay
min	Minute
mRNA	Messenger RNA
n	Nano
N protein	Nucleocapsid protein
nAbs	Neutralizing antibodies
NK cells	Natural killer cells
ORF	Open reading frame
PBS	Phosphate-buffered saline
PBST	PBS supplemented with Tween
PC	Polycarbonate
PMMA	Poly(methyl methacrylate)
POC	Point-of-care
POM	Polyoxymethylene
PRNT	Plaque reduction neutralization test
R_0	Basic reproduction number

RAG	Recombination activating gene
RBD	Receptor binding domain
RNA	Ribonucleic acid
ROC	Receiver operating characteristics
RT	Room temperature
S protein	Spike protein
s-NHS	*N*-Hydroxysulfosuccinimide
SA	Streptavidin
SARS-CoV	Severe acute respiratory syndrome coronavirus
SARS-CoV-2	Severe acute respiratory syndrome coronavirus 2
sgRNA	Subgenomic RNA
SPR	Surface plasmon resonance
TCR	T cell receptor
TLR	Toll-like receptor
TMB	3,3',5,5'-Tetramethylbenzidine
TMPRSS2	Transmembrane protease serine subtype 2
VOC	Variant of concern
WHO	World Health Organization

Contents

1 Introduction

In human history, large outbreaks of infectious diseases have often had remarkable influence on society, economy and development. A commonly known example of such global outbreaks, referred to as pandemics, was the so-called "Black Death", a global outbreak of bubonic plague in the 14th century, killing about one third of the population at that time. However, already the bible mentions pandemic outbreaks and even older documents serve as registers for early disease outbreaks like the Athenian Plague of 430 B.C. Despite advances in medicine and natural sciences over several decades, another well-known pandemic killed more people within one year than the Black Death within a century during the Spanish Flu outbreak in 1918. Since then, the world has seen several other pandemics, some of them still ongoing like the HIV pandemic, others mainly contained like Ebola.[1]

Nowadays, countries try their best to prepare for future disease outbreaks. The World Health Organization (WHO) develops R&D Blueprints, defining possible diseases that might become a worldwide threat and research activities that will come into action once an outbreak is recognized. These roadmaps are hoped to help combating future pandemics.[1] A similar approach was used by the Johns Hopkins Center for Health Security together with the World Economic Forum and the Bill and Melinda Gates Foundation by hosting "Event 201" in October 2019, a tabletop exercise, where an outbreak of a novel coronavirus was simulated, focusing on challenges and necessary measures to contain the pandemic. While this simulation revealed some gaps in pandemic preparedness and proposed possible solutions, the organizers would not have imagined how real their scenario would become within a few months.[2]

Only two months after "Event 201", the first cases of a novel disease, caused by a previously unknown coronavirus, SARS-CoV-2 (severe acute respiratory coronavirus 2), were found in Wuhan, China.[3] The disease was later named COVID-19 (coronavirus disease 2019) by the WHO and the outbreak was declared a pandemic in March 2020.[4] At that time, the Vice President of the European Commission, *Josep Borrell*, stated that

> *"COVID-19 will reshape our world. We don't know yet when the crisis will end. But we can be sure that by the time it does, our world will look very different."*[5]

And while the pandemic is still going on three years later, a lot has changed. Unprecedented research efforts have focused on SARS-CoV-2, allowing for the authorization of vaccines within one year after the initial outbreak, and various medications as well as tests for COVID-19 were

developed. One research focus was the evaluation of the immune response to infection with SARS-CoV-2 or vaccination against it, giving indications on the protection individuals have thanks to their immune system. This urgent research need has been a major focus of this thesis by contributing with the development of rapid, automated antibody tests for SARS-CoV-2.

While many well-known companies as well as research groups have presented different types of antibody tests over the last years, most of them are relatively unflexible and fixed to one designated application. Most commonly, either enzyme-linked immunosorbent assays (ELISAs) or lateral-flow assays (LFAs) are applied with their operating principles being outlined in detail later in this thesis. ELISAs are preferably applied in high-throughput analysis using big automated analysis devices suitable for the analysis of hundreds of samples per day. For this application they are very useful, but if more than one parameter is to be determined simultaneously or results are required within few minutes, they are not suitable. Moreover, whenever an ELISA is adapted for another analyte of interest, time-extensive optimization studies are necessary to define appropriate concentrations of all reagents. LFAs on the contrary are suitable for rapid analyses within about 15 min but they often face severe matrix problems when applying blood samples and read-out is done by eye, giving rise to human bias. Furthermore, they sometimes fail to mimic the interaction of antibodies and viral proteins occurring in the body by applying denatured viral proteins and just as ELISA assays they commonly only test for one parameter at once. While many more antibody test types could and will be described, these examples already give a good expression of what is needed in the field of serodiagnostics: people long for a platform that gives reliable results within few minutes, not only for one parameter but for as many different parameters of interest as possible. The COVID-19 pandemic showed how rapidly a pandemic state can change and research as well as public health interests shift with it. Therefore, flexible testing systems are required. New demands have to be implemented within very short timeframes, optimally by expanding existing offers, not by replacing them. To achieve such a flexible system, ready to be used for antibodies to different proteins as well as different antibody classes, for the semi-quantitative serosurveillance or for the measurement of other antibody features was the main goal of this thesis. This ambitious goal could be achieved by combining a well-optimized analysis platform in its first application for human serodiagnostics with high-quality antigens produced in eukaryotic cells to perfectly mimic the situation in the human body. The application of microarray technology allowed for the determination of various different parameters at once, while specialized surface treatment of microarray chips enabled the analysis of human blood without troublesome matrix influence. Finally, detection by chemiluminescence facilitated highly sensitive signal readout in quantitative manner.

But before the presentation of these results on the development of rapid, automated chemiluminescence microarray immunoassays (CL-MIAs) for the detection of antibodies to SARS-CoV-2 and possible application fields for these assays, the following chapters will give a comprehensive

overview over the relevant background knowledge. First, SARS-CoV-2 will be introduced with its main features, changes over the last years and its method of action in the human body. Then, the fundamentals of immunology and antibody formation and the different possibilities to detect antibodies, especially for SARS-CoV-2, will be outlined to provide the necessary background to understand and contextualize the results obtained in the course of this dissertation.

2 Theoretical Background

In the following, the theoretical basis of the thesis at hand will be elucidated by taking a closer look on three main topics: the virus SARS-CoV-2, the reaction of the immune system to infections and different types of serological assays used to evaluate the reaction of the immune system with special focus on SARS-CoV-2.

2.1 SARS-CoV-2

2.1.1 Characteristics and Replication

SARS-CoV-2 first emerged in December 2019, and proved its pathogenicity over the following months and years. Yet, it is not the first coronavirus to cause a large-scale outbreak: the related viruses severe acute respiratory syndrome coronavirus (SARS-CoV) and Middle Eastern respiratory syndrome coronavirus (MERS-CoV) spread over many countries back in 2003 and 2012, respectively. All these viruses belong to the family of *Coronaviridae*, more precisely the *Betacoronavirus* genus and the *Sar-/Merbecovirus* subgenera, and are enveloped, positive-sense single-stranded RNA viruses.[6]

SARS-CoV-2 shares a high sequence identity with SARS-CoV (about 80%) and MERS-CoV (about 50%), but even higher similarities were found to a number of bat-derived SARS-like coronaviruses (about 88%), suggesting that bats were the original hosts of the novel virus before it infected humans, making it a zoonotic virus.[7]

Its large genome has an approximate length of 30 kb encoding 16 nonstructural proteins forming the replicase complex, nine accessory proteins and four structural proteins within 14 open reading frames (ORFs). About two thirds of the genome consist of two ORFs, ORF1a and ORF1b that code for the viral replicase complex, while the structural proteins are encoded in the remaining third together with accessory proteins.[8,9] These structural proteins are highly relevant from an immunological point-of-view as they are most apparent to the human body after an infection and are likely to induce a reaction of the human immune system. Three of the structural proteins are presented on the surface of SARS-CoV-2, namely the spike (S), envelope (E) and membrane (M) protein, while the nucleocapsid (N) protein is contained within the virions as shown schematically in Figure 2.1. It can bind to packaging signal regions in the viral RNA and lead to the formation of stable single genome condensates. These condensates can interact with S, E and M proteins, leading to final virion packaging.[10] As will become

apparent in the results section of this thesis, the focus of serological tests lies on the S protein and the N protein. An immune reaction to the latter is highly specific for a previous infection with SARS-CoV-2 as will become clear throughout Section 2.1.3, while the determination of the body's reaction to the S protein is of significant importance due to its involvement in the infection process.
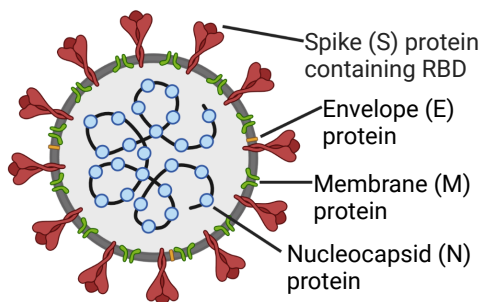

Figure 2.1: Schematic structure of SARS-CoV-2 with its structural proteins.[11]

The cell entry of SARS-CoV-2 is mediated by the S protein. In active virions, the S protein is present as a homotrimer with each monomer containing a S1 and a S2 subunit. The S2 domain anchors the protein to the membrane and later mediates membrane fusion. The receptor binding domain (RBD) within the S1 domain can bind to angiotensin-converting enzyme 2 (ACE2), a cell surface enzyme with relevance in maintaining normal blood pressure that was already the receptor for SARS-CoV as well as for the endemic alphacoronavirus HCoV-NL63 that causes mild upper respiratory tract infections like the related HCoV-229E, HCoV-OC43 and HCoV-HKU1.[8,12]

When a SARS-CoV-2 virion binds to an ACE2 receptor on the cell surface as shown in Figure 2.2 a, the S protein is subsequently proteolytically cleaved at two cleavage sites, starting with the separation of the protein into its S1 and S2 subunits and then further activating the S2 subunit at the S2' cleavage site.[13] These so-called priming processes are usually mediated by the serine protease TMPRSS2 (transmembrane protease serine subtype 2) at the cell surface, but can generally also occur due to the proteinase furin (for S1/S2 cleavage) or by cathepsin proteases, depending on the step in the SARS-CoV-2 reproduction cycle and the type of infected cell.[14] After the cleavage steps, a highly antigenic fusion peptide is exposed, leading to a conformation change followed by membrane fusion and cell uptake of the virion.[15]

Once a virion has entered a cell by clathrin-mediated endocytosis, uncoating and the release of genomic RNA (gRNA) into the cytoplasm takes place (Figure 2.2 b).[16] This gRNA is recognized as messenger RNA (mRNA) by ribosomes in the cell and translation of ORF1a and ORF1b takes place. The resulting replicase polyproteins are cleaved, resulting in the viral polymerase (Figure 2.2 c) that can then engage in RNA synthesis within replication organelles formed from cell membranes. They produce RNA templates for RNA replication as well as subgenomic RNAs (sgRNAs) encoding structural and accessory proteins (Figure 2.2 d and e) that are then further processed to sg-mRNAs used for translation of the structural proteins (Figure 2.2 f). Once all necessary proteins as well as new gRNA has been produced, virion assembly starts by coating of the RNA with N proteins, followed by budding of these nucleocapsid structures into

the endoplasmatic reticulum-Golgi intermediate compartment (ERGIC, Figure 2.2 g), where they acquire a lipid bilayer containing S, M and E proteins. These new virions can then leave the host cell and continue to infect other cells (Figure 2.2 h and i).[17] Therefore, if the host's immune system reacts rapidly to the presence of the spike antigen, possibly the infection of cells and the spreading of the virus within the body can be prevented. This emphasizes the necessity for rapid immunological tests to detect whether an individual possesses protection from infection or possibly needs preventive support by vaccination as will be detailed in Section 2.1.3.
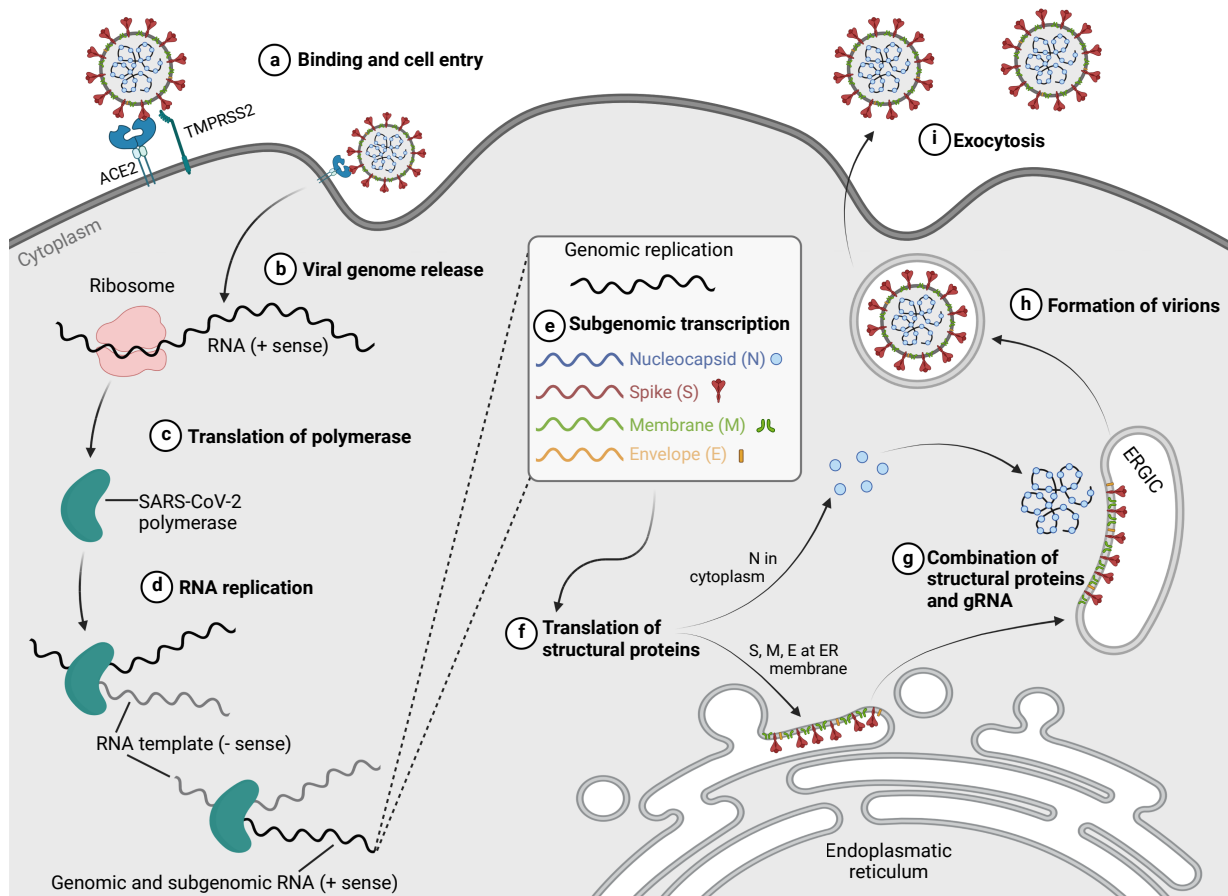
Figure 2.2: Cell entry and replication cycle of SARS-CoV-2.[11,18]

But this determination of protection is aggravated by an intrinsic feature of SARS-CoV-2. Similar to many other viruses, it is able to adjust to its host by mutations, therefore evading the immune system. Especially amino acid changes within the S protein are a very important factor, influencing the invasion of cells, replication, transmission and antibody production.[19] First mutations within the S protein occurred already in early 2020, making a variant with a D614G mutation predominant worldwide. In the following overview of main variants that evolved since the beginning of the pandemic, only key mutations in the S protein will be stated for clarity. In December 2020, the alpha variant (Pango lineage B.1.1.7), carrying an additional

N501Y mutation in the S protein, came up and dominated the cases for approximately 6 months. During that time, also the beta (B.1.351, additional E484K and K417N mutation) and gamma (P.1, additional E484K and K417T mutation) variants came up but did not reach the same abundance worldwide. Instead, in May 2021 the delta variant (B.1.617.2, D614G mutation as well as L452R, T478K, P681R) was first found in India and rapidly spread, dominating the cases until late 2021, when the omicron variant (B.1.1.529 with D614G, N501Y, E484A, T478K and P681H) and its subvariants BA.1 - BA.5 appeared.[20,21] The change of predominant variant worldwide is also shown graphically in Figure 2.3, indicating the percentage of sequences from selected variants within all available sequences per day. The figure shows how fast a change in predominant variant can occur. Within few weeks a new mutation can spread over the whole world, casting doubts on all previous research results as the new variant might behave substantially different and previously gained immunity to another variant might have become useless.
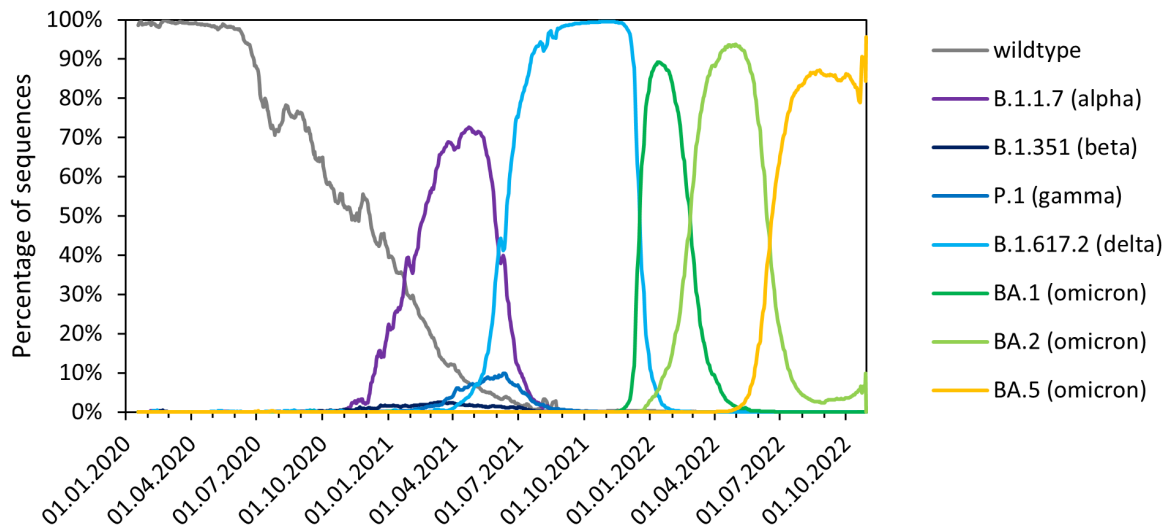

Figure 2.3: Percentages of selected variants within all available sequences worldwide from January 2020 to November 2022 (wildtype data contains the first known sequence as well as very closely related early variants like B.1); Data obtained using CoV-Spectrum.[22]

Therefore, it is of utmost importance to have diagnostic analytical tools available that can be adjusted as rapidly as the virus changes. Not only is it necessary to produce antigens from new upcoming variants shortly after their appearance in high quality but also does it have to be possible to exchange antigens as soon as new ones are made available. The best tool to enable serological surveillance with variants coming up would be an analytical test that is able to include all new variants without having to replace old ones so that samples from any place and any time point can be analyzed with the same test, showing responses to different variants. While for the detection of an active infection, only sequencing of the viral genome found in a

sample proved successful, there are serological test formats like microarray immunoassays that can accomplish multiplex measurements of antibody responses to different mutants at once, as will be shown later on in this work.

Over the course of the pandemic, many of the variants of SARS-CoV-2 were defined as "variants of concern" (VOC) due to their high transmissibility (measured for example using the basic reproductive number R_0 that states the number of new cases generated from a single case)[23] or symptom severity, which will be discussed in more detail in the following section.

2.1.2 Pathogenesis

While many coronaviruses are known to infect humans, most of them only lead to mild symptoms.[7] In contrast, SARS-CoV-2 infection can result in severe symptoms and death just as it had been the case for the closely related SARS-CoV in 2003. SARS-CoV-2 infection leads to the so-called coronavirus disease 2019 (COVID-19) that predominantly shows respiratory symptoms, but also has some additional manifestations that can be explained with the tissue tropism of SARS-CoV-2. As explained beforehand, ACE2 and TMPRSS2 as well as furin are relevant for the cell entry of SARS-CoV-2. ACE2 and TMPRSS2 are co-expressed in high levels in ciliated and secretory nasal cells, while additionally furin is present on certain bronchial cells. Furthermore, differentiated enterocytes, present in the gastrointestinal tract, show high levels of ACE2, explaining enteric infections.[15]

The most pronounced transmission routes of SARS-CoV-2 as shown in Figure 2.4 are also in accordance with the tissue tropism as the primary way of transmission is thought to be the contact to small respiratory droplets (diameter > 5 µm) from infected persons. Another possibility is the transmission by aerosols (diameter < 5 µm) or fecal-oral transmission.[8]

Generally, most patients experience flu-like symptoms with the most common symptoms being fever, cough and dyspnea, in some cases progressing to acute respiratory distress syndrome (ARDS) or pneumonia, possibly leading to death. Other symptoms can be headaches, nausea, vomiting, diarrhea, pharyngitis or fatigue, among others.[8,24] Higher age coincides with more severe disease progress, as do several risk factors including cardiovascular disease, hypertension, diabetes or cancer. On the contrary, children usually show milder symptoms.[25] In severe cases where patients develop ARDS, the cause of this life threatening complication often lies within a patients immune system due to the manifestation of a cytokine storm. As the virus infects cells, they secrete cytokines and release them as will be elucidated later. This leads to severe inflammation processes and damages in the surrounding tissue. Apart from the lung, also other organs like for example the kidneys can be damaged by the extreme immune reaction following SARS-CoV-2 infection.[26]

While the original wildtype coronavirus led to such severe or even critical symptoms in 19%
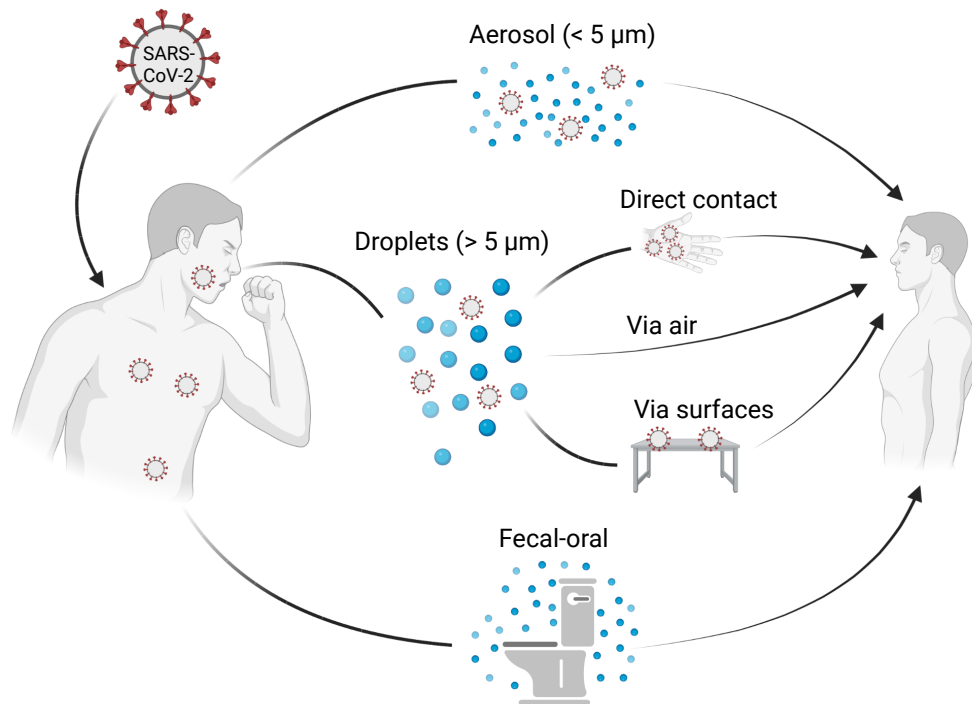
Figure 2.4: Transmission routes of SARS-CoV-2.[11]

of cases, with a 2.3% lethality, the numbers varied significantly for different variants. The early variants alpha, beta and gamma already showed a slightly higher transmissibility (e.g. for gamma, a R_0 of 3.4 compared to 2.5 for the wildtype was reported), disease severity and lethality (e.g. for alpha: 1.55 - 1.73 times more lethality). Another increase was reached with the delta variant that was predominant for a long period of time and showed very high transmissibility ($R_0 = 7$, facilitated also by shorter median incubation periods of 4.5 days) and increased lethality (2.37 times higher). In contrast to this development, the currently predominant variant omicron leads to a less severe course of disease with 0.71 times lower lethality. Still, the transmissibility further increased to a R_0 of 10 with a median incubation time of 3 days. This development can be explained from an evolutionary viewpoint as diseases with a high lethality often limit their transmissibility by killing their hosts before transmission can occur, while high transmissibility with low lethality can help a virus thrive.[23]

Another factor that influences the current disease outcomes in contrast to the situation in the beginning of the pandemic is the availability of medication and vaccines for SARS-CoV-2 which will be outlined in the following.

2.1.3 Treatment and Vaccination

When the pandemic began in early 2020, researchers worldwide put enormous research effort into the development of vaccines and the search for possible antiviral drugs.

Meanwhile, several possible treatments are available for certain patient groups profiting from them. Very early on during the pandemic, common antiviral drugs were tested for their efficacy in patients with COVID-19.[27] Over the years, further antivirals were developed with two main mechanisms of action: 1) drugs that target viral proteins or RNA and 2) drugs targeting host proteins or processes relevant for viral cell entry. Another approach is the use of convalescent plasma or intravenous immunoglobulin obtained from convalescent patients or even the use of monoclonal antibodies that can be very helpful as a treatment for high risk patients despite the high cost and difficult production.[19] Still, as is common for viral infection, no single drug was found to specifically treat COVID-19 in all patients, but decisions on suitable medication have to be made with respect to a patient's health status so that drugs are often only applied in high risk patients with certain comorbidities or in severely ill patients. For all other people, the best measure against COVID-19 is considered vaccination, making it one of the most powerful tools in putting an end to the pandemic.

In the field of vaccine development, there has also been made huge progress over the past years. Until December 2021, already nine different vaccines had been approved by the WHO. They mainly applied three different techniques: 1) mRNA vaccines (e.g. BNT162b2 from Pfizer/BioNTech), 2) non-replicating viral vector vaccines (e.g. AZD1222 from Oxford/Astra Zeneca) and 3) inactivated virus vaccines (e.g. CoronaVac from Sinovac).[28] As a forth vaccine principle, also protein based vaccines (e.g. NVX-CoV2373 from Novavax) have gained approval in several countries.[29] The different principles are also represented in Figure 2.5.
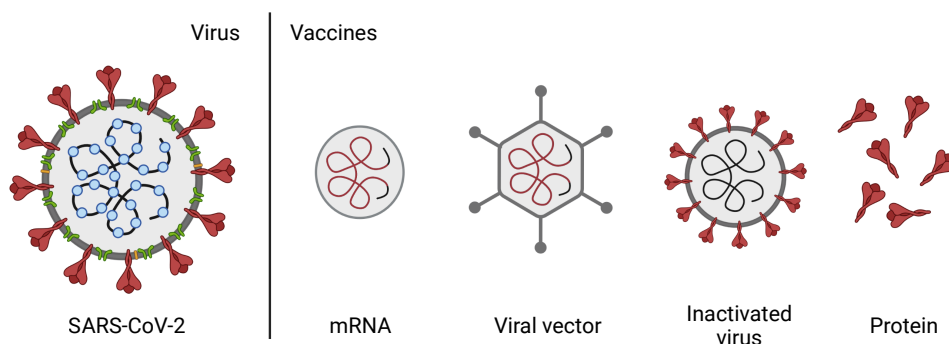

Figure 2.5: Different principles for SARS-CoV-2 vaccines.[11]

All these vaccines focus on inducing an immune response to parts of the SARS-CoV-2 S protein so that optimally the cell entry of the virus can be prevented by inhibition of the RBD-ACE2 binding. Here again the availability of suitable immunological tests like antibody assays

is crucial to test for vaccine efficacy. They are applied already early in vaccine trials to assess whether the vaccine can induce an immune reaction and are later continuously used to detect whether the available vaccines are still sufficient or whether adaptation of the vaccine or booster vaccination is necessary to retain protection. Another principle to test for the effectivity of vaccines is monitoring of infections in vaccinated and unvaccinated study groups but here no estimate of protection for a single person can be given until an infection occurs, an event one wants to prevent by vaccination. Therefore, rapid serological tests are needed to assess without high work or time expenditure whether a person is still protected or needs another vaccine dose or maybe a different, more effective vaccine type. Optimally, such tests can also distinguish immunity after vaccination from that after infection so that even unnoticed breakthrough infections after vaccination can be detected, enabling a broad immune profile of the population.

Already during the development of the first vaccines, it became clear in clinical trials that they can reduce the risk of infection with over 90% protection for many vaccine candidates.[30] Over time, it became evident that breakthrough infections can still occur after vaccination, especially with the upcoming SARS-CoV-2 variants, but that vaccination still provided significant protection from severe symptoms and complications including ICU admission, intubation or respiratory failure.[31] With respect to the variants, it was found that notable protection remains even from the initial vaccines especially for earlier variants like alpha, beta and even delta, while reduced protection was indicated for the omicron variant, giving rise to the development of adjusted vaccines.[32–34] The efficacy of these adjusted vaccines should be monitored in the future to make sure that they lead to the development of antibodies specific to the new variants, while still being applicable for older circulating variants. Therefore, suitable multiplex serological tests are necessary that can do these determinations for different variants simultaneously. A perfect example are microarray immunoassays like the ones this dissertation aimed on developing, as will be explained in more detail in Chapter 2.3.1.6.

The following chapter will focus on the function of the immune system and the different ways of providing immunity after vaccination to give a deeper understanding of the processes occurring in the body after an infection or vaccination with focus on the production of antibodies that are the main research interest for this dissertation.

2.2 Immunology

While the aim of this thesis was the development of antibody tests for SARS-CoV-2 that overcome all the drawbacks presented by commonly used test techniques, one has to first gain a deeper understanding of the fundamentals of human immunology to be able to fully grasp the

importance of antibodies within the human immune reaction. Only then can also be understood why the rapid and reliable determination of antibodies plays a decisive role in the coercion of pandemics.

2.2.1 Fundamentals

Immunology is a field of research that found its beginnings in the late 18th century with *Edward Jenner*. He discovered in 1796 that smallpox in humans could be prevented by infecting them with cowpox - also called vaccinia - a related virus that was not fatal for humans. He called this process vaccination and about 200 years later, smallpox was announced eradicated by the WHO thanks to *Edward Jenner*'s discovery.[35]

At the time of inventing vaccines, *Jenner* did not know anything about the causative agents of diseases. Here, *Robert Koch* contributed substantially in the 19th century by realizing that microorganisms cause diseases, a knowledge that lead to the development of further vaccines, for example by *Louis Pasteur* against cholera and rabies.[35] Other important contributors were the Russian natural scientist *Ilya Ilich Metchnikoff* and the German physician *Paul Ehrlich* who were awarded the Nobel Prize for Medicine in 1908.[36]

Both of them had focused on different aspects of immunology during their research. *Ehrlich* proposed "bodies" in the blood of immunized individuals that were able to protect themselves as well as also other individuals upon injection of so-called "anti-toxic serum". He therefore provided the basis for what we today know as antibodies, while he was rather sceptical about *Metchnikoff's* results, which he considered as inconclusive to many investigators.[37] *Metchnikoff* had discovered that certain mobile cells could ingest and digest foreign material introduced into an organism. He called them phagocytes and the process phagocytosis and recognized that it was an important process in inflammation and elimination of pathogens.[38]

The two subsystems that the immune system can be divided into and that were in part already investigated by *Metchnikoff* and *Ehrlich* - albeit not under the same notation as today - are an innate component, representing the rapid "first line of defense", and an adaptive component, being more specific but not as fast as the innate response. Figure 2.6 shows the main elements of the innate and the adaptive immune system and Table 2.1 gives a short comparison of the main differences between these two components that will also be outlined in more detail in the following sections.

2.2.2 Innate Immune System

The innate immune system (also called native immunity) consists of mechanisms that are present even before infection occurs. Its major components are epithelial barriers that block

Table 2.1: Comparison of innate and adaptive immunity.[39,40]

Feature	Innate immunity	Adaptive immunity
Time of response	Immediately after entry and recognition of a pathogen	Days to weeks after the entry of a pathogen
Specificity	Not highly specific, recognition by pattern recognition receptors	Highly specific due to antigen specific B and T cell receptors
Memory	Limited, response is the same with every exposure	Yes, responsiveness is enhanced by repeated exposure
Cellular component	Phagocytes, dendritic cells, eosinophils, NK cells, mast cells	B and T cells
Humoral component	Complement proteins	Antibodies

the entry of pathogens (like skin and mucosa), phagocytic cells (like for example macrophages), natural killer cells (NK cells) and various plasma proteins including proteins of the complement system.[41] Other features of the innate immune system include fever, interferons and pattern-recognition molecules.[42]

These pattern recognition molecules help the innate immune system to distinguish pathogens from host structures. A common kind of these molecules are Toll-like receptors (TLRs) that are able to recognize pathogen structures and thus to activate immune cells. Many of them recognize bacterial features like peptidoglycan or lipopolysaccharides, but for the detection of viruses there are also TLRs recognizing double-stranded (ds) RNA.[43] TLRs can induce the production of for example cytokines helpful in fighting an infection.[41,43]

For the mentioned production of cytokines and other actions, the cells that form part of the innate immunity are needed as depicted in Figure 2.6. Many different cell types are included with some of them sharing tasks. One group are phagocytes as discovered by *Metchnikoff*. These specialized leukocytes (mainly macrophages, dendritic cells, eosinophils and neutrophils) can uptake microbes and render them harmless. Macrophages and dendritic cells additionally have an important role in antigen presentation to T cells, making them a link to the innate immune system. Mast cells initiate inflammatory reactions by releasing e.g. histamine, enzymes and cytokines. Another important cell type are natural killer (NK) cells that can induce apoptosis of cells infected for example by viruses. Additionally, they also secret cytokines that lead to macrophage activation.[40,44]

Cytokines generally are low molecular weight messengers that can alter the behavior of cells, e.g. by promoting the growth of certain leucocytes (interleukins), activating them or acting as
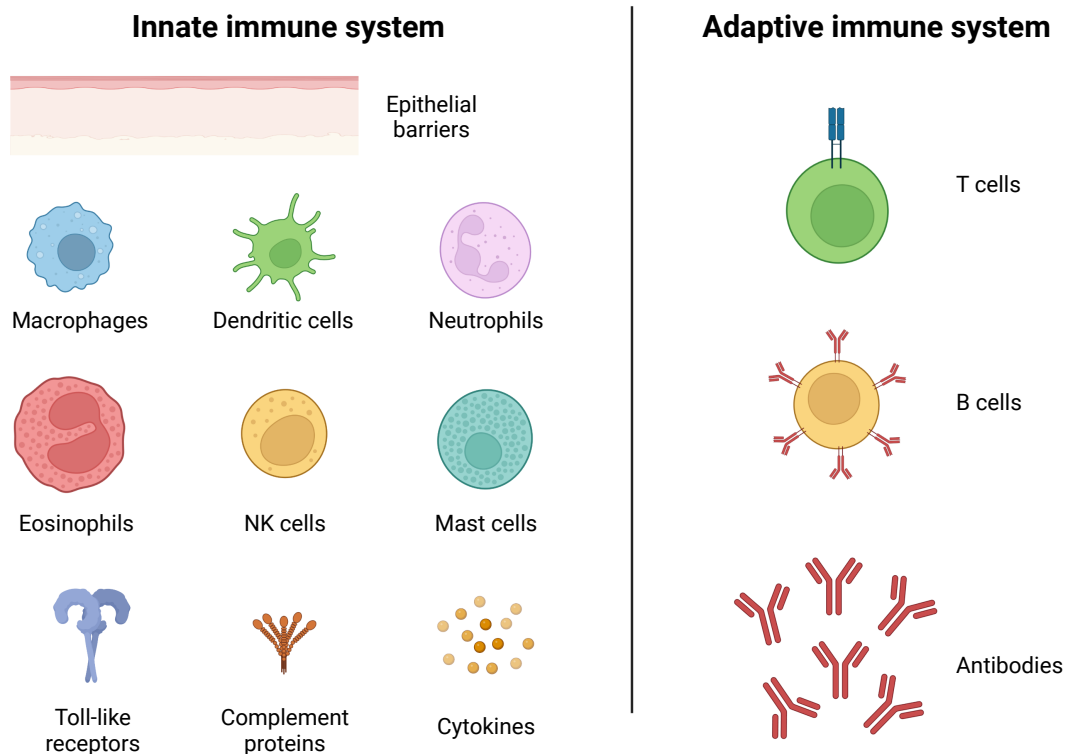
Figure 2.6: Components of the innate and the adaptive immune system.[11]

chemoattractants (chemokines). A special group of cytokines are called interferons. Upon viral infection, especially interferon α and β are produced, leading to reduced replication within the cell, also hindering virus proliferation.[45]

Finally, the complement system as the last part of innate immunity presented herein is made up from more than 30 proteins mainly found in plasma. Whenever the complement system is activated, a sequential cascade of enzymatic reactions takes place (known as complement activation pathways) and leads to a physiological response like chemoattraction of immune cells or apoptosis. While initially after its discovery in the 1890s, complement was thought to be important only in the innate immune system, later research in the 1970s found it to play a role also in the adaptive immune system, showing how closely the two subsystems of the immune system act together.[46]

2.2.3 Adaptive Immune System

The adaptive immune system mainly consists of T and B lymphocytes as cellular components and antibodies as humoral components. Both T and B lymphocytes are relatively small with diameters of 8 - 10 µm. They normally have large nuclei but only few mitochondria, ribosomes

and lysozymes, but as soon as they are activated, they enlarge and increase their number of organelles.[44]

2.2.3.1 T Cells

B and T cells can be activated by specific antigens binding to antigen receptors presented on the cell surface (B cell and T cell receptors, BCR and TCR, respectively). For T cell activation, it is necessary that these antigens are presented on the surface of antigen-presenting cells (APCs, for example dendritic cells or macrophages). In contrast to B cells, they do not recognize intact antigens but only peptide fragments that can be found on so-called MHC (major histocompatibility complex) proteins on the surface of APCs. The TCRs necessary for this recognition are membrane bound and consist of two disulfide-bond linked polypeptide chains with each having a constant and a variable domain, similar to antibodies as will be described later. Each T cell expresses one type of TCR, obtained from site-specific recombination of different TCR gene fragments during the development of T cells in the thymus. The detailed mechanisms to obtain TCR diversity are similar to those used in B cells and will be explained later.[47]

When a T cell coincides with an APC presenting the correct antigen within the peripheral lymphoid organs, binding of the TCR and the MHC with antigen takes place. To achieve an activation of the T cell, additional co-stimulation (mediated for example by the surface protein CD28 on T cells binding to CD80/CD86 proteins on APCs as shown in Figure 2.7) is necessary.[48] As a third activation signal, the secretion of cytokines from the APC is used.[49] Upon activation, T cells differentiate into active cells with pre-defined functions. T cells carrying the CD4 receptor (CD4$^+$ cells) mainly become T helper cells that are able to 1) produce cytokines necessary to attract other immune cells and 2) to stimulate B cells so that antibodies are generated.[44] Alternatively, CD8$^+$ cells convert into cytotoxic T cells upon activation. These are able to attack and destroy infected cells (e.g. in viral infections) by expressing ligands for cell death receptors or liberating cytolytic granules, leading to apoptosis.[50,51] Additionally, memory T cells are of interest. They can be either CD4$^+$ or CD8$^+$ T cells after exposure to the respective antigen and are long-lived cells that can give rapid protection upon re-exposure to the antigen.[52]

2.2.3.2 B Cells

The second relevant cell type in adaptive immunity are B cells. As shown in Figure 2.8, they are produced in the bone marrow and have their origin in hematopoietic stem cells differentiating into common lymphoid progenitors (CLP) upon signalling from the surrounding stromal cells. Therefore, B cells share their origin in CLPs with for example NK cells and T cells, but
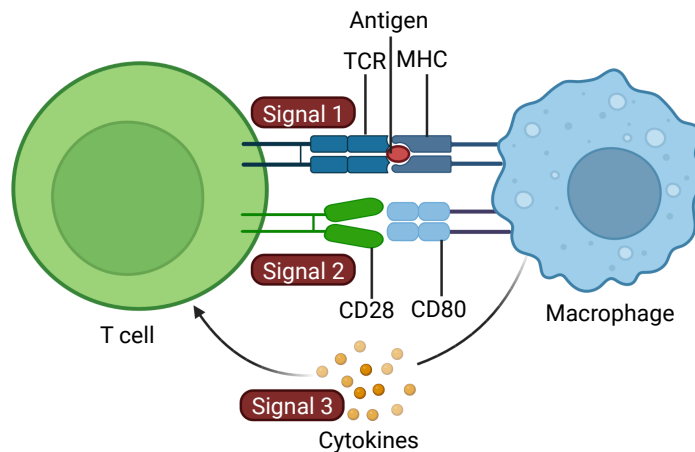
Figure 2.7: Antigen specific activation of T cells by different signals.[11]

in contrast to these cells, they further develop into pro-B cells, considered the first actual B cell stage in the development process.[53] While for the development of T cells, the progenitor cells have to migrate to the thymus and differentiate into early thymic progenitors there, B cells remain in the bone marrow for another development step as the microenvironment of the stromal cells in the bone marrow is crucial by delivering all stimuli and factors needed for the activation of relevant transcription factors.[44] For a B cell to become functional, it has to express a B cell receptor (BCR) that consists of a heavy (H) and a light (L) chain. Secreted B cell receptors are known as antibodies and will be treated later on. Each B cell carries one specific receptor that is formed during its development in the bone marrow. Its formation starts during the pro-B cell stage by recombination-activating gene (RAG)-dependent rearrangement of gene segments for the BCR. First, the antigen binding region of the H chain is formed by rearrangements and recombination of three germ-line genes - V (variable), approx. 65 different segments, D (diversity), approximately 30 different segments and J (joining) genes, approximately 5 segments - followed by formation of L chains with antigen binding regions made up from V and J genes, where again various different segments are available, leading to about 10^{12} different combinations.[35,54,55] These can then pair with the H chains to form immunoglobulin M (IgM) that is presented on the surface as BCR and initiates the entrance of the immature B cell into the spleen.[56] When the B cells get into contact with antigens that bind to their BCR, crosslinking of BCRs occurs for some antigens (e.g. polysaccharides from bacteria that contain repetitive motifs) and leads to activation of the cell. For protein antigens that usually only contain the BCR binding motif once, a second activating signal is needed. Therefore, B cells can internalize antigens and present fragments of them via MHC proteins. These are recognized by T helper cells that give a second confirmatory signal leading to proliferation of the B cell.[35,39] Alternatively, the B cells can enter germinal centers after T helper cell-dependent antigen contact.[55] These

germinal centers exhibit an microenvironment of lymphoid tissue suitable for cell proliferation, somatic hypermutation and selection by antigenic affinity.[44] When somatic hypermutation occurs, point mutations are introduced into the V regions of the H and L chains at very high rates, leading to mutant BCRs. These B cells are screened for their antigen affinity and those with higher affinity than the original BCR preferably mature further into antibody secreting cells. This is an important difference to the diversification process in TCRs which is in main parts very similar, e.g. it uses the same V(D)J recombinase including the RAG proteins, but no somatic hypermutation occurs. Therefore, TCRs retain low antigen affinity, while BCRs elicit very high affinities with K_D values in the order of 0.01 - 100 nM.[47] Additionally, class switch recombination can occur in B cells, leading to the production of different antibody isotypes apart from IgM that is found on immature B cells.[35]
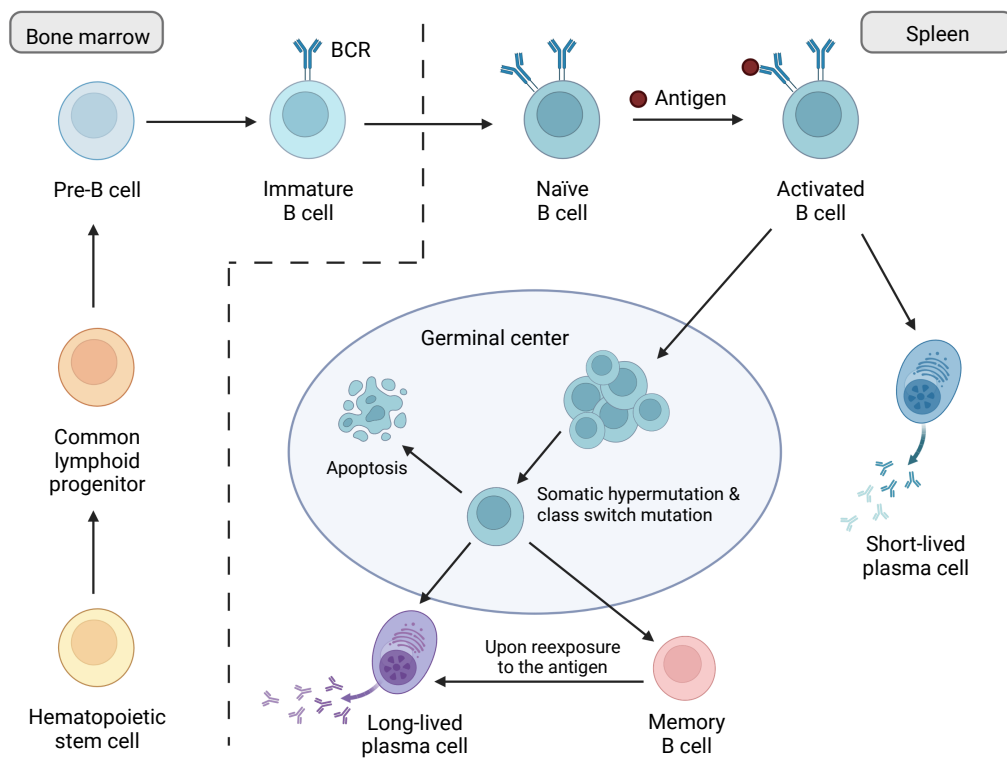

Figure 2.8: Development stages of B cells.[11]

During the whole process of B cell development and maturation, various checkpoints have to be passed. During early development, negative selection makes sure that B cells acting in an autoreactive manner are rendered harmless (e.g. by receptor editing, apoptosis or anergy), avoiding the later production of autoantibodies. On the other hand, positive selection enables the survival of only those B cells that recognize their respective antigen.[57] Further selection steps occur in later developmental stages as described before, so that only few B cells ultimately reach the state of long-lived plasma cells or memory B cells.

Memory B cells are long lived cells that were once stimulated by their respective antigen and had undergone proliferation, possibly class switch and selection in a germinal center. They divide very slowly and present a BCR on their surface without secreting antibodies but upon another contact with the antigen they proliferate and differentiate into plasma cells, allowing for a much faster response than would be possible from naïve B cells. Memory B cells can circulate for many years and therefore give a robust protection. Plasma cells on the other hand only present low amounts of their BCR on the surface. Additionally, they can neither act as antigen presenting cells anymore, nor are they able to undergo a class switch. Their main function is the continuous secretion of antibodies which will be treated in the following section.[53,58]

2.2.3.3 Antibodies

Antibodies form part of the humoral immune response which is the response mediated by secreted macromolecules. They are secreted by B cells (plasma cells) and are effector molecules in contrast to the membrane bound BCRs which also are immunoglobulins but function as sensors for antigens.[39] Secreted antibodies can act by different mechanisms: 1) neutralization of pathogens, e.g. by preventing their entry into human cells, 2) agglutination of two or more pathogens with the same antigen to form an aggregate that can more easily be eliminated, 3) activation of the complement system, 4) opsonization (tagging) of pathogens to label them for the recognition by macrophages or neutrophils.[39]
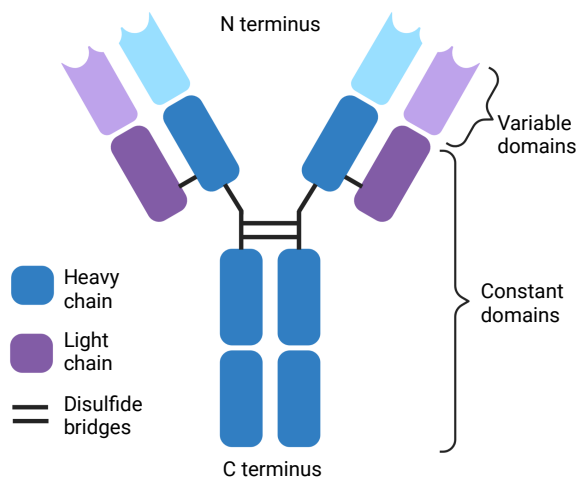

Figure 2.9: Schematic structure of an antibody.[11]

Antibodies consist of four polypeptide chains as shown in Figure 2.9, two identical heavy chains and two identical light chains like BCRs. The light chain consists of two domains and the heavy one of four to five domains. The N terminal domains of the chains are variable and are relevant for antigen binding. In this area, somatic hypermutation leads to optimized affinity for the respective antigens. This variability is possible due to three complementary determining regions (CDRs) in the N terminal domains of light and heavy chain which consist of protruding loops formed from 9 - 11 amino acids between anti-parallel β sheets. This gives rise to very diverse 3D structures, allowing for the recognition of a big variety of antigens. The remaining domains towards the C terminus are constant and are able to e.g. interact with complement proteins. The four chains of an antibody

are linked by disulfide bonds complemented by non-covalent interactions for further stabilization. Due to their symmetrical Y-shaped structure, antibodies contain two identical antigen binding sites that can interact with antigens like virusal proteins.[39]

The affinity of an antibody as measure of its ability to bind to an antigen strongly can be calculated as association constant of the antigen-antibody complex as shown in Equations 2.1 and 2.2 with A being free antigen, B being free antibody and AB the antigen-antibody complex at equilibrium. K_a is the association constant that is used as a measure of affinity. It is given in M^{-1}, while the reciprocal dissociation constant K_d (in M) also often is used for expressing binding strength of an antibody.[59]

$$A + B \overset{k_a}{\underset{k_d}{\rightleftharpoons}} AB \tag{2.1}$$

$$K_a = \frac{1}{K_d} = \frac{k_a}{k_d} = \frac{[AB]}{[A][B]} \tag{2.2}$$

Affinity maturation by somatic hypermutation leads to an increased affinity with a greater rate constant k_a and association constant K_a, respectively. Antibodies which elicit higher affinity can form a stronger bond to their antigen, giving them more protective force than ones with lower affinity. To evaluate affinities, different methods are available like surface plasmon resonance or isothermal titration calorimetry (ITC). The latter often is referred to as gold standard as it can be used to measure affinities of antibodies and ligands in solution without any immobilization or chemical modification. It thus is a label free method that utilizes the slow titration of antibody and antigen by measuring the heat formed or absorbed during the process of antibody-antigen complex formation. Thereby, the enthalpy ΔH of the complex formation reaction can be measured and used to determine binding affinity K_a according to Equation 2.3 (with ΔG as the change in Gibbs free energy, ΔS the change in entropy, R as gas constant and T as absolute temperature).[60]

$$\Delta G = -RT \ ln \ K_a = \Delta H - T\Delta S \tag{2.3}$$

Another important measure is the avidity, which can be referred to as the total binding strength consisting of affinity and valency.[61] This valency of an antibody depends on its class. Generally, five different classes of antibodies (immunoglobulins) are known. Each B cell only produces one of these classes, a switch to a different antibody class can be achieved by class switch recombination in germinal centers. Differences between the classes apart from the valency are found within the constant part of the heavy chains of the antibody. IgM is the first immunoglobulin that is expressed during the development of B cells, therefore it is the primary response to pathogens. Its main function is the opsonization of antigen.

During the secondary response to a pathogen at a later timepoint of disease, mainly IgG is formed as shown in Figure 2.10. IgG antibodies have a molecular mass of approx. 150 kDa and are capable of efficiently neutralizing toxins and viruses as well as opsonizing antigens.
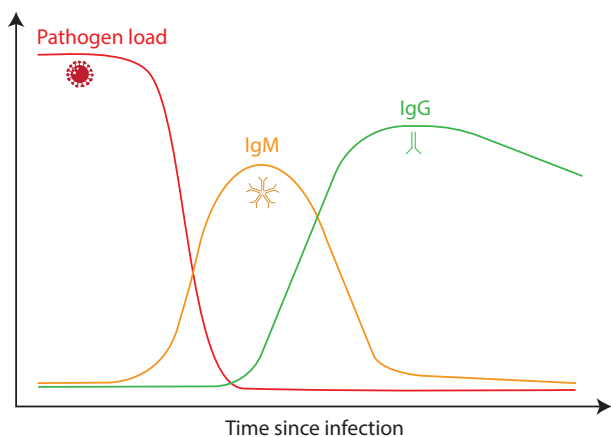

Figure 2.10: Timescale of IgM and IgG development after infection.

Figure 2.11 (a) shows the 3D structure of an IgG molecule with two heavy and light chains as well as a carbohydrate component bound to a conserved N glycosylation site within the heavy chains.[62] Another class of antibodies, IgD, is also produced relatively early when B cells leave the bone marrow but its function remains unclear. The fourth antibody class, IgA, is relevant due to its protection of the mucosal surfaces from toxins, viruses and bacteria by neutralizing them or preventing their binding to the surface. The last known class is IgE, which plays a role in hypersensitivity and allergy as well as the immune reaction to
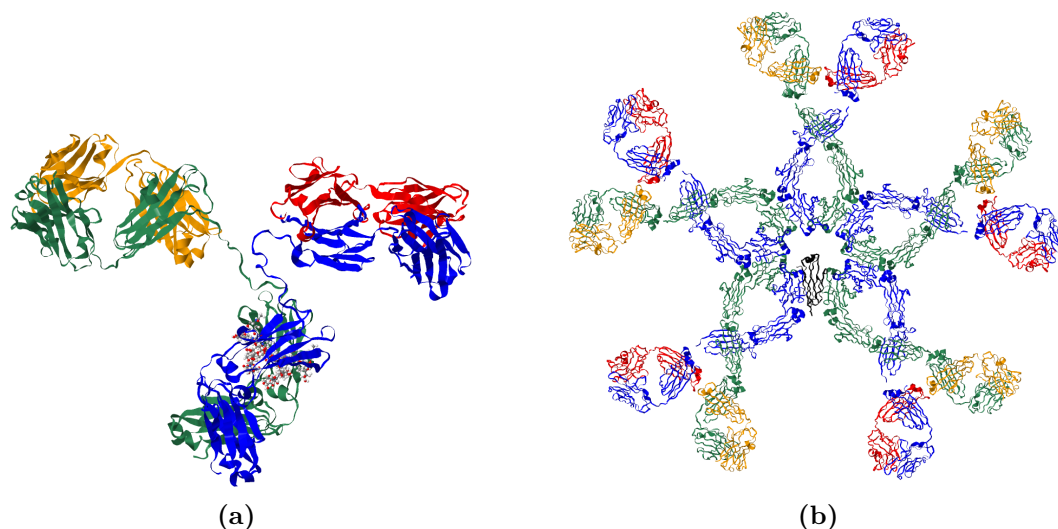
parasites.[40] While IgD, IgE and IgG are found as monomers, IgA is usually present in dimers and IgM occurs as pentamers with the monomers being held together by a J chain, allowing them to bind to antigens with a total of ten antigen binding sites.

Generally, IgM elicits lower affinity than IgG due to its early formation and early fading in contrast to IgG that can undergo affinity maturation over time, but IgM has a high avidity due to the high number of possible interaction sites (high valency). A representation of an IgM molecule is provided in Figure 2.11 (b). The different classes are found in different concentrations in the serum with IgG being the most abundant followed by IgA, while IgE and especially IgD (as it is normally not secreted) can only be found in low concentration. IgG also has the longest half-life of the antibody classes with 23 days while in comparison the half-life of IgM is only 5 days.[39]

When comparing secreted antibodies and membrane bound BCRs, the main difference is a hydrophobic α helical transmembrane domain and a short cytosolic domain at the C terminal end of the heavy chain. Upon activation of a B cell by antigen contact and differentiation into a plasma cell, expression of the heavy chain is upregulated and alternative mRNA processing occurs, leading to the loss of the membrane anchor. Therefore, the BCR cannot be linked to the cell membrane anymore and is secreted as an antibody.[39] These antibodies then recognize their respective antigen and can carry out their previously described functions.

With this chapter, the importance of the immune system and all its components working hand in hand should have become apparent. At the same time, the importance of antibodies

Figure 2.11: (a) 3D representation of an IgG antibody obtained using X-ray diffraction;[63] (b) 3D representation of an IgM antibody obtained with synchrotron X-ray solution scattering and molecular graphics modelling;[64] heavy chains are shown in blue and green, light chains in orange and red, J chain in IgM shown in black; images generated with Jmol.[65]

was stressed: they are highly specific, form and fade dynamically and therefore can be used to assess time courses of infections or efficiency of vaccines. But to make this possible, reliable serological tests are required, allowing for the deeper analysis of antibodies specific to a disease. Therefore, the next chapter will focus on different test principles and bioanalytical platforms that have been developed and investigated by research groups around the world.

2.3 Serological Assays and Analysis Platforms

2.3.1 Serological Assays

Serological assays can be applied for the detection of antibodies in blood samples. They can be helpful in a variety of settings as they can provide important information at different stages of an infection. Early after disease onset, they can help to monitor a patient's immune reaction to an infection by testing for the early formed IgM antibodies, while serological assays for the determination of IgG are helpful after the acute stage of infection, where the pathogen is not detectable anymore. They are used to detect previous infection that had gone unnoticed by the patient, but they are also valuable for safety testing of blood products to prevent the transfusion of blood infected with e.g. hepatitis C or other chronic infections leading to antibody formation. Additionally, they are helpful in epidemiological studies or for the determination of vaccine-

induced immunity and its decay over time. Apart from the detection of IgM and IgG antibodies separately, another interesting target for serological assays are neutralizing antibodies that can prevent the infection of cells and disease progression.[66]

During the development of a serological assay, different considerations have to be made. The assay should aim on reaching very high sensitivity, which can be calculated as shown in Equation 2.4, meaning that it gives the fraction of samples that were classified as containing antibodies within all samples known to contain antibodies. A low sensitivity of a serological test means that positive samples are relatively likely to be falsely classified as negative.

$$Sensitivity = \frac{Number\ of\ true\ positive\ results}{Number\ of\ all\ positive\ samples} \times 100 \qquad (2.4)$$

At the same time, another aim should be to achieve high specificity, calculated according to Equation 2.5 as the fraction of samples correctly classified as negative within all samples known to not contain antibodies.[67]

$$Specificity = \frac{Number\ of\ true\ negative\ results}{Number\ of\ all\ negative\ samples} \times 100 \qquad (2.5)$$

Additionally, it has to be considered whether the evaluation of a serological test will be done quantitatively or qualitatively, i.e. that it only gives a binary statement on the presence or absence of antibodies or also a numerical classification of the amount of antibodies relative to a standard. To be able to distinguish negative from positive samples, a classifier has to be defined as the borderline between positive and negative. For this purpose, receiver operating characteristic (ROC) curve analysis is a suitable tool. To obtain a ROC curve, an appropriately large, known sample set is tested with the test of choice, giving a response for each of the samples. Subsequently, arbitrary thresholds are set at different values throughout the whole signal range and for each threshold, the true positive rate (sensitivity) and false positive rate (1 − specificity) are calculated and plotted against each other. The resulting plot can then be used to determine the optimal cut-off value.

Figure 2.12 shows exemplary ROC curves of varying quality: while curves close to the dashed black line (x = y, representing a random classification) belong to tests with very bad selectivity for positive and negative samples, the optimal ROC curve would run along the axes as shown in green. If such a rectangular curve shape is seen, the optimal cut-off value belongs to the point (0,1) in the left upper corner, where 100% sensitivity and specificity can be achieved. If deviations from the optimal curve are found, the cut-off value is defined depending on needs and interests as to optimize either sensitivity or specificity.

Another relevant consideration is the amount of automation, the number of measurements per time interval, the duration of a single measurement and the necessary laboratory equip-

ment. This gives rise to various different test formats ranging between highly automated high-throughput tests and very easy-to-use point-of-care tests as well as to different bioanalytical platforms suitable for the execution of these tests. The following sections will outline some examples for serological test formats and bioanalytical platforms used for SARS-CoV-2 as well as other pathogens.
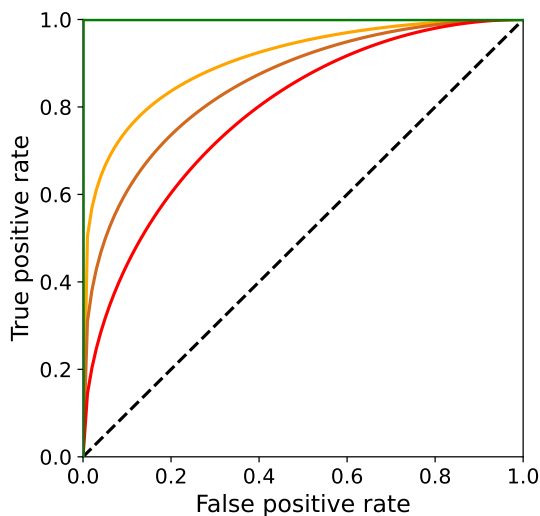
For the main goal of this thesis, which was to enable the rapid, sensitive and specific analysis of antibodies to SARS-CoV-2 using a highly automated test with low work expenditure that can easily be adapted to rapid changes of requirements during the pandemic, first a suitable test format together with an appropriate analysis platform had to be selected. The following sections will also show the rationale for this decision that was made even before the assay development which will then be elucidated in Chapter 4.

Figure 2.12: Exemplary ROC curves.

2.3.1.1 Hemagglutination (Inhibition) Assays

A very early example for serological tests are hemagglutination inhibition assays that had been developed in the 1940's for the detection of IgM as well as IgG antibodies to influenza.[68] The assay principle is based on the process of agglutination, where certain receptors found on the surface of red blood cells bind to the hemagglutinin glycoprotein present on the surface of influenza virions. This creates a lattice of red blood cells and virus particles that keeps the blood cells in suspension, giving the test solution a light red colour. On the contrary, when no agglutination occurs, the blood cells sink to the bottom of the used test tube or microtiter plate well, forming a red circle with sharp edges. To test for the presence of antibodies, the virus of interest is incubated with serum containing antibodies. Subsequently, the treated virus is added to a suspension of red blood cells, whereas the more agglutination can occur the less antibodies were present in the serum sample. While initially the test principle was only used for influenza and other viruses like mumps,[69] measles[70] or rubella[71] that intrinsically have the ability to force blood cell agglutination by their surface proteins, its application was also made feasible for other viruses like SARS-CoV-2.[72,73] In an exemplary serological test published by *Ertesvåg et al.*, anti-erythrocyte nanobodies are coupled with the RBD domain from SARS-CoV-2. These nanobodies can therefore bind to red blood cells which can subsequently be cross-linked by the binding of SARS-CoV-2 RBD-specific antibodies, leading to visible ag-

glutination.[74] Hemagglutination tests as well as hemagglutination inhibition tests are relatively cost efficient and easy to perform, which has paved their way as gold standard in the detection of vaccine-elicited immune protection against influenza, but they also have several drawbacks like a limited range of pathogens susceptible to the test type without severe adaptations, difficulties in interpreting low levels of agglutination or its inhibition, the influence of non-specific agglutination or inhibiting agents and generally a relatively low sensitivity and specificity.[69,73]

2.3.1.2 Complement Fixation Tests

An alternative are complement fixation tests that are mainly used for the determination of IgG antibodies. They make use of the complement proteins that are able to bind to antigen-antibody complexes and additionally are able to lyse certain labeled erythrocytes. For doing a complement fixation test with a serum sample, first the patient's complement proteins in the sample are destroyed by heat treatment. The serum is then mixed with the viral antigen of interest to allow for binding of antibodies to this antigen, forming antigen-antibody complexes. Subsequently, exogenous complement (e.g. from guinea pig serum) is added and binds to these complexes, thus being "fixed" to them. When now so-called indicator erythrocytes are added, unfixed complement will lead to hemolysis. On the contrary, no lysis of the erythrocytes will occur, if the complement was fixed by antigen-antibody complexes.[66] Complement fixation has been used already in the early 20th century by *Wassermann* for the serological detection of an infection with *Treponema pallidum*, causative agent of syphilis, a test that had been widely used and optimized over the following decades.[75–77] Additionally, it was also used for the detection of other infections by means of antibodies to the respective pathogen, e.g. for typhus fever by detecting antibodies against *Rickettsia prowazeki*[78] or Q fever caused by *Coxiella burnetii*.[79] It furthermore found application in monitoring of the immune response after vaccination of cattle against *Bacillus anthracis*,[80] and, more recently, complement fixating activity of patient sera after SARS-CoV-2 infection was also investigated.[81] Nevertheless, complement fixation is very labor intensive and can hardly be automated. Therefore, it has mainly been replaced by immunoassays.

2.3.1.3 Enzyme-linked Immunosorbent Assays and Related Methods

Immunoassays can be defined as bioanalytical methods in which the interaction of an antigen and an antibody is used for the determination of an analyte, hence making them generally applicable for serological testing.[82] First examples of immunoassays date back to the 1960s when radioimmunoassays were first described.[83] Here, radioactively labeled analyte is competing for binding sites with the analyte in a sample and radioactivity is measured to determine the antigen amount in the sample. Although the principle proved very successful for the detection

of small amounts of an analyte, a high technical expenditure and the need for an isotope laboratory resulting in high costs for analyses led to the development of other assay methods like for example the enzyme-linked immunosorbent assay (ELISA).

The ELISA principle has been developed by two different working groups independently in 1971.[84,85] In contrast to the previously applied radioimmunoassays, ELISA is based on the labeling of antigen with an enzyme instead of a radioactive isotope. This made the production easier, more affordable and allowed for prolonged storage of the prepared conjugates. *Peter Perlmann*, one of the developers of the ELISA technique, conjugated alkaline phosphatase to rabbit IgG and let it incubate with an IgG containing sample on a cellulose immunosorbent treated with anti-rabbit IgG serum. After washing, a colorimetric substrate of alkaline phosphatase was added, giving a measurable color reaction with absorbance dependent on the amount of labeled antigen that had bound to the surface in competition with the IgG in the sample.[85] In current ELISAs, mostly horseradish peroxidase (HRP) is used as enzyme label, also leading to a color reaction upon addition of a substrate for the enzyme, e.g. 3,3,5,5-tetramethylbenzidine (TMB). HRP has the advantage of being significantly smaller than alkaline phosphatase (40,000 Da compared to 86,000 Da), leading to less sterical hindrance. Additionally, it is less expensive than other options. As an alternative to colorimetric readout by measuring OD, also fluorescence or (chemi)luminescence can be applied. The former needs a light source for excitation, followed by measurable light emission and leads to similar detection limits of the analyte as colorimetric detection, while the latter does not require an external light source and can give up to ten times lower detection limits.[86]

Other necessary elements to perform an ELISA are a suitable solid phase allowing for the adsorbance of biomolecules (mostly polystyrene 96-well plates are used), washing buffers for cleaning between different assay steps and blocking agents for the prevention of unspecific binding to the solid phase. As blocking reagents for example casein, bovine serum albumin (BSA) or fish gelatin are used, binding permanently to the solid phase.[86]

Among ELISAs, different principles can be distinguished. In a direct ELISA, a purified sample is added to the solid support and the analyte of interest binds to the surface. After blocking and washing, an enzyme-labeled primary antibody recognizing the analyte is introduced, followed by detection with one of the previously described techniques. The assay is highly specific but requires purified samples and not all primary antibodies are readily available with enzyme labels. To overcome this, indirect ELISAs can be used, where the primary antibody is unlabeled and is bound by a secondary antibody (e.g. species-specific). This principle is the method of choice when detecting antibodies in serum samples, as will be explained in more detail in the following. Another ELISA principle that overcomes the need for purified samples to be immobilized on the microtiter plate are sandwich antibodies. Here, the analyte of interest is captured between an immobilized and a dissolved antibody. This principle has gained widespread suc-

cess in antigen tests to determine an active infection with e.g. SARS-CoV-2. As a last general principle, competitive ELISAs can be named. Here, the analyte of interest is immobilized and the primary antibody is incubated with a sample containing the analyte. Hence, part of the primary antibodies are already occupied and cannot bind to the immobilized analyte, leading to lower detectable signals with increasing analyte in the unknown sample. This assay principle has the drawback of a relatively long assay duration but gives a high specificity and is often used in quantitative assays.[86]

Target molecules of ELISA can either be various antigens including proteins or also small molecules, but as well antibodies, as it is the case for serological ELISAs. Depending on the target molecule, the immobilized biomolecule as well as the biomolecules used for detection have to be adapted: in an indirect serological ELISA, the respective antigen is immobilized, primary antibodies from a blood sample bind to it and are detected using a suitable secondary antibody with enzyme label (e.g. anti-human IgG or anti-human IgM) as depicted in Figure 2.13 (a).[87,88] Alternatively, sandwich-like assay procedures are possible, where the specific antibody is sandwiched between an immobilized antigen and a dissolved, enzyme-labeled protein, requiring the interaction of both antigen binding sites of the antibody (Figure 2.13 (b)).[89] This principle is more specific as cross-reactivity of secondary antibodies can be avoided, but also expensive and laborious due to the need of conjugation of antigen and detection enzyme.

Classical ELISA is a very widely used technique in clinical serological diagnostics. It allows for relatively sensitive and specific detection of analytes and can be done as a high-throughput method, especially when using automated ELISA platforms. Nevertheless, some drawbacks have to be considered: ELISA generally is tedious and laborious, it takes relatively long with assay durations of several hours and contains many manual pipetting steps that have to be carried out with high precision to avoid errors. Additionally, usually only one analyte can be
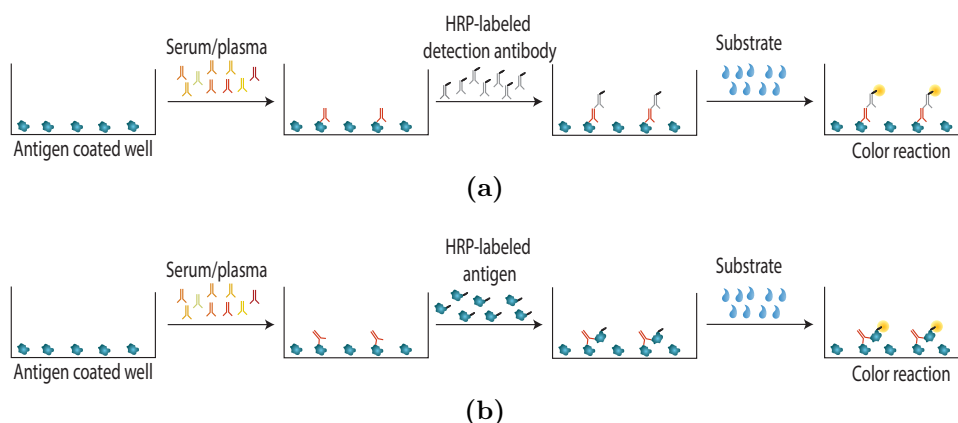

Figure 2.13: (a) Indirect ELISA for detection of antibodies; (b) Sandwich-like ELISA for detection of antibodies.

determined per well of the microtiter plate, implying limited multiplexing options. Furthermore, specialized laboratory equipment is needed, making it hard to carry out ELISAs in a field setting.[86]

A measure to improve the sensitivity of an ELISA is the use of a different detection principle. As mentioned beforehand, apart from colorimetric assays, also assays applying chemiluminescence (CL) for signal generation can be found. They are often referred to as chemiluminescence immunoassays (CLIA).[90] CL can for example be generated using HRP by just exchanging the respective substrates from TMB to luminol and hydrogen peroxide as shown in Figure 2.14. Upon contact to hydrogen peroxide, HRP catalyzes the formation of hydroxyl radicals (OH$^\cdot$) and superoxide anion radicals (O$_2^{-\cdot}$). Subsequent reaction of the chemiluminescence substrate luminol with these radicals leads to the formation of a luminol radical and in a second step luminol endoperoxide. This unstable compound eliminates nitrogen, resulting in a 3-aminophthalate triplet dianion in excited state that converts into the singlet dianion by intersystem crossing (ISC). This excited state-dianion can relax to its ground state while emitting visible light ($\lambda = 425$ nm) that can be recorded e.g. by means of a CCD camera.[91] Due to the relatively high quantum efficiency of 0.001 to 0.1, very low detection limits down to 10^{-18} - 10^{-21} mol can be reached with CL.[92] Other than the detection method, CLIAs work analogous to ELISAs with better sensitivities but also the need for equipment suitable for the detection of CL. Another related assay principle for serological assays are electro-chemiluminescence immunoassays (ECLIAs) that apply ruthenium-based tracers able to emit light of a defined wavelength following a redox reaction upon application of a voltage instead of enzyme labels.[93]
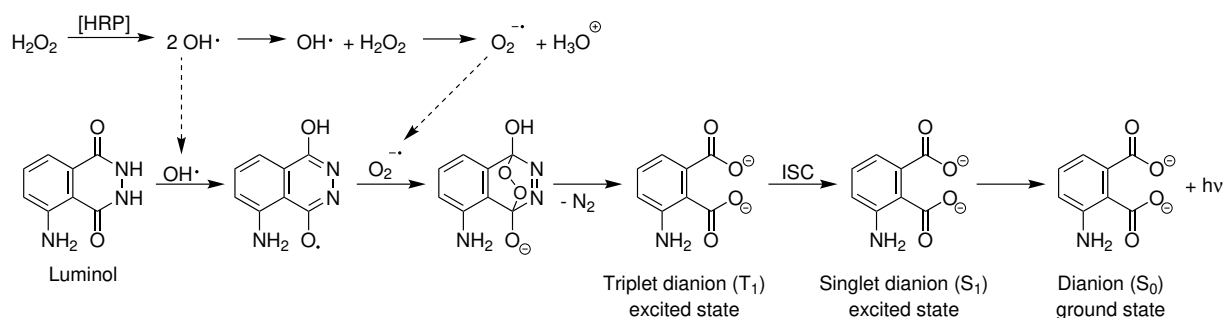

Figure 2.14: Chemical principle behind the HRP-catalyzed CL reaction of luminol and hydrogen peroxide.

2.3.1.4 Immunofluorescence Assays

The immunofluorescence assay (IFA) is a microscopical method for the detection of antibodies. It uses uninfected control cells as well as cells infected with the pathogen of interest that are fixed to wells on glass microscope slides. Subsequently, a serum sample containing antibod-

ies is added and the antibodies can bind to their specific antigens presented on the surface of the infected cells. To detect bound antibodies, a fluorescent dye-conjugated anti-species antibody (e.g. anti-IgM or anti-IgG) is added and labels all positions where antibodies from serum have bound. Their presence is verified using a fluorescence microscope.[94] This assay principle has been applied in numerous diseases, for example in the detection of HIV infections via the presence of antibodies[95] or for serological investigations in visceral leishmaniasis[96] but also for SARS-CoV-2 antibody detection.[97,98]

The IFA is a relatively inexpensive technique as long as a fluorescence microscope is available. It can also be helpful to characterize the exact position of antibodies binding to antigens on a cell. But it also has some drawbacks, as its interpretation is subjective, fluorescence often is subject to background problems and non-specificity issues and it does not give quantitative results - these can alternatively easily be obtained using ELISA techniques. An additional problem has to be considered with all assays using active virus to generate infected cells as the according biosafety level for the respective pathogen has to be reached by the testing laboratory.[99]

2.3.1.5 Lateral Flow Assays

The previously described immunoassay principles are suitable in laboratory settings, as they require specialized equipment, extensive working steps (e.g. pipetting or culturing of cells) or specially trained staff. They may give reliable results but as a drawback, obtaining these results takes relatively long time.

But nowadays, near-patient biochemical testing that is also known as point-of-care (POC) testing gains more and more importance. It refers to tests that can be done by healthcare professionals within close proximity to a patient. Results are gained within short timeframes, on the one hand due to rapid test formats, on the other hand because of the reduced need for transport and sample preparation. It potentially even allows for diagnostic measures at pharmacies or other decentralized institutions, enabling easier access to healthcare and diagnostic tests.[100]

An exemplary assay principle that is well-suited for POC antibody testing as no expensive specialized laboratory equipment is required, are lateral flow assays (LFAs) as depicted in Figure 2.15. These are membrane-strip based immunoassays in which the sample is transported without any external influence by capillary force. The sample is applied to an adsorbent sample pad containing buffer ions and surfactants stabilizing the analytes in the sample. It then moves on over the conjugation pad where it takes up the specific detection biomolecules - e.g. for serological SARS-CoV-2 LFAs the respective SARS-CoV-2 protein of interest conjugated to gold nanoparticles or latex microspheres. Additionally, the conjugation pad usually contains positive

control antibodies to check for correct assay procedure. The analyte bound to the detection molecules then migrates on to the detection zone made from a nitrocellulose membrane where a control and analyte line with capture molecules is positioned (e.g. anti-human IgG on the analyte line for serological assays). Here, the nanoparticles bound to analyte are captured and give a visible line that can be read out by eye or using a suitable reader.[101] Generally, also the detection of different analytes in one assay is possible by preparing multiple analyte lines.[102,103] Additionally, a quantitative readout can be generated by preparing several subsequent lines of the same antibody with the number of lines visible after sample addition being proportional to the amount of analyte or by reading out the intensity of the test line and calibrating with a suitable standard.[104,105]
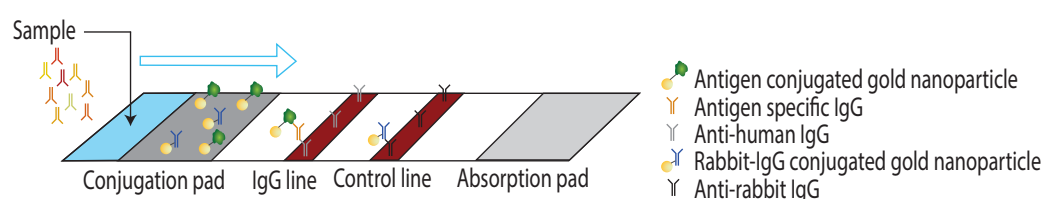

Figure 2.15: Principle of lateral flow assays.

The most critical component of a LFA is the applied membrane. Here, mostly nitrocellulose is used with pore sizes ranging from 0.05 µm to 12 µm. Different pore sizes and their distribution crucially influences the capillary flow time needed for the sample liquid to fill the membrane strip. Another influence factor is the applied detection method. Most LFAs apply gold or latex nanoparticles as mentioned. They make qualitative interpretation by eye easily feasible but have limitations for quantitative readout. Other options are fluorescent, paramagnetic or enzyme labels allowing for a better quantitative evaluation but no longer for manual readout.

In conclusion, LFAs have several advantages against other assay types. They are rapid and easy to perform, as they do not require pipetting or washing steps but only the addition of sample is necessary. Tests are also easy to store and for many sample types, measurements are possible without any sample pre-treatments. Therefore, they are widely applied in many areas and also in the field of SARS-CoV-2 serology, where hundreds of different LFAs have been reported, many of them also being commercially available.[106–108] There are even examples for competitive LFAs allowing for the detection of neutralizing SARS-CoV-2 antibodies.[109] Nevertheless, LFAs also have several drawbacks limiting their application. They normally are not as sensitive as e.g. ELISAs as no enhancement of the response by enzyme reaction is achieved. Depending on the sample matrix, problems like pore blocking might occur and false positive results can result in some matrices.[110]

2.3.1.6 Microarray Immunoassays

Most assay types described so far are widely applied for serological investigations for many different diseases as they allow for the detection of different antibody classes. But most of them lack the possibility of multianalyte detection within a single measurement. Therefore, another available principle for serological tests are microarray immunoassays. They consist of small reactive reagent spots (containing e.g. proteins, but also DNA, aptamers, cells or other recognition elements) immobilized on a solid support either by non-covalent interactions like van der Waals forces or hydrogen bonds or by covalently linking them to the support. Hundreds of spots can be placed onto small supports, allowing for spatially resolved analysis of various analytes in a single measurement. Microarrays have been widely applied for the analysis of microorganisms, small molecules like drugs or toxins or proteins including antibodies.[111] Recently, several examples of microarrays for detection of antibodies to SARS-CoV-2 can be found.[112,113] An exemplary microarray immunoassay for SARS-CoV-2, applying immobilized antigens and reagent flows to enable short assay times, is shown in Figure 2.16. The general procedure on the molecular level is comparable with the ELISA principle but in contrast the reactions are miniaturized and located on reagent spots not whole microtiter plate wells. Many microarray immunoassays apply chemiluminescence for signal generation as it gives rise to very sensitive assays, but also fluorescence is widely used. Within the microarray immunoassays, one can distinguish statically incubated assays from flow-based assays where all assay steps are carried out in continuous or discontinuous flow, leading to reduced interaction time, significantly reducing total measurement times. Additionally, in flow-based microarray immunoassays the sample is lead towards the antigens on the microarray very closely by the sample stream, enabling short diffusion distances between analyte and antigen, again also giving rise to very short analysis times. A drawback is that most flow-based systems do not allow for high throughput.[111]
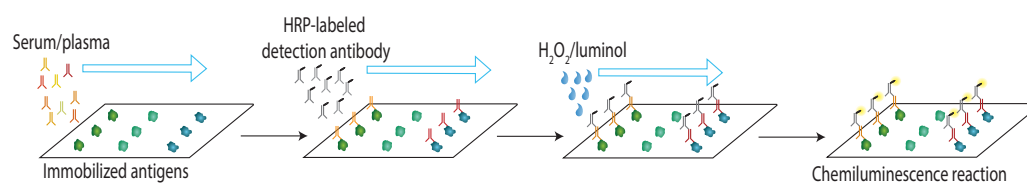

Figure 2.16: Flow-based microarray immunoassay for the detection of specific antibodies.

A crucial factor in microarrays is the selection of a suitable solid support. Relevant factors are the presence of functional groups needed for the immobilization of the capture molecules and the equal distribution of these groups over the surface. Additionally, the surface should optimally not be prone to unspecific binding as to avoid false positive results. In contrast to the desired, highly specific antigen-antibody interaction that is to be measured in a serological assay, also undesired unspecific interactions can occur that are referred to as unspe-

cific binding. In contrast to specific interactions they usually have lower affinity but might be more abundant, therefore blocking interaction sites for specific binding. Reasons for unspecific interactions with the surface can be manifold and can often only be reduced by introducing blocking reagents. These themselves introduce another risk of unspecific binding to them instead of the surface, showing that in the best case a surface would be optimized with respect to unspecific binding so that no blocking is necessary. This has proven especially difficult in serological assays for human diagnostics, as human serum is a very demanding matrix that is prone to unspecific binding due to its high protein content.[114,115] In case of protein immobilization, the surface also has to be capable of stabilizing the protein and preventing it from denaturatio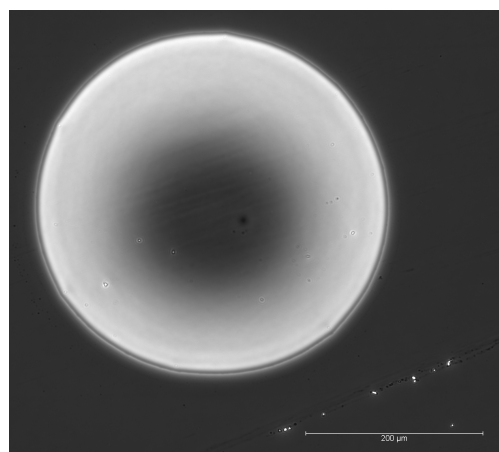n. The main used support material is derivatized glass. An example of derivatization are poly-L-lysine coated glass surfaces, allowing for the non-covalent immobilization of capture molecules and often used in DNA microarrays. Other options include aldehyde-, amine- or epoxy-modified glass surfaces allowing for covalent immobilization.[116,117] Other possible microarray materials are silicon,[118] polystyrene[119] or polycarbonate.[120] Reagents can be deposited on the surface by contact printing or by contact-free printing methods like piezo dispensing.[111,116] An exemplary microscope image of a reagent spot on a glass microarray chip is shown in Figure 2.17, giving an impression of the small spot size.

Figure 2.17: Microscope image of a contact-printed protein spot; scale bar indicates 200 µm.

Microarrays have various advantages over other assay principles as they enable the parallel analysis of up to hundreds of analytes in a single measurement. As was explained beforehand, this is of particular interest for SARS-CoV-2 antibody assays as the virus changes rapidly and serological assays should have the possibility of extension to new variants. Moreover, they should give multidimensional information by not only considering a single antigen but different antigens from the virus. This advantage of microarrays might also be helpful when serological assays are used to detect infections that had not been noticed by the patient or in which no pathogen detection had taken place during the active infection: a microarray can not only carry antigens from one pathogen but several pathogens simultaneously, making it possible to assign the causative pathogen for an infection in the aftermath. Especially with native antigens produced in eukaryotic cell lines being readily available for a multitude of pathogens, the road for innovative microarray immunoassays is well-paved. What is needed now are microarray immunoassays that can easily and rapidly be adjusted to the requirements of the pandemic situation by changing the used antigens as well as adjusting the assay to new

general analysis targets.

One example for such general targets would be the POC application of antibody assays. For this purpose, often LFAs are used due to the rapid availability of results. There are currently barely alternatives available when it comes to rapid measurements without needing specialized laboratory equipment and trained personnel but still, LFAs have severe drawbacks with respect to matrix influence as well as quantitative interpretation of results. Here again, microarray immunoassays are optimal substitutes that make way for new serological POC assays. Especially flow-based microarrays are suited as they allow for very short assay times and can be highly automated by using microarray platforms as will be detailed later. For SARS-CoV-2, antibody measurements at the point of care, e.g. hospital or medical practice are of interest as the rapid assessment of a patients immune status can then be used for important medical decisions like administration of booster vaccines without requiring long waiting times to obtain results from centralized diagnostic laboratories.

These influence factors show the necessity for multiparameter POC serological assays for SARS-CoV-2, an aim that can best be reached by developing innovative microarray immunoassays on a suitable analysis platform. Such analysis platforms for microarray immunoassays as well as other assay techniques will be discussed in Section 2.3.2. But before concentrating on assay platforms, the following section will focus on one more assay principle that is highly relevant in serological testing as it gives an estimate of protection from infection by antibodies, which is often the main information people want to gain from an antibody test.

2.3.1.7 Neutralization Tests

Neutralization tests are highly relevant in serological testing. In comparison to the determination of total IgM or IgG, they only detect those antibodies that can efficiently prevent the infection of cells by neutralization of the virus.

Early representatives of neutralization tests usually relied on the cultivation of cells and their infection with the virus of interest. When cells are infected by a virus, they will be destroyed over time and the virus can progress by infecting neighboring cells. These areas of viral infection and cell destruction are referred to as plaques and can often be recognized by eye or using a microscope, e.g. as clear or turbid spots, sometimes visually even comparable to bacterial colonies, depending on the mechanisms of action of a virus. The formation of these plaques had been used for the detection of viruses already in the 1950s, when *Henderson et al.* reported a method for the determination of arthropod-borne virus plaques by overlaying cell monolayers with agar to make the plaques well visible upon their formation.[121] The technique was later adapted for various viruses, e.g. by *Russell et al.* who reported tests not only for the identification of dengue virus, but also the application of the so-called plaque reduction

neutralization test (PRNT) for the determination of neutralizing antibodies.[122,123] Therefore, different dilutions of a serum containing neutralizing antibodies are incubated with the virus of interest so that antibodies can neutralize the virions and render them unable to infect cells. Then, the virus suspension is added to a suitable cell monolayer, for some assay procedures overlaid with solutions containing agar or methyl cellulose and fetal bovine serum, and subsequently incubated so that plaque formation can occur. After a suitable incubation time, the resulting plaques are counted and compared to the number of plaques in a serum-free assay. The antibody titer is determined as the highest serum dilution without evidence for viral infection or with a defined percentage of plaque reduction.[124,125] If plaques are not well visible by eye or microscope, the use of immunocytochemistry for the detection of infected cells is possible, where virus on infected cells is labeled with a suitable antibody and then detected by e.g. a colorimetric reaction.[124] Alternatively, also the use of imaging cytometry has been proven useful for the detection of virus infected cells rather than plaques in shorter assay times.[126]

The PRNT is still the gold standard for detection of neutralizing antibodies due to its high specificity and reliability. For example, comparison studies of SARS-CoV-2 PRNTs with other antibody assays determining total antibody count showed notable differences in detected titers with results from PRNT being more predictive for the protective force of the antibodies.[125,127] Still, PRNTs also have several drawbacks. Due to the need for prolonged incubation of cells to enable plaque formation they are very time-consuming. Additionally, they are relatively laborious and require specialized laboratories (e.g. biosafety level 3 for viruses like SARS-CoV-2), as active virus is used for the tests. Another drawback is that results depend heavily on the assay conditions, e.g. the used cell line, viral strains, further reagents and results between laboratories may differ, making standardized protocols necessary.[128,129]

To overcome the necessity for biosafety level 3 (BSL 3) facilities, there are neutralization tests available for different diseases that are based on pseudovirus expressing the respective viral antigen of interest on their surface instead of the active virus. Various different types of pseudoviruses have been developed and applied for this purpose like for example hemagglutinin-pseudotype retroviruses based on influenza virus[130] or SARS-CoV-2 pseudovirus neutralization tests using vesicular stomatitis virus[131] or lentivirus.[132]

But these tests are still laborious and time-consuming due to the need for cell culture, so that surrogate assays were developed as an alternative. Early, non-cell-based alternatives were so-called blocking ELISAs. Therefore, usually monoclonal antibodies were expressed that were able to efficiently neutralize the virus of interest. Microtiter plates were coated with either inactivated virus or solely a specific recombinant antigen from the virus and serum samples were incubated to give neutralizing antibodies the chance to bind to the respective antigen. Detection was then done using labeled monoclonal neutralizing antibodies and measuring the inhibition of signal by binding sites occupied with neutralizing antibodies from a serum sam-

ple. Examples of such blocking ELISAs in literature include assays for human diagnostics, e.g. for rabies neutralizing antibodies,[133] as well as for veterinarian purposes, for example for neutralizing antibodies after foot-and-mouth disease vaccination[134] or neutralizing antibodies to porcine circovirus after vaccination.[135] While they are notably faster than PRNTs, these blocking ELISAs still bear the risk that antibodies might be able to bind to the respective antigen with higher affinity than the used monoclonal detection antibody but this blocking of the binding site might still not be strong enough to prevent binding of the virus to a cell and infecting it.

Therefore, another cell-free neutralization assay type has been developed shortly after the beginning of the COVID-19 pandemic: surrogate neutralization assays measuring the actual inhibition of binding between SARS-CoV-2 RBD and human ACE2 protein by neutralizing antibodies. Such assays were reported in classical ELISA format in microtiter plates with either ACE2 or RBD bound to the microtiter plate and the counterpart used as detection reagent with a suitable enzyme label as shown in Figure 2.18.

Another approach aims on not only making assay results available within few hours as in ELISA tests but within few minutes, for example by the application of LFAs for neutralizing antibodies, giving results within 10 minutes.[109] But as explained beforehand, LFAs still present certain disadvantages, making other techniques necessary for rapid neutralization tests. Here again, microarray immunoassays are the perfectly suited tool for the application of surrogate neutralization assays that can be used in POC settings within very short analysis times while being easily adjustable and even paving the way for quantitative interpretation of obtained results. But still, suitable analysis platforms are necessary for any assay type to find widespread application in research or in a commercial context. Therefore, the next chapter will give an
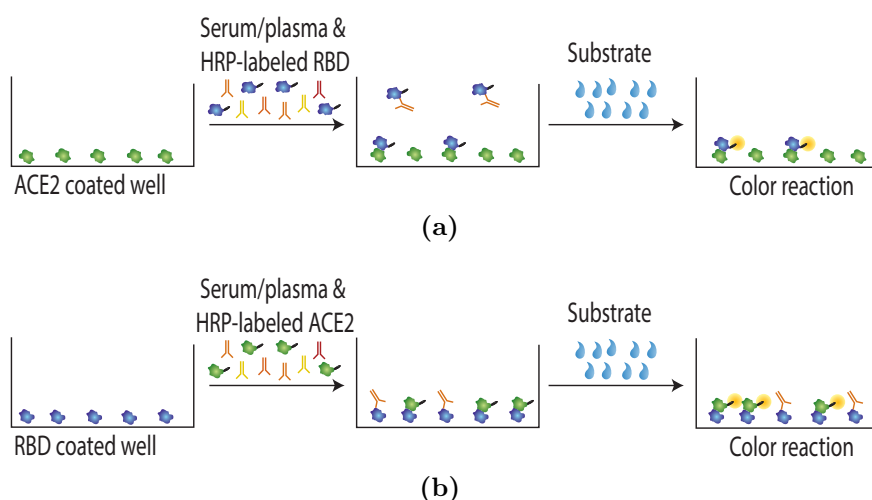

(a)

(b)

Figure 2.18: Different formats for competitive ELISAs for detection of neutralizing SARS-CoV-2 antibodies: (a) Immobilized ACE2; (b) Immobilized RBD.

overview over different analysis platforms used for serological assays, especially with respect to SARS-CoV-2.

2.3.2 Bioanalytical Platforms for SARS-CoV-2 Serology

During the pandemic, enormous development effort was put into the development of SARS-CoV-2 antibody assays either on existing or even on new, specially designed analysis platforms. Some of them will be introduced in the following. It is important to point out that most of the presented serological SARS-CoV-2 platforms were developed in parallel to the results obtained in this dissertation as the laboratory work for the dissertation started shortly after the begin of the pandemic when nearly no antibody tests were yet available. Therefore, this work had to compete with huge international research efforts for novel serodiagnostic tests. To stress the obtained results, it was decided to present some of the immunoassays and platforms developed in parallel by international, well-known research groups. Subsequently, the detailed objectives of this work will be outlined to define the research gap that this dissertation aimed on filling and information on the chemical basis for the applied techniques will be given, followed by the presentation of the obtained results that can be benchmarked against the alternative systems described in the current chapter.

2.3.2.1 ELISA Platforms and Related Systems

Especially in the field of ELISAs and all related immunoassay techniques, a variety of bioanalytical platforms for the detection of SARS-CoV-2 antibodies can be found. Many of them are also widely applied by virological laboratories for high-throughput screenings of patients not only for SARS-CoV-2 but also for many other diseases, as these commercial platforms normally have reagent kits available for different diseases.

Two widespread used ELISAs with CE marking and FDA-EUA-approval for SARS-CoV-2 antibodies were developed by EUROIMMUN AG in early 2020 to be used for the detection of IgA and IgG antibodies. One of them uses recombinantly produced S1 protein in native form and was reported to have 94.4% sensitivity and 99.6% specificity by the manufacturer, while the other one uses a recombinantly manufactured N protein where potentially cross-reactive regions were removed, resulting in 94.6% sensitivity and 99.8% specificity.[136] These assays can be conducted manually, but for high-throughput measurements normally an analysis platform like the EUROLabWorkstation is used, enabling the analysis of up to 15 microtiter plates in one run in a fully automated manner, allowing for more than 200 results per hour.[137] Especially the S1 ELISA was extensively tested by research groups, confirming the good performance with values for sensitivity between 75% - 97.5% and specificity between 90.0% - 100%.[138–140]

While the EUROIMMUN assays are well suited for a diagnostic laboratory, they still have some drawbacks. Apart from the general disadvantages of ELISAs like the relatively long analysis time, they normally only detect antibodies to one antigen at a time. To improve this and enable results for various antigens within single measurements, research groups focused on developing multiplex ELISA systems for SARS-CoV-2 antibodies. *Byrum et al.* reported the open multiplex-ELISA platform multiSero consisting of an ELISA array of printed recombinant antigens (N, S1 and RBD, while generally up to 48 different antigens could be immobilized), a portable Nautilus plate reader (possible to build for less than \$1500) and a modular, python-based evaluation software as shown in Figure 2.19.[141] The analysis platform was shown to enable a good sensitivity of 95% with a specificity of 99%.

This platform therefore combines the microarray principle with well-known ELISA technology, allowing for significantly more results in the same time compared to conventional ELISA. Still, the platform bears the disadvantage of long incubation times on the ELISA plate, giving rise to an assay time of about 4 h, making faster biosensors desirable.[141] Other research groups also reported similar results using the commercial CoViDiag platform by Innobiochips that even allows for the detection of antibodies to five antigens (S1, N, RBD, S2 and the N terminal S1 domain) in an ELISA format.[142]
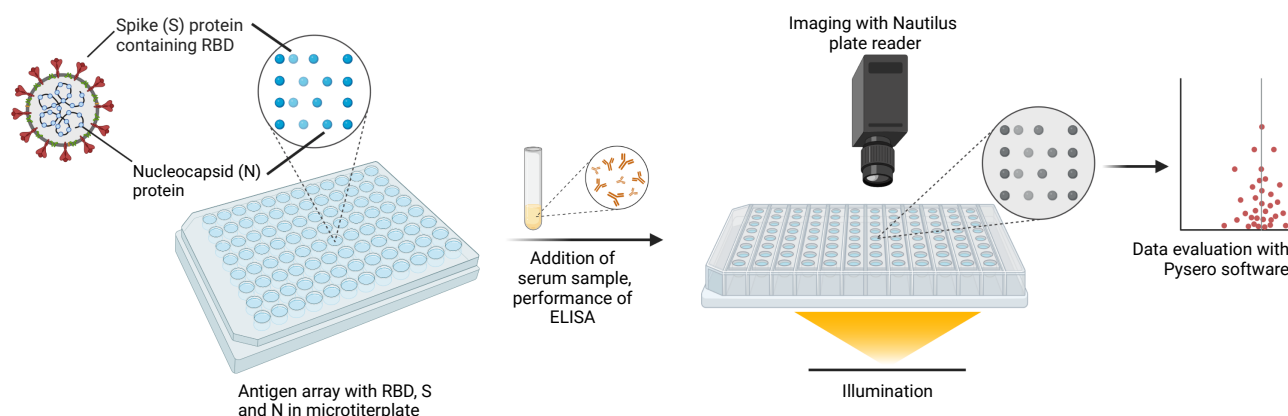

Figure 2.19: Principle and workflow of the multiSero analysis platform.[11,141]

An approach to overcome some of the limitations of ELISA including high costs and portability problems especially for automated systems was the development of a microfluidic on-chip ELISA by *González-González et al.*[143] They used commercially available microfluidic chips and an in-house built automated microfluidic analysis platform that enabled automated antigen coating, blocking, sample transport and detection. To make the assay more affordable, they evaluated the use of a smartphone camera instead of a microplate reader for detection with favorable results.[143] The on-chip ELISA showed good accordance with a classical ELISA and allowed for a cheaper and more portable analysis setup, but still the measurement time could

not be significantly reduced, making most ELISA assays only applicable in fields were results are not required within few minutes.

A novel approach to bring the ELISA technique into POC diagnostics was taken by the company GENSPEED Biotech GmbH, which developed a so-called µ-ELISA that is conducted on a mobile analysis platform.[144] It determines not only antibodies to one antigen but allows for multiplex analysis of three different antigens (RBD, N and S protein). In the future, the test might still be further extendable as enough space for a maximum of eight different antigens is available. In contrast to conventional ELISAs, it can give results within 20 minutes. This short analysis time is made possible by a test chip with a microfluidic channel. A sample is applied to the channel and travels along it due to capillary flow. Within the channel, the three antigens are immobilized and antibodies can bind to them. After the addition of detection antibodies, enzyme labels and chemiluminescence substrates, a photodiode array is used to read out the photons generated by the enzyme reaction.[144] The assay was shown to have very high sensitivity of 100% as well as high specificity of 93%.[145] A drawback in the possible applications of the test principle is that it can only be applied for the analysis of IgG antibodies.

2.3.2.2 Microparticle-based Platforms

Another possibility that is widely used in research but also in commercial tests is the application of micro- or nanoparticles in bioanalytical platforms. This principle bears the advantage of freely moving particles instead of statically immobilized particles. Therefore, particle-based assays enable a better binding of antibodies due to improved accessibility. Additionally, by using magnetic particles often the background influence can be reduced as only the antigen coated beads are evaluated and less unspecific binding occurs on the bead surface compared to the big surface of microtiter plate wells.

An exemplary commercial microparticle-based platform that uses chemiluminescence for detection (CLIA) is offered by YHLO Biotech Co. with the iFlash system. It can be processed fully automated, gives quantitative results with respect to a WHO standard and the biggest available analyzer allows for up to 1200 results per hour with the first result being available after 30 minutes. The test uses magnetic nanoparticles coated with the respective antigen (S or N protein). Detection of either IgG or IgM is then done with NSP-DMAE-NHS acridinium ester labeled secondary antibodies that can emit light by chemiluminescence after triggering.[146] An additional opportunity is the detection of neutralizing antibodies by immobilization of RBD on the magnetic beads and detection with acridinium ester labeled ACE2, for which a sensitivity of > 90% and a specificity of > 98% was stated.[147] Both assay principles are shown in Figure 2.20. Comparison studies for the IgM/IgG assay found sensitivities of 35% (IgM) - 77% (IgG) and specificities of 94% (IgM) - 100% (IgG).[139,146] For the surrogate neutralization test, good accor-

dance was found with other surrogate assays while comparison with a PRNT showed slightly less accordance, proving that surrogate tests might not be able to perfectly mimic processes occurring in cells upon infection.[148,149]

Another example for a commercial microparticle platform used for the analysis of SARS-CoV-2 antibodies - mainly by research groups and not primarily in routine diagnostics - is the Luminex platform that applies xMAP technology. A big advantage of this assay platform is its ability to generate multiplex assays by using spectrally distinct populations of carboxylated paramagnetic beads. Antigens of interest can be covalently immobilized on these beads followed by incubation with a blood sample. Apart from serum samples, also the use of dried blood spots is possible in Luminex assays. The binding of IgG or IgA antibodies can then be detected using fluorescing, R-phycoerythrin-labeled anti-human IgG or IgA antibodies, respectively.[150] While the incubation steps can be done in microtiter plates, a suitable platform has to be used for the assay readout. The analysis is then done by a flow-cytometry-based principle using two lasers of which one characterizes the bead type by its spectral properties while the second one excites the fluorescent label on the detection antibodies, allowing for the quantification of bound analyte. For different Luminex assays for SARS-CoV-2, sensitivities of 75.3% - 88.7%
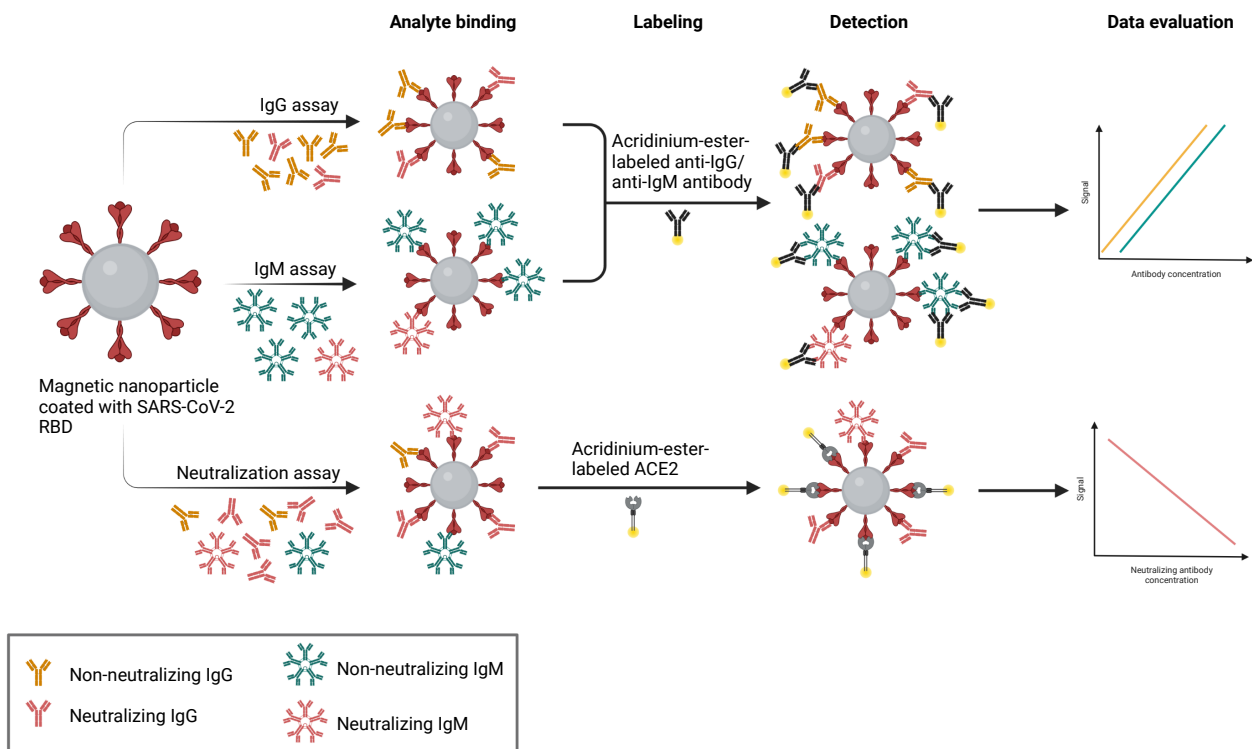

Figure 2.20: YHLO tests for the determination of anti-SARS-CoV-2 IgG, IgM and neutralizing antibodies.[11,146,147]

and specificities of 99% - 100% were reached.[150,151] Generally, Luminex assays are advantageous as they allow for the simultaneous detection of different analytes, enabling the obtainment of more results per time than for classical singleplex formats. Still, relatively long assay times have to be considered as well as the specialized instrumentation necessary for the readout.

2.3.2.3 Electrochemical Sensors

All previously described bioanalytical platforms still present with relatively high assay times and often also high costs are a drawback. Additionally, as mentioned previously it would be desirable to have miniaturized systems that can be applied in POC settings without any specialized laboratory equipment. An example for an assay platform targeting some of these aspects is the SPEEDS platform (Serological testing Platform for rapid ElectrochEmichal Detection of SARS-CoV-2) developed by *Peng et al.*[152] It enables the analysis of serum IgG or IgM against the SARS-CoV-2 RBD within 13 minutes, can be stored for prolonged periods of time and can be batch-fabricated at low cost. The SPEEDS platform consists of an electrochemical immunosensor with three screen-printed electrodes on a PET film that can be connected with a commercial potentiostat for signal readout that then transfers the measurement result to a smartphone as represented in Figure 2.21 (a). In the preparation of the immunosensor, RBD is immobilized on the working electrode via streptavidin-biotin binding. Antibodies from a sample are then captured on the RBD and subsequently labeled with an alkaline-phosphatase-labeled detection antibody specific for the respective antibody class, IgM or IgG. For detection, p-aminophenyl phosphate is added and degraded to benzoquinone in a reaction catalyzed by alkaline phosphatase as shown in Figure 2.21 (b). The resulting chronoamperometric current is proportional to the amount of bound antibody and can be measured with the potentiostat. The sensor system was calibrated with monoclonal anti-SARS-CoV-2 IgG and IgM, resulting in measurement ranges from 10 ng mL^{-1} - 60 µg mL^{-1} and 1.6 ng mL^{-1} - 50 µg mL^{-1}, respectively, which is in the expected range for serum antibody content and additionally is a very wide measurement range. Measurements of patient samples were very promising, although only a relatively low number of 30 samples was tested. This makes the SPEEDS assay a good option in POC settings, where fast results for single samples are required.[152]

Another electrochemical sensor was developed by *Yakoh et al.* by using a label-free paper-based bioanalytical platform called COVID-19 ePAD.[153] This approach overcomes the need for labeled antibodies or other detection reagents that are necessary in most serological assays. Label-free assays are desirable to avoid costs, unspecific binding and preparation time as well as to reduce measurement duration. As in the SPEEDS platform, three electrodes (working electrode, counter electrode and reference electrode) are printed onto a substrate by screen printing. As substrate, a paper strip with defined hydrophilic reaction zones is used
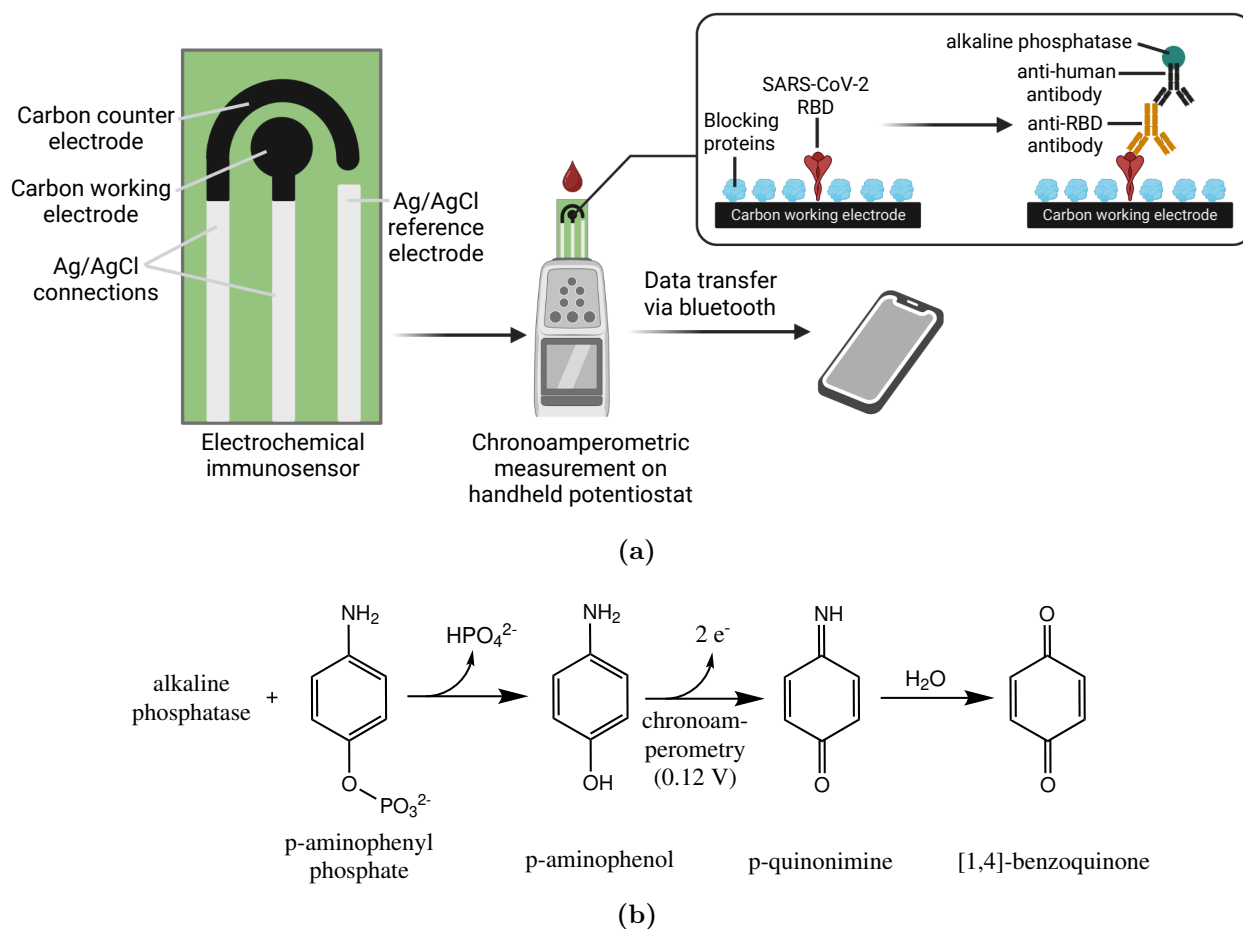
(a)

(b)

Figure 2.21: (a) Components and assay principle of the SPEEDS platform; (b) Alkaline phosphatase catalyzed electron generation. [11,152]

that can subsequently be folded to give stacked layers of electrodes and reaction space. The SARS-CoV-2 RBD is covalently immobilized on the bottom layer of the sensor, followed by blocking. In the measurement, a serum sample is added to the bottom layer and incubated. After a washing step, the ePAD is folded and the redox indicator $[Fe(CN)_6^{3-/4-}]$ is added on top. The electrochemical response is detected by squarewave voltammetry, a technique giving rise to very low background currents and therefore very low detection limits. Binding of antibodies to the immobilized RBD leads to the formation of rigid antigen-antibody complexes on the electrode and therefore to disruption of the redox conversion in the redox indicator as it forbids the charge transfer of the redox probe. This can be recorded as a decreased current response in comparison to a reference measurement without antibodies. The test is supposed to give qualitative results within 30 minutes and was evaluated with 17 patient sera, where a better detection limit compared to a LFA could be found and all but one sample were classified correctly. [153] The COVID-19 ePAD is relatively cheap to produce and is one of few label

free systems available. Nevertheless, further evaluation with additional sera has to be done to evaluate the test performance.

2.3.2.4 Surface Plasmon Resonance Sensors

A technique that had previously been mentioned as useful for the measurement of antibody affinities but that can also be applied for the detection of antibodies is surface plasmon resonance (SPR). It is an optical principle that stands out due to its ability to detect minimum changes in refractive index upon binding of biomolecules. SPR sensors usually contain coin metals, mostly gold, and a monochromatic p-polarized light source. This light source is used to excite plasmons at the interface between metal and biomolecules like SARS-CoV-2 proteins immobilized on a polymer layer. Depending on the binding of antibodies to the proteins on the gold surface, the resonance wavelength of the plasmons shifts and therefore the refractive index changes. *Basso et al.* presented a SPR sensor for the detection of antibodies to N and S protein of SARS-CoV-2.[154] The respective protein was immobilized on a gold surface via self-assembled monolayers of alkanethiols, a serum sample was added and response units were measured after removing unbound proteins with phosphate buffered saline (PBS). The respective changes in refractive index are represented in Figure 2.22. With this principle, a change in refractive index was found for positive samples, while in negative samples the response before and after serum addition and washing was the same. The SPR assay can be done within under 10 minutes and SPR chips can be used for up to 10 subsequent measurements by regeneration with glycine HCl solution at pH 3.[154] Therefore, the SPR sensor is a time efficient and sensitive, label-free method for the detection of SARS-CoV-2 antibodies when the necessary equipment is available.
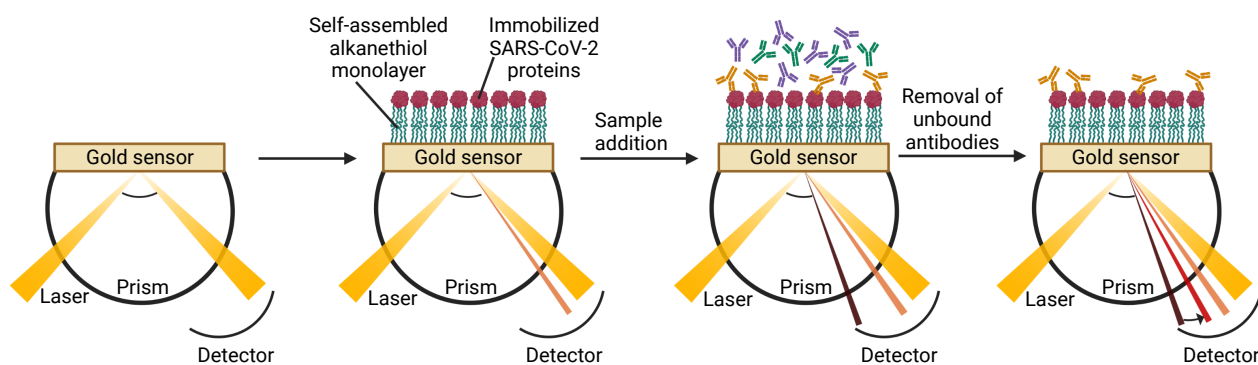

Figure 2.22: Changes in refractive index after antigen immobilisation, serum addition and washing of SPR sensor surface.[11,154]

To stress the possible applications of SPR sensors even more, *Djaileb et al.* presented a SPR assay on a portable instrument that gave quantitative results for antibodies to the N protein within 15 minutes. This sensing platform could be used for rapid, on-site measurements in

POC settings.[155] Nevertheless, SPR sensors are only suitable for evaluating one single antigen within a measurement, which represents a drawback of the method.

2.3.2.5 Microarray Platforms

While many of the previously described bioanalytical platforms had several advantages over other techniques, they often only allow for the detection of antibodies to a single protein within one measurement. Especially with the upcoming variants of SARS-CoV-2, there is an increased need for multiplex assays. Additionally, they can also be useful for the distinction of antibodies from infection and vaccination, as vaccination can only induce antibodies to one antigen in contrast to infection. An optimal technique for multiplex measurements are microarrays as described in the previous chapter, where different general assay principles were explained. They only require low amounts of antigen for the production of small spots and allow for the spatially resolved evaluation of the results. While they are often applied simply for the detection of antibodies, they can give even more information. For the conduction of microarrays, several analytical platforms have been reported in literature.

An example is a bioanalytical microarray platform for SARS-CoV-2 epitope mapping reported by *Musicò et al.*[156] They used linear epitopes from SARS-CoV-2 proteins on a silicon-based microarray platform that allows for the oriented immobilization of peptides and reported the screening of patient samples for epitopes with extended antibody binding and suspected higher immunogenicity. In preparation of the microarrays, silicon slides are coated with the polymer MCP6 and subsequently spotted with the peptides using a non-contact spotter. Subsequently, serum samples are incubated, followed by incubation of a fluorescence-labeled secondary antibody for the detection of IgG or IgM antibodies with subsequent excitation and readout of fluorescence intensity. With this principle, notable variations in the immune reaction of different patients were found, but still immunodominant regions on SARS-CoV-2 proteins could be identified that might be helpful in the development of other serological tests.[156] Other research groups also reported microarrays for epitope mapping, e.g. by immobilizing 1968 spots on glass microscope slides[157] or by applying non-porous nitrocellulose films for the microarray production.[158] This principle of epitope mapping is promising to detect the main immunogenic regions on a protein of interest, but one still has to consider that the three-dimensional structure of peptides might significantly differ from that within the whole protein so that the informative value of epitope analysis in microarrays might be limited. Additionally, most of the respective mircoarrays exhibit relatively long assay durations of several hours.

Nevertheless, microarrays are very useful when whole proteins are immobilized. *Hedde et al.* presented a microarray analysis platform that can be applied widely due to its low price of \$200 and the option of easily 3D printing it.[112] The platform is optimized for the use in

areas with weak infrastructure and it can generate results from few drops of blood from a finger prick within 2 - 4 hours. This so-called CoVAM test[159] on the TinyArray imager[112] uses 67 antigens from ten different respiratory viruses as to not only evaluate the immune response to SARS-CoV-2 but also to other possibly relevant pathogens. The TinyArray imager consists of a camera module with different pass filters suitable for the recording of fluorescence from an microarray. Fluorescence excitation is done with LEDs and microarray chips consist of a nitrocellulose-coated microarray surface on which antigens are deposited. Anti-IgG and -IgA antibodies conjugated to quantum dot fluorophores are used for detection. This microarray platform proved to be well applicable for the determination of SARS-CoV-2 antibodies with a sensitivity of 92.9% and a specificity of 97.7%.[159] It can easily be adapted to further pathogens and might be well applicable in low-budget settings, but the relatively long assay duration might still be limiting its application.

Another promising microarray platform is the Microarray Chip Reader system that was used in the course of this dissertation. The newest device generation is represented in Figure 2.23.

Figure 2.23: Newest device generation of the bioanalytical platform MCR, the MCR-R.

It is a fully automated microarray platform that can be programmed in a modular manner due to its optimized tubing system. It can be applied for various formats of microarray immunoassays but is specialized for the application in flow-based chemiluminescence microarray immunoassays (CL-MIAs). The centerpiece of this platform is the flow cell unit with a CCD camera for the detection of chemiluminescence on a microarray chip. The development of the MCR family dates back to 1999 when *Weller et al.* presented the first prototype of a multiplex chemiluminescence immunosensor called PASA (parallel affinity sensor array).[160] First applications focused on environmental contaminants like trinitrotoluene or atrazine, while during the later development stages a variety of different analytes were considered while continuously expanding the analysis platform. A second generation was presented in 2004, the Immunomat used for the detection of antibiotics in milk.[161] This platform showed a higher degree of automation than the previous generation and was also used for the immunoassay-based detection of bacteria.[162] Further improvements were necessary to broaden the application spectrum, therefore a novel, three-layer chip design was developed to enable high flow rates as required for rapid microarray immunoassays. These optimized chips were applied in the third generation analysis device MCR 3 that was also used during the dissertation at hand. Its design was suitable to be used as automated, portable stand-alone equipment with sufficient reagent

storage to conduct a measurement day by only inserting microarray chips and samples.[111] This platform was used for the detection of bacteria,[163] viruses[164] or small molecules,[165] but also antibodies in pig sera.[166] During the course of this dissertation, the first ever application of the MCR 3 for human serodiagnostics was tested, followed by application of the subsequent device generation MCR-R shown in Figure 2.23. The next section will outline the detailed objectives during this development process and the chemical background of the used microarray chips.

3 Objectives of This Work

At the beginning of this dissertation in early 2020, very little was known about SARS-CoV-2, how it would evolve over the following years and how the human immune system would react to an infection or if immunization by vaccination was possible at all. But it was apparent already back then that powerful analytical platforms would be necessary to learn more about the virus and its impact. A main focus were different methods for direct detection of an infection, but on the long run it appeared even more important to research the reaction of the human body to SARS-CoV-2. For this purpose, antibody tests were considered highly relevant as they could give information on previous infections, the current state of protection and generally are a good indicator of the immune status for a pathogen.

Research groups as well as the diagnostic industry all over the world rapidly focused on developing suitable antibody tests for different purposes: some of the early developed tests were focused on the application in routine laboratories with several hundreds of conducted tests per day while others tried to enter the POC market by developing so-called rapid antibody tests that could be conducted in short time without needing a diagnostic laboratory. What the vast majority of these tests had in common was that they were relatively unflexible. Especially those tests developed for research purposes in smaller research groups without decades of experience in antibody test development were unwieldy when it came to adapting them to the rapid changes during the dynamic pandemic situation. Changes required time-extensive optimization studies, recombinant antigens were not available from the commercial producers as fast as necessary due to the high demand.

With this insight, the research gap and objective of this dissertation were to focus on the development of flexible, rapid SARS-CoV-2 multiparameter antibody tests that could be adjusted to whatever needs the pandemic might bring with it. The Institute of Water Chemistry (IWC) had been developing and optimizing an analysis platform over the past 20 years, resulting in a well-applicable platform for research purposes, the MCR. But so far the MCR devices had only been applied in research fields where alternative, "gold standard" methods had already been available and could be used as a benchmark for new assays. Additionally, the platform had been applied in environmental and water chemistry but not for human serological diagnostics which is known to be a technically very challenging field. Therefore, the pandemic was the perfect opportunity to put assay development on the MCR to a new level by requiring rapid promising results to be able to keep up with other research groups that had significantly more

experience, manpower and resources for the assay development available.

Hence, the availability of a MCR 3 device was one of the cornerstones necessary for this work. Furthermore, native, recombinant antigens from eukaryotic cell lines were available from ISAR Bioscience GmbH, a cooperating local company, making the research results independent of the commonly occurring supply difficulties for SARS-CoV-2 antigens from international suppliers. This also brought the advantage of being able to use high-quality antigens that were similar to how the respective proteins occurred in the human body, while some other researchers as well as commercial producers had to rely on less suitable cell lines for protein expression.

It was decided to focus on flow-based CL-MIAs as the general knowledge on their development was present at the IWC and as they were perfectly suited for the aim of the work. This technique allowed for multiplex assays that can easily be expanded with further immobilized proteins that might become relevant as soon as the virus would start to mutate. Additionally, even in the beginning antibodies to several different proteins of SARS-CoV-2 were of interest, making assays necessary that could detect them simultaneously. With this multiplex principle, not only more reliable results could be obtained but also different research questions could be approached. The flow-based principle enabled short analysis times which would be the biggest advantage over most of the concurring systems that would usually take several hours until first results were available.

On the basis of these foundations and with the big advantages of the microarray principle on the MCR in sight, first steps could be made towards the development of novel, flexible antibody assays. While the results will be described in the next chapter, some basic principles for the microarray chip production that had already been investigated in the previous years and that have to be understood to fully comprehend the development process and presented assays, will be detailed here.

For the detection of SARS-CoV-2 antibodies on the MCR platform, different microarray chip materials were investigated in the course of this dissertation, including modified glass, polycarbonate (PC) plates and PC foils. The first two had previously been used for different applications,[117,120] but this dissertation aimed on further expanding the range of microarray chip materials by using thinner PC foils as will be elucidated in the results section. The chemical details behind the used modified surfaces will shortly be explained in the following to give an impression of the molecular basis behind the microarray chips.

To prepare glass chips, commercial microscopy slides are used, treated with acid to obtain hydroxy groups on the surface and subsequently silanized with (3-glycidyloxypropyl)trimethoxysilane (GOPTS) to obtain reactive epoxy functionalities on the surface as can be seen in Figure 3.1. These can then react with the polyetheramine Jeffamine® ED 2003 at elevated temperature, resulting in a polymer-monolayer on the surface that exhibits terminal amine groups available for the covalent immobilization of antigens. The polymer-layer is helpful to avoid

unspecific binding by shielding the surface from the assay reagents. Additionally, it allows for higher antigen density by acting as mobile brushes helping to avoid sterical hindrance between immobilized antigens.
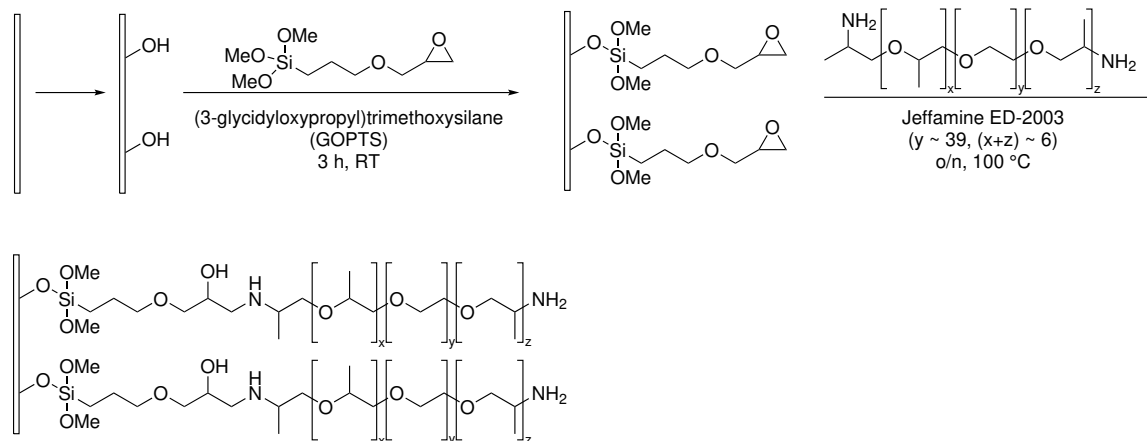

Figure 3.1: Reaction scheme for the surface modification of microscopy glass slides with Jeffamine® ED 2003.

Figure 3.2 shows different options for the immobilization of proteins: for diepoxy PEG immobilization (Figure 3.2 (A)), an epoxide functionality is coupled to the chip surface together with a PEG spacer. The reactive epoxide groups then readily react with amine groups on added proteins, giving *beta*-hydroxy amines. Alternatively, DSC activation can be used (Figure 3.2 (B)). Here, the amine groups are activated using active ester coupling strategy. They form carbamates with *N,N'*-disuccinimidyl carbonate (DSC), resulting in urea derivatives after reaction with amine groups from the respective proteins to be immobilized. As a third option, EDC/s-NHS activation is applicable (Figure 3.2 (C)). In this immobilization strategy, not the chip surface but carboxy groups on the antigen are activated by forming an active ester with 1-ethyl-3-(3-dimethylaminopropyl)carbodiimide (EDC) followed by substitution with *N*-hydroxysulfosucciniminide (s-NHS) to form an even better leaving group. After a nucleophilic attack from the amine group on the surface of a microarray chip, an amide bond is obtained between chip surface and immobilized protein.

The production of glass microarray chips is time-consuming and requires significant amounts of harmful chemicals like acids and organic solvents. Therefore, a faster and more environmentally friendly alternative was developed by using polymer-coated PC microarray chips. To obtain them, Jeffamine® ED 2003 is carboxy-modified using succinic anhydride as shown in Figure 3.3. Subsequently, the PC surface is coated with the modified Jeffamine by screen printing. Then again the EDC/s-NHS strategy can be used for the immobilization of proteins. The terminal carboxy groups on the surface are activated as explained beforehand and amide bonds are formed with amine groups from the respective antigens as shown in Figure 3.4. This
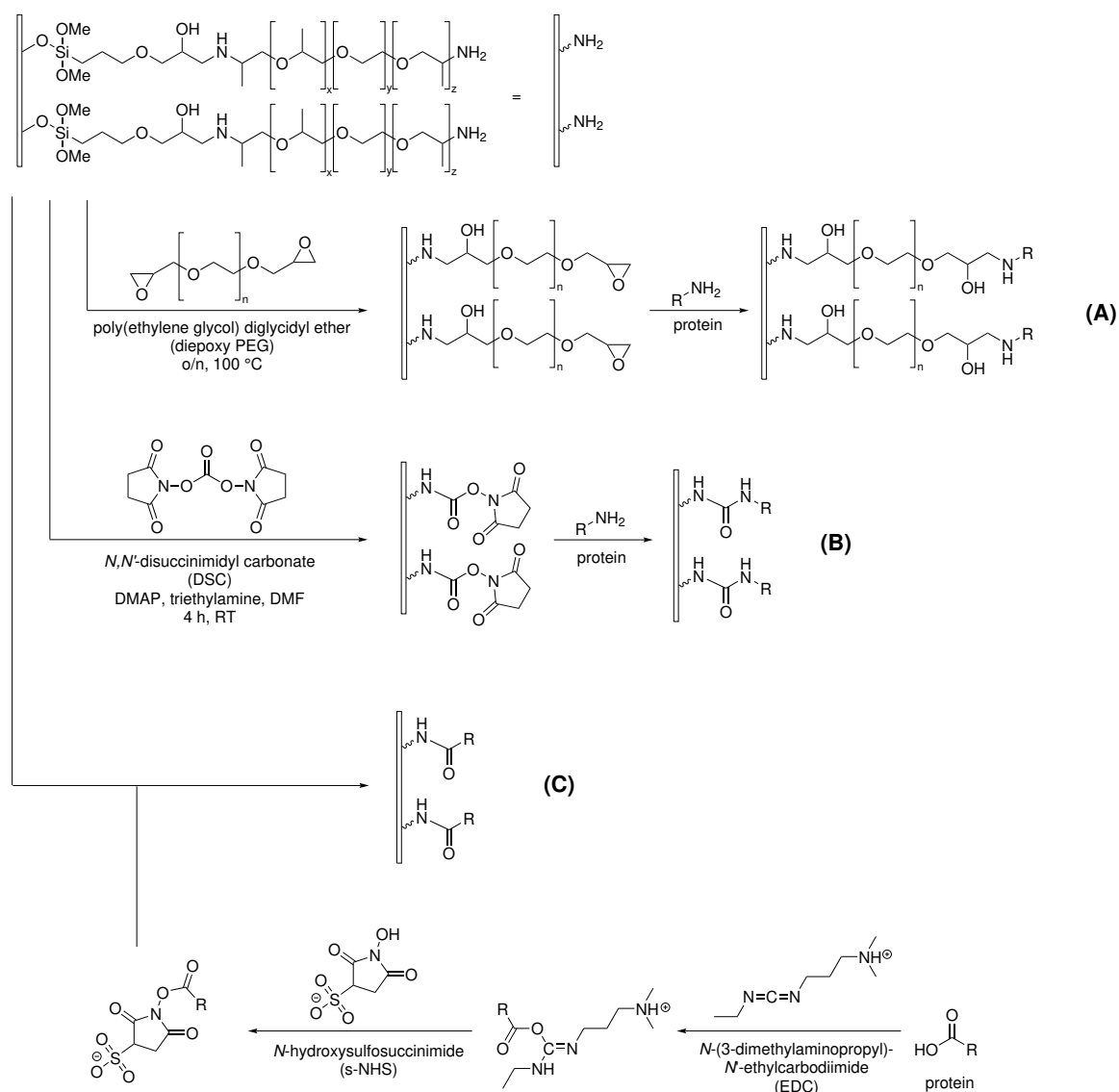
Figure 3.2: Reaction schemes for different covalent immobilization strategies for proteins on glass microarray chips: (A) Diepoxy PEG, (B) DSC, (C) EDC/S-NHS.

production process is significantly faster than the production of glass chips, but the PC chips are less researched than the glass chips that have been applied for over a decade already.
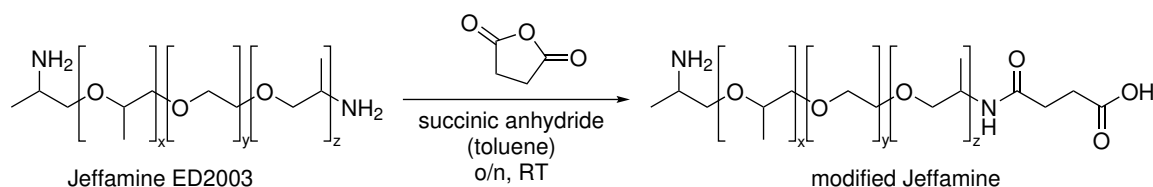

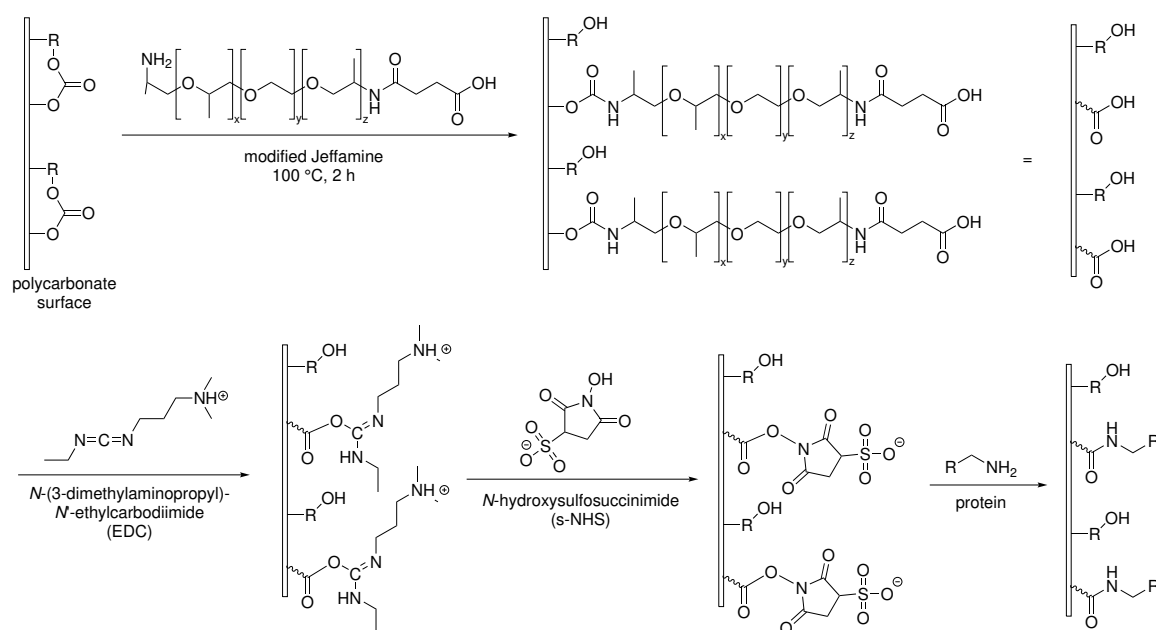**Figure 3.3:** Reaction scheme for the carboxy modification of Jeffamine® ED 2003.

Figure 3.4: Reaction scheme for the immobilization of antigens on the PC microarray chip surface.

This general principle of preparing microarray chips is another huge asset of the measurement principle applied in this dissertation. In contrast to many other assay systems that rely on adsorption and electrostatic interactions for the immobilization of antigens, microarrays on the MCR apply covalent binding to enable a more stable bond between antigen and surface and preventing the loss of antigen while at the same time exhibiting a surface optimized for minimal unspecific binding.

Therefore, the optimal pre-conditions were available to generate urgently needed antibody tests for flexible applications that could answer research questions as well as medical diagnostic questions within significantly shorter assay times than those promised by commonly used techniques.

Nevertheless, despite these good premises, several challenges had to be faced within this dissertation. Due to the rapidly evolving pandemic, results had to be gained within short timeframes to contribute to the knowledge gain without being overtaken by other researchers developing alternative assays in shorter times. This was especially challenging, as main parts of the experimental design, experiment conduction and data evaluation and interpretation for this dissertation were done by one person while other research groups and especially diagnostic companies had significantly bigger teams at hand working on the development of assays. Furthermore, it was unknown whether the MCR 3 or the newer generation, MCR-R, were at all suitable for the analysis of human blood samples as this had never been tested before. Hence, the chip chemistry as explained beforehand had to be investigated in detail to be able to con-

duct all necessary optimizations to enable measurements in blood without obtaining undesired unspecific binding. Therefore, control samples that had been classified by alternative tests would have to be acquired to benchmark all developments against other reliable tests.

Even after facing these fundamental challenges, the outcome of the PhD project was still unclear. It had to be investigated whether antibodies could be detected with sufficient sensitivity and specificity to be competitive with alternative assays, and it was unclear whether results could possibly be interpreted in a quantitative manner. Moreover, it became apparent early in the pandemic, that analysis of different antibody classes as well as of neutralizing antibodies might become increasingly important while the spread of the virus progressed. Therefore, many additional challenges were to be expected during the work, again stressing the need for a flexible analysis system that could face all these upcoming challenges within the short times that were required by the dramatic worldwide pandemic situation.

The previous chapter already showed some of the assays that were developed in parallel to this work to point out the immense research efforts that were taken up to fight the pandemic in all possible ways. But it should also have become clear that all developed assays had their specific drawbacks and that none of these examples could fulfill the requirements of being highly specific and sensitive, optimally also quantitative while being easily and rapidly adjustable to all situative changes, being easy to use and giving results within few minutes while answering research and diagnostic questions that might come up over the course of the pandemic.

Therefore, the challenges and expectations at the beginning of this dissertation were huge and it was not possible to anticipate where the path might lead. The following chapter will now present how these challenges could be solved and where the path over three pandemic years led by presenting the results obtained in the quest for the development of rapid automated CL microarray immunoassays for SARS-CoV-2 serological assessments.

4 Results

4.1 Publication 1: Automated, flow-based chemiluminescence microarray immunoassay for the rapid multiplex detection of IgG antibodies to SARS-CoV-2 in human serum and plasma (CoVRapid CL-MIA)

CoVRapid - Rapid detection of SARS-CoV-2 antibodies by flow-based microarray immunoassay
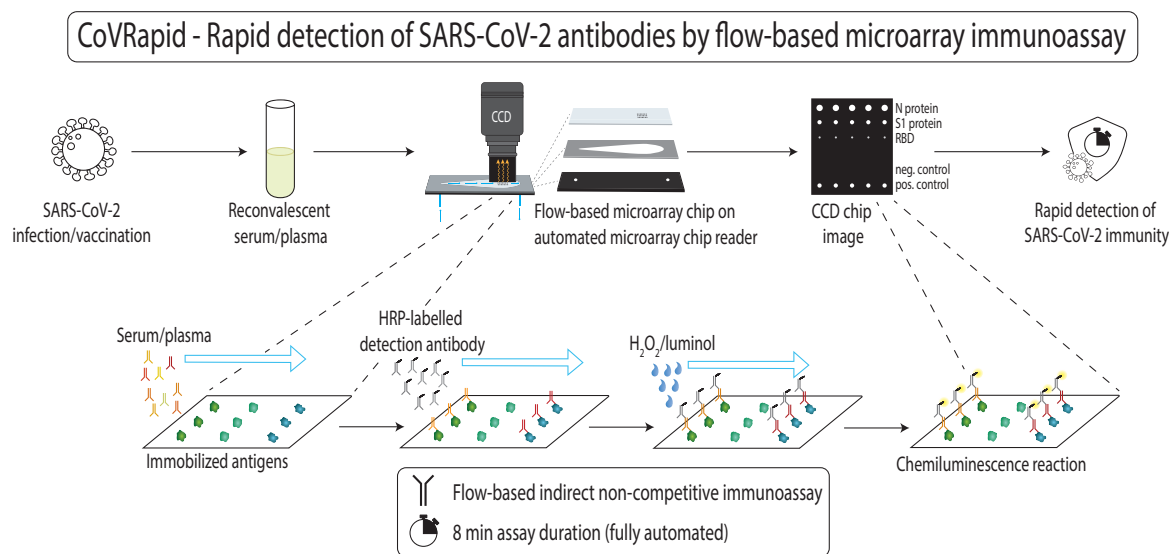
4.1.1 Publication Summary and Author Contributions

In this publication, the first example of a chemiluminescene microarray immunoassay (CL-MIA) for the detection of IgG antibodies in human blood on the analysis platform MCR 3 was presented. For the measurements, amino modified glass chips were used, allowing for the covalent immobilization of antigens on the chip surface. It enabled the simultaneous detection of antibodies to the SARS-CoV-2 RBD, S1 and N protein within eight minutes. Therefore, the so-called CoVRapid CL-MIA was significantly faster than commonly applied ELISA tests while

giving additional multiplex information due to its microarray format. In the beginning of the assay development process, different surface activation strategies were tested for their suitability in the immobilization of SARS-CoV-2 antigens. After determining the optimal immobilization method, which was active ester coupling using DSC, the concentrations of immobilized antigens as well as secondary detection antibody were optimized. With these optimized conditions, a linear correlation between positive sample ratio and the measured CL signal could be obtained, showing that semi-quantitative measurements of IgG antibodies were possible. To further evaluate the test capability for qualitative evaluations, 65 patient samples were classified with the CoVRapid CL-MIA after definition of cut-off values using ROC curve analysis as well as with two commercial SARS-CoV-2 antibody tests. In consequence, the CoVRapid CL-MIA was shown to be the most sensitive and specific of the compared tests with both 100% sensitivity and specificity. Therefore, a high performing test could be developed within a very short development timeframe to keep up with the pandemic development although no previous experience with human serodiagnostics on the used analysis platform MCR 3 had been available at the IWC.

Own contribution:

- Design of experiments

- Development of measurement program on MCR 3

- Conduction of measurements with support from R. Koros (B. Sc. student supervised by J. Klüpfel)

- Data analysis

- Writing of manuscript

RESEARCH PAPER

Automated, flow-based chemiluminescence microarray immunoassay for the rapid multiplex detection of IgG antibodies to SARS-CoV-2 in human serum and plasma (CoVRapid CL-MIA)

Julia Klüpfel[1] · Rosa Carolina Koros[1] · Kerstin Dehne[2] · Martin Ungerer[2] · Silvia Würstle[1] · Josef Mautner[3,4] · Martin Feuerherd[4] · Ulrike Protzer[4,5] · Oliver Hayden[6] · Martin Elsner[1] · Michael Seidel[1]

Abstract
In the face of the COVID-19 pandemic, the need for rapid serological tests that allow multiplexing emerged, as antibody seropositivity can instruct about individual immunity after an infection with SARS-CoV-2 or after vaccination. As many commercial antibody tests are either time-consuming or tend to produce false negative or false positive results when only one antigen is considered, we developed an automated, flow-based chemiluminescence microarray immunoassay (CL-MIA) that allows for the detection of IgG antibodies to SARS-CoV-2 receptor-binding domain (RBD), spike protein (S1 fragment), and nucleocapsid protein (N) in human serum and plasma in less than 8 min. The CoVRapid CL-MIA was tested with a set of 65 SARS-CoV-2 serology positive or negative samples, resulting in 100% diagnostic specificity and 100% diagnostic sensitivity, thus even outcompeting commercial tests run on the same sample set. Additionally, the prospect of future quantitative assessments (i.e., quantifying the level of antibodies) was demonstrated. Due to the fully automated process, the test can easily be operated in hospitals, medical practices, or vaccination centers, offering a valuable tool for COVID-19 serosurveillance.

✉ Michael Seidel
michael.seidel@mytum.de

1 Institute of Hydrochemistry, Chair of Analytical Chemistry and Water Chemistry, Technical University of Munich, Elisabeth-Winterhalter-Weg 6, 81377 Munich, Germany

2 ISAR Bioscience GmbH, Semmelweisstr. 5, 82152 Planegg, Germany

3 Helmholtz Zentrum München, German Research Center for Environmental Health, Haematologikum, Research Unit Gene Vectors and Technical University of Munich, Children's Hospital, Marchioninistraße 25, 81377 Munich, Germany

4 Institute of Virology, Technical University of Munich / Helmholtz Zentrum München, Trogerstr. 30, 81675 Munich, Germany

5 German Center for Infection Research (DZIF), Munich partner site, 81675 Munich, Germany

6 Heinz-Nixdorf-Chair for Biomedical Electronics, Technical University of Munich, TranslaTUM, Einsteinstr. 25, 81675 Munich, Germany

Introduction

The global COVID-19 pandemic has kept the world in suspense for about a year now. The first cases of the novel coronavirus infection were reported in Wuhan, China, in December 2019 and assigned to the respective pathogen in January 2020 [1]. Since then, worldwide more than 90,000,000 people were infected with over 1,900,000 deaths resulting from COVID-19 (as of January 2021) [2].

The causative agent, SARS-CoV-2, is a betacoronavirus that is related to other zoonotic coronaviruses that circulate worldwide, causing common colds. SARS-CoV-2 has a large RNA genome, encoding for a number of structural proteins, namely the spike glycoprotein (S), the nucleocapsid protein (N), the membrane glycoprotein (M), and the envelope protein (E). Posttranslational modifications are essential for most of the proteins like the glycosylated membrane proteins and the phosphorylated N protein, which binds to viral genomic RNA [3]. In the course of a SARS-CoV-2 infection, the body reacts with the production of antibodies to a variety of these proteins,

⬡ Springer

starting with IgM antibodies followed by the longer lasting IgG antibodies that can be found in the blood for several months after an infection. A very relevant factor in the body's battle against the infection—and also for later immunity—is antibodies to the S protein, especially the receptor-binding domain (RBD) located in the S1 fragment. This domain binds to the human angiotensin-converting enzyme 2 (ACE2) and subsequently leads to the entry of the virus into the cell [4]. To assess whether an individual already underwent a SARS-CoV-2 infection and, hence, might be immune to reinfection due to protective antibodies, antibody tests are a helpful tool.

But these tests are not only relevant in context of previous infections. Since the emergence of SARS-CoV-2, a number of potential vaccine candidates have been developed [4] with the first ones already being applied [5]. Here, antibody tests might be helpful in testing the efficiency and the duration of immunity after vaccination. In addition, announcements have already been made (for example, by airlines) that access to certain locations and activities might be coupled to a proof of SARS-CoV-2 immunity. Here, rapid on-site antibody tests will be beneficial.

Therefore, we developed a chemiluminescence microarray immunoassay (CL-MIA) chip for the rapid, flow-based analysis of IgG antibodies to three different SARS-CoV-2 antigens—RBD, S1, and the N protein—in human serum and plasma in a fully automated analysis device, the Microarray Chip Reader 3. This device has previously been used for different tests, ranging from the quantification of bacteria by on-chip isothermal DNA amplification [6] over the detection of antibodies to viruses in pig blood [7] to the quantitative detection of antibiotic residues in milk [8] but here we present the first diagnostic application in human blood, the CoVRapid CL-MIA.

The test principle is an indirect non-competitive immunoassay that is carried out on microarray glass chips containing up to 100 covalently bound reagent spots per flow cell. The mode of operation is shown in Fig. 1 in comparison to other immunoassay techniques frequently applied for SARS-CoV-2 antibody detection. The flow-based principle of the CoVRapid test (Fig. 1a) allows for very short assay times below 10 min and is therefore even faster than many of the so-called rapid tests, which usually are lateral flow tests (Fig. 1c), and give qualitative results within 5 to 20 min [9]. These tests additionally have the disadvantage that they are sensitive to matrix effects resulting in relatively low sensitivity and the possibility of false positive results, which is undesired in the context of antibody testing [10]. Another relevant factor is the use of adsorbed, denatured antigens for most lateral flow assays that lack the three-dimensional structure that is relevant for the binding of neutralizing antibodies. In the CoVRapid CL-MIA, this crucial point can be accounted for, since the test uses native antigens from mammalian expression systems, containing all structural features and posttranslational

modifications that are also present in antigens in infected human cells. A very specific kind of tests that is often used when quantitative high-throughput analysis is desired is ELISA tests (Fig. 1b). Here, antigen (often denatured) is adsorbed to wells and sample as well as labelled antibody and substrate are incubated within the wells. Therefore, many manual steps are necessary that might give rise to errors and prevent in-field applications, as extensive and expensive laboratory equipment is necessary. Additionally, since equilibrium conditions must be established, incubation times of usually several hours are needed prior to readout. Finally, only antibodies to one single antigen can be detected, meaning that false negative results would be obtained if patients formed antibodies to a different antigen that is not tested for [11]. This problem is overcome by microarrays that allow for multiplex analysis of various antigens, usually within hours [12]. Table 1 shows a comparative overview over different commercial SARS-CoV-2 antibody tests with respect to assay principle, assay time, tested antigens, and test performance. As is obvious from the information in Table 1, our CoVRapid test compares favorably and presents novelty in terms of work expenditure, multiplex capability, and assay time. Analysis is accomplished in a fully automated manner within 8 min giving information about antibodies to three different SARS-CoV-2 antigens simultaneously. The respective antigens are covalently immobilized in their native state using established coupling chemistry that can easily be applied to other proteins. This enables the expansion of the test to other antigens within a short development timeframe. The surface chemistry of the test, finally, also allows for negligible matrix influence, allowing even the analysis of hemolytic samples. With all these benefits and its high diagnostic sensitivity and specificity, the CoVRapid CL-MIA can be a valuable tool in COVID-19 serosurveillance.

Experimental

Chemicals, reagents and materials

All chemicals, unless stated otherwise, were purchased from Sigma-Aldrich, subsidiary of Merck (Darmstadt, Germany) and Carl Roth (Karlsruhe, Germany). Chemiluminescence reagents were used from the Elistar Supernova reagent kit from Cyanagen (Bologna, Italy). A peroxidase-labelled anti-human IgG antibody (Fc fragment) from goat was purchased from Sigma-Aldrich (A0170, 5.6 mg mL^{-1}).

For the preparation of spotting, blocking, and running buffers, phosphate-buffered saline (PBS, 137 mM NaCl, 2.68 mM KCl, 8.09 mM Na$_2$HPO$_4$•2 H$_2$O, and 1.47 mM KH$_2$PO$_4$, pH 7.2–7.4) was used. To obtain spotting buffer, 10% (w/v) trehalose dihydrate and 0.005% (w/v)

Table 1 Overview over different assay principles and commercial SARS-CoV-2 antibody tests in comparison to CoVRapid CL-MIA (*n.s.*, not specified)

Assay principle	Test, *manufacturer*	Used antigen	Assay duration	Specificity in %	Sensitivity in %	Literature
Lateral flow assay	Panbio™ COVID-19 IgG/IgM Rapid Test Device, *Abbott Laboratories*	n.s.	10–20 min	99.4	93.0	[13]
	STANDARD™ Q COVID-19 IgM/IgG Duo Test, *SD Biosensor Inc*	N	15 min	100	64.9	[14]
Enzyme-linked immunosorbent assay (ELISA)	SARS-CoV-2 ELISA IgG, *EUROIMMUN AG*	S1	2 h	98	82.5	[14]
	EDI™ Novel Coronavirus COVID-19 IgG ELISA, *Epitope Diagnostics Inc*	N, S	< 2 h	98	85.6	[14]
Chemiluminescence immunoassay (CLIA)	MAGLUMI 2019-nCoV IgG, *Shenzhen New Industries Biomedical Engineering Co*	n.s.	n.s.	88.9–98	70.1–95.0	[14, 15]
	LIAISON® SARS-CoV-2 S1/S2 IgG, *DiaSorin S.p.A*	S1, S2	35 min	96.8–99	81.4–82.4	[14, 15]
	iFlash-SARS-CoV-2, *Shenzhen Yhlo Biotech Co. Ltd.*	N, S	> 12 min	92.9–100	76.9–93.0	[15, 16]
	SARS-CoV-2 IgG, *Abbott Laboratories*	N	29 min	99–100	64.5–92.6	[13, 14, 16]
	Elecsys® Anti-SARS-CoV-2, *Roche Diagnostics GmbH*	N	18 min	100	80.5–83.5	[14, 16]
Microarray immunoassay (MIA)	xMAP SARS-CoV-2 Multi-Antigen IgG Assay, *Luminex Corporation*	N, S1, RBD	2.5 h	99.3	96.3	[17, 18]
	CoVRapid CL-MIA, *Technical University of Munich*	N, S1, RBD	8 min	100	100	This work

Pluronic® F127 were added. For blocking buffer, 0.05% (*v/v*) Tween® 20 and 1% (w/v) bovine serum albumin were added to PBS. As running buffer, PBS with 0.1% (v/v) Tween® 20 was used.

SARS-CoV-2 antigens

Recombinant SARS-CoV-2 spike S1 protein with mouse Fc-tag (expressed in HEK293 cells) was purchased from Biozol
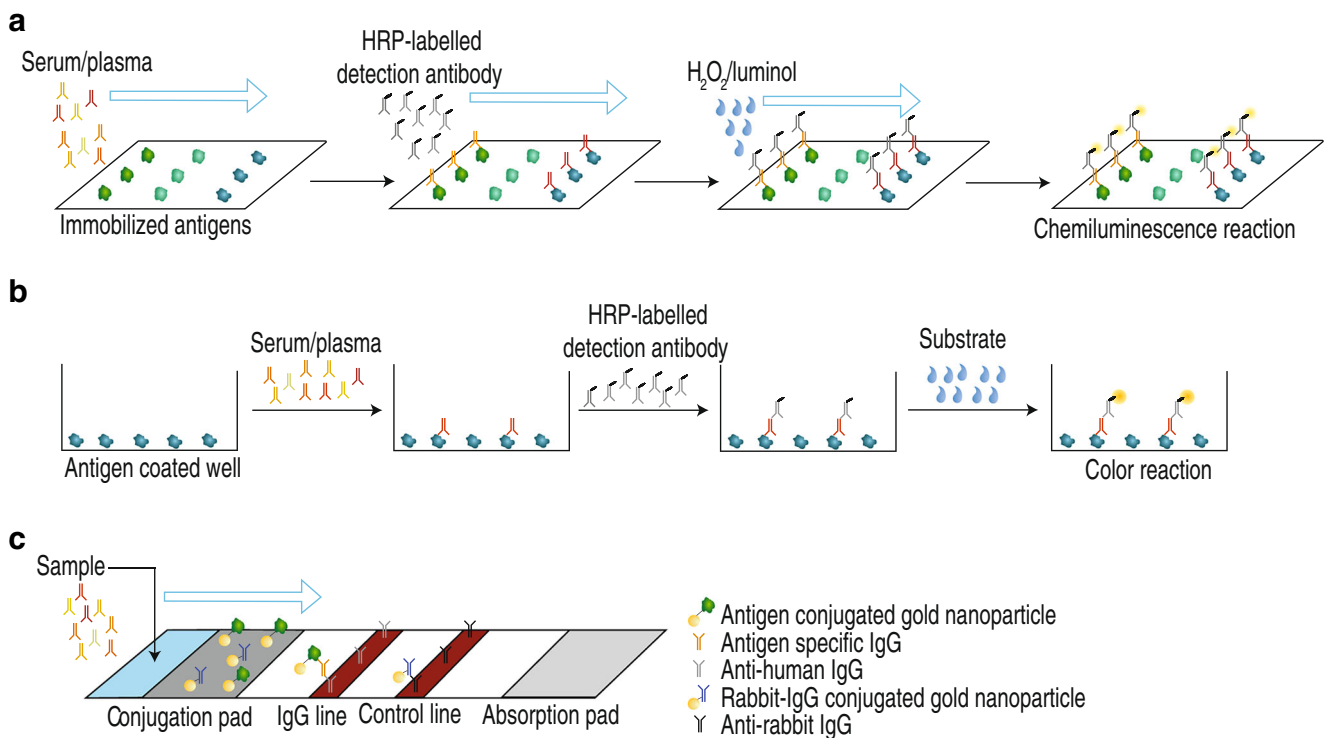
Fig. 1 Overview over different antibody test principles. **a** Flow-based CL-MIA. **b** ELISA. **c** Lateral flow immunoassay

(Eching, Germany) and produced by Sino Biological (Beijing, China).

Recombinant SARS-CoV-2 spike RBD protein with His-tag and recombinant SARS-CoV-2 nucleocapsid protein with Strep-tag were produced by ISAR Bioscience (Planegg, Germany).

Spike protein RBD-His consists of the amino acids corresponding to the receptor-binding domain (RBD), which was derived from the S protein nucleotide sequence (positions 22517 to 23183, amino acid 319 to 541, RVQP....CVNF) of the SARS-CoV-2 Wuhan Hu-1 genome (GenBank accession number MN908947) followed by six histidines. Nucleocapsid protein N-strep consists of the amino acids corresponding to the N protein nucleotide sequence (positions 28290 to 29549) of the SARS-CoV-2 Wuhan Hu-1 genome (GenBank accession number MN908947) followed by a streptavidin tag (NP-Strep). The complementary DNA sequences adapted for hamster codon usage were produced synthetically by GeneArt (Life Technologies) by adding signal sequences METPAQLLFLLLLWLPDTTG before starting and cloned into the plasmid vector pcDNA5/FRT via BamHI and XhoI. The resulting vectors were called pcDNA5/CoV-RBD-His and pcDNA5/CoV-NP-Strep, respectively, and allow for expression and secretion of RBD-His or NP-Strep into the culture medium of mammalian cells under the control of the human cytomegalovirus (CMV) immediate-early enhancer/promoter and selection for stable clones with Hygromycin B after co-transfection with plasmid pOG44. The vectors were transfected by using Lipofectamine 2000 Reagent (Invitrogen, #11668-019) into Flip-InTM-Chinese hamster ovary (CHO) cells (Life Technologies), together with the plasmid pOG44, providing site-directed recombination. After selection of a stably expressing clone in Ham's F12 supplemented with 10% fetal bovine serum and 600 μg ml^{-1} Hygromycin B, the clones were adapted to ProCHO5 medium (Lonza, #BE12-766Q) supplemented with 4 mM L-Glutamin (Biochrom, #K0283).

CHO-spike-RBD-His cells and CHO-spike-NP-Strep cells were grown in suspension in ProCHO5, 4 mM L-Glutamin and 600 μg ml^{-1} Hygromycin B in flasks to submaximal density at 37 °C and then centrifuged. The cells were continuously grown at 37 °C, with splitting every 3–4 days. The supernatants were cleared by centrifugation at 400g for 5 min and subsequent filtration with a 0.22-nm sterile filter (TPP, #99722). The resulting RBD-His or NP-Strep protein-containing medium was immediately frozen and stored at −20 °C until protein purification. Starting from a mix of cell clones, single clones are being selected and further propagated.

For protein purification, thawed CHO-RBD-His supernatants (0.5 L) were diluted 1:2 in 20 mM sodium phosphate, 0.3 M NaCl, pH 8.0, and loaded on an equilibrated 1-mL HisTrapTM excel column (GE Healthcare 17-3712-05).

After washing the column with 20 mM sodium phosphate, 0.3 M NaCl, pH 8.0, RBD-His was eluted with 4 × 1 mL 20 mM sodium phosphate, 0.3 M NaCl, 0.25 M imidazole, pH 8.0. Protein content was determined by OD 280 measurement and the relevant fractions were dialysed (Slyde-A-Lyzer Dialysis Cassette, 10000 MWCO, Thermo Scientific # 66380) against phosphate-buffered saline (PBS from Roth: 137 mM NaCl, 2.7 mM KCl, 10 mM Na$_2$HPO$_4$, 2 mM KH$_2$PO$_4$, pH 7.4, 0.2 μm filtered and steam sterilized) at 4 °C for 16 h.

0.5 L CHO-NP-Strep supernatants were diluted 1:2 in 50 mM sodium phosphate, 0.3 M NaCl, pH 8.0, and loaded on an equilibrated 1-mL StrepTrapTM HP column (GE Healthcare 28-9075-46). After washing the column with 50 mM sodium phosphate, 0.3 M NaCl, pH 8.0, NP-Strep was eluted with 4 × 1 mL 20 mM sodium phosphate, 0.3 M NaCl, 2.5 mM desthiobiotin (Sigma, #D1411) pH 8.0. Protein content was determined by OD 280 measurement and the relevant fractions were dialysed (Slyde-A-Lyzer Dialysis Cassette, 10,000 MWCO, Thermo Scientific # 66380) against PBS at 4 °C for 16 h.

Serum and plasma samples

Serum and plasma samples were either purchased from Sigma-Aldrich (Darmstadt, Germany) or obtained from Helmholtz Zentrum München, German Research Center for Environmental Health, Haematologikum (Munich, Germany) and the Institute of Virology, Technical University of Munich (Munich, Germany). All procedures were in accordance with the Helsinki Declaration of 1975, as revised in 2000.

All patient data were anonymized before obtainment of the samples. Patient samples were handled in laboratories approved for biosafety level 2.

Chip surface chemistry

The immunoassay was performed on glass slides with surface modifications based on a procedure described elsewhere [19]. In short, microscopy glass slides were cleaned thoroughly and activated by acid treatment for subsequent silanization with (3-glycidyloxypropyl)trimethoxysilane. The silanized slides were then coated with Jeffamine® ED-2003. The prepared, polyether amine functionalized chips were stored under inert gas until protein immobilization was done.

Microarray chip production

Depending on the immobilization protocol for antigen microarray preparation, the polyether amine functionalized glass slides were activated before spotting or used without activation. Activation was necessary for DSC and diepoxy PEG immobilization strategies, while for EDC/s-NHS

immobilization, the functionalized glass slides could be used without further treatment.

For N,N′-disuccinimidyl carbonate (DSC) activation, a mixture of 16 mg N,N′-disuccinimidyl carbonate, 0.8 mg 4-(dimethylamino)pyridine, and 25 μL triethylamine in 320 μL dimethylformamide per chip was prepared. Subsequently, 600 μL of this mixture was pipetted onto the top side of a functionalized glass slide that was then covered with another slide (top side pointing downward). The chip sandwiches were incubated at RT and low humidity for 4 h, subsequently separated and sonicated in methanol for 15 min. After drying them in nitrogen stream, they were directly used for spotting.

For preparation of a reactive epoxy group on the chip surface, poly(ethylene glycol) diglycidyl ether (diepoxy PEG) activation was used. Therefore, 600 μL of diepoxy PEG was pipetted onto the top side of a functionalized glass slide that was then covered with another slide (top side pointing downward). The chip sandwiches were incubated at 100 °C overnight, subsequently separated and sonicated in methanol for 15 min. After drying them in nitrogen stream, they were directly used for spotting.

Alternatively, diepoxy PEG activation was done by pre-spotting the chips with a solution of diepoxy PEG in water (50% v/v) on the micro-contact spotter BioOdyssey Calligrapher® MiniArrayer from Bio-Rad (Hercules, USA) equipped with a solid pin SNS 9 from ArrayIT (Sunnyvale, USA). After pre-spotting and overnight incubation at 100 °C, the chips were also sonicated in methanol for 15 min and used for spotting after drying.

Spotting solutions were prepared by diluting the antigens and positive controls with spotting buffer for DSC and diepoxy PEG activated chips. For spotting without previous activation of the polyether diamine chip surface (EDC/s-NHS spotting), 2 mg/mL 1-ethyl-3-(3-dimethylaminopropyl)carbodiimide (EDC) and N-hydroxysulfosuccinimide (s-NHS) were added to spotting buffer. Antigen and positive control solutions of desired concentration (if necessary, previously diluted with spotting buffer) were then mixed with EDC/s-NHS solution (50% v/v). As positive control, anti-peroxidase and anti-human IgG antibodies were used, while as negative control spotting buffer was applied.

The spotting solutions were then pipetted into a 384-well plate (10–40 μL per solution depending on the number of spotted chips) and inserted into the micro-contact spotter together with the prepared glass chips. Spotting was done in five replicates for each spotting solution with a grid spacing of 900-μm distance between replicates and 1300-μm distance between the spotted rows. The spotting process was carried out at 20 °C and 55% humidity. After spotting, the chips were incubated at 20 °C and 55% humidity overnight.

For microarray chip assembly, the spotted chips were connected to a PMMA carrier containing in- and outlet holes using double-sided adhesive foil with cut-outs forming two flow channels. The assembled chips were then filled with blocking buffer and stored at 4 °C until measurement.

Microarray measurements

Microarray measurements were carried out on the Microarray Chip Reader, 3rd generation (MCR 3), manufactured by GWK Präzisionstechnik GmbH (Munich).

Before the beginning of measurements on the microarray chip reader MCR 3, the system was flushed with running buffer and water using the respective flushing program. Subsequently, all necessary reagents (horseradish peroxidase (HRP)-labelled anti-human IgG diluted with running buffer to the desired concentration and chemiluminescence reagents luminol and hydrogen peroxide) were placed in the device. The tubes were loaded with the corresponding liquids using the load program. In the beginning of each measurement day, the blank program was executed to record the CCD camera background signal for an exposure time of 60 s. For measurements, a prepared microarray chip was inserted into the MCR 3 chip tray and the measurement program for the respective flow cell was carried out. Samples were prepared by diluting 100 μL of serum or plasma sample with running buffer to a final volume of 1 mL, out of which 900 μL was used for the measurement. The total assay process is summarized in Table 2. The sample was flown over the chip slowly, followed by the HRP-labelled detection antibody and the chemiluminescence reagents, which had been pre-mixed in 50 μL segments. The exposure time for the recording of the measurement image was 60 s, followed by thorough washing of the system, leading to a total measurement time of 7 min 45 s.

Data evaluation

The detected CL signals were corrected with the previously recorded blank image, stored as txt files and processed with the evaluation software MCR spot reader (Stefan Weißenberger, Munich, Germany). On the background-corrected CL images, a grid was set to define the position of the spots. For each spot, the mean value of the ten brightest pixels was calculated. Means and standard deviations were calculated for the five replicates per row and spots that deviated more than 10% from the mean were excluded (maximum two excluded spots per row).

The resulting mean values and standard deviations for all rows were used for further analysis and graphical evaluation using Python 3.

Table 2 Main assay steps on the MCR 3 with details to used volumes and flow rates; a video showing the measurement process is provided in the Supplementary Information

Step	Volume	Flow rate	
Sample injection	900 μL	10 μL s^{-1}	
Flushing	1000 μL	10 μL s^{-1}	
	2000 μL	500 μL s^{-1}	
Detection antibody injection	200 μL	100 μL s^{-1}	
	800 μL	10 μL s^{-1}	
Flushing	1000 μL	10 μL s^{-1}	
	2000 μL	500 μL s^{-1}	
CL reagents injection	400 μL	150 μL s^{-1}	
Image acquisition	-	-	
Flushing of whole system	11 mL	250 μL s^{-1}	(flushing of sample syringe)
	8 mL	500 μL s^{-1}	(flushing of tubes and chip)

Comparison measurements with commercial antibody tests

Comparison measurements with the commercial recomLine and recomWell tests from Mikrogen GmbH (Neuried, Germany) for the detection of SARS-CoV-2 specific IgG were conducted according to the manufacturer's specifications.

Results and discussion

Optimization of immobilization strategy

Four different methods of surface activation and antigen immobilization were tested (DSC, diepoxy PEG, diepoxy PEG pre-spotting, EDC/s-NHS). A schematic representation of the chemical background of each of these methods is presented in Fig. 2a) (for a more detailed view, Supplementary Information Fig. S1 shows the respective reaction schemes). The pre-functionalized microarray glass chips present PEG spacers with terminal amino groups on their surface. Antigens then can be immobilized in an undirected manner via either amino groups (e.g., from lysine) in DSC and diepoxy PEG immobilization or via carboxy groups (e.g., from glutamic acid) in EDC/s-NHS immobilization. For DSC, the full chip surface was activated, for diepoxy PEG activation of the full surface as well as only activation of the antigen spots by pre-spotting was tested. For EDC/s-NHS, the antigen carboxy groups are activated and spotted onto an amino functionalized chip without surface activation.

After spotting, the chips are assembled with a PMMA carrier and an adhesive foil containing two flow channels as shown in Fig. 2b), resulting in a microarray chip as in Fig. 2c) that can be inserted into the measurement device MCR 3.

Figure 3 shows the resulting chemiluminescence signals for measurements of a SARS-CoV-2 serology negative (a) and positive (b) sample for the SARS-CoV-2 antigens N,

RBD, and S1, as well as the positive control (anti-human IgG) and the background signal (spotting buffer).

With all tested methods, the antigen CL signals were higher for the positive sample compared to the negative one, while for the background a very low signal and for the positive control a high signal were found, showing the general applicability of all methods. Pre-spotting of diepoxy PEG gave similar results as whole chip activation with diepoxy PEG with slightly lower signal for the positive sample. Therefore, the time-consuming pre-spotting process was considered unnecessary.

With the negative sample in Fig. 3a, only slight unspecific binding of antibodies to the antigens could be seen for DSC and diepoxy PEG, while for EDC/s-NHS especially for the N protein a relatively high signal was found (2231 a.u. compared to 630 a.u. for diepoxy PEG). This unspecific binding also diminishes the obtained positive/negative signal ratio, which is found as 3.0 (N), 6.3 (RBD), and 5.7 (S1) for EDC/s-NHS, while diepoxy PEG immobilization gave values of 7.7, 19.3, and 10.7 and DSC yielded 7.4, 21.9, and 9.1, respectively. Additionally, many of the EDC/s-NHS spots on the microarray chip were very variable, while the other immobilization methods gave uniform, round spots. As in EDC/s-NHS activation not the chip surface but carboxy groups of the proteins in solution are activated, cross-linking of the proteins might occur, leading to conformational changes and a change of activity over the course of the spotting process.

As the positive/negative signal ratios obtained with DSC and diepoxy PEG immobilization were comparable for all spotted rows, it was decided to use DSC immobilization for all further experiments due to the low time expenditure of 4 h for the surface activation before spotting compared to overnight activation with diepoxy PEG.

We therefore were able to develop different strategies for the covalent immobilization of proteins on glass microarray chips in their native conformation, benefitting from the expertise of our research group in the production of different kinds
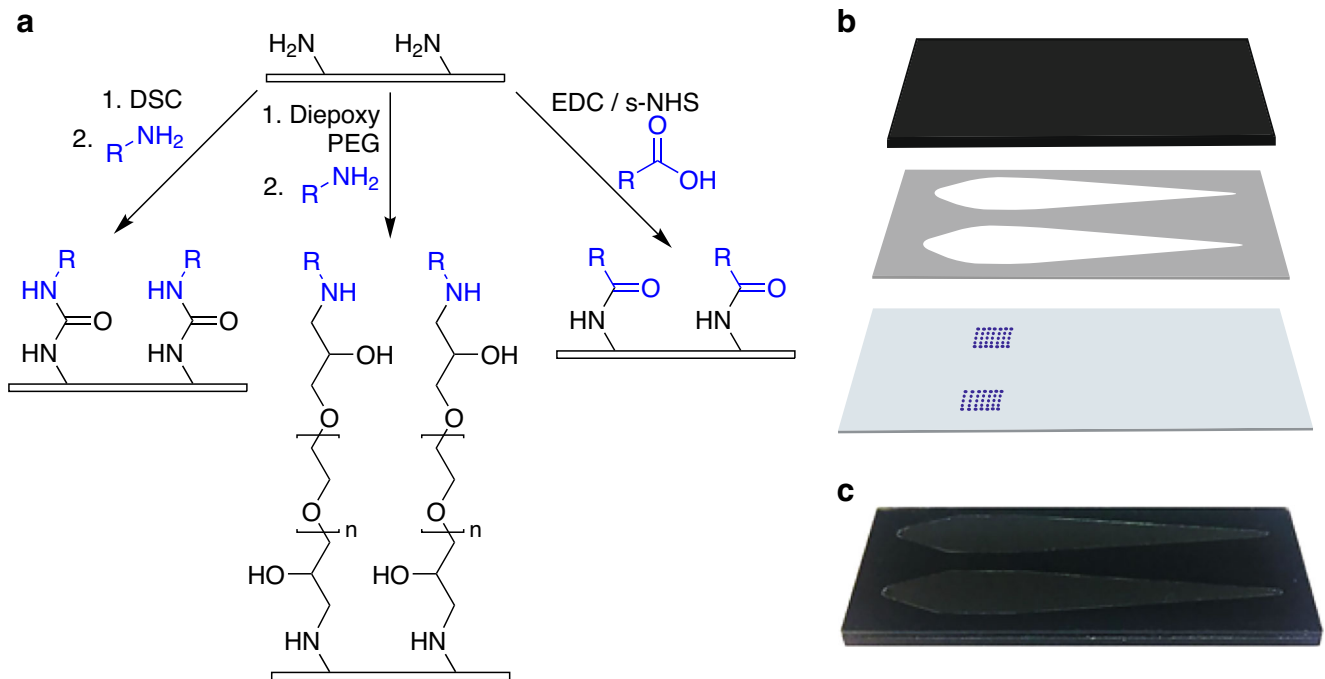
Fig. 2 Microarray chip spotting and assembly. a Schematic overview of antigen immobilization strategies, with DSC and diepoxy PEG immobilization being two-step processes (chip surface activation followed by antigen immobilization) and EDC/s-NHS as one-step process (antigen activation in spotting solution), antigens shown in blue, immobilization is done via amino or carboxy groups of the amino acid side chains. b Chip assembly from carrier (top), adhesive foil with flow channels (middle), and glass microarray chip (bottom). c Photograph of an assembled chip

of microarrays. An important factor is the spotting buffer, containing trehalose and Pluronic® F127 [19]. Trehalose is also used in protein freeze-drying processes as a protective agent, mimicking the hydrogen bonds between polar functional groups of the protein and water [20], while pluronics are poloxamers that are widely applied in pharmaceutical industry and microfluidic technology as non-ionic surfactants to prevent protein aggregation and adsorption [21, 22]. The immobilization methods can also be easily applied to other native proteins, allowing for the rapid adaption and extension of the microarray.

Optimization of antibody and antigen concentrations

After determination of the optimal immobilization method, different immobilized antigen concentrations and secondary
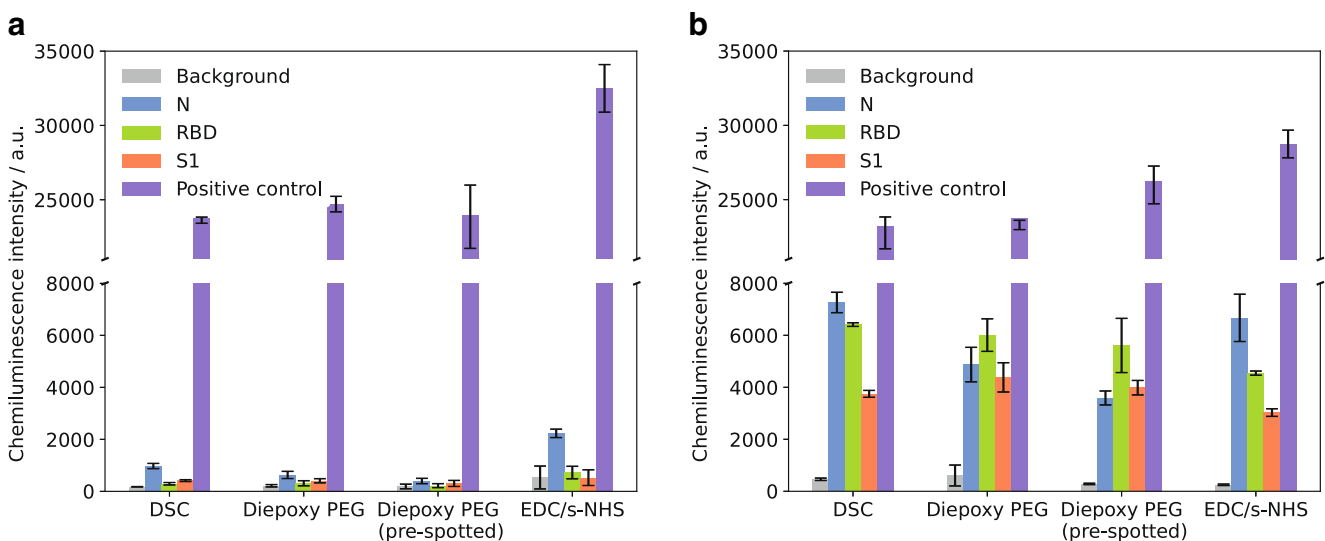
Fig. 3 Measurement results for different immobilization methods. a SARS-CoV-2 serology negative sample. b SARS-CoV-2 serology positive sample; error bars represent replicate measurements on different chips, $n = 3$

antibody concentrations were tested. For the antigen concentrations, undiluted antigen (250 µg mL^{-1} for N and S1 protein, 350 µg mL^{-1} for RBD) and subsequent twofold dilutions were tested until a dilution of 1:8. For the HRP-labelled secondary antibody, five different concentrations, namely 11.2 µg mL^{-1} (1:500 dilution of stock solution), 5.6 µg mL^{-1} (1:1000), 2.8 µg mL^{-1} (1:2000), 1.4 µg mL^{-1} (1:4000), and 0.7 µg mL^{-1} (1:8000), were used. The same SARS-CoV-2 serology positive sample was used for all measurements. The results are presented in Fig. 4a with one set of bars for each secondary antibody concentration and each bar representing a certain antigen concentration in the spotting solution as indicated. Figure 4b shows examples of images of a microarray chip with bright spots in rows representing spotted antigens.

It is clearly visible that the chemiluminescence signal increases with increasing secondary antibody concentration. In the same course, the background signal increases but to a lower extent compared to the specific antigen signals. For

secondary antibody concentrations from 0.7 to 5.6 mg mL^{-1}, a significant increase can be seen upon doubling of the concentration, while a further increase to 11.2 mg mL^{-1} only gives slightly higher signals for all antigens. Thus, as a compromise between high signal intensities and low expenditure of secondary antibody, a concentration of 5.6 mg mL^{-1} was used for all further measurements.

For the decision on the optimal spotted antigen concentration, not only the chemiluminescence intensities as displayed in Fig. 4a were taken into account but also the appearance of the spots on the microarray chip as shown in Fig. 4b. Here, three blocks of spots can be seen with the four columns within each block representing the different concentrations of antigens, decreasing from left to right. The three blocks correspond to the different antigens, starting with N protein on the left side, RBD in the middle and S1 protein on the right-hand side, as also shown in Fig. 4a. The flow direction of sample and reagents during the measurements is from lower
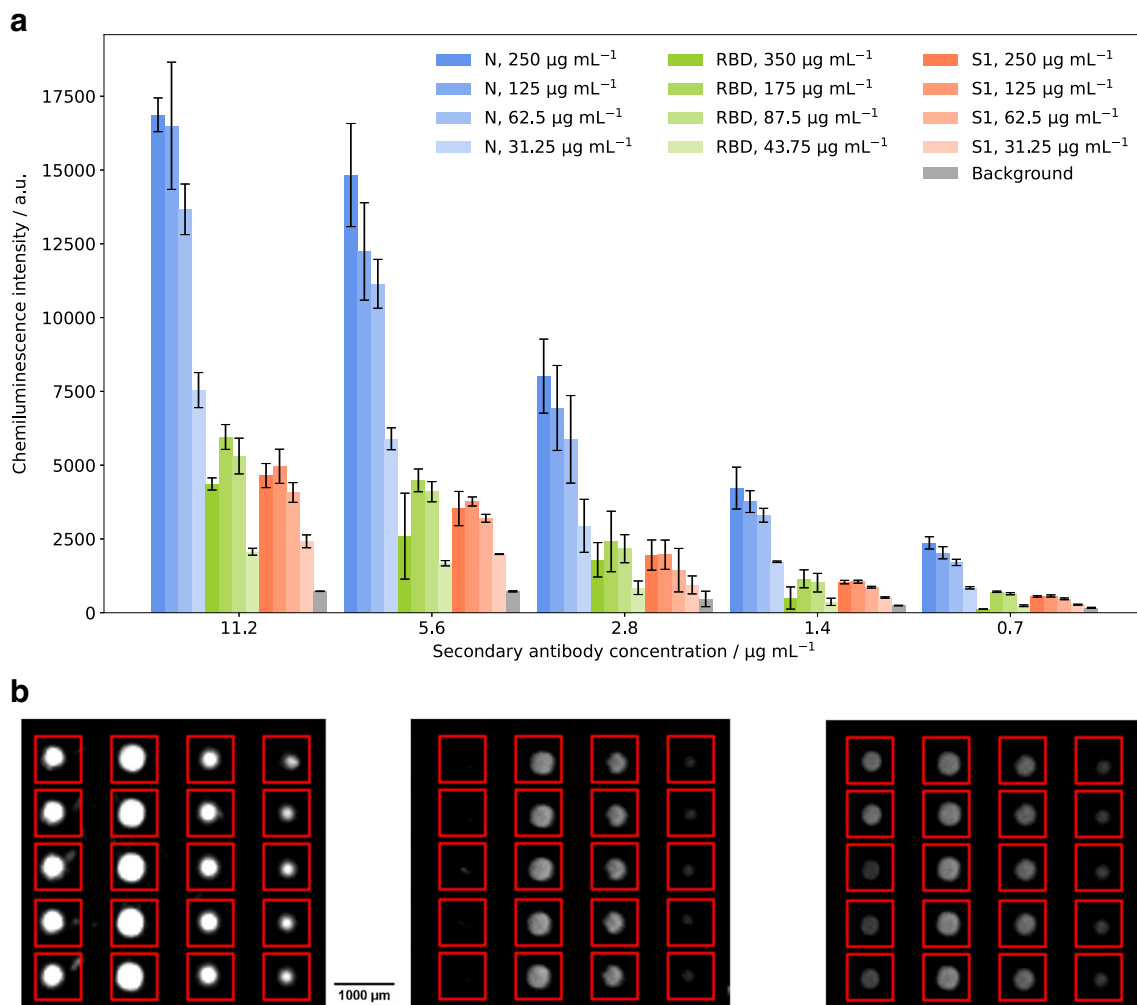
Fig. 4 **a** Measurements of different immobilized antigen dilutions using different secondary antibody concentrations; error bars represent replicate measurements on different chips, $n = 3$. **b** Exemplary chip images (columns from left to right: N undiluted, N 1:2, N 1:4, N 1:8; RBD undiluted, RBD 1:2, RBD 1:4, RBD 1:8; S1 undiluted, S1 1:2, S1 1:4, S1 1:8, rows represent replicates of the same antigen dilution)

towards higher concentrations of the antigens (right to left in Fig. 4b).

For the intensities, the same trends can be seen regardless which secondary antibody concentration was used. For the N protein, a signal increase is seen with increasing concentration of antigen on the chip. For S1 and RBD, this is true for all diluted samples (concentrations between 31.25 and 175 µg mL^{-1} as indicated above). For the spotting of undiluted antigen, lower intensities than for the 1:2 dilution are found, indicating either a lower immobilization efficiency with less immobilized antigen molecules on the surface or a lower activity of the protein. When looking at the antigen spots, an increase in diameter is seen up to the 1:2 dilution, while for the undiluted spotting row, notably smaller and less uniform spots are seen for all antigens, especially for the S1 protein, where the spots are barely visible. This can be attributed to the drying of the spots during the incubation time after spotting. In the undiluted antigen samples, no stabilizing agents were added, leading to rapid drying of the spots and activity loss of the protein. Especially for the S protein, it has already been shown that antibody recognition depends strongly on the used protein expression systems; therefore, also slight conformational changes upon drying of the spots might have an influence [3]. Additionally, it is possible that protein agglomerated or adsorbed to the wells of the microwell plate before spotting, reducing the concentration on each spot. For the diluted antigen samples, we aimed at reducing these effects by using the spotting buffer containing trehalose and Pluronic® F127. As these additives had a beneficial effect on signal intensity (for S1 and RBD) as well as on spot appearance (for all antigens) but still a high antigen concentration was desired, all further experiments were done using 1:2 dilutions of the antigens with spotting buffer, resulting in concentrations of 175 µg mL^{-1} (RBD) and 125 µg mL^{-1} (S1, N) in the spotting solution.

Dilution measurements

To evaluate the correlation between antibody concentration and chemiluminescence signal that is needed for the development of prospective future quantitative tests, COVID-19 reconvalescent plasma was diluted with a negative control sample. Antibody measurements of samples with positive plasma ratios between 0 and 100% were performed for RBD and S1 protein as they are the most immunogenic antigens [3] and, therefore, most promising for a quantitative application. A determination of the SARS-CoV-2 N protein was not attempted, as its sequence was shown to be more conserved over different corona viruses [11] implying that cross reactivity and, hence, cross sensitivity to antibodies to endemic corona viruses might be possible [23].

Figure 5 shows the resulting chemiluminescence intensities for seven different mixture ratios of serology positive and negative samples. Besides the RBD and S1 protein, also the background signal is shown for comparison. A linear correlation between antibody concentration in the sample and chemiluminescence intensity can clearly be seen with linear regressions almost perfectly fitting the measured data ($R^2 = 1.00$ for RBD and S1, $R^2 = 0.94$ for the background signal). The slight slope for the background signal can be explained as different blood samples were used, naturally resulting in different background values. For prospective future applications, this matrix influence can easily be avoided by a background correction of the measurement data as was done in all following experiments.

While for the measurement point at 1% positive sample ratio only a slight difference to the pure negative sample can be seen, the following measurement point at 10% positive sample ratio already can be distinguished well from the negative sample. The greater slope for the RBD compared to the S1 protein can be assigned to the different spotted concentrations (175 µg mL^{-1} and 125 µg mL^{-1}, respectively). From these results, we conclude that a future development towards a quantitative test is possible. If a standard sample with a known, high concentration of antibodies to the RBD and S1 protein is available, a calibration of the test can be done, allowing for a simple quantitative interpretation of measurements that might give a more detailed information about an individual's SARS-CoV-2 serological status.

Measurement and classification of patient samples and comparison with results of commercial antibody tests

To define cutoff values used for the assignment of positive and negative results, receiver operating characteristic (ROC) curves were used. They illustrate the trade-off between correctly identified positive samples and false positives in a diagnostic test, allowing for the selection of a suitable cutoff value for a given question [24]. In a ROC curve, the cutoff value is shifted over a range of values and sensitivity and specificity are calculated for each cutoff. Resulting pairs of sensitivity and $1 - $specificity are plotted together with a diagonal line ($x = y$). A perfect test will result in a right triangle that intersects the point [0,1], representing 100% sensitivity and specificity. A calculation of the area under the curve (AUC) for a perfect test will give a value of 1.0, while the worst possible result (resembling a toss coin) is an AUC of 0.5, achieved by a ROC curve matching the diagonal. Depending on the diagnostic question of interest, a cutoff can be chosen with respect to highest possible sensitivity or specificity. In the context with SARS-CoV-2 antibody detection, high specificity is desirable, as a false positive result might mislead tested individuals to be less cautious as they presume to be immune to SARS-CoV-2 infection.

To determine ROC curves for the test presented herein, 65 serum and plasma samples (32 from individuals without previous SARS-CoV-2 infection, 33 from reconvalescent COVID-19 patients) were tested, the resulting

Fig. 5 Linear regression ($m = 7$) for measurements of samples with different ratios of SARS-CoV-2 serology positive plasma for RBD and S1 protein; error bars represent replicate measurements on different chips, $n = 3$
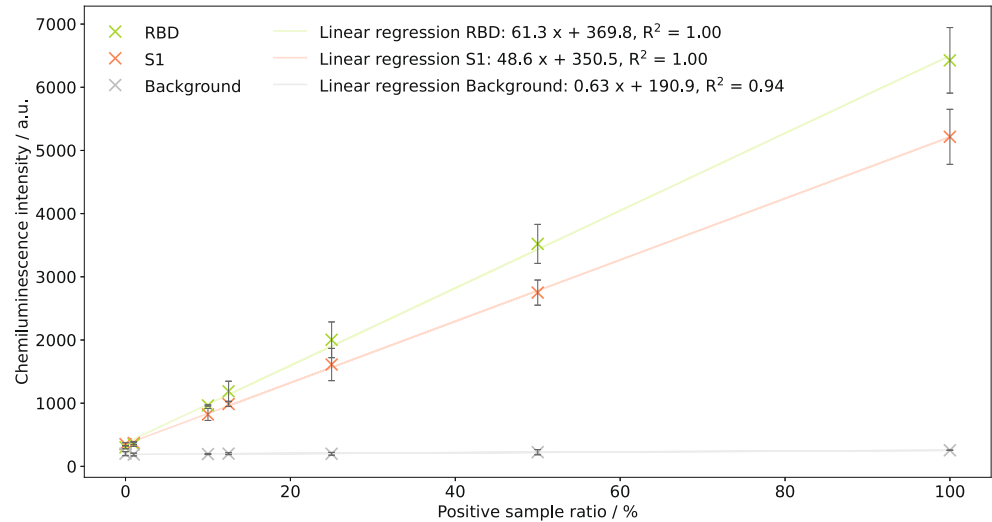
chemiluminescence values were background-corrected and then used for the ROC determination. Results for the three tested antigens as well as for the combination of them on the chip are shown in Fig. 6. For the combined antigens, a sample was considered positive when it gave signal above cutoff for at least one antigen.

For all antigens, a high AUC above 0.99 was determined. Literature states that an AUC value above 0.9 represents good accuracy of a test [24, 25]. Especially for the N protein, an optimal ROC curve with an AUC of 1.0 was found.

Cutoff values were defined such that the highest possible specificities resulted for each antigen as especially in antibody

testing, a false positive result is considered more harmful than a false negative one as it dissembles a non-existing immunity. The respective cutoff values, given in background-corrected chemiluminescence intensity, are 2860 for the N protein (100% sensitivity, 100% specificity), 800 for RBD (93.9% sensitivity, 100% specificity), and 1700 for the S1 protein (87.9% sensitivity, 100% specificity). Still, the given values for sensitivity must be considered with caution, as it cannot be guaranteed that all reconvalescent patients actually had formed antibodies to all antigens.

The determined cutoff values were then used to take a closer look at the measurement results for all patient samples.

Fig. 6 ROC curves and respective AUC values for different antigens, obtained from measurements of 65 patient samples; **a** N protein, **b** RBD, **c** S1 protein, **d** combination of all antigens on the chip
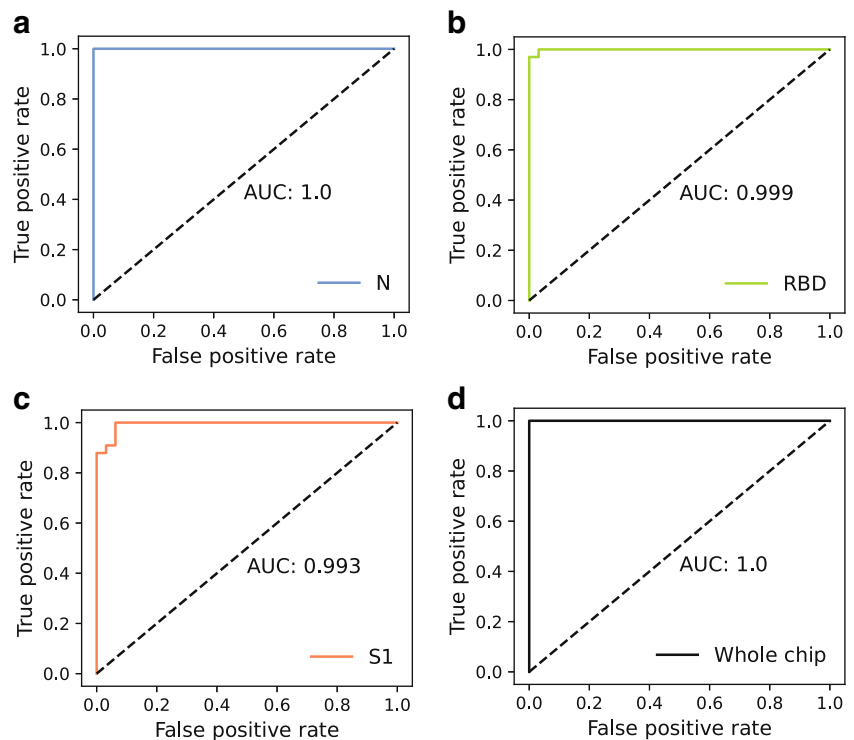
The background-corrected chemiluminescence values were normalized with respect to the cutoff values and the resulting values are shown in Fig. 7a for the negative samples and in Fig. 7b and c for the positive samples. For the patients without

previous SARS-CoV-2 infection, most samples showed higher normalized intensities for the N protein than for RBD and S1. This was the expected result, as for the N protein a cross reactivity with endemic coronaviruses could not
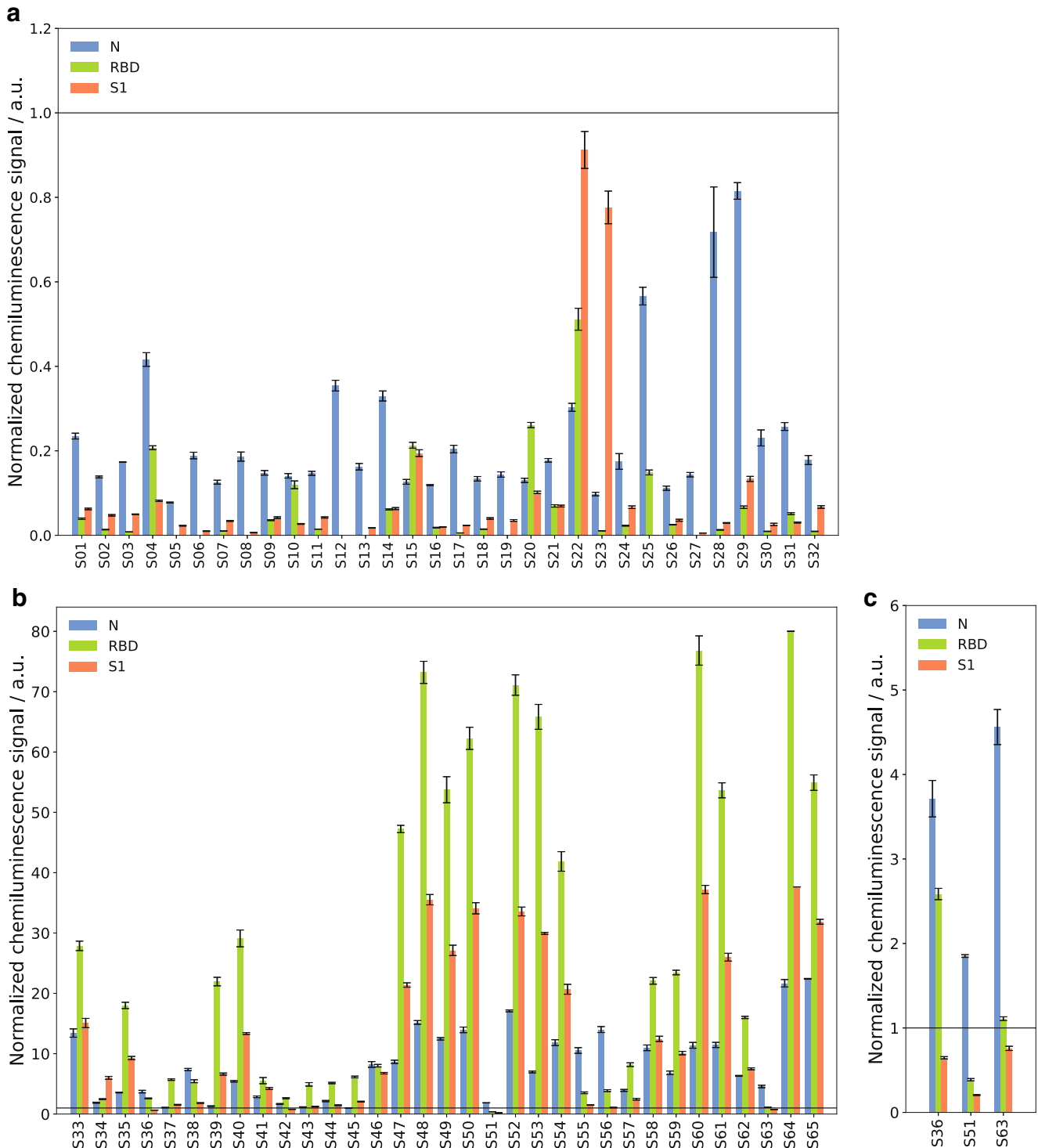
Fig. 7 CoVRapid CL-MIA results for 65 patient samples. **a** Results for 32 SARS-CoV-2 serology negative samples. **b** Results for 33 SARS-CoV-2 serology positive samples. **c** Detailed representation of positive samples with measurement signal below the cutoff for at least one antigen; all values are normalized with respect to the cutoff values determined by ROC curve analysis; error bars represent standard deviation of replicate spots on one chip, $n = 5$

completely be excluded due to high sequence similarity. Comparison measurements with the recomLine test from Mikrogen showed that the vast majority of all patients had formed antibodies to the N protein of at least one of the endemic coronaviruses 229E, NL63, OC43, and HKU1. For the negative sample S22, which shows a lower intensity for N than for S1 and RBD, it is possible that a recent, undetected infection with SARS-CoV-2 was present and IgG antibodies had already started to form to a low extent or that the patient had overcome COVID-19 at a very early stage of the pandemic and the antibody amount in the blood had already declined below the detectable level. Confirmation would be possible by follow-up measurements of the patient or by consulting his case file, which both were not possible due to the sample obtainment strategy. Sample S23 shows a low intensity for both N protein and RBD, while a relatively high signal for S1 is detected. As the RBD is contained within the S1 protein and tended to give higher signals compared to the S1 in our test, this indicates that no specific antibodies to SARS-CoV-2 S1 have been formed. Instead, as the used S1 protein carried a mouse Fc fragment, it might be possible that the patient had formed human anti-mouse antibodies (HAMA) that have been shown to interfere with immunoassay measurements [26]. Still, with the defined cutoff values, all negative samples were correctly classified as negative for all three antigens, resembling a specificity of 100% for the CoVRapid CL-MIA.

For the SARS-CoV-2 serology positive samples in Fig. 7b the trend already seen in the dilution measurements again is visible, as for most patients a higher intensity is found for RBD compared to S1 due to the higher immobilized concentration. Few samples show a different behaviour with comparable intensities for S1 and RBD or even higher signal for S1, indicating that antibodies to other S1 regions than the RBD might have been formed. In comparison to the signals for the N protein, most samples show higher intensities for S1 and RBD, which is

expected as the spike protein is considered more immunogenic than the nucleocapsid [3].

The measured intensities spread over a broad range from slightly above 1 (cutoff) to over 70. As no information on the clinical course of the patients was available, it can only be suspected that higher intensities may be related to either more recent or more severe disease. Still, all knowingly positive samples were found positive for at least one of the tested antigens, resembling 100% sensitivity.

For a total of three of the positive samples only for one or two of the antigens, a signal above the cutoff was determined. As in Fig. 7b no clear interpretation of samples with low signal is possible, these samples are shown in more detail in Fig. 7c. The reason for this outcome might be that the patients still were in an early stage of infection where few antibodies had been formed yet, or that the antibody amount in the blood was already declining due to a prolonged time since infection. This emphasizes that a quantitative test will be helpful in the future. When comparing the results obtained with the commercial multiplex test recomLine from Mikrogen, for S51 and S63, only a positive result for the N protein could be found, while S1 and RBD were negative, confirming the CoVRapid result. This is also in accordance with literature findings showing that antibodies to different proteins form independently which possibly leads to significantly different reactions to different antigens at certain points of time after symptom onset [27, 28].

Comparison tests were done not only with the recomLine test (N, RBD, and S1 protein) but also with the N specific recomWell ELISA from Mikrogen. The principal antibody test used for the sample classification that Fig. 7 refers to was the iFlash test from YHLO. Here, samples are classified with regard to antibodies for either the N or S1 protein.

Overall, a good performance of all tests was found as depicted in Table 3. While our CoVRapid test classified all samples correctly (with respect to iFlash classification), with the recomLine

Table 3 Classification of patient samples by different anti-SARS-CoV-2 IgG tests. The iFlash-SARS-CoV-2 IgG was used as reference classification for 62 samples, while three samples were only tested with the alternative tests CoVRapid CL-MIA, recomLine SARS-CoV-2 IgG, and recomWell SARS-CoV-2 IgG (one of the samples specified as

"Not classified" was ordered from a commercial supplier as negative control, two were obtained from reconvalescent COVID-19 patients). For the recomWell test, two samples gave values in the borderline area of the test and were therefore excluded

	iFlash	CoVRapid	recomLine	recomWell	
AB positive	31	100 0	100 0	96.7 3.3	Positive (%) Negative (%)
AB negative	31	0 100	3.2 96.8	3.3 96.7	Positive (%) Negative (%)
Not classified	3	66.7 33.3	66.7 33.3	66.7 33.3	Positive (%) Negative (%)
Total	65	65	65	63	Total

test, one false positive sample was found (positive for S1, negative for RBD and N). With the recomWell test, two samples gave results in the borderline area and were therefore excluded. Additionally, this test gave one false negative and one false positive result. This gives the CoVRapid test the highest sensitivity and specificity (100% each) while recomLine obtained values of 100% and 96.8%, respectively, and recomWell showed the highest deviations with 96.7% each.

Conclusion

We developed a rapid, flow-based CL-MIA that allows for the fully automated detection of IgG antibodies to three different SARS-CoV-2 antigens, namely N, S1, and RBD, from human serum or plasma within as few as 8 min. The test showed a very high diagnostic sensitivity and specificity of 100% with 65 tested patient samples and thus performed better than two commercial tests for the same sample set. Additional advantages of the CoVRapid CL-MIA over the other test systems are the rapid analysis without extensive manual pipetting steps due to an automated flow-based principle of the assay. Due to this principle, the assay is more sensitive than common lateral flow "rapid tests" while still being very fast and easy to conduct without extensive manual steps in contrast to ELISA tests.

Due to the microarray principle, the simultaneous detection of antibodies to different antigens is possible with the CoVRapid CL-MIA, giving a more detailed insight into the individual immune response and diminishing the risk of false negative results. With our specialized microarray chip surface chemistry, we also achieved a negligibly small matrix influence that can be further reduced by on-chip matrix controls, enabling even the analysis of hemolytic blood samples.

With respect to the microarray chip production, also the covalent immobilization strategy for native proteins has to be emphasized in comparison to common assays that are based on the adsorption of denatured proteins. With native proteins, an environment comparable to the human cell is created, giving a realistic impression of the human immune response. Additionally, future adaption of the test for example by immobilization of antigens containing mutations is easily possible using the same antigen production and immobilization strategies as described herein.

This test is not only valuable in clinical surroundings to check whether a patient already overcame a SARS-CoV-2 infection and, especially, whether he still has antibodies that probably render him immune to fresh infection. It additionally can be very helpful in the upcoming time in connection with the SARS-CoV-2 vaccination that is already carried out in many countries and will be in the following months in many more. The test can be used to assess whether a vaccination has been successful and, hence, can aid in the control of vaccination status dependent admission criteria on-site.

Future research activities are planned to enlarge the scope of applications of the test. One aim is to transfer the microarray from glass to polycarbonate chips, making the fabrication even more economic. Additionally, the dual detection of IgM and IgG antibodies to SARS-CoV-2 and also to other respiratory viruses such as influenza will be expedited, as the flow-based concept is predestined for a two-step detection of different parameters. The detection of IgM antibodies furthermore would allow for a rapid diagnostic tool, e.g., in emergency rooms where patients with respiratory symptoms could be diagnosed rapidly after admission and subsequently be treated accordingly right from the beginning of their hospitalization. Another possible field of application would be a general vaccination monitoring for diseases such as measles, hepatitis A and B, or SARS-CoV-2 to allow for a rapid titer check by quantitative CL-MIA directly followed by vaccination if necessary.

Overall, we bring forward a valuable diagnostic tool that can easily be customized to different applications and already proved very successful in the context of SARS-CoV-2 serology testing.

Declarations

References

1. Zhu N, Zhang D, Wang W, Li X, Yang B, Song J, et al. A novel coronavirus from patients with pneumonia in China, 2019. N Engl J Med. 2020;382:727–33. https://doi.org/10.1056/NEJMoa2001017 .

2. World Health Organization. WHO Coronavirus disease (COVID-19) dashboard. 2020. https://covid19.who.int/. Accessed 15 Jan 2021.

3. Zhang X-Y, Guo J, Wan X, Zhou J-G, Jin W-P, Lu J, et al. Biochemical and antigenic characterization of the structural proteins and their post-translational modifications in purified SARS-CoV-2 virions of an inactivated vaccine candidate. Emerg Microbes Infect. 2020;9:2653–62. https://doi.org/10.1080/22221751.2020.1855945 .

4. Krammer F. SARS-CoV-2 vaccines in development. Nature. 2020;586:516–27. https://doi.org/10.1038/s41586-020-2798-3 .

5. Tanne JH. Covid-19: Pfizer-BioNTech vaccine is rolled out in US. BMJ. 2020;371:m4836. https://doi.org/10.1136/bmj.m4836 .

6. Kober C, Niessner R, Seidel M. Quantification of viable and non-viable Legionella spp. by heterogeneous asymmetric recombinase polymerase amplification (haRPA) on a flow-based chemiluminescence microarray. Biosens Bioelectron. 2018;100:49–55. https://doi.org/10.1016/j.bios.2017.08.053 .

7. Wutz K, Meyer VK, Wacheck S, Krol P, Gareis M, Nölting C, et al. New route for fast detection of antibodies against zoonotic pathogens in sera of slaughtered pigs by means of flow-through chemiluminescence immunochips. Anal Chem. 2013;85:5279–85. https://doi.org/10.1021/ac400781t .

8. Kloth K, Rye-Johnsen M, Didier A, Dietrich R, Märtlbauer E, Niessner R, et al. A regenerable immunochip for the rapid determination of 13 different antibiotics in raw milk. Analyst. 2009;134: 1433–9. https://doi.org/10.1039/b817836d .

9. Kubina R, Dziedzic A. Molecular and serological tests for COVID-19 a comparative review of SARS-CoV-2 coronavirus laboratory and point-of-care diagnostics. Diagnostics (Basel). 2020. https://doi.org/10.3390/diagnostics10060434 .

10. Adams ER, Ainsworth M, Anand R, Andersson MI, Auckland K, Baillie JK, et al. Antibody testing for COVID-19: a report from the National COVID Scientific Advisory Panel. Wellcome Open Res. 2020;5:139. https://doi.org/10.12688/wellcomeopenres.15927.1 .

11. Kilic T, Weissleder R, Lee H. Molecular and immunological diagnostic tests of COVID-19: current status and challenges. iScience. 2020;23:101406. https://doi.org/10.1016/j.isci.2020.101406 .

12. Hedde PN, Abram TJ, Jain A, Nakajima R, Ramiro de Assis R, Pearce T, et al. A modular microarray imaging system for highly specific COVID-19 antibody testing. Lab Chip. 2020;20:3302–9. https://doi.org/10.1039/d0lc00547a .

13. Batra R, Olivieri LG, Rubin D, Vallari A, Pearce S, Olivo A, et al. A comparative evaluation between the Abbott Panbio™ COVID-19 IgG/IgM rapid test device and Abbott Architect™ SARS CoV-2 IgG assay. J Clin Virol. 2020;132:104645. https://doi.org/10.1016/j.jcv.2020.104645 .

14. Naaber P, Hunt K, Pesukova J, Haljasmägi L, Rumm P, Peterson P, et al. Evaluation of SARS-CoV-2 IgG antibody response in PCR positive patients: comparison of nine tests in relation to clinical data. PLoS One. 2020;15:e0237548. https://doi.org/10.1371/journal.pone.0237548 .

15. Plebani M, Padoan A, Negrini D, Carpinteri B, Sciacovelli L. Diagnostic performances and thresholds: the key to harmonization in serological SARS-CoV-2 assays? Clin Chim Acta. 2020;509:1–7. https://doi.org/10.1016/j.cca.2020.05.050 .

16. Parai D, Dash GC, Choudhary HR, Peter A, Rout UK, Nanda RR, et al. Diagnostic comparison of three fully automated chemiluminescent immunoassay platforms for the detection of SARS-CoV-2 antibodies; 2020.

17. Denise M. Hinton FDA. xMAP SARS-CoV-2 Multi-Antigen IgG Assay Emergency Use Authorization. 2020. https://www.fda.gov/media/140257/download. Accessed 15 Jan 2020.

18. Luminex Corporation. xMAP®SARS-CoV-2 Multi-Antigen IgG Assay Package Insert. 2020. https://www.fda.gov/media/140256/download. Accessed 15 Jan 2020.

19. Wolter A, Niessner R, Seidel M. Preparation and characterization of functional poly(ethylene glycol) surfaces for the use of antibody microarrays. Anal Chem. 2007;79:4529–37. https://doi.org/10.1021/ac070243a .

20. Carpenter JF, Crowe JH. An infrared spectroscopic study of the interactions of carbohydrates with dried proteins. Biochemistry. 1989;28:3916–22. https://doi.org/10.1021/bi00435a044 .

21. Lee HJ, McAuley A, Schilke KF, McGuire J. Molecular origins of surfactant-mediated stabilization of protein drugs. Adv Drug Deliv Rev. 2011;63:1160–71. https://doi.org/10.1016/j.addr.2011.06.015 .

22. Luk VN, Mo GC, Wheeler AR. Pluronic additives: a solution to sticky problems in digital microfluidics. Langmuir. 2008;24:6382–9. https://doi.org/10.1021/la7039509 .

23. Gralinski LE, Menachery VD. Return of the Coronavirus: 2019-nCoV. Viruses. 2020. https://doi.org/10.3390/v12020135 .

24. Gardner IA, Greiner M. Receiver-operating characteristic curves and likelihood ratios: improvements over traditional methods for the evaluation and application of veterinary clinical pathology tests. Vet Clin Pathol. 2006;35:8–17. https://doi.org/10.1111/j.1939-165x.2006.tb00082.x .

25. Trivedi SU, Miao C, Sanchez JE, Caidi H, Tamin A, Haynes L, et al. Development and evaluation of a multiplexed immunoassay for simultaneous detection of serum IgG antibodies to six human coronaviruses. Sci Rep. 2019;9:1390. https://doi.org/10.1038/s41598-018-37747-5 .

26. Klee GG. Human anti-mouse antibodies. Arch Pathol Lab Med. 2000;124:921–3. https://doi.org/10.1043/0003-9985(2000)124<0921:HAMA>2.0.CO;2 .

27. Ayouba A, Thaurignac G, Morquin D, Tuaillon E, Raulino R, Nkuba A, et al. Multiplex detection and dynamics of IgG antibodies to SARS-CoV2 and the highly pathogenic human coronaviruses SARS-CoV and MERS-CoV. J Clin Virol. 2020;129:104521. https://doi.org/10.1016/j.jcv.2020.104521 .

28. Shrock E, Fujimura E, Kula T, Timms RT, Lee I-H, Leng Y, et al. Viral epitope profiling of COVID-19 patients reveals cross-reactivity and correlates of severity. Science. 2020. https://doi.org/10.1126/science.abd4250 .

4.2 Publication 2: Fully Automated Chemiluminescence Microarray Analysis Platform for Rapid and Multiplexed SARS-CoV-2 Serodiagnostics

Economic and fast polycarbonate chip production

Whole blood measurements

CL microarray immunoassays

for SARS-CoV-2 serodiagnostics

Sequential IgM/IgG detection

Distinction of reconvalescence/vaccination

Serosurveillance
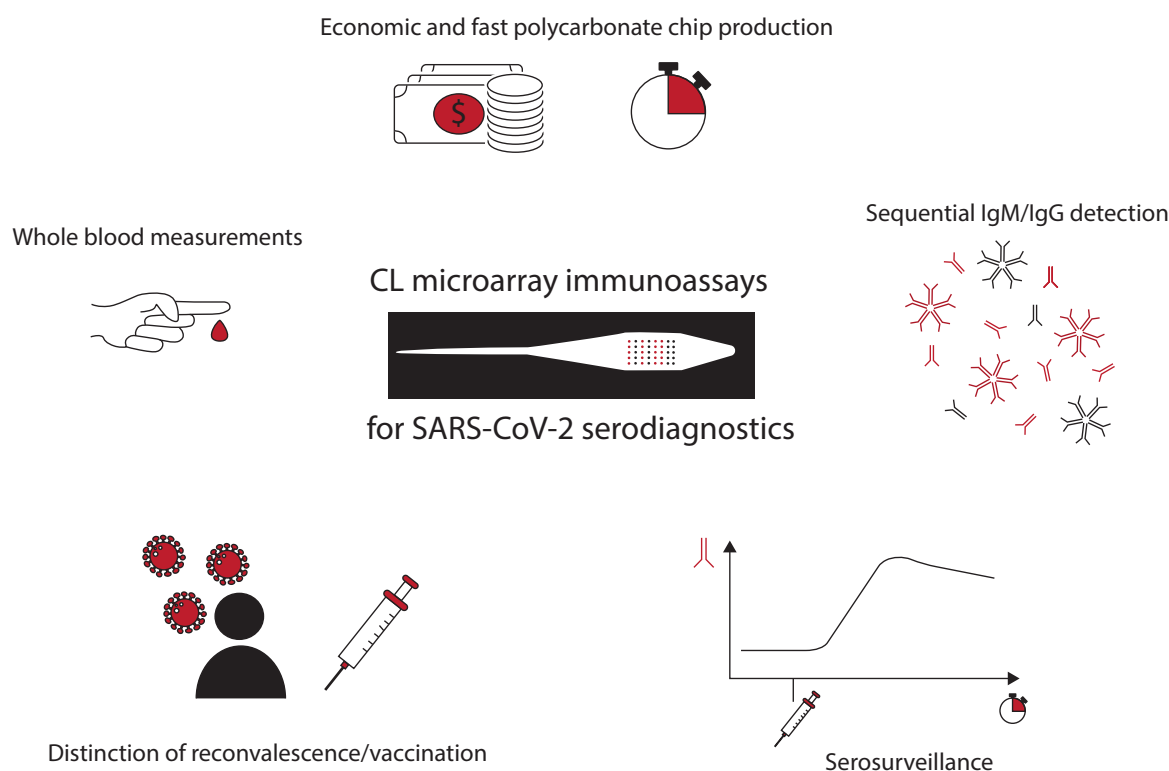
4.2.1 Publication Summary and Author Contributions

This publication was an expansion of the previous results in various aspects. First, a new measurement device (MCR-R) was available, so the measurement program had to be adapted. Secondly, the production of glass chips was very time extensive so that the application of easier to fabricate polycarbonate chips was tested and as a third aspect, a novel injection procedure was established to reduce the sample volume and the measurement duration. With the resulting polycarbonate microarray chips for CL-MIA measurements of SARS-CoV-2 antibodies on the MCR-R, it was possible to obtain qualitative results equal to those previously presented with glass chips in Publication 1 but with a reduction of measurement time by more than 50% (3 min 45 s) and a reduction of sample volume by 92% (8 µL). This general measurement principle was then applied to different research questions with respect to SARS-CoV-2. Thereby, it could be shown that a distinction of reconvalescent, vaccinated and naïve individuals was

possible due to the microarray character. For vaccinated individuals the possibility of close serosurveillance after vaccination was presented, which can prove very useful when deciding about the timing of booster vaccinations. While previous measurements had been done using serum or plasma samples, it was now shown that also whole blood can be applied without undesired matrix effects. This is of utmost importance for a possible application of the assay principle in POC diagnostics as it allows for the direct use without needing any sample pre-processing steps, making results available even faster. Additionally, one major improvement was the sequential detection of different antibody types. Previously, only IgG had been detected, while in this publication for the first time the sequential measurement of IgM and IgG was presented, giving important information about the time course of antibody formation.

Therefore, this publication presented an optimized assay and its versatility, making it applicable for numerous research questions comping up during the pandemic.

Own contribution:

- Design of experiments

- Development and extension of measurement program on MCR-R

- Conduction of measurements with support from S. Paßreiter (M. Sc. student supervised by J. Klüpfel) and N. Weidlein (Research intern supervised by J. Klüpfel)

- Data analysis

- Writing of manuscript

Fully Automated Chemiluminescence Microarray Analysis Platform for Rapid and Multiplexed SARS-CoV-2 Serodiagnostics

Julia Klüpfel, Sandra Paßreiter, Nina Weidlein, Martin Knopp, Martin Ungerer, Ulrike Protzer, Percy Knolle, Oliver Hayden, Martin Elsner, and Michael Seidel*

ACCESS | Metrics & More | Article Recommendations | SI Supporting Information

ABSTRACT: Lateral-flow immunoassays and laboratory diagnostic tests like enzyme-linked immunosorbent assays (ELISAs) are powerful diagnostic tools to help fight the COVID-19 pandemic using them as antigen or antibody tests. However, the need emerges for alternative bioanalytical systems that combine their favorable features—simple, rapid, and cost-efficient point-of-care (POC) analysis of lateral-flow immunoassays and higher reliability of laboratory tests—while eliminating their disadvantages (limited sensitivity and specificity of lateral-flow assays and prolonged time and work expenditure of laboratory analysis). An additional need met by only a few tests is multiplexing, allowing for the analysis of several immunorecognition patterns at the same time. We herein present a strategy to combine all desirable attributes of the different test types by means of a flow-based chemiluminescence microarray immunoassay. Laminated polycarbonate microarray chips were developed for easy production and subsequent application in the fully automated microarray analysis platform MCR-R, where a novel flow cell design minimizes the sample volume to 40 μL. This system was capable of detecting IgG antibodies to SARS-CoV-2 with 100% sensitivity and specificity using recombinant antigens for the SARS-CoV-2 spike S1 protein, nucleocapsid protein, and receptor binding domain. The analysis was accomplished within under 4 min from serum, plasma, and whole blood, making it also useful in POC settings. Additionally, we showed the possibility of serosurveillance after infection or vaccination to monitor formerly unnoticed breakthrough infections in the population as well as to detect the need for booster vaccination after the natural decline of the antibody titer below detectable levels. This will help in answering pressing questions on the importance of the antibody response to SARS-CoV-2 that so far remain open. Additionally, even the sequential detection of IgM and IgG antibodies was possible, allowing for statements on the time response of an infection. While our serodiagnostic application focuses on SARS-CoV-2, the same approach is easily adjusted to other diseases, making it a powerful tool for future serological testing.
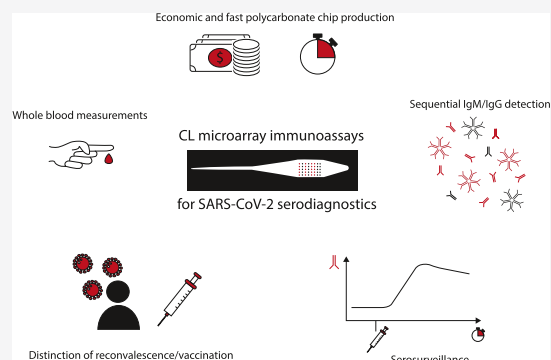
The SARS-CoV-2 pandemic has been affecting the world for almost 2 years already with more than 242 infections and more than 4.9 million deaths from COVID-19.[1] In the beginning of the pandemic, major research efforts focused on the development of polymerase chain reaction-based tests for the detection of active infection and on the development and authorization of vaccines that were pursued as our key back to normality. Since then, enormous scientific accomplishments have made it possible that by now, billions of people already obtained one of the available authorized vaccines.[2] But at the same time, new challenges are arising. To date, it is not completely clear what importance the antibody titer has for the protection against an infection with SARS-CoV-2,[3,4] especially as breakthrough infections are occurring after vaccination. Therefore, quantitative methods for rapid and thorough serosurveillance are crucial. Repeated multiplex assessment of antibody levels after vaccination can help detecting breakthrough infections that might otherwise go unnoticed as they often are asymptomatic. Broad monitoring in the population can help generate significant knowledge on the relevance of the antibody response for SARS-CoV-2, but to this end, rapid, inexpensive multiplex methods with minimal sample preparation and high sensitivity and specificity are required.

Currently available antibody tests for SARS-CoV-2 are widely applied and have been extensively reviewed.[5−9] Still, every serological test principle has its advantages and drawbacks, as outlined in our earlier publication.[10] For example, enzyme-linked immunosorbent assays (ELISAs)[11] give very reliable results and are well-suited for the simultaneous analysis of a large number of samples, but they

require trained staff and specialized laboratory equipment. This restricts their use to diagnostic laboratories and the results are not available immediately. When considering tests in point-of-care (POC) settings, for example, in medical practices or clinical settings, the main requirements are fast results at a relatively low sample throughput and easy handling and operation without the need for a laboratory environment. While most often lateral-flow assays (LFAs) are applied,[12] they usually lack multiplexing capacity and typically have lower diagnostic sensitivities and specificities compared to laboratory-based tests, which may give rise to false-positive as well as false-negative results.

Based on our expertise in automated, flow-based chemiluminescence microarray immunoassays (CL-MIAs),[13−17] we aimed to develop serological assays for SARS-CoV-2 that use three important SARS-CoV-2 antigens in parallel. A first prototype based on glass microarray chips from 2021[10] was promising, but not yet optimized for production cost or manufacturing time; further, except for a first proof-of-principle study, its range of possible applications was not yet explored.

Here, we therefore bring forward a new microarray chip design for fast and reliable analysis with a minimal sample volume of serum, plasma, or even whole blood. The production of polycarbonate microarray chips is much more time efficient than using glass slides. This strategy had previously only been used for the detection of DNA and small molecules,[18] while herein the first application in the detection of antibodies from blood samples is shown. Specifically, for blood matrices, sensitivity is normally compromised by high unspecific binding, which needs to be avoided by surface blocking.[19] Here, we were able to develop a chemically modified chip surface that can be used without any blocking procedure, thus dramatically reducing background interferences and manufacturing time. Second, we developed a sample injection procedure on a new benchtop analysis device. This design proved instrumental in preventing the carry-over of the sample between measurements, significantly reducing the necessary sample volume to below 20 μL (8−16 μL depending on the sample type), which would make fingerstick blood tests possible. Reducing the measurement time to under 4 min is an important feature for onsite testing and is even faster than most of the common LFA "rapid antibody tests".

Third, after showing the general analytical performance of the novel microarray chip, we demonstrate a range of important serodiagnostic applications, with focus on multiplex detection of antibodies: (i) to distinguish vaccinated and convalescent individuals, (ii) for thorough monitoring in the population after vaccination to serologically detect asymptomatic breakthrough infections as well as critical reduction of antibody titer over time, (iii) for sequential automated detection of different antibody classes, and (iv) to enable the use of whole blood for the measurements. Taken together, these features make the microarray chip attractive for applications in decentralized or even POC settings with little to no sample preparation.

■ EXPERIMENTAL SECTION

Chemicals, Reagents, and Materials. All chemicals, unless stated otherwise, were purchased from Sigma-Aldrich, subsidiary of Merck (Darmstadt, Germany) and Carl Roth (Karlsruhe, Germany). Chemiluminescence (CL) reagents were used from the Elistar Supernova reagent kit from Cyanagen (Bologna, Italy). A peroxidase-labeled anti-human

IgG antibody (Fc fragment) from goat was purchased from Sigma-Aldrich (A0170, 5.6 mg mL^{-1}) in addition to a peroxidase-labeled anti-human IgM antibody (μ-chain specific) from goat (A6907-1 mL, 0.55 mg mL^{-1}). Spotting and running buffer was produced as described elsewhere.[10]

SARS-CoV-2 Antigens. Recombinant SARS-CoV-2 spike S1 protein with mouse Fc-tag (expressed in HEK293 cells) was purchased from Biozol (Eching, Germany) and produced by Sino Biological (Beijing, China). Recombinant SARS-CoV-2 spike RBD protein with His-tag and recombinant SARS-CoV-2 nucleocapsid protein with Strep-tag were produced by ISAR Bioscience (Planegg, Germany), as described elsewhere.[10]

Blood Samples. Blood samples were either purchased from Sigma-Aldrich (Darmstadt, Germany), obtained from the Institute of Virology, Technical University of Munich (Munich, Germany), or from ISAR Bioscience (Planegg, Germany). All procedures were in accordance with the Helsinki Declaration of 1975, as revised in 2000. All patient data were anonymized before the measurements. Patient samples were handled in laboratories approved for biosafety level 2.

Microarray Chip Production. The immunoassay was performed on polycarbonate (PC) surfaces with chemical modifications based on a procedure described elsewhere.[15,18] In short, a polyetheramine with terminal carboxylate functionality on one terminus was produced by chemically modifying Jeffamine ED-2003 with succinic anhydride by dissolving the reagents in toluene, stirring at room temperature overnight, and removing the toluene. Chips were then coated with this modified Jeffamine by screen printing, heated to 100 °C for 2 h, washed with water, and stored at low humidity until protein immobilization was performed.

Covalent protein immobilization was accomplished using the EDC/s-NHS strategy. To prepare the coupling reagents, 1 mg mL^{-1} 1-ethyl-3-(3-dimethylaminopropyl)carbodiimide (EDC) and N-hydroxysulfosuccinimide (s-NHS) were added to the spotting buffer. Antigen solutions (without further dilution) and positive controls (1:2 diluted with spotting buffer) were then mixed with EDC/s-NHS solution (50% v/v). Anti-peroxidase and anti-human IgG antibodies were used as the positive control, while spotting buffer was applied as the negative control. For IgM measurements, anti-human IgM antibody was used as an additional positive control. Onto a 384-well plate, 20 μL per spotting solution was transferred and inserted into the microcontact spotter together with the prepared PC chips. Spotting was done in five replicates for each spotting solution with a grid spacing of 1100 μm distance between replicates and 1040 μm distance between the spotted rows. The maximum number of different spotting solutions was 20. The spotting process was carried out at 20 °C and 55% humidity. After spotting, the chips were assembled directly by connecting them to a POM carrier containing inlet and outlet holes using double-sided adhesive foil with cut-outs forming the flow channel. All chips were stored at 4 °C until measurement. No blocking of the chips was required.

Microarray Measurements. Prior to measurements on the microarray chip reader MCR-R, the system was flushed with water. Subsequently, the CL reagents luminol and hydrogen peroxide were inserted into the device as well as the respective detection antibody solutions (peroxidase-labeled anti-human IgG diluted 1:1000 with running buffer; additionally, for IgM measurements, peroxidase-labeled anti-human IgM diluted 1:1000 with running buffer) and all tubes were
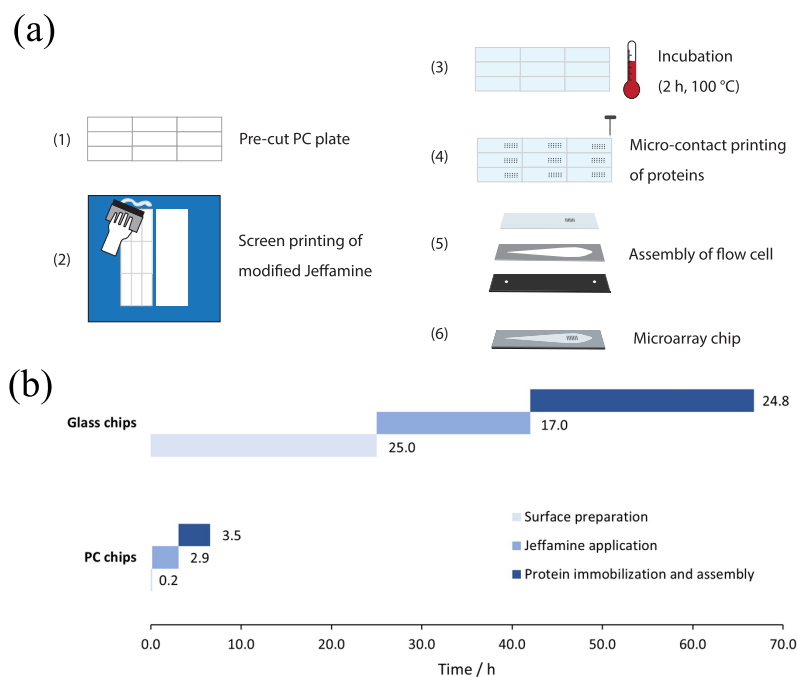
Figure 1. (a) Schematic overview of the PC chip production process, and (b) comparison of production times for glass and PC microarray chips.

loaded with the corresponding liquids. In the beginning of each measurement day, a darkframe image was recorded for an exposure time of 60 s for consideration of the CCD camera background signal. For measurements, 40 μL of diluted serum, plasma, or whole blood sample were injected into the chip. The dilution was performed with running buffer, where the dilution factor depended on the respective sample type. The chip was then inserted into the MCR-R chip tray and the measurement was started. The fully automated flow-based assay then consisted of detection of antibody transport over the chip and subsequent flushing and injection of luminol and hydrogen peroxide. The image was acquired for 60 s, followed by a final flush of the chip.

For the sequential IgM/IgG detection, an incubation time before the measurement was necessary (60 s), followed by the previously described process that was carried out for both the IgM detection antibody and the IgG detection antibody. The total measurement duration for single IgG acquisition was 3 min 45 s, while the sequential IgM/IgG detection took 7 min 55 s (including 60 s sample incubation). A more detailed overview of the assay steps, volumes, and flow rates is given in the Supporting Information (Table S1).

Data Evaluation. The detected CL signals were stored as txt-files and processed with the evaluation software MCR spot reader (Stefan Weißenberger, Munich, Germany). On the darkframe-corrected CL images, a grid was emplaced to define the position of the spots. For each spot, the mean value of 10 brightest pixels was calculated. Means and standard deviations were obtained for the five replicates per row, and spots that deviated more than 10% from the mean were excluded. The resulting mean values and standard deviations for all rows were used for further analysis and graphical evaluation with Python 3.

■ **RESULTS AND DISCUSSION**

Development of a CL-MIA on PC Microarray Chips. We previously reported the development of a SARS-CoV-2 antibody microarray immunoassay based on glass microarray chips as a proof of principle for future application in serodiagnostics. Herein, we present a much-improved microarray chip approach using a new chip material together with a newly developed flow cell layout and a novel sample injection principle as well as first examples for possible applications of this microarray chip in the field of SARS-CoV-2 POC serodiagnostics.

A major advantage of the new chip principle is the reduced production time and cost to make the microarray chips competitive for commercial POC antibody tests. For the previously described glass chips, a total production time of about 66 h over 4 days was needed to produce chips for 18 measurements.[10] The process involved three overnight incubation steps as well as lengthy washing and activation steps, as laid out in a more detailed tabulation from Bemetz et al.[18]

For the PC chips described herein, Jeffamine ED-2003 was modified with a carboxylate functionality on one terminus to allow protein immobilization as had been shown before.[18] This modified Jeffamine paste was applied to the preslitted PC plates using screen printing and subsequently let to react at an elevated temperature for 2 h. Afterward, spotting was accomplished using EDC/s-NHS coupling chemistry, activating the carboxylate functionalities on the chip surface and covalently immobilizing the proteins via amino groups from amino acid side chains as shown in the Supporting Information (Figure S1). For this immobilization procedure, no lengthy activation of the complete surface was necessary, as the activation reagents were spotted on the chip together with the respective proteins. Furthermore, experiments showed that overnight incubation of the chips after spotting can be disregarded reducing the total production time by 90% to 6.6 h, as also illustrated in Figure 1, together with a schematic overview of the whole production process.

In addition, the production of PC chips proved significantly cheaper, with the cost of raw materials and chemicals per chip
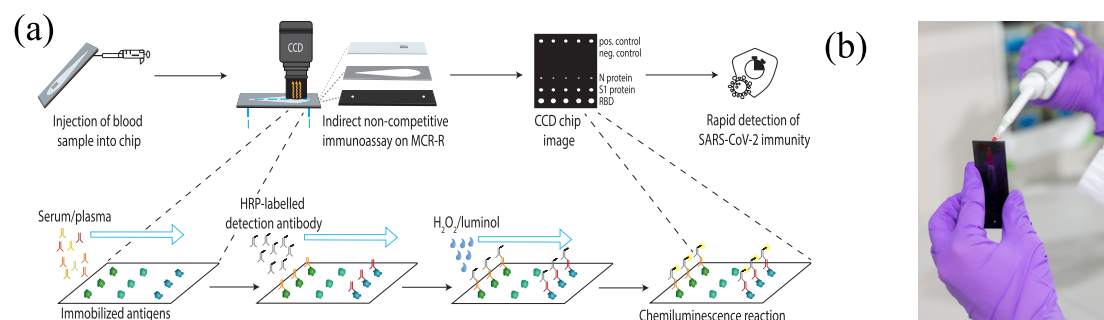
Figure 2. (a) Measurement process of the indirect noncompetitive microarray immunoassay with manual sample injection and (b) image of the sample injection process.

below 2€ for PC compared to 30€ for glass chips, lower reagent expense for PC chip production, and also significantly lower work expenditure.

For measurements of the novel PC chips, herein, a new analysis platform (MCR-R by GWK Präzisionstechnik) is presented for the first time. This benchtop device is optimized for POC applications: it is relatively small and does not require a specialized laboratory surrounding for operation. It contains storage containers for system liquids, a microarray chip loading unit, and a CCD camera. More detailed information on the device can be found in the Supporting Information.

While formerly, a sample syringe was used to transport serum or plasma samples to the microarray chip, we developed a direct chip injection method for the PC microarray chips using customary pipettes. Therefore, significantly less sample volume is needed and no relevant contamination of the device with human blood takes place. This makes the process applicable to consecutive measurements of samples from different people without carry-over. Additionally, the direct chip injection allows a very short measurement time of 3 min 45 s.

After the insertion of the chip into the device, it is flushed automatically, and the detection antibody is flown over the chip slowly. After another flushing step, the chip is filled with a luminol/hydrogen peroxide mixture and a CCD image is taken. The whole process of this indirect noncompetitive immunoassay is shown in Figure 2.

To minimize the sample volume and to allow for a uniform distribution of the sample in the chip upon injection, different flow cell designs were tested. Figure 3 shows some of the most promising designs, with (I) being the standardized flow cell layout that had been used for all previous designs. Layouts (II) and (III) aimed on canalizing the sample flow upon injection
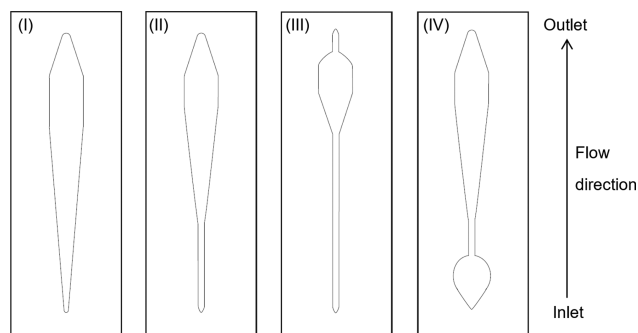
to mimic the flow obtained by injection via a syringe pump and tubes, while at the same time reducing the necessary sample volume by minimizing the width of the flow cell. Design (IV) contains a sample reservoir to compensate for variations in injection speed during the course of manual pipette injection.

Testing of the different flow cells showed that the average signal intensities were comparable for all designs, but designs (II), (III), and (IV) showed a more even distribution of samples within the chip, while for design (I), bubble formation occurred more frequently leading to unwetted areas within the flow cell. When also considering the sample volume and spot area, design (II) was chosen, as it reduced the necessary volume from about 60 μL for design (I) to 40 μL, but still left a spot area big enough for future expansion of the chip to accommodate additional spotted rows.

To test for the optimal sample dilution when directly injecting the sample into the chip compared to the previous device-based injections, 1:2, 1:5, and 1:10 dilutions of serum samples (40 μL sample volume containing 20, 8, or 4 μL of serum, respectively) were measured by direct injection and the results for the background signal, SARS-CoV-2 receptor binding domain (RBD), and N protein were compared to values obtained by the sample syringe injection of a 1:10 dilution (1 mL sample volume containing 100 μL of serum).

The results are shown in Figure 4, demonstrating a clear correlation between the sample dilution and CL intensity for the tested negative (sample 1) and positive (samples 2–4) samples. Dilution of negative sample 1 shows that the background signal increased slightly with increasing serum amount but was still very low, resulting in a good signal-to-noise ratio. For the negative sample, the signals for the SARS-CoV-2 antigens are in the range of the background with the exception of the N protein signal for syringe injection, indicating slight unspecific or cross-reactive binding of IgG antibodies to the immobilized protein during the long sample interaction time (200 s), while the shorter interaction time for the direct chip injection seems to be beneficial. For the positive samples, a significantly elevated CL signal compared to the negative sample 1 was found for all dilutions. As expected, lower amounts of serum in the sample resulted in lower signals. It was decided to use a dilution of 1:5 for all further measurements as it represents a good compromise between the low sample volume (8 μL) and high CL signal.

After defining the standard conditions for measurements on the MCR-R as PC chips (spotted using EDC/s-NHS) with direct injection of 40 μL of 1:5 serum dilution, these optimized conditions were benchmarked against the results obtained previously with glass chips by applying the traditional
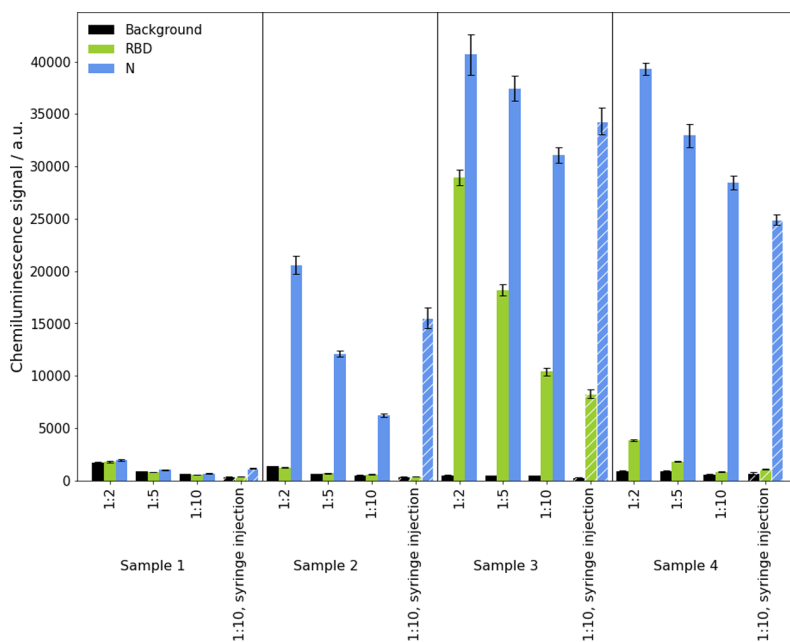

Figure 3. Different flow cell designs. The immobilized spots are located in the upper third of the flow cell.

Figure 4. Measurements of four different SARS-CoV-2 serology-negative (sample 1) or serology-positive (samples 2−4) serum samples on PC microarray chips in different dilutions by direct chip injection (filled bars) and syringe injection (hatched bars) (error bars indicate the standard deviation of replicate spots on the chip, $n = 5$).
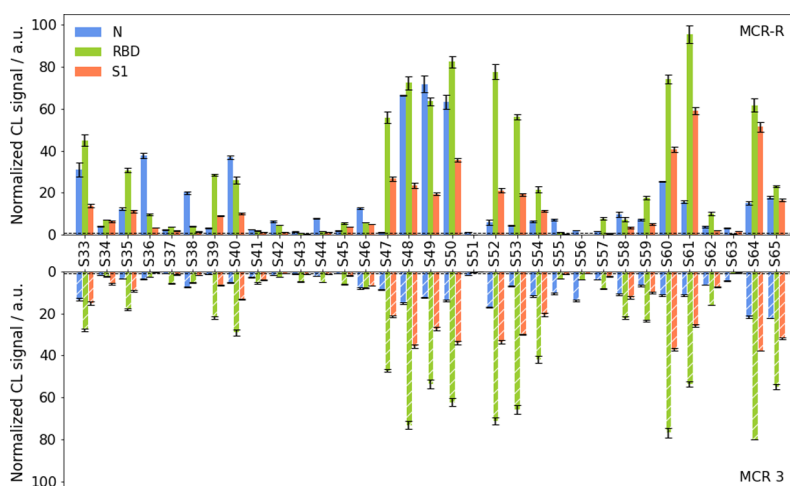

Figure 5. Performance comparison for the optimized assay on MCR-R (top) and the previous assay on MCR 3 (bottom) on a sample set of 33 SARS-CoV-2 serology-positive samples (CL values are background-corrected and normalized with respect to the cut-off values, cut-off value shown with dotted lines, error bars indicate the standard deviation of replicate spots on the chip, $n = 5$).

automated injection mode. Therefore, the same set of 65 positive or negative samples that had been used for the assessment of the glass chips (preclassified using commercial antibody tests)[10] were measured using the novel PC chips and the results were compared directly. The receiver operating characteristic (ROC) curve analysis (ROC curves shown in the Supporting Information) gave cut-off values after background correction of 560 for the N protein (glass chips: 2860), 1000 for the S1 protein (glass chips: 1700), and 400 for the RBD (glass chips 3:800). While all cut-offs could be notably reduced, the greatest change was obtained for the N protein, supporting the hypothesis of reduced binding of potentially cross-reactive antibodies upon shorter sample interaction time. Such binding might result from antibodies to structurally closely related endemic coronaviruses[20−22] that show lower

affinity to the SARS-CoV-2 N protein compared to specific antibodies and thus only bind when left to interact for a longer time span, as in the case of syringe injection.

With these optimized cut-off values, it was possible to determine the results below the cut-off for all 32 negative samples. The results of the 33 positive samples (normalized with respect to the cut-off values) can be seen in Figure 5. On the top, the new results are shown, while on the bottom, the previously published results for glass chips are depicted. It can be clearly seen that analogous trends in signal intensity are found for both assays. Differences in intensity for the N protein can be attributed to the significantly reduced cut-off value, while the overall reduced signal for some samples was probably caused by the storage of the samples for about 6 months between the measurements.

Figure 6. CCD chip images of measurements of (a) SARS-CoV-2 serology-negative sample, (b) sample from a vaccinated individual, and (c) sample from a COVID-19 reconvalescent person (column 1: negative control, column 2: RBD, column 3: S1 protein, column 4: N protein, column 5: positive control, rows A−E represent replicates of the same spot).
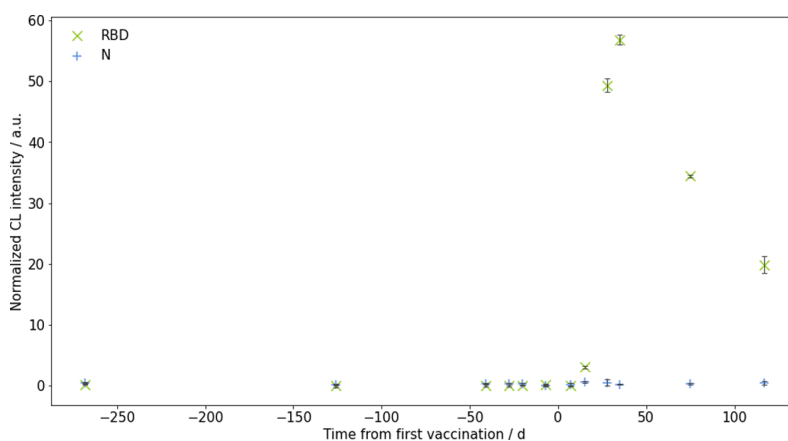

Figure 7. Repeated antibody determination of the same person before and after vaccination with the Biontech/Pfizer mRNA vaccine (vaccination on days 0 and 21, values are background-corrected and normalized with respect to cut-off, error bars indicate the standard deviation of triplicate measurements).

In the PC chip assay, all positive samples gave a signal above the cut-off value for at least one of the three proteins, which is the decision criterion for classification of a sample as positive. Therefore, it is concluded that the novel PC chip assay with its 100% diagnostic sensitivity and specificity can keep up with the previously reported glass chips regarding the correct sample classification, while at the same time showing various advantages as described beforehand.

Application for Distinction of Reconvalescent and Vaccinated Individuals. The most common SARS-CoV-2 antibody tests suffer from the restriction of relying on only one antigen. When only antibodies to the N protein are registered, they are only suitable for the detection of antibodies after infection. In contrast, tests that rely on the S protein or the RBD pattern cannot distinguish whether antibodies were formed as a reaction to vaccination or as a result of previous infection. In contrast, with the microarray chips presented herein, it can clearly be distinguished whether antibodies were formed after infection or vaccination due to the multiplex nature of the microarray. Figure 6 shows examples of chip images of different serotypes: a COVID-19 serology-negative sample that only gives a signal for the positive control in column 5 (Figure 6a), a sample from a vaccinated person (Figure 6b) that shows an elevated signal for the S1 protein (column 3) and the RBD (column 2), and a sample from a reconvalescent COVID-19 patient (Figure 6c) that also presents antibodies to the N protein (column 4). This feature of the test can be very helpful to detect whether a vaccinated person was infected despite the protection posed by the vaccination.

Application in Serosurveillance after Vaccination. After the start of COVID-19 vaccination campaigns in the end of 2020, interest arose in the durability of the antibody response after vaccination and the possibility of breakthrough infections. Therefore, we investigated whether the test principle presented herein is suitable for monitoring the antibody status after vaccination and possibly detecting asymptomatic breakthrough infections. Therefore, samples of an individual were taken at 12 different time points in a period between 268 days before vaccination with the Pfizer/Biontech vaccine until 117 days after the first vaccine dose (96 days after the second dose). Figure 7 shows the resulting normalized CL intensities for measurements of the N protein as well as the RBD.

It can be clearly seen that the signal for the N protein remains relatively constant during the whole time span. The normalized values lie between 0.06 and 0.54 au and are therefore way below the cut-off value of 1.0, which shows that no SARS-CoV-2 breakthrough infection of the proband occurred during the time span of the measurements. If an infection had occurred, it would have been noticed in an increase of the N signal as well as the RBD signal, and therefore, a possibly otherwise unnoticed infection could have been detected serologically. For the RBD, values below the cut-off are found at all times between 268 days before vaccination until 7 days after the first vaccine dose (normalized signal between −0.03 and 0.18 au), while at 15 days after the first vaccination, the signal already reached a value of 3.10 au, a factor of 3.1 above the cut-off. The maximum signal was reached about 3 weeks later (35 days after the first dose, 14 days after the second dose) with a signal of 56.83 au. These results are in very good agreement with the results from the Pfizer/Biontech clinical study.[23] Further measurements at 75 and 117 days after the first vaccine dose then showed a
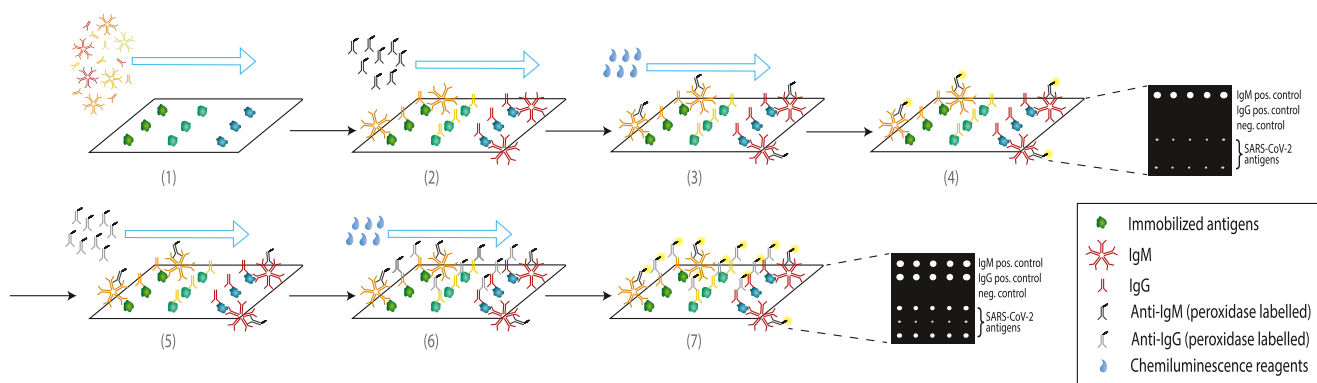
Figure 8. Schematic representation of the sequential IgM/IgG assay on the MCR-R with the assay steps (1) sample injection, (2)/(5) detection antibody flow, (3)/(6) CL reagents flow, and (4)/(7) CCD image acquisition. During the measurement process, two images are recorded that can easily be distinguished and assigned by considering the IgM/IgG-positive control rows.
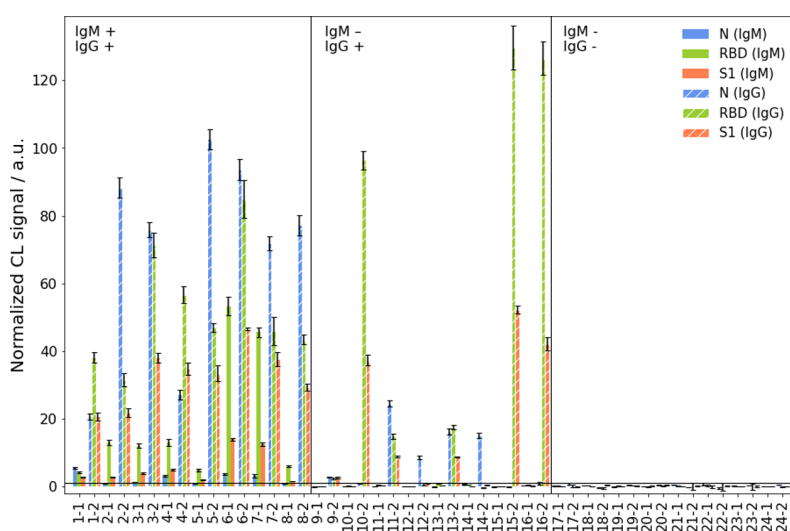

Figure 9. Sequential detection of SARS-CoV-2 IgM and IgG for samples containing either both antibody classes (left), only IgG (middle), or none (right). Filled bars represent IgM measurements (sample denominator -1), while hatched bars represent IgG measurements (sample denominator -2) (CL values are background-corrected and normalized with respect to cut-off values, error bars indicate the standard deviation of replicate spots on the chip, $n = 5$).

declining signal with 34.41 and 19.88 au, respectively. This was also in accordance with the expectations due to the short half-life of the mRNA from the vaccine in the human body and the findings from reconvalescent patients, which also showed a notable loss of antibodies over the course of few months after infection. The same trend is probable after vaccination and could serve as an indicator that a regular booster vaccination may be necessary.

Therefore, our PC microarray chips can be used for continuous monitoring of antibody titers after vaccination for the serological detection of breakthrough infections and also as an application in rapid titer control to decide whether a booster vaccination might be necessary if values below the cut-off are found. Currently, there is ongoing discussion about the significance of antibody levels as more and more breakthrough infections after vaccination occur. To date, it is still not completely clear whether there is a correlation between antibody titer and the risk for a breakthrough infection so that thorough serological monitoring is crucial to gain representative information. But while we herein only show this scope of application for SARS-CoV-2, an adaptation of the test for other diseases can easily be accomplished, paving the

way for a rapid general vaccination control as may be advisable, for example, by medical officers for people working in areas of particular risk of certain diseases.

Application for the Rapid, Sequential Detection of IgM and IgG Antibodies. All results presented so far refer to the detection of IgG antibodies that usually start to form a few weeks after an infection. Even before that, IgM antibodies are formed so that a detection of both IgM and IgG can give important information about the course of an infection, even though it has been shown that for COVID-19, IgM production occurs relatively late and therefore not notably before IgG can be detected already.[24,25] But still, information about the presence or absence of IgM antibodies is valuable in assessing how long ago the infection has occurred as the IgM titers plummet faster than the IgG titers.

Therefore, we developed a sequential IgM/IgG assay that allows for the detection of both antibody classes within one measurement in under 8 min. The assay principle is shown in Figure 8 with the first step being the manual sample injection. Afterward, the chip is incubated for 60 s at room temperature to allow the sterically demanding IgM pentamers to bind to the immobilized proteins. Subsequently, the anti-IgM detection

antibody is washed over the chip, followed by luminol and hydrogen peroxide and image acquisition. The second assay part then is analogous to the assay of IgG only and repeats the IgM assay steps with the anti-IgG detection antibody. In the second image acquisition, the combined signal from the labeled anti-IgM and anti-IgG antibodies is recorded as the antibodies from the first assay step are still bound to the chip. Hence, one has to subtract the signal from the IgM image from the second image's signal to calculate the IgG signal.

Figure 9 shows the results of sequential IgM/IgG measurements for a total of 24 samples that had been classified by the Institute of Virology of TUM using an YHLO iFlash antibody test. Eight of them had been determined as IgM- and IgG-positive for SARS-CoV-2, another eight were IgG-positive but not IgM-positive, and eight were negative controls. The calculation of the pure IgG signal was done as well as a background correction and normalization with respect to the cut-off values that had been defined for the singular IgG assay. For each sample, two groups of bars are presented, the first one representing the IgM signal and the second one representing the IgG signal.

For all samples, a correct classification was possible. For the IgM- and IgG-positive samples, values above the cut-off for at least one of the proteins were obtained in all IgM and IgG measurements. For the negative control samples, all detected signals were found below the cut-off values. The IgM-negative, IgG-positive samples all gave a positive signal in the IgG measurements, while being negative in the IgM measurements. Therefore, our test can be applied for the rapid sequential detection of IgM and IgG in a single measurement, giving indications about the onset of antibody production. Additionally, the intensity values also give indications on the amount of antibodies formed. Application of this assay principle may be even more helpful for application to other diseases that show an earlier beginning of IgM production so that an even more detailed temporal classification of an infection is possible.

Another important remark is that even incubation times of 60 s after the sample injection into the chip do not lead to false-positive results, indicating very low unspecific binding for intermediate incubation times. The same cut-off values can be applied to measurements directly after injection and measurements after incubation, making the assay stable against slight delays in the sample injection and chip insertion that might occur in a clinical setting. Additionally, it was shown that the binding of antibodies to the immobilized antigens is very stable and flushing of the chip does not remove notable amounts of bound antibodies, preventing false-negative results in the IgG measurement.

Application for the Rapid Point-of-Care Detection of Antibodies in Whole Blood. All results presented so far were obtained using plasma or serum samples, which is common in immunoassays such as ELISAs, but have disadvantages as the sample preparation by centrifugation is necessary. When using whole blood for the antibody determination, this separation step can be omitted, but often problems such as high background, contamination of devices with cells, or unspecific binding of sample components occur, leading to false-positive results.

For the PC microarray chips presented here, a low influence of these aspects was expected due to the short interaction times of the sample and chip surface. Previous measurements had shown low background values for serum and plasma measurements. Consequently, we compared plasma and

anticoagulated whole blood samples from the same donors (21 different samples). Due to the hematocrit (volume percentage of red blood cells in whole blood, usually ∼50% of the blood volume), twice the volume of whole blood was used compared to plasma (16 and 8 μL, respectively) and filled to 40 μL with the running buffer. Chips were then measured directly without incubation, giving background values in the same range for plasma and whole blood.

As no elevation of the background occurred when using whole blood, the resulting signals for the SARS-CoV-2 antigens from plasma and whole blood were compared. The results are shown in Figure 10 with readout intensity of plasma samples
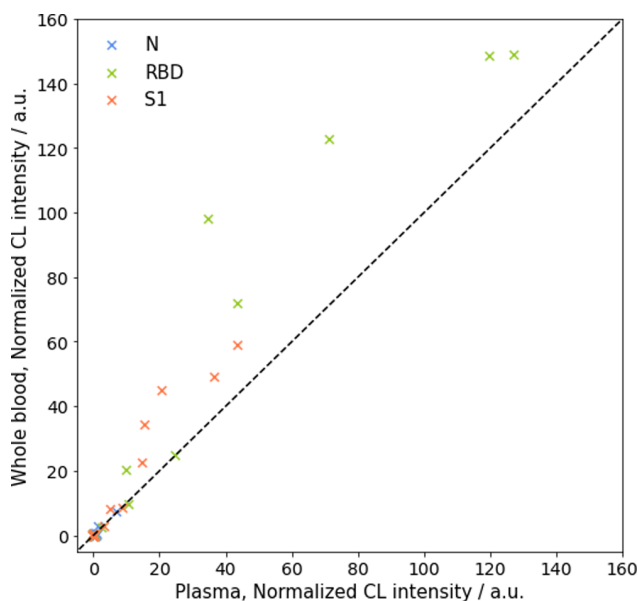

Figure 10. Comparison of results from whole blood and plasma measurements for a set of 21 samples (CL values are background-corrected and normalized with respect to cut-off values).

on the x-axis and whole blood samples on the y-axis (after background correction and normalization with respect to the previously defined cut-off values). A very good correlation is found especially for low CL signals corresponding to negative samples. Importantly, no data point is misclassified when comparing the analysis of whole blood and plasma, making both sample types applicable for the detection of SARS-CoV-2 antibodies in blood. Remarkably, again the same cut-off value can be used for both whole blood and plasma, as already characterized for IgM and IgG.

When looking at positive samples, still the same clear trends are seen in whole blood and plasma but with slightly higher deviations from the diagonal of the regression line in Figure 10. For the positive samples measured herein, generally higher signals are found for whole blood compared to plasma. A reason for this observation might be found in the hematocrit effect, as the exact amount of solid and liquid components in each blood sample is unknown. But as this outcome was seen for different samples whereas no positive sample gave a notably higher signal in plasma compared to whole blood, another reason is possible as well, for example, systematic losses of antibodies during the sample preparation to obtain plasma. Nevertheless, as the presented test does not aim at giving quantitative results but only at classifying samples as positive or

negative, it is concluded that whole blood can be applied as a sample material just as good as plasma.

This makes the assay even more interesting for POC applications, as the necessary amount of 16 μL of whole blood per measurement might even be obtained from a finger prick. Blood could then be transferred directly into the chip, making the bedside sampling and direct analysis possible without the sample preparation time. Due to the direct chip injection, the main part of the measurement device MCR-R is not contaminated with blood upon measurement, allowing for measurements of different patients without any risk of carry-over.

◼ CONCLUSIONS

We herein present for the first time the performance of a new PC-based microarray chip for use in SARS-CoV-2 serodiagnostics on the microarray platform MCR-R. The new development pushes the boundaries toward competitive performance in realistic applications: it gives significantly faster results in under 4 min, is cost-economic, and avoids contamination of the device with body fluids by use of one-way microarray chips. Only small sample volumes are necessary, and no extensive sample preparation is required. This makes the device promising for POC applications for SARS-CoV-2 and other serologically interesting diseases.

Some of them were already demonstrated herein, namely, progress measurements after vaccination, distinction of antibodies formed after SARS-CoV-2 infection, and vaccination and rapid sequential detection of IgM and IgG antibodies. Furthermore, whole blood can be used as a sample, making it especially interesting in POC settings as no extensive sample preparation is necessary and blood from a finger prick can be transferred to the device, giving results within minutes.

With all of these advantages, the new microarray chip outperforms many commercial tests by its versatility that still leaves potential for various further serodiagnostic objectives and improvements. While so far, we only focused on SARS-CoV-2 serological questions, the microarray can easily be adapted or extended to also cover serologic analyses for other diseases by simply adding further proteins to the array. Trials with influenza proteins and endemic coronaviruses are already in planning. For the future, we envision that our approach may allow for a complete vaccination status check-up within one single measurement in few minutes from a drop of blood.

◼ ASSOCIATED CONTENT

Ⓢ Supporting Information

The Supporting Information is available free of charge at https://pubs.acs.org/doi/10.1021/acs.analchem.1c04672.

Additional assay details including reaction schemes; figures for obtained ROC curves; and photographs and detailed description of the analysis platform (PDF)

◼ AUTHOR INFORMATION

Corresponding Author

Michael Seidel − *Institute of Hydrochemistry, Chair of Analytical Chemistry and Water Chemistry, Technical University of Munich, 85748 Garching, Germany;* ⓞ orcid.org/0000-0002-1961-5641; Email: michael.seidel@mytum.de

Authors

Julia Klüpfel − *Institute of Hydrochemistry, Chair of Analytical Chemistry and Water Chemistry, Technical University of Munich, 85748 Garching, Germany*

Sandra Paßreiter − *Institute of Hydrochemistry, Chair of Analytical Chemistry and Water Chemistry, Technical University of Munich, 85748 Garching, Germany*

Nina Weidlein − *Institute of Hydrochemistry, Chair of Analytical Chemistry and Water Chemistry, Technical University of Munich, 85748 Garching, Germany*

Martin Knopp − *Heinz-Nixdorf-Chair for Biomedical Electronics, Technical University of Munich, TranslaTUM, 81675 München, Germany*

Martin Ungerer − *ISAR Bioscience GmbH, 82152 Planegg, Germany*

Ulrike Protzer − *Institute of Virology, Technical University of Munich/Helmholtz Zentrum München, 81675 München, Germany; German Center for Infection Research (DZIF), 81675 München, Germany*

Percy Knolle − *Institute of Molecular Immunology/ Experimental Oncology, Technical University of Munich, 81675 München, Germany*

Oliver Hayden − *Heinz-Nixdorf-Chair for Biomedical Electronics, Technical University of Munich, TranslaTUM, 81675 München, Germany*

Martin Elsner − *Institute of Hydrochemistry, Chair of Analytical Chemistry and Water Chemistry, Technical University of Munich, 85748 Garching, Germany;* ⓞ orcid.org/0000-0003-4746-9052

Complete contact information is available at: https://pubs.acs.org/10.1021/acs.analchem.1c04672

Author Contributions

J.K. conceived the experiments; J.K., S.P., and N.W. conducted the experiments under the supervision of J.K.; J.K. analyzed the results and wrote the manuscript with input from the co-authors; M.K. adapted the MCR-R software for sequential measurements; M.U. provided recombinant SARS-CoV-2 RBD and N protein; U.P. and P.K. provided patient samples; O.H. provided Bio2 laboratory workspace at TranslaTUM; and M.E. and M.S. supervised the project and were responsible for funding acquisition and resources.

Notes

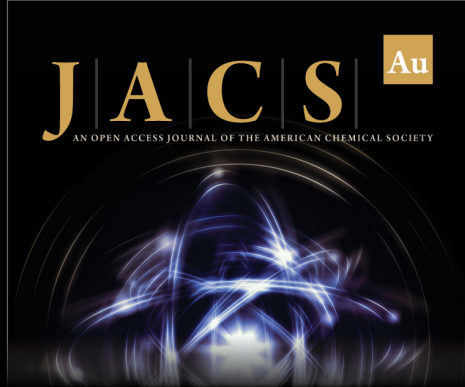The authors declare no competing financial interest.

◼ ACKNOWLEDGMENTS

◼ REFERENCES

(1) World Health Organization. WHO Coronavirus disease (COVID-19) dashboard. https://covid19.who.int/ (accessed Sep 15, 2021).

(2) Ritchie, H.; Mathieu, E.; Rodés-Guirao, L.; Appel, C.; Giattino, C.; Ortiz-Ospina, E.; Hasell, J.; Macdonald, B.; Beltekian, D.; Roser, M. Coronavirus Pandemic (COVID-19) *Our World in Data* 2021.

(3) Føns, S.; Krogfelt, K. A. *Pathog. Dis.* 2021, 79, No. ftaa069.

(4) Abbasi, J. *JAMA* 2021, 326, 1781−1782.

(5) Tantuoyir, M. M.; Rezaei, N. *Cell Biol. Int.* 2021, 45, 740−748.

(6) Lisboa Bastos, M.; Tavaziva, G.; Abidi, S. K.; Campbell, J. R.; Haraoui, L.-P.; Johnston, J. C.; Lan, Z.; Law, S.; MacLean, E.; Trajman, A.; Menzies, D.; Benedetti, A.; Ahmad Khan, F. *BMJ* **2020**, *370*, No. m2516.

(7) Kubina, R.; Dziedzic, A. *Diagnostics* **2020**, *10*, No. 434.

(8) Adams, E. R.; Ainsworth, M.; Anand, R.; Andersson, M. I.; Auckland, K.; Baillie, J. K.; Barnes, E.; Beer, S.; Bell, J. I.; Berry, T.; Bibi, S.; Carroll, M.; Chinnakannan, S. K.; Clutterbuck, E.; Cornall, R. J.; Crook, D. W.; Silva, T. de.; Dejnirattisai, W.; Dingle, K. E.; Dold, C.; Espinosa, A.; Eyre, D. W.; Farmer, H.; Fernandez Mendoza, M.; Georgiou, D.; Hoosdally, S. J.; Hunter, A.; Jefferey, K.; Kelly, D. F.; Klenerman, P.; Knight, J.; Knowles, C.; Kwok, A. J.; Leuschner, U.; Levin, R.; Liu, C.; López-Camacho, C.; Martinez, J.; Matthews, P. C.; McGivern, H.; Mentzer, A. J.; Milton, J.; Mongkolsapaya, J.; Moore, S. C.; Oliveira, M. S.; Pereira, F.; Perez, E.; Peto, T.; Ploeg, R. J.; Pollard, A.; Prince, T.; Roberts, D. J.; Rudkin, J. K.; Sanchez, V.; Screaton, G. R.; Semple, M. G.; Slon-Campos, J.; Skelly, D. T.; Smith, E. N.; Sobrinodiaz, A.; Staves, J.; Stuart, D. I.; Supasa, P.; Surik, T.; Thraves, H.; Tsang, P.; Turtle, L.; Walker, A. S.; Wang, B.; Washington, C.; Watkins, N.; Whitehouse, J. *Wellcome Open Res.* **2020**, *5*, No. 139.

(9) Carinci, F.; Moreo, G.; Limongelli, L.; Testori, T.; Lauritano, D. *Appl. Sci.* **2020**, *10*, No. 4506.

(10) Klüpfel, J.; Koros, R. C.; Dehne, K.; Ungerer, M.; Würstle, S.; Mautner, J.; Feuerherd, M.; Protzer, U.; Hayden, O.; Elsner, M.; Seidel, M. *Anal. Bioanal. Chem.* **2021**, *413*, 5619−5632.

(11) Liu, W.; Liu, L.; Kou, G.; Zheng, Y.; Ding, Y.; Ni, W.; Wang, Q.; Tan, L.; Wu, W.; Tang, S.; Xiong, Z.; Zheng, S. *J. Clin. Microbiol.* **2020**, *58*, No. e00461-20.

(12) Trombetta, B. A.; Kandigian, S. E.; Kitchen, R. R.; Grauwet, K.; Webb, P. K.; Miller, G. A.; Jennings, C. G.; Jain, S.; Miller, S.; Kuo, Y.; Sweeney, T.; Gilboa, T.; Norman, M.; Simmons, D. P.; Ramirez, C. E.; Bedard, M.; Fink, C.; Ko, J.; León Peralta, E. J. de.; Watts, G.; Gomez-Rivas, E.; Davis, V.; Barilla, R. M.; Wang, J.; Cunin, P.; Bates, S.; Morrison-Smith, C.; Nicholson, B.; Wong, E.; El-Mufti, L.; Kann, M.; Bolling, A.; Fortin, B.; Ventresca, H.; Zhou, W.; Pardo, S.; Kwock, M.; Hazra, A.; Cheng, L.; Ahmad, Q. R.; Toombs, J. A.; Larson, R.; Pleskow, H.; Luo, N. M.; Samaha, C.; Pandya, U. M.; Silva, P. de.; Zhou, S.; Ganhadeiro, Z.; Yohannes, S.; Gay, R.; Slavik, J.; Mukerji, S. S.; Jarolim, P.; Walt, D. R.; Carlyle, B. C.; Ritterhouse, L. L.; Suliman, S. *BMC Infect. Dis.* **2021**, *21*, No. 580.

(13) Kunze, A.; Dilcher, M.; Abd El Wahed, A.; Hufert, F.; Niessner, R.; Seidel, M. *Anal. Chem.* **2016**, *88*, 898−905.

(14) Seidel, M.; Niessner, R. *Anal. Bioanal. Chem.* **2014**, *406*, 5589−5612.

(15) Wolter, A.; Niessner, R.; Seidel, M. *Anal. Chem.* **2007**, *79*, 4529−4537.

(16) Kober, C.; Niessner, R.; Seidel, M. *Biosens. Bioelectron.* **2018**, *100*, 49−55.

(17) Wutz, K.; Meyer, V. K.; Wacheck, S.; Krol, P.; Gareis, M.; Nölting, C.; Struck, F.; Soutschek, E.; Böcher, O.; Niessner, R.; Seidel, M. *Anal. Chem.* **2013**, *85*, 5279−5285.

(18) Bemetz, J.; Kober, C.; Meyer, V. K.; Niessner, R.; Seidel, M. *Anal. Bioanal. Chem.* **2019**, *411*, 1943−1955.

(19) Zhang, W.; Ang, W. T.; Xue, C.-Y.; Yang, K.-L. *ACS Appl. Mater. Interfaces* **2011**, *3*, 3496−3500.

(20) Tamminen, K.; Salminen, M.; Blazevic, V. *Clin. Immunol.* **2021**, *229*, No. 108782.

(21) Gralinski, L. E.; Menachery, V. D. *Viruses* **2020**, *12*, No. 135.

(22) Kilic, T.; Weissleder, R.; Lee, H. *iScience* **2020**, *23*, No. 101406.

(23) Mulligan, M. J.; Lyke, K. E.; Kitchin, N.; Absalon, J.; Gurtman, A.; Lockhart, S.; Neuzil, K.; Raabe, V.; Bailey, R.; Swanson, K. A.; Li, P.; Koury, K.; Kalina, W.; Cooper, D.; Fontes-Garfias, C.; Shi, P.-Y.; Türeci, Ö.; Tompkins, K. R.; Walsh, E. E.; Frenck, R.; Falsey, A. R.; Dormitzer, P. R.; Gruber, W. C.; Şahin, U.; Jansen, K. U. *Nature* **2020**, *586*, 589−593.

(24) Hormati, A.; Poustchi, H.; Ghadir, M. R.; Jafari, S.; Jafari, N.; Ashtari, A.; Ahmadpour, S. *Iran. J. Allergy, Asthma Immunol.* **2021**, *20*, 244−248.

(25) Zhou, C.; Bu, G.; Sun, Y.; Ren, C.; Qu, M.; Gao, Y.; Zhu, Y.; Wang, L.; Sun, L.; Liu, Y. *J. Med. Virol.* **2021**, *93*, 2857−2866.

Supporting Information

Fully automated chemiluminescence microarray analysis platform for rapid and multiplexed SARS-CoV-2 serodiagnostics

Julia Klüpfel[1], Sandra Paßreiter[1], Nina Weidlein[1], Martin Knopp[2], Martin Ungerer[3], Ulrike Protzer[4,5], Percy Knolle[6], Oliver Hayden[2], Martin Elsner[1], Michael Seidel[1]*

[1]Institute of Hydrochemistry, Chair of Analytical Chemistry and Water Chemistry, Technical University of Munich, Lichtenbergstraße 4, 85748 Garching, Germany

[2]Heinz-Nixdorf-Chair for Biomedical Electronics, Technical University of Munich, TranslaTUM, Einsteinstr. 25, 81675 München

[3]ISAR Bioscience GmbH, Semmelweisstr. 5, 82152 Planegg

[4]Institute of Virology, Technical University of Munich / Helmholtz Zentrum München, Trogerstr. 30, 81675 München

[5]German Center for Infection Research (DZIF), Munich partner site, 81675 München

[6]Institute of Molecular Immunology/ Experimental Oncology, Technical University of Munich, Ismaningerstr. 22, 81675 München

Table of contents:

Supplemental experimental data

Supplemental figures

Supplemental information

Table S1. Main assay steps on the MCR-R (steps that only apply to the sequential IgM/IgG detection are shown in italic)

Step	Volume	Flow rate	Comment
Sample injection	40 µL	-	done manually
Sample incubation			*60 s*
Flushing of chip	*2000 µL*	*500 µL s^{-1}*	
IgM detection antibody injection	*800 µL*	*10 µL s^{-1}*	
Flushing of chip	*2000 µL*	*500 µL s^{-1}*	
CL reagents injection	*400 µL*	*150 µL s^{-1}*	
Image acquisition	*-*	*-*	*60 s exposure*
Flushing of whole fluidic system	*7500 µL*	*500 µL s^{-1}*	
Flushing of chip	2000 µL	500 µL s^{-1}	
IgG detection antibody injection	800 µL	10 µL s^{-1}	
Flushing of chip	2000 µL	500 µL s^{-1}	
CL reagents injection	400 µL	150 µL s^{-1}	
Image acquisition	-	-	60 s exposure
Flushing of whole fluidic system	7500 µL	500 µL s^{-1}	

Figure S1: Reaction scheme of surface modification and covalent protein immobilization on polycarbonate surfaces
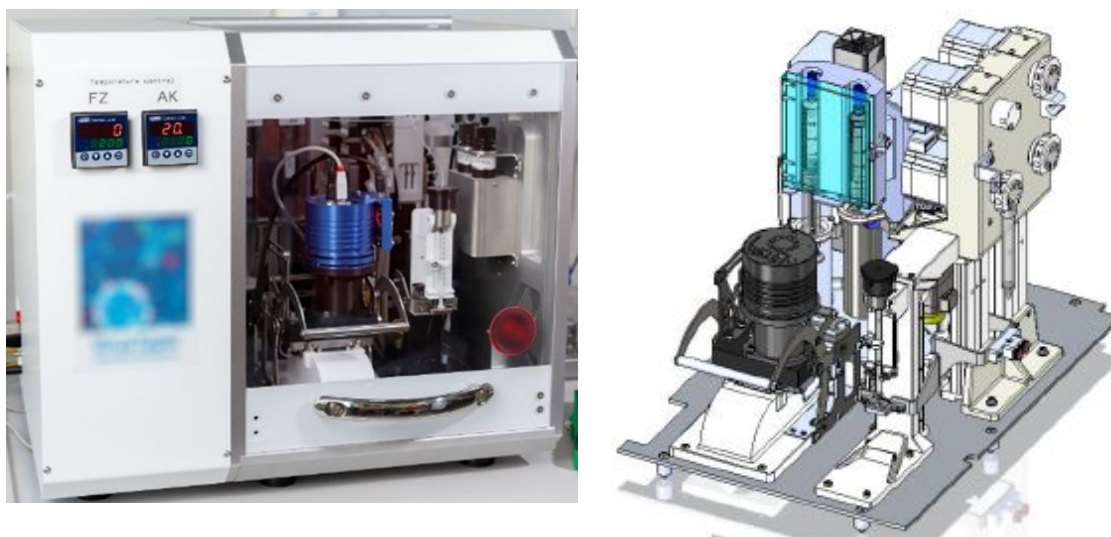
Figure S2: Automated microarray platform MCR-R; left: physical image of the device, right: schematic depiction of the main device elements: camera unit, syringe pumps and valves (copyright of right image: GWK Präzisionstechnik GmbH)

Description of the MCR-R:

The MCR-R was developed by the Chair of Analytical Chemistry (TUM) together with GWK Präzisionstechnik GmbH (Munich). It is the currently newest generation of Microarray Chip Readers (MCR) and offers versatile application possibilities for both research and routine application. Its main components are a CCD camera locate above a microarray chip loading unit (shown in black in the front left of Figure S2 (right image). Behind the camera unit, two syringes for the dosage of peroxidase labelled detection antibodies are located, on the right of the camera unit a syringe pump for sample injection can be found. Behind this syringe pumps, the valve tower is seen, containing four valves and a syringe pump for the transport of chemiluminescence reagents, running buffer and cleaning reagents. With its size of 50 x 50 cm, the device is suitable for benchtop placing, a recently presented version of the MCR-R is even smaller than the one used in this manuscript while having the same functionality.

For the application in research, the device offers a software toolbox allowing for the design of different measurement programs, e.g. for sequential programs using two different detection antibodies, programs with syringe injection of the sample or direct sample injection into the microarray chip and many more options, allowing for the development of optimized assays for the applications of interest.

For routine application of the device, only the necessary measurement programs are activated and can then be used by any user who had a short training on the device, even without a deeper technical or chemistry background. Only few manual steps (filling reagent syringes and containers, starting the measurement program, entering a microarray chip) have to be done, while the whole assay is done completely automatically. The data evaluation software is tailormade for every application so that all relevant evaluation steps are done on the device for routine applications. Therefore, the device is suitable for point-of-care applications as it is easy to use, shows a high degree of automation, is small enough to find space in hospitals or medical practices and can be used for various different microarray applications with relevance at the point of care.
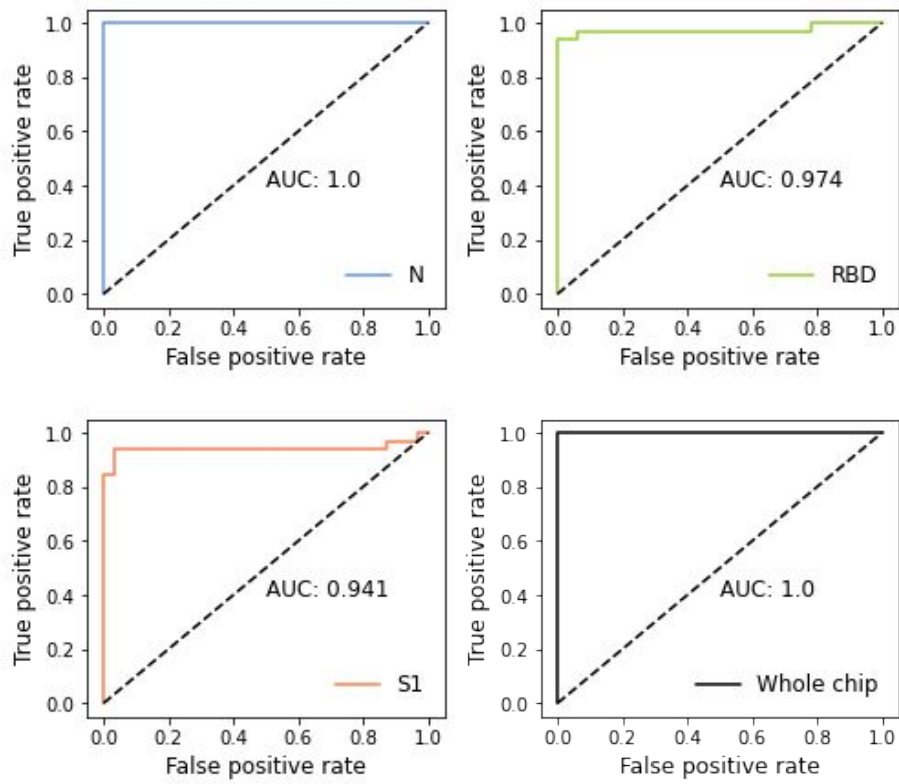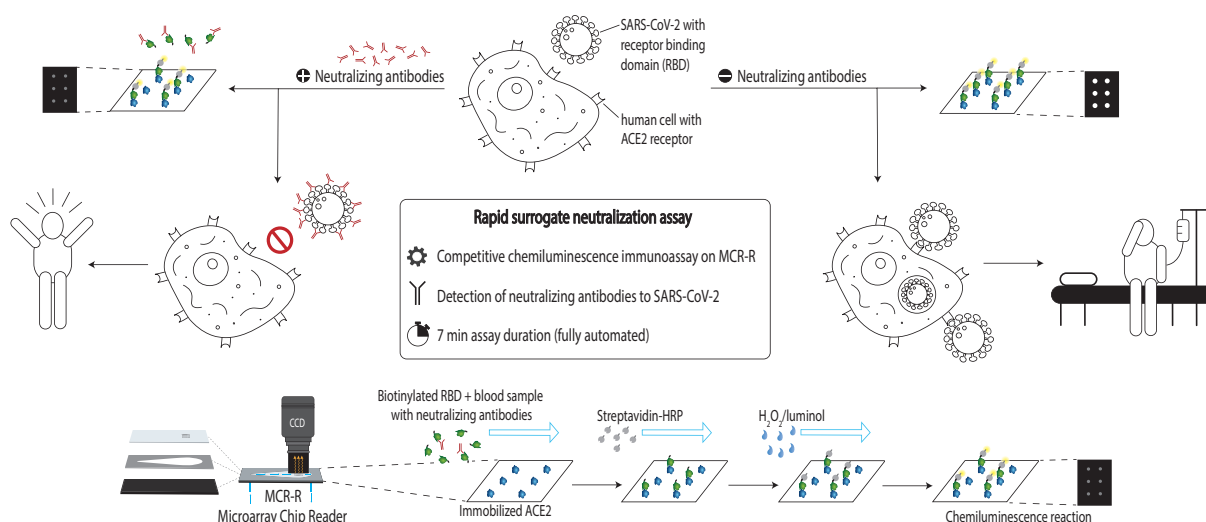
Figure S3: ROC curves obtained for N protein, RBD, S1 protein and combined ROC curve for the whole microarray chip

4.3 Publication 3: Automated detection of neutralizing SARS-CoV-2 antibodies in minutes using a competitive chemiluminescence immunoassay

4.3.1 Publication Summary and Author Contributions

With the two previous publications it was already possible to keep up to the speed of antibody test research and development all over the world, answering new upcoming research questions rapidly after they came up and providing optimized tests that could keep pace with other newly developed tests. Another research question that came up over time and grew more and more important with the progressing pandemic was the detection of neutralizing antibodies to SARS-CoV-2. These antibodies are able to inhibit the binding of SARS-CoV-2 RBD to the human ACE2 receptor and thus prevent the cell entry of the virus. While the previously described assays aimed on the direct detection of antibodies using anti-IgG or anti-IgM detection antibodies, the detection of neutralizing antibodies focused on a different principle as the binding of RBD to ACE2 and its inhibition by antibodies is measured in a competitive immunoassay. Thus, a lower measurement signal correlates with a high amount of neutralizing antibodies. Compared to the previous developments this is a completely different assay principle, making the development of a suitable microarray very challenging, especially as no other rapid neutralization tests that gave results within few minutes were available at the time.

As a first step before measuring inhibition, first the protein-receptor interaction between

ACE2 and RBD was studied. Tests were done on different chip surfaces (polycarbonate chips with 0.25 or 1 mm thickness and glass chips) and with both immobilized ACE2 as well as immobilized RBD while detecting the binding of the respective biotinylated counter-protein with peroxidase-labeled streptavidin. It was shown that all tested variants could generally be applied but glass chips with immobilized ACE2 gave the most promising results for inhibition measurements. In consequence, a measurement program for neutralization measurements was developed, allowing for results within seven minutes.

To evaluate the performance of this competitive binding inhibition test, first the concentration dependence of the inhibition was tested. By diluting a positive sample and comparing it to a measurement of a negative sample, it was found that up to a 1:100 dilution of positive sample still could be distinguished from a negative one, which compared well to a measurement without sample. In consequence, a cohort of 80 samples (33 SARS-CoV-2 serology negative, 47 positive) was tested to further evaluate the assay performance and compare the rapid neutralization assay on the MCR-R to a surrogate neutralization ELISA, the previously established total IgG antibody assay and a commercial neutralization test. Here, all positive and negative samples could be classified correctly and results from the competitive assay on the MCR-R and the other neutralization assays were well comparable. Moreover, when comparing with the total IgG assay, the importance of neutralization measurements was stressed as some samples were shown to have developed a high amount of antibodies but only a low amount of neutralizing antibodies binding to the correct RBD epitopes. Finally, monitoring of neutralizing antibodies after vaccination was done and showed that the neutralizing antibody titer increases shortly after the second vaccine dose, decreases rapidly afterwards and can then be boostered again by a third dose. Therefore, the newly developed neutralization assay is a very useful tool, giving important additional information on a person's immune status within few minutes.

Own contribution:

- Design of experiments (together with S. Paßreiter)

- Development of measurement program on MCR-R

- Evaluation of different chip materials

- Protein-receptor interaction measurements

- Data analysis

- Writing of the manuscript (together with S. Paßreiter)

The manuscript was written in shared first authorship of J. Klüpfel and S. Paßreiter.

RESEARCH PAPER

Automated detection of neutralizing SARS-CoV-2 antibodies in minutes using a competitive chemiluminescence immunoassay

Julia Klüpfel[1] · Sandra Paßreiter[1] · Melina Rumpf[1] · Catharina Christa[2] · Hans-Peter Holthoff[3] · Martin Ungerer[3] · Martin Lohse[3] · Percy Knolle[4] · Ulrike Protzer[2,5] · Martin Elsner[1] · Michael Seidel[1]

Abstract
The SARS-CoV-2 pandemic has shown the importance of rapid and comprehensive diagnostic tools. While there are numerous rapid antigen tests available, rapid serological assays for the detection of neutralizing antibodies are and will be needed to determine not only the amount of antibodies formed after infection or vaccination but also their neutralizing potential, preventing the cell entry of SARS-CoV-2. Current active-virus neutralization assays require biosafety level 3 facilities, while virus-free surrogate assays are more versatile in applications, but still take typically several hours until results are available. To overcome these disadvantages, we developed a competitive chemiluminescence immunoassay that enables the detection of neutralizing SARS-CoV-2 antibodies within 7 min. The neutralizing antibodies bind to the viral receptor binding domain (RBD) and inhibit the binding to the human angiotensin-converting enzyme 2 (ACE2) receptor. This competitive binding inhibition test was characterized with a set of 80 samples, which could all be classified correctly. The assay results favorably compare to those obtained with a more time-intensive ELISA-based neutralization test and a commercial surrogate neutralization assay. Our test could further be used to detect individuals with a high total IgG antibody titer, but only a low neutralizing titer, as well as for monitoring neutralizing antibodies after vaccinations. This effective performance in SARS-CoV-2 seromonitoring delineates the potential for the test to be adapted to other diseases in the future.

Keywords SARS-CoV-2 · COVID-19 serology · Protein-receptor interaction · Chemiluminescence immunoassay · Neutralizing antibodies · Competitive immunoassay

Julia Klüpfel and Sandra Paßreiter contributed equally.

✉ Michael Seidel
michael.seidel@mytum.de

1 Institute of Water Chemistry, Chair of Analytical Chemistry and Water Chemistry, Technical University of Munich, Lichtenbergstr. 4, 85748 Garching, Germany

2 Institute of Virology, Technical University of Munich/Helmholtz Zentrum München, Trogerstr. 30, 81675 Munich, Germany

3 ISAR Bioscience GmbH, Semmelweisstr. 5, 82152 Planegg, Germany

4 Institute of Molecular Immunology/Experimental Oncology, Technical University of Munich, Ismaningerstr. 22, 81675 Munich, Germany

5 German Center for Infection Research (DZIF), 81675 Munich, Germany

Introduction

Since its outbreak in late 2019, the SARS-CoV-2 pandemic affected the lives of billions of people around the world. At the time of writing this manuscript, the World Health Organization (WHO) reported 613 million confirmed cases and 6.5 million deaths [1]. To monitor SARS-CoV-2 infections, especially those that go unnoticed [2], diagnostic methods to determine the presence of antibodies were rapidly developed [3–6]. However, these tests screen for antibodies to multiple epitopes and, therefore, cannot provide information about the effective protective immunity that is gained in the form of those antibodies that truly prevent the cell entry of SARS-CoV-2 [7].

Essential for this cell entry is the binding of the viral receptor binding domain (RBD), located within the SARS-CoV-2 spike protein (S1 fragment), to the human angiotensin-converting enzyme 2 (ACE2) receptor at the cell surface. This receptor is, for example, strongly expressed in lung

tissue. Those antibodies that are capable of specifically binding to the RBD and, thereby, of preventing cell entry, are called neutralizing antibodies [8]. Studies have shown that the levels of neutralizing antibodies (nAbs) decrease over time and that certain patient groups even develop only low level of nAbs in the first place [9, 10]. Therefore, the determination of the neutralizing capacity of SARS-CoV-2 antibodies is of great interest for understanding SARS-CoV-2 immunity [11] and for giving recommendations on booster vaccines in point-of-care settings in the future as is currently already done for other infectious diseases.

The standard method for the detection of neutralizing antibodies is plaque reduction neutralization tests (PRNTs) [12]. Here, serum samples are incubated with active virus, and subsequently, eukaryotic cells are infected with the virus and incubated for several days. When evaluating the amount of formed plaques (regions of cell destruction due to viral infection), one can see if neutralization of the virus by antibodies in the serum occurred or if cells were infected at undiminished velocity. This assay principle is not only time-intensive, but also requires highly skilled staff and biosafety level 3 laboratory facilities, which often are not available [12]. An alternative are surrogate assays that do not use active virus but rely on non-infectious viral proteins (especially the spike protein) instead [13]. This makes the assays faster and the use of BSL3 laboratories obsolete, so that assays become accessible for many laboratories. Although these assays might miss some neutralizing antibodies to other proteins than the spike protein and its receptor binding domain, they generally give a good estimate of neutralizing antibodies in a sample compared to virus-based neutralization tests [14–16]. Since 2020, various surrogate assays have been presented in scientific literature or even made commercially available, most of them by applying ELISA techniques [17–20], but also luciferase assays [21] or bead-based Luminex assays [22] can be found. Many of the reported surrogate assays showed a performance equivalent to PRNTs in significantly less time with only a few hours instead of days. Very few examples of rapid, point-of-care neutralization tests with turnaround times below 1 h can be found in terms of lateral flow assays [23, 24] or cellulose pull-down tests [25], but these tests often suffer from bias when readout is done by eye and even digital readout is easily influenced by varying quality of blood samples or the exact time point of readout, sometimes making even relative quantification difficult. But still, such fast assays are required, for example, to test for neutralizing antibodies at a medical practitioner and to then immediately give a booster vaccination if necessary or for verification of vaccination status, border control, or for the screening for possible donors for convalescent plasma [24, 26]. Even though currently, reliable threshold values for reasonable protection are not known yet, this will probably change in the future as it has already been shown

that neutralizing antibody levels are highly predictive of immune protection [27]. And already now, the public readily makes use of rapid antibody tests offered by pharmacies which only give information on binding but not on neutralizing antibodies. Here, rapid neutralization assays would be a valuable tool in order to not give people a false feeling of protection in case they have antibodies binding to other motifs on SARS-CoV-2 rather than neutralizing antibodies.

Therefore, we developed a competitive chemiluminescence immunoassay for the measurement of neutralizing SARS-CoV-2 antibodies. Due to the flow-based detection principle and the short sample incubation time, results are available significantly faster than for statically incubated assays.

As a prerequisite for the neutralization assay, first the protein-receptor interaction between SARS-CoV-2 RBD and human ACE2 had to be assessed in detail on the analysis platform Microarray Chip Reader – Research Edition (MCR-R, described in detail in Klüpfel et al. [28]) to be able to define suitable conditions for the subsequent measurement of the inhibition of this binding in a competitive assay. While previous works with this analysis platform included various immunoassay formats for the detection of bacteria [29], small-molecule antibiotics [30, 31], toxins [32, 33], or antibodies [34, 35], for example, by sandwich immunoassay or chip-based amplification [36, 37], no example for the measurement of protein-receptor interaction as well as its inhibition has been presented on the MCR so far. Therefore, this first example of such an assay on the platform opens the door into a broad field with multiple potential applications that have so far been served by other methods including radioligand binding assays, surface plasmon resonance, isothermal titration calorimetry [38], or classical immunoassay techniques like ELISA [39].

Figure 1 shows the measurement principles for the protein-receptor binding assay as well as for the subsequent competitive neutralization assay.

The determination of the protein-receptor interaction is possible in two ways: immobilization of the (a) RBD or (b) ACE2 protein on the chip surface. In a first step, the respective complementary biotinylated protein (ACE2 in the case of (a), RBD in the case of (b)) is injected into the chip, leading to formation of RBD-ACE2 complexes at the chip surface. Subsequently, these complexes can be detected when horseradish peroxidase (HRP)-labeled streptavidin is flushed over the chip surface, because the streptavidin binds to the biotin label and catalyzes a chemiluminescence (CL) reaction in the presence of H_2O_2 and luminol resulting in a measurable bright light signal.

Other assay principles and analysis platforms had been used previously for the detection of RBD-ACE2 binding. A similar but more time-consuming approach is interaction measurement by ELISA, which has shown that a sigmoidal
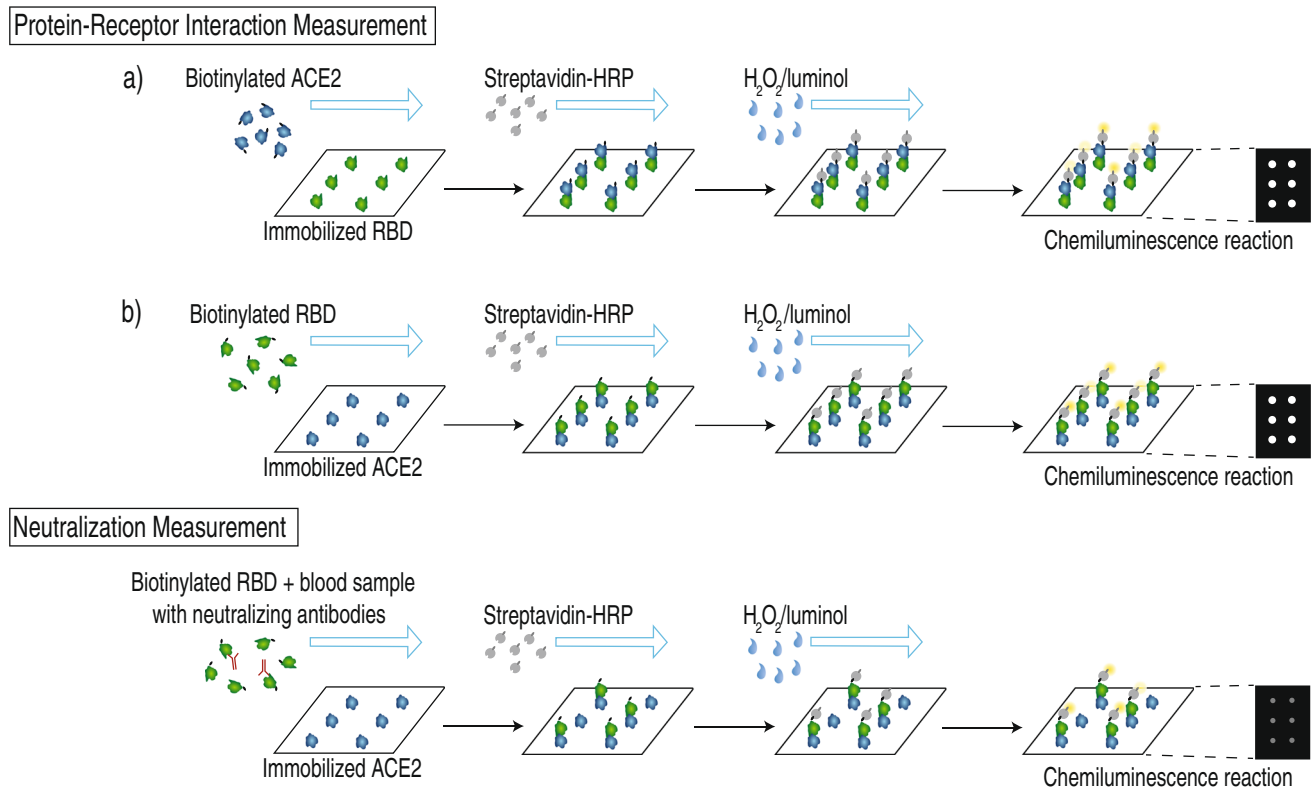
Fig. 1 Overview over immunoassay principles for protein-receptor interaction measurements (top) and neutralization antibody measurements (bottom) for SARS-CoV-2 on the MCR-R

binding curve is obtained from the interaction of SARS-CoV-2 RBD and ACE2.

Generally, various examples for the measurement of ligand-receptor interaction using more time-extensive ELISA methods can be found in literature [40–42]. In such bimolecular binding reactions, a hyperbola would be expected when titrating receptor with ligand or vice versa, unless secondary effects influence the binding. A common example for such effects is cooperativity where binding of one ligand molecule to the receptor influences the affinity of subsequent ligand molecules on the receptor [43]. In consequence, a sigmoidal curve is found as has been shown for ELISA measurements of RBD-ACE2 interaction [39, 44].

Thus, these protein-receptor interaction measurements were not only used to find the most suitable orientation of the assay but mainly for the determination of optimal concentrations of the respective protein on the surface and in solution as to give high signal when no neutralizing antibodies are present but to also be susceptible to minimal amounts of inhibition, corresponding to a position at the steepest part of the respective sigmoidal binding curve. As the use of immobilized ACE2 was found to be beneficial regarding necessary reagent concentrations, this orientation was used for inhibition measurements to detect neutralizing antibodies. Additionally, this first assay development stage was also

used to evaluate different immunochip materials, showing that amino-modified glass slides were most suitable.

After the evaluation of these general conditions, the next development step is the inhibition of the protein-receptor interaction by neutralizing antibodies. For this neutralization assay, a serum sample is mixed with biotinylated RBD and injected into the microarray chip with immobilized ACE2 as shown in Fig. 2 (bottom). As is typical in such competitive assays, the signal will be brighter the fewer neutralizing antibodies are present, because when neutralizing antibodies bind to the biotinylated RBD, they prevent RBD-ACE2 complexes at the chip surface and, therefore, inhibit the chemiluminescence signal.

In addition to presenting the first method for detecting protein-receptor interaction and its inhibition with the analysis platform MCR-R, we also present a comparison of different microarray chip materials for their application in these assays. To evaluate the performance of the novel competitive assay for the detection of neutralizing SARS-CoV-2 antibodies, we show the successful measurement of 80 serum samples. We further show that these results also correlate well to a total IgG antibody assay and a neutralization ELISA. Finally, the possibility of monitoring neutralizing antibodies after vaccination is presented. These results show that surrogate neutralization assays can be performed in less
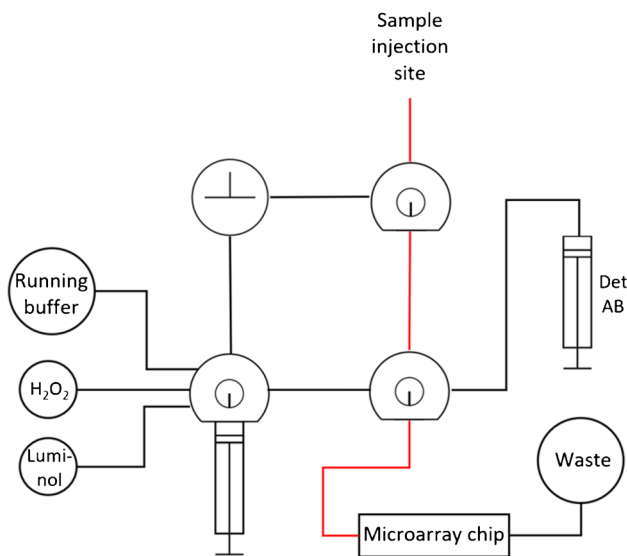
Fig. 2 Simplified tubing plan of the MCR-R with newly added sample injection site using a syringe adapter (sample path marked in red); additional tubes not used in the assay are omitted for clarity

than 10 min by competitive chemiluminescence immunoassays using a flow-based detection principle. They open the way to point-of-care diagnostic tests in this field of immune diagnostics.

Experimental

Chemicals, reagents, and materials

Standard chemicals were obtained from Sigma-Aldrich, subsidiary of Merck (Darmstadt, Germany), VWR (Rednor, USA) and Carl Roth (Karlsruhe, Germany). Hydrogen peroxide and luminol solution was bought from Cyanagen (Bologna, Italy) in the Elistar Supernova reagent kit. Streptavidin-Peroxidase was purchased from Biozol (VEC-SA-5004). A peroxidase-labeled anti-human IgG antibody (Fc fragment) from goat was obtained from Sigma-Aldrich (A0170, 5.6 mg mL^{-1}).

Spotting buffer was produced as described elsewhere [45], while as running buffer, Dulbecco's phosphate-buffered saline with 0.1% (*v/v*) Tween® 20 was used.

SARS-CoV-2 antigens

Human ACE2 protein was ordered from Sino Biological (Beijing, China). Recombinant SARS-CoV-2 spike RBD proteins with His-tag from wild-type virus (wt RBD) as well as the delta variant (delta RBD) were produced by ISAR Bioscience (Planegg, Germany) with the wt RBD being taken from the S protein nucleotide sequence of the

SARS-CoV-2 Wuhan Hu-1 genome (GenBank accession number MN908947, positions 22517 to 23183), while the delta RBD contained the following mutations: L452R and T478K. Details on the procedures were published before [45, 46]. Shortly, CHO cells were transfected with plasmid vectors containing the DNA sequences for the RBD proteins with an added His-tag and subsequently grown at 37 °C. The supernatants were centrifuged and filtered and subsequently purified using HisTrap columns. Protein content after elution was determined by OD$_{280}$ measurement and the relevant fractions were dialyzed.

The biotinylation of wt RBD and human ACE2 was done using the EZ-Link Micro Sulfo-NHS-LC biotinylation kit (Thermo Scientific #21935 or #A39257) with 20-fold molar excess according to the standard procedure instruction, followed by removal of excess biotin by dialysis against 1 L PBS for 16 h at 4 °C, using Slide-A-Lyzer™ Dialysis Cassettes, 7 K MWCO, 0.5 mL (Thermo Scientific #66373).

Serum and plasma samples

Serum and plasma samples were either purchased from Sigma-Aldrich (Darmstadt, Germany), obtained from the Institute of Molecular Immunology and the Institute of Virology, Technical University of Munich (Munich, Germany) or collected in the course of this study. All procedures were in accordance with the Helsinki Declaration of 1975, as revised in 2000.

All patient data were anonymized before use of the samples. Patient samples were handled in laboratories approved for biosafety level 2.

Chip surface preparation

The chemiluminescence immunoassays were performed either on glass or polycarbonate (PC) slides or PC foils with surface modifications based on procedures described previously [28, 47, 48], that were applied with some alterations and optimizations. Shortly, glass microscopy slides were surface modified by silanization and subsequent coupling of the polyetheramine Jeffamine® ED-2003. For the optimized production of glass chips, incubation times for acid treatments before silanization were reduced to 15 min, and volumes of silanization reagent and Jeffamine® ED-2003 were reduced to 300 µL to allow for upscaling and lower prices per unit.

PC sheets (1-mm thickness) were prepared using carboxy-modified Jeffamine as detailed in previous works [28, 48] with an alteration of the incubation temperature to 90 °C. Shortly, Jeffamine® ED-2003 was carboxy-modified by coupling of succinic anhydride and subsequently, PC sheets were coated with the molten polymer by screen printing. PC foils (0.25-mm thickness) were treated equally.

Microarray chip production

Before spotting proteins on the chip surface, most glass chips were activated using *N,N′*-disuccinimidyl carbonate (DSC) activation [45]. A mixture of 8 mg N,*N′*-disuccinimidyl carbonate, 0.4 mg 4-(dimethylamino)pyridine and 12.5 μL triethylamine in 160 μL dimethylformamide per chip was prepared, and 300 μL of this mixture were incubated between two functionalized glass slides in sandwich principle at RT for 30 min, followed by manual cleaning and sonication in methanol. After drying, they were either directly used for spotting or stored at 4 °C until spotting.

Spotting solutions were prepared as antigens or positive control antibody diluted with spotting buffer as described earlier [45]. As positive control, anti-peroxidase antibody was used, while as negative control spotting buffer was applied.

For spotting without previous activation of the chip surface (EDC/s-NHS spotting [28], applied to all PC chips and certain glass chips), 1 mg mL^{-1} 1-ethyl-3-(3-dimethylaminopropyl)carbodiimide (EDC) and 1 mg mL^{-1} N-hydroxysulfosuccinimide (s-NHS) were added to spotting buffer and mixed with prediluted or undiluted antigen and positive control solutions (50% v/v).

Spotting was then done using the the BioOdyssey Calligrapher miniarrayer from Bio-Rad (Hercules, USA) with a SNS9 spotting pin using the same procedure applied for our previous SARS-CoV-2 assays [28]. In short, five replicates per spot were transferred onto the glass or PC chips (transverse to intended flow direction on the microarray chip) with up to 20 different solutions in flow direction (spotting rows). The chips were assembled with a polyoxymethylene (POM) carrier containing in- and outlet holes and a double-sided adhesive foil with a cut-out flow channel and stored at 4 °C until measurement.

Microarray measurements for total IgG antibody detection

Microarray measurements were done on the microarray platform MCR-R, which was obtained from GWK Präzisionstechnik (Munich, Germany) and has been described in detail in a previous publication [28]. As presented there, the device had to be flushed at the beginning of a measurement day and was subsequently loaded with the necessary reagents, followed by a darkframe image to correct for camera background. For measurements, plasma or serum samples were prepared by diluting 20 μL of sample with 205 μL PBST and a measurement chip was inserted into the chip unit. The measurement was started, and the sample was injected into a valve of the MCR-R using an adapter for low residual volume syringes. The sample filled the tubing from valve to chip and was then pushed over the chip

by a syringe pump transporting running buffer. The overall simplified tubing plan is shown in Fig. 2, while detailed information on the measurement program is summarized in the Supporting Material (Section S1).

To obtain an optimal interaction between sample and immobilized antigens, a stopped flow was applied, allowing for the incubation of small sample aliquots on the chip for 5 s. After the sample transport, the chip was flushed slowly with peroxidase-labeled anti-human IgG antibody, followed by chemiluminescence reagents. The camera exposure time was 60 s; afterwards the tubing as well as the sample injection adapter were flushed thoroughly, giving a total time of 6.5 min per measurement including manual steps.

Microarray measurements for protein–protein interaction measurement

To detect protein–protein interaction between human ACE2 and RBD, a measurement program with a duration of 3 min 45 s that had previously been used for an antibody assay, was applied [28]. 40 μL samples of either biotinylated RBD or ACE2 were prepared in concentrations of 0, 0.05, 0.1, 0.5, 1, 5, 10, 20 μg mL^{-1} or 0, 0.5, 1, 5, 10, and 50 μg mL^{-1}, respectively. For measurements, a sample was injected into a chip directly, the chip was inserted into the MCR-R, and the measurement was started immediately.

Microarray measurements for neutralizing antibody detection

To detect the inhibition of RBD-ACE2 binding by neutralizing antibodies, a solution of biotinylated RBD in PBST with a concentration of 10 μg mL^{-1} was prepared. 20 μL of this solution were mixed with 20 μL of serum, plasma, or whole blood sample and injected into a microarray chip that was then inserted into the MCR-R, where the automated measurement was started immediately. The measurement program was equal to the one used for protein–protein interaction measurements.

Neutralization ELISA measurements

The neutralization ELISA was conducted as described previously by Richardson et al. [46]. Shortly, ELISA plates were coated with 60 ng ACE2 per well for 1 h, followed by washing (with PBST) and blocking steps (milk powder solution for 1 h). Serum samples were incubated in 1:2 dilution together with 18 ng of biotinylated RBD per well for 1 h, followed by incubation of streptavidin peroxidase for 1 h. After addition of TMB substrate and stopping of the reaction with H$_2$SO$_4$, absorbance was determined at a wavelength of 450 nm.

Surrogate neutralization assay on YHLO iFlash 1800

A commercial and certified surrogate paramagnetic particle chemiluminescence immunoassay (CLIA) by the manufacturer YHLO Biotechnology (Shenzhen, China) for quantification of neutralizing antibodies was performed. Neutralizing antibodies in sera are linked to SARS-CoV-2 RBD antigen-coated paramagnetic microparticles. The remaining microparticles are competitively bound by acridinium-ester labeled ACE2 conjugates. The number of neutralizing antibodies is calculated in AU mL^{-1} [arbitrary units per milliliter] and correlates inversely to the reaction mixtures relative light units (RLU) [49, 50]. The lower limit of quantification is 4 AU mL^{-1}, and the upper limit of quantification is 800 AU mL^{-1}. Seropositivity is given for values above 10 AU mL^{-1} according to the manufacturer's instructions. Results can be adapted to WHO International Standard (NIBSC code 20/136) by conversion (AU mL^{-1} × 2.4 = IU mL^{-1} [international units per milliliter]).

Data evaluation

The detected CL signals were corrected with the previously recorded blank image, stored as txt-files, and processed with the evaluation software "MCR-Analyser" (Martin Knopp, Munich, Germany) [51]. On the background-corrected CL images, a grid was set to define the position of the spots. For each spot, the mean value of the ten brightest pixels was calculated. Means and standard deviations were calculated for the five replicates per row and spots that deviated more than 10% from the mean were excluded.

The resulting mean values and standard deviations for all rows were used for further analysis and graphical evaluation using Python 3.

Results and discussion

Measurement of SARS-CoV-2–ACE2 interaction

To pre-define obligatory parameters for the neutralization assay, first a protein-receptor interaction assay was established, aimed at finding optimal concentrations of the used proteins as well as optimal chip material.

First, it was tested whether the immobilization of ACE2 or RBD was more suitable and what dilution of the immobilized protein was optimal. For immobilized ACE2, two-fold dilutions between 1:2 (0.5 mg mL^{-1}) and 1:16 were spotted on the same chips and different concentrations of biotinylated RBD ranging from 0 to 20 µg mL^{-1} were added in an automated non-competitive immunoassay, giving the CL intensity curves shown in Fig. 3. While the 1:2 and 1:4

dilution gave comparable results, the higher dilutions gave significantly lower signals. In sigmoidal interaction curves, optimally the increasing part of the curve should span over a concentration range of at least one log value, while at the same time also covering a big range of intensity values. These criteria are best met by the highest tested concentrations. As the 1:2 and 1:4 dilution gave comparable results, it is assumed that a maximum occupation of the small spot surface was obtained with the 1:4 dilution, and additional ACE2 could not be bound covalently to the surface. Still, a 1:2 dilution of ACE2 was used for further experiments to make sure that the maximum possible amount of protein was bound to the surface. The respective EC50 value for the 1:2 dilution was 5.7 µg mL^{-1}, which was considered a suitable concentration of RBD for the use in the inhibition measurements of the subsequent neutralization assay.

In contrast to immobilizing ACE2, it is also generally possible to immobilize the SARS-CoV-2 RBD. While we were able to prove the general applicability of this principle (results shown in Supplementary Material) and also its advantages for future simultaneous evaluation of neutralizing antibody responses to different SARS-CoV-2 variants, we focused on the more economic and currently also more reliable principle with immobilized ACE2.

Apart from the assay orientation and reagent concentrations, also different chip materials, namely amino-modified glass and carboxy-modified polycarbonate in different thicknesses (1 mm and 0.25 mm), were evaluated. Similar experiments had been done for a total IgG antibody assay for SARS-CoV-2 before (results shown in Supporting Material), showing that glass chips performed best, followed by thin PC foils. The re-assessment was done as the detection mechanism for the neutralization assay differs from that of the total IgG antibody assay; thus, a different outcome would be possible.

Therefore, human ACE2 (0.5 mg mL^{-1}) was immobilized on DSC glass chips as well as on PC sheet (1 mm) and foil (0.25 mm) chips and tested with biotinylated RBD as described before. To additionally account for the influence of interaction time between RBD and ACE2, an incubation of RBD in the chip for 2 min before starting the measurement was tested, giving a notably higher interaction time compared to the standard interaction time of 10 s.

The resulting CL values are shown in Fig. 4, indicating that for the glass chips higher endpoint CL values were obtained (about 60,000 a.u. compared to 30,000 a.u.). Especially for the PC sheet chips a very steep curve was found, indicating a very small working range for the subsequent neutralization assay. For PC foil chips, no endpoint plateau was reached, indicating that even higher concentrations of RBD would be necessary. In consequence, glass chips again were considered more suitable than PC chips for both interaction and the following inhibition measurements. The reason for this outcome can be found in
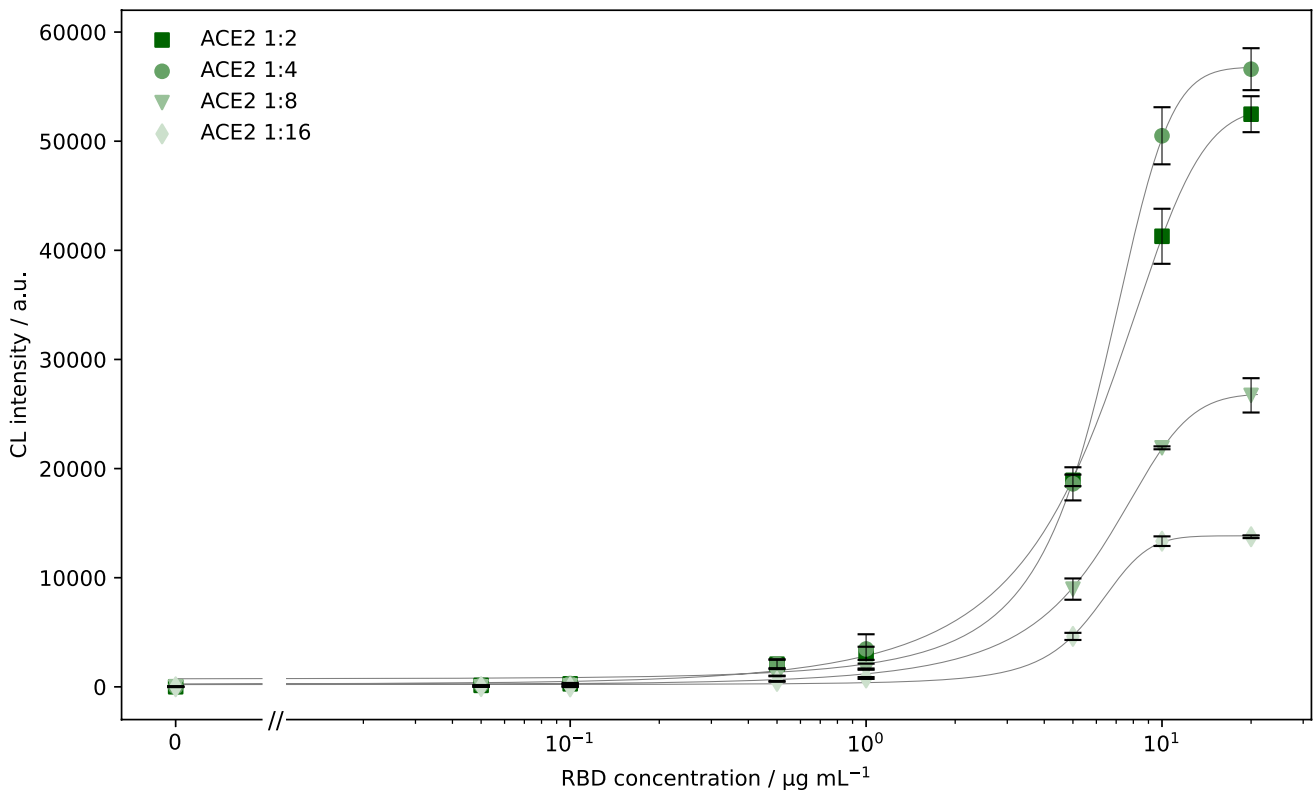
Fig. 3 Comparison of different immobilized ACE2 concentrations for determination of ACE2-RBD binding (CL signals are background-corrected, error bars show standard deviations of triplicate measurements, curves were fitted using 4-parameter logistic fit, linear axis scaling is used left of the axis break to include 0 µg mL^{-1})

the different immobilization strategy on PC, possibly resulting in insufficient amounts or inept orientation of immobilized ACE2.

For the tested incubation times on glass chips, it was found that after a 2-min incubation, the concentration of streptavidin-peroxidase could be significantly lowered (1:10,000 instead of 1:2500 dilution) while still giving comparable endpoint CL intensities as the 10-s incubation. Furthermore, the longer incubation led to a significantly reduced EC50 value of 1.8 µg mL^{-1} compared to 5.7 µg mL^{-1}. Therefore, prolonged incubation is a helpful tool if one wants to evaluate solely a protein-receptor interaction, but inhibition experiments showed that the 2-min incubation was not suitable for the detection of neutralizing antibodies as the inhibition was overestimated, even in negative samples, possibly due to non-specific binding of serum proteins to either immobilized ACE2 or biotinylated RBD. Hence, glass chips with 10-s sample incubation were used for further evaluations.

Concentration dependency of neutralization measurements

As a next development step, it was tested what influence the addition of SARS-CoV-2 seropositive and negative samples

had on the obtained signal and whether the signal inhibition after addition of positive samples was concentration-dependent. Therefore, a competitive binding inhibition assay format was used. Chips were spotted with ACE2 (0.5 mg mL^{-1}) and biotinylated RBD was mixed with either a positive sample in different dilutions or a negative sample to a final RBD concentration of 5 mg mL^{-1} to be close to the previously defined EC50 value. It was expected that with a SARS-CoV-2 seronegative sample no signal change would occur, while for a positive sample, the signal would decline in a concentration-dependent way in comparison to a measurement without serum.

Figure 5 shows the measurement results that confirmed these expectations. While a 1:2 diluted negative sample gave results around 25,000 a.u.—just like a measurement with 5 µg mL^{-1} RBD without serum addition—the positive sample gave a significantly reduced signal in a 1:2 dilution (below 1,000 a.u.) and showed a concentration-dependent signal increase upon higher dilutions until a 1:160 dilution could not be distinguished from a negative sample anymore.

This experiment showed that the measurement of neutralizing antibodies is generally possible with the presented assay principle and that positive samples can be
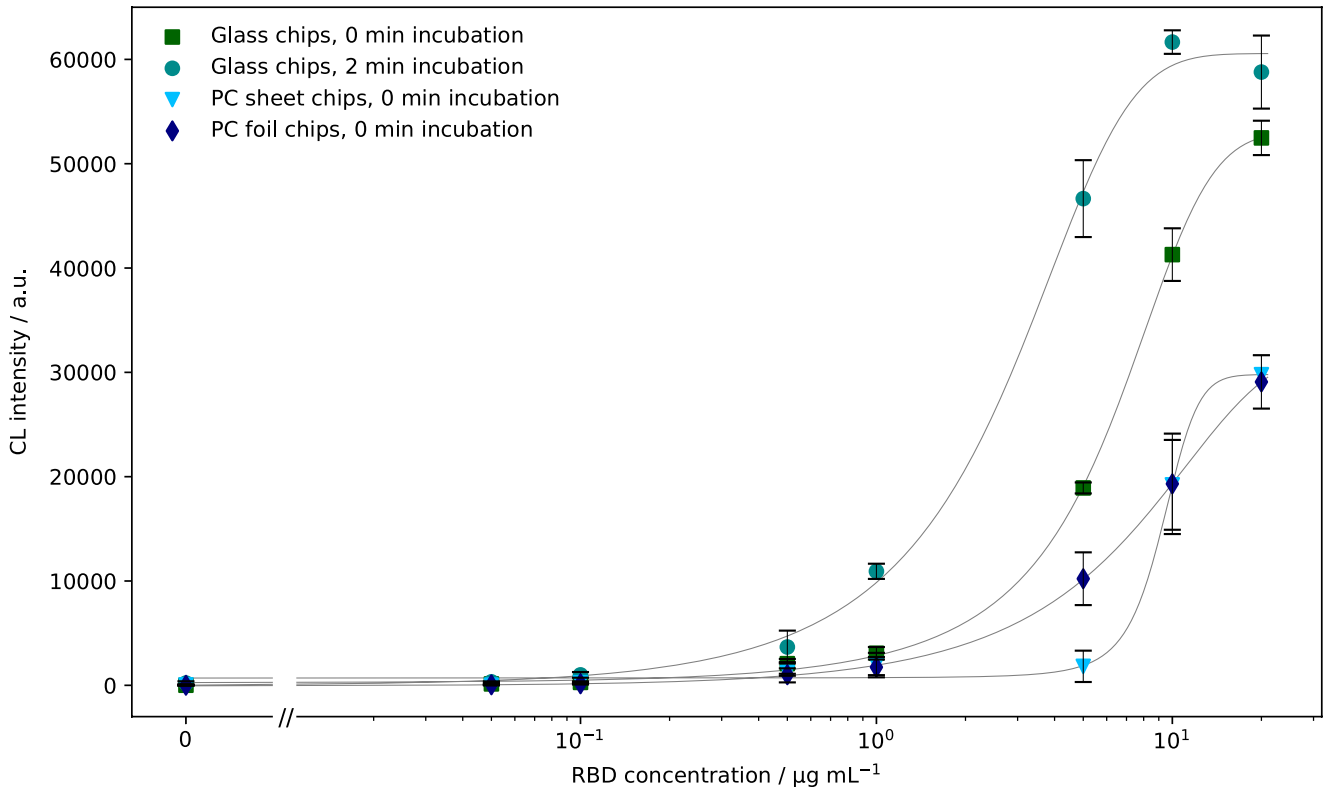
Fig. 4 Comparison of different chip materials and incubation times for determination of ACE2-RBD binding (CL signals are background-corrected, error bars show standard deviations of triplicate measurements, curves were fitted using 4-parameter logistic fit, linear axis scaling is used left of the axis break to include 0 μg mL^{-1})
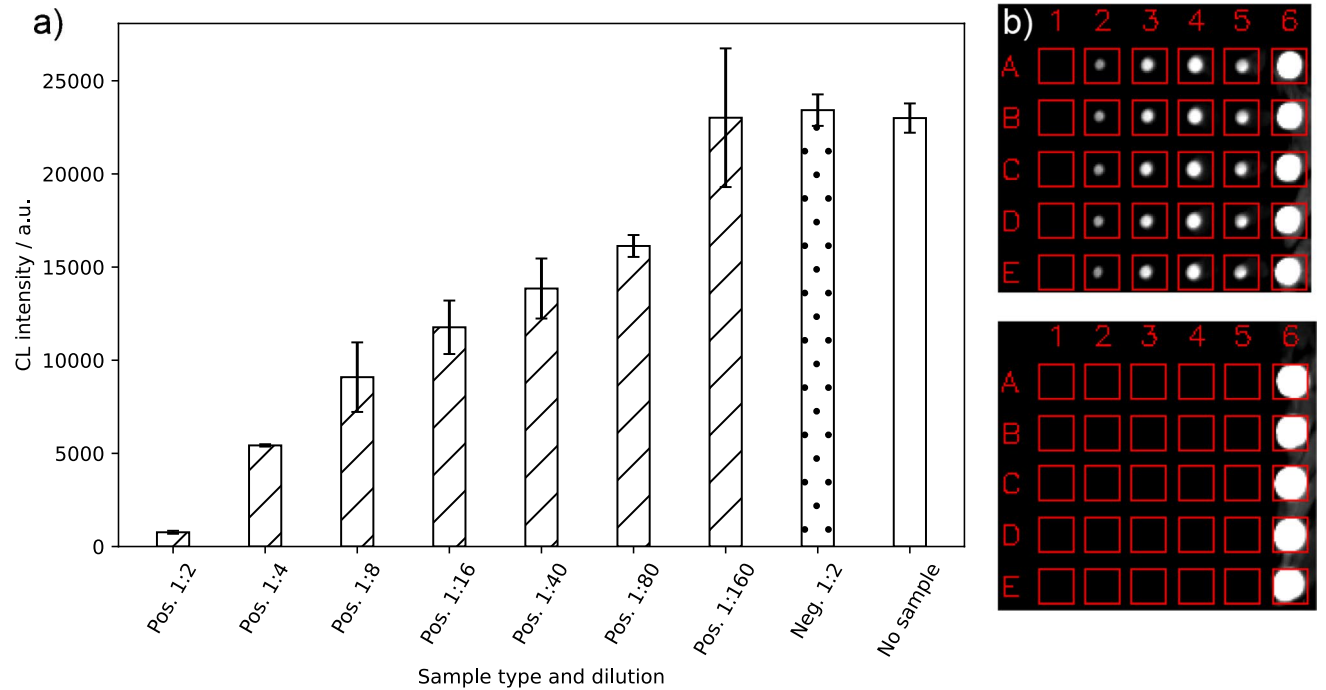

Fig. 5 a Inhibition measurements using different dilutions of a SARS-CoV-2 seropositive sample, a negative control sample and a measurement without addition of serum sample (CL signals are background-corrected, error bars show standard deviations of triplicate measurements), **b** measurement images for a seronegative (top) and seropositive (bottom) sample at 1:2 dilution (Column 1: negative control, 2–5: ACE2 in different dilutions from 1:16 to 1:2, 6: positive control)
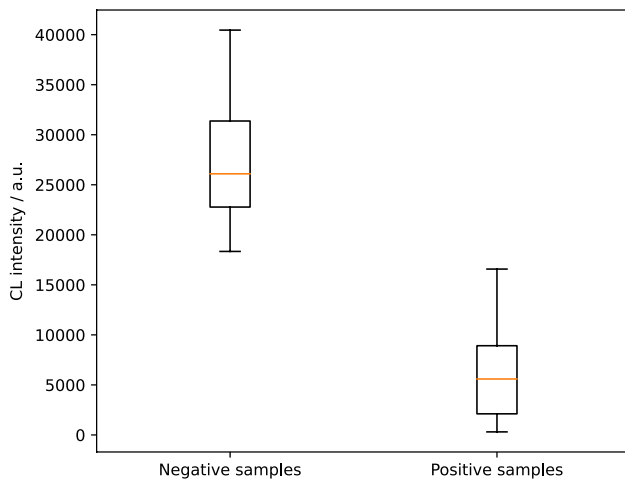
Fig. 6 Neutralization measurements of 33 SARS-CoV-2 seronegative and 47 positive samples (CL signals are background-corrected)

detected over a relatively broad concentration range, while negative samples give high intensities as anticipated. In continuation, the assay was tested with a higher number of positive and negative samples to reveal its applicability as some positive samples might only lead to a very slight signal reduction while negative samples could possibly inhibit due to non-specific binding to either RBD or ACE2.

Detection of neutralizing antibodies in blood samples and comparison with alternative methods

To evaluate the performance of the neutralization assay, a total of 80 samples (33 SARS-CoV-2 seronegative, 47 positive) were measured. They were well distinguishable with positive samples giving low CL intensities and negative ones giving high intensities as shown in Fig. 6. A two-tailed unpaired t test on the data resulted in a P value < 0.0001 for a significance level of $\alpha = 0.05$, emphasizing the statistically significant differences between the sample groups.

In parallel, for 15 positive and 17 negative samples, comparison measurements were done for confirmation using a surrogate neutralization ELISA. While the measured signals differed for some samples (see Fig. 7), the general trends are very similar in both assays. The differences for some samples can be explained with the different interaction times: while in the statically incubated ELISA assay the sample is let to interact for 1 h, in our neutralization chemiluminescence immunoassay, the interaction time is only a few seconds until the chip is flushed and the detection process is started. Nonetheless, the accordance between the two neutralization assays is very high despite the different assay principles.

To investigate the correlation between the total amount of IgG antibodies and the neutralizing activity of
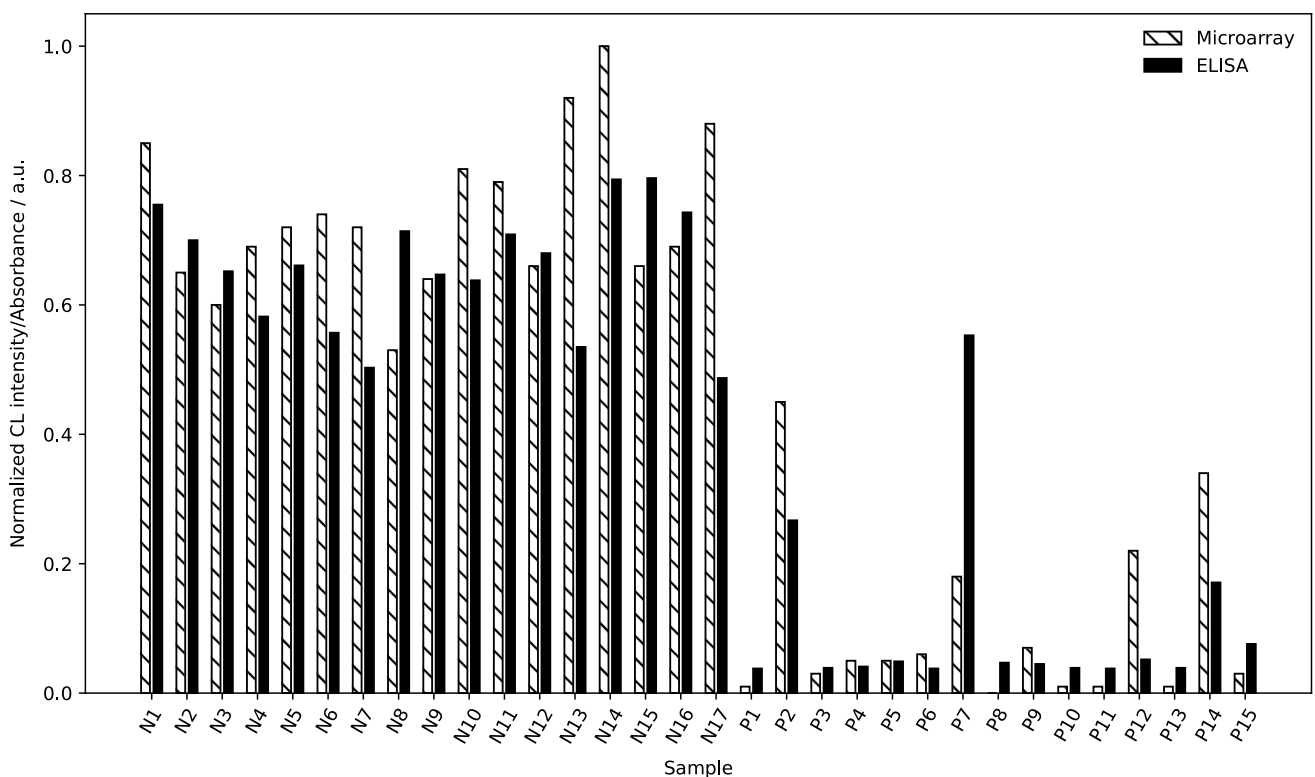
Fig. 7 Comparison of neutralization ELISA and neutralization CL-MIA (CL signals are background-corrected and normalized for easier comparison, ELISA results are given as measured absorbance)

antibodies, 57 samples were tested with a total IgG antibody CL-MIA detecting all antibodies binding to SARS-CoV-2 RBD but not necessarily inhibiting the binding of RBD to ACE2. This assay type had been developed on the MCR-R before [45] and was now improved by using a novel injection approach as detailed in the experimental section to allow for higher reproducibility and lower background intensities. With this procedure, the influence of non-specific binding could be reduced significantly, which had been a problem in some samples before as human IgG binds to surfaces readily and will be detected in the total IgG antibody assay with the anti-IgG detection antibody leading to the possibility of false positive results. For the neutralization assay, in contrast, the direct chip injection procedure could be sustained as not IgG but biotinylated RBD is detected.

Figure 8 shows the correlation between the neutralization assay and total IgG antibody assay signal. Positive and negative samples can be separated clearly. All negative samples give high signals in the neutralization assay and low signal in the total IgG antibody assay. For many positive samples, also a correlation between both assays is visible (indicated by the gray diagonal line in Fig. 8), but for some samples, very high intensities (approx. 65,000 a.u.) were measured in the total IgG antibody assay while only giving intermediate signal in the range of 5,000–15,000 a.u. in the neutralization assay while a very low signal of approx. 1,000 a.u. would have been expected. This indicates that there were antibodies in that samples that could bind to RBD but not in an epitope that would inhibit the binding of RBD to ACE2. This shows the importance of neutralization tests as total IgG antibody tests do not necessarily give an indication on the protective effect of these antibodies, whereas neutralization assays have proven to give important additional information.

To find out whether the assay could be carried out in a point-of-care manner to gain important information fast and without the need of a specialized laboratory, measurements in whole blood were done. For both positive and negative samples, comparable results were found in whole blood and plasma when considering the hematocrit value and therefore diluting the plasma sample stronger than the whole blood. Therefore, point-of-care applications of the neutralization immunoassay by performing measurements on a drop of capillary blood appear to be a viable option in the future.

Hence, we could show that the measured CL signals are concentration-dependent, and results are well comparable with an alternative surrogate assay format and relatable to total IgG measurements, making the assay very promising for a true quantitative application using international reference standards. While calibration of the assay with such standard material would be easily possible, the respective WHO standard (NIBSC code 20/136 [52], issued in 2020) was not available due to depletion of stocks during the time of our measurements, while a replacement had not yet been issued [53]. Therefore, we compared our results to a commercial surrogate neutralization assay from YHLO, allowing for quantification of neutralizing antibodies in the range of 4 to 800 AU mL^{-1}. A total of 64 samples were analyzed using both assays, showing a good correlation between both assays. Among 31 samples that had been pre-classified as seronegative and were also found as negative in the neutralization assay on the MCR-R, one sample taken from a person 14 days after the first SARS-CoV-2 vaccination dose was found to contain neutralizing antibodies by the YHLO assay. This discrepancy can be credited to a slightly higher sensitivity of the YHLO assay due to its longer incubation time, while our neutralization assay cannot detect extremely low antibody numbers shortly after the onset of antibody

Fig. 8 Correlation of results from total IgG antibody assay and neutralization assay (CL signals are background-corrected, dotted lines show separation between positive and negative samples, solid line shows correlation between total antibody signal and neutralization signal in positive samples)
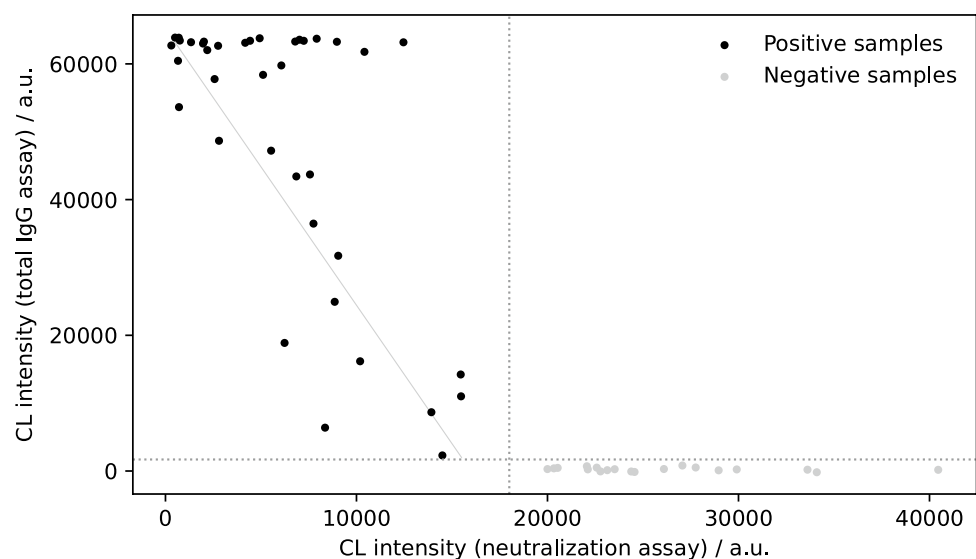
production. Additionally, YHLO and MCR measurements were done on different sample aliquots that were exposed to different storage conditions, possibly influencing the sample quality. The remaining 30 negative samples were concludingly found as negative in both neutralization assays. For the 33 tested seropositive samples, concentrations between 26 and 800 AU mL^{-1} (upper limit of quantification) were obtained in the YHLO assay with a good correlation to the results obtained on the MCR-R. Correlation analysis resulted in a Pearson R of -0.87 (negative correlation between AU mL^{-1} and chemiluminescence signal was expected due to the competitive assay format with decreasing signal for increasing antibody concentration). A graphical representation of the correlation can be found in the Supplementary Material (Fig. S4). The CL values obtained for samples at or above the upper limit of quantification for the YHLO assay range over a relatively large range down to CL values of few 100 a.u., indicating that the linear range of the novel assay on the MCR-R might be shifted to even higher neutralizing antibody titers, making it powerful for the analysis of strongly positive samples as are expected shortly after vaccination, while already being able to correctly identify samples with significantly lower titers.

Monitoring of neutralizing antibodies after vaccination

As the general detection of neutralizing antibodies was shown to be possible with our assay, we tested if it was applicable in the monitoring of neutralizing antibodies after vaccination. It is well known that antibody titers drop over time, so it was tested whether this drop could also be observed with our neutralization assay. Therefore, a total of 11 samples from the same person were measured—the first one was taken 7 days before the first Pfizer/Biontech vaccine dose, followed by a sample 7 days after the first and second dose. The first two doses were administered 21 days apart, while the third dose was given 237 days after the first. The first and the last tested sample were taken 454 days apart.

The results for the neutralization measurements are shown in Fig. 9. For the first two samples, very high CL intensities are obtained, as no antibodies had been formed yet, while for the third sample, the intensity was as low as 0.07, showing that after the second vaccine dose, a high amount of neutralizing antibodies had been formed. Over the following weeks, the intensity increases again as the antibody titer drops, reaching a value of 0.61 211 days after the first vaccination. A significant increase in neutralizing antibodies was again seen at the measurement date 15 days after the third vaccination with a value of 0.06. In the following, the measured intensities increased again, but at a lower rate compared to the increase after two doses of vaccine so that still a value of 0.40 was found 210 days after the third vaccination. This is an indication of improved sustainability of neutralizing antibodies formed after booster vaccination.

Therefore, it was shown that a monitoring of neutralizing antibodies after vaccinations is possible with our assay and that also changes in the rate of antibody decline after subsequent booster vaccinations can be monitored.

Conclusion

We were able to develop a rapid method for the detection of neutralizing antibodies in blood samples. While we currently only applied the method to detect SARS-CoV-2 immunity, it can be easily adapted to various other diseases

Fig. 9 Neutralizing antibody monitoring after SARS-CoV-2 vaccinations; vertical lines indicate vaccine doses (CL signals are background-corrected and normalized with respect to the maximum signal)
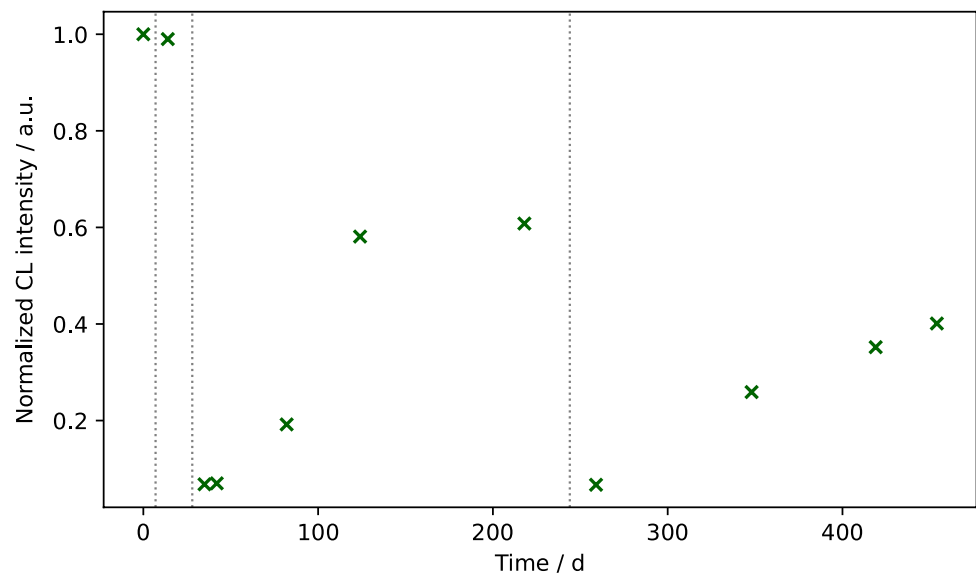
in the future. To further improve the assay for SARS-CoV-2, future research will focus on the use of immobilized RBD to allow for a simple determination of EC50 values and binding behavior for different variants as well as on the applicability of different chip materials. While so far PC chips were not competitive compared to glass chips, it was successfully shown that they could generally be used so that surface optimization might be fruitful.

More importantly, to our present knowledge, the neutralization assay on the MCR-R is faster than all other published surrogate neutralization assays with its measurement duration of 7 min. To stress the general relevance of neutralization assays, we showed that the determination of neutralizing antibody titers is crucial to detect the true protective effect of antibodies as not all persons with a high total antibody count also showed high neutralizing titers, whereas only neutralizing antibodies can help to prevent the infection of cells with SARS-CoV-2.

The neutralization CL-MIA showed outstanding performance in the measurement of serum samples from 80 persons and was proven to give results comparable to a neutralization ELISA and a commercial chemiluminescence immunoassay for neutralization measurements, while being significantly faster. It can thus also be applied to various questions like the monitoring of neutralizing antibodies after vaccinations or infections and can also be used in a point-of-care manner due to its simplicity and speed. In the future, also a quantitative evaluation of measurements will be possible as soon as a new international reference standard will be available. Therefore, it might be applied in pharmacies or at medical practices to give information about the presence of neutralizing antibodies and the need for booster vaccinations on-site.

We here present a powerful tool for the detection of neutralizing antibodies to SARS-CoV-2 that has a huge potential for future applications with respect to other diseases.

Declarations

Ethics approval The study was approved by the Ethics Commission of the Technical University of Munich, Rechts der Isar Hospital (reference 22/21 S-SR) and was conducted in accordance with the declaration of Helsinki.

Consent to participate All samples were collected with informed consent.

Consent for publication All samples were collected with informed consent.

Conflict of interest The authors declare no competing interests.

References

1. WHO. WHO Coronavirus Disease (COVID-19) dashboard. 2022. https://covid19.who.int/. Accessed 28 Sept 2022.
2. Schneider J, Mijočević H, Ulm K, Ulm B, Weidlich S, Würstle S, Rothe K, Treiber M, Iakoubov R, Mayr U, Lahmer T, Rasch S, Herner A, Burian E, Lohöfer F, Braren R, Makowski MR, Schmid RM, Protzer U, Spinner C, Geisler F. SARS-CoV-2 serology increases diagnostic accuracy in CT-suspected, PCR-negative COVID-19 patients during pandemic. Respir Res. 2021. https://doi.org/10.1186/s12931-021-01717-9.
3. Ayouba A, Thaurignac G, Morquin D, Tuaillon E, Raulino R, Nkuba A, Lacroix A, Vidal N, Foulongne V, Le Moing V, Reynes J, Delaporte E, Peeters M. Multiplex detection and dynamics of IgG antibodies to SARS-CoV2 and the highly pathogenic human coronaviruses SARS-CoV and MERS-CoV. J Clin Virol. 2020. https://doi.org/10.1016/j.jcv.2020.104521.
4. Burbelo PD, Riedo FX, Morishima C, Rawlings S, Smith D, Das S, Strich JR, Chertow DS, Davey RT, Cohen JI. Sensitivity in detection of antibodies to nucleocapsid and spike proteins of severe acute respiratory syndrome coronavirus 2 in patients with coronavirus disease 2019. J Infect Dis. 2020. https://doi.org/10.1093/infdis/jiaa273.
5. Faustini SE, Jossi SE, Perez-Toledo M, Shields AM, Allen JD, Watanabe Y, Newby ML, Cook A, Willcox CR, Salim M,

Goodall M, Heaney JL, Marcial-Juarez E, Morley GL, Torlinska B, Wraith DC, Veenith TV, Harding S, Jolles S, Ponsford MJ, Plant T, Huissoon A, O'Shea MK, Willcox BE, Drayson MT, Crispin M, Cunningham AF, Richter AG. Development of a high-sensitivity ELISA detecting IgG, IgA and IgM antibodies to the SARS-CoV-2 spike glycoprotein in serum and saliva. Immunology. 2021. https://doi.org/10.1111/imm.13349.

6. Gillot C, Douxfils J, Cadrobbi J, Laffineur K, Dogné J-M, Elsen M, Eucher C, Melchionda S, Modaffarri É, Tré-Hardy M, Favresse J. An original ELISA-based multiplex method for the simultaneous detection of 5 SARS-CoV-2 IgG antibodies directed against different antigens. J clin med. 2020. https://doi.org/10.3390/jcm9113752.

7. Kojima N, Klausner JD. Protective immunity after recovery from SARS-CoV-2 infection. Lancet Infect Dis. 2022. https://doi.org/10.1016/S1473-3099(21)00676-9.

8. Hoffmann M, Kleine-Weber H, Schroeder S, Krüger N, Herrler T, Erichsen S, Schiergens TS, Herrler G, Wu N-H, Nitsche A, Müller MA, Drosten C, Pöhlmann S. SARS-CoV-2 cell entry depends on ACE2 and TMPRSS2 and is blocked by a clinically proven protease inhibitor. Cell. 2020. https://doi.org/10.1016/j.cell.2020.02.052.

9. Haveri A, Ekström N, Solastie A, Virta C, Österlund P, Isosaari E, Nohynek H, Palmu AA, Melin M. Persistence of neutralizing antibodies a year after SARS-CoV-2 infection in humans. Eur J Immunol. 2021. https://doi.org/10.1002/eji.202149535.

10. Wall EC, Wu M, Harvey R, Kelly G, Warchal S, Sawyer C, Daniels R, Hobson P, Hatipoglu E, Ngai Y, Hussain S, Nicod J, Goldstone R, Ambrose K, Hindmarsh S, Beale R, Riddell A, Gamblin S, Howell M, Kassiotis G, Libri V, Williams B, Swanton C, Gandhi S, Bauer DLV. Neutralising antibody activity against SARS-CoV-2 VOCs B.1.617.2 and B.1.351 by BNT162b2 vaccination. Lancet. 2021; https://doi.org/10.1016/S0140-6736(21)01290-3

11. Rathe JA, Hemann EA, Eggenberger J, Li Z, Knoll ML, Stokes C, Hsiang T-Y, Netland J, Takehara KK, Pepper M, Gale M. SARS-CoV-2 serologic assays in control and unknown populations demonstrate the necessity of virus neutralization testing. J Infect Dis. 2021. https://doi.org/10.1093/infdis/jiaa797.

12. Bewley KR, Coombes NS, Gagnon L, McInroy L, Baker N, Shaik I, St-Jean JR, St-Amant N, Buttigieg KR, Humphries HE, Godwin KJ, Brunt E, Allen L, Leung S, Brown PJ, Penn EJ, Thomas K, Kulnis G, Hallis B, Carroll M, Funnell S, Charlton S. Quantification of SARS-CoV-2 neutralizing antibody by wild-type plaque reduction neutralization, microneutralization and pseudotyped virus neutralization assays. Nat Protoc. 2021. https://doi.org/10.1038/s41596-021-00536-y.

13. Perera RAPM, Ko R, Tsang OTY, Hui DSC, Kwan MYM, Brackman CJ, To EMW, Yen H-L, Leung K, Cheng SMS, Chan KH, Chan KCK, Li K-C, Saif L, Barrs VR, Wu JT, Sit THC, Poon LLM, Peiris M. Evaluation of a SARS-CoV-2 surrogate virus neutralization test for detection of antibody in human, canine, cat, and hamster sera. J Clin Microbiol. 2021. https://doi.org/10.1128/JCM.02504-20.

14. Tan CW, Chia WN, Qin X, Liu P, Chen MI-C, Tiu C, Hu Z, Chen VC-W, Young BE, Sia WR, Tan Y-J, Foo R, Yi Y, Lye DC, Anderson DE, Wang L-F. A SARS-CoV-2 surrogate virus neutralization test based on antibody-mediated blockage of ACE2-spike protein-protein interaction. Nat Biotechnol. 2020; https://doi.org/10.1038/s41587-020-0631-z

15. Liu K-T, Gong Y-N, Huang C-G, Huang P-N, Yu K-Y, Lee H-C, Lee S-C, Chiang H-J, Kung Y-A, Lin Y-T, Hsiao M-J, Huang P-W, Huang S-Y, Wu H-T, Wu C-C, Kuo R-L, Chen K-F, Hung C-T, Oguntuyo KY, Stevens CS, Kowdle S, Chiu H-P, Lee B, Chen G-W, Shih S-R. Quantifying neutralizing antibodies in patients with COVID-19 by a two-variable generalized additive model. mSphere. 2022; https://doi.org/10.1128/msphere.00883-21

16. Embregts CWE, Verstrepen B, Langermans JAM, Böszörményi KP, Sikkema RS, de Vries RD, Hoffmann D, Wernike K, Smit LAM, Zhao S, Rockx B, Koopmans MPG, Haagmans BL, Kuiken T, GeurtsvanKessel CH. Evaluation of a multi-species SARS-CoV-2 surrogate virus neutralization test. One Health. 2021. https://doi.org/10.1016/j.onehlt.2021.100313.

17. Wisnewski AV, Liu J, Lucas C, Klein J, Iwasaki A, Cantley L, Fazen L, Campillo Luna J, Slade M, Redlich CA. Development and utilization of a surrogate SARS-CoV-2 viral neutralization assay to assess mRNA vaccine responses. PLoS ONE. 2022. https://doi.org/10.1371/journal.pone.0262657.

18. Sholukh AM, Fiore-Gartland A, Ford ES, Miner MD, Hou YJ, Tse LV, Kaiser H, Zhu H, Lu J, Madarampalli B, Park A, Lempp FA, St Germain R, Bossard EL, Kee JJ, Diem K, Stuart AB, Rupert PB, Brock C, Buerger M, Doll MK, Randhawa AK, Stamatatos L, Strong RK, McLaughlin C, Huang M-L, Jerome KR, Baric RS, Montefiori D, Corey L. Evaluation of cell-based and surrogate SARS-CoV-2 neutralization assays. J Clin Microbiol. 2021. https://doi.org/10.1128/JCM.00527-21.

19. Abe KT, Li Z, Samson R, Samavarchi-Tehrani P, Valcourt EJ, Wood H, Budylowski P, Dupuis AP, Girardin RC, Rathod B, Wang JH, Barrios-Rodiles M, Colwill K, McGeer AJ, Mubareka S, Gommerman JL, Durocher Y, Ostrowski M, McDonough KA, Drebot MA, Drews SJ, Rini JM, Gingras A-C. A simple protein-based surrogate neutralization assay for SARS-CoV-2. JCI Insight. 2020. https://doi.org/10.1172/jci.insight.142362.

20. Münsterkötter L, Hollstein MM, Hahn A, Kröger A, Schnelle M, Erpenbeck L, Groß U, Frickmann H, Zautner AE. Comparison of the Anti-SARS-CoV-2 Surrogate neutralization assays by TECO-medical and DiaPROPH-Med with samples from vaccinated and infected individuals. Viruses. 2022. https://doi.org/10.3390/v14020315.

21. Kim SJ, Yao Z, Marsh MC, Eckert DM, Kay MS, Lyakisheva A, Pasic M, Bansal A, Birnboim C, Jha P, Galipeau Y, Langlois M-A, Delgado JC, Elgort MG, Campbell RA, Middleton EA, Stagljar I, Owen SC. Homogeneous surrogate virus neutralization assay to rapidly assess neutralization activity of anti-SARS-CoV-2 antibodies. Nat Commun. 2022. https://doi.org/10.1038/s41467-022-31300-9.

22. Fenwick C, Turelli P, Pellaton C, Farina A, Campos J, Raclot C, Pojer F, Cagno V, Nusslé SG, D'Acremont V, Fehr J, Puhan M, Pantaleo G, Trono D. A high-throughput cell- and virus-free assay shows reduced neutralization of SARS-CoV-2 variants by COVID-19 convalescent plasma. Sci Transl Med. 2021. https://doi.org/10.1126/scitranslmed.abi8452.

23. Lake DF, Roeder AJ, Kaleta E, Jasbi P, Pfeffer K, Koelbela C, Periasamy S, Kuzmina N, Bukreyev A, Grys TE, Wu L, Mills JR, McAulay K, Gonzalez-Moa M, Seit-Nebi A, Svarovsky S. Development of a rapid point-of-care test that measures neutralizing antibodies to SARS-CoV-2. J Clin Virol. 2021. https://doi.org/10.1016/j.jcv.2021.105024.

24. Fulford TS, Van H, Gherardin NA, Zheng S, Ciula M, Drummer HE, Redmond S, Tan H-X, Boo I, Center RJ, Li F, Grimley SL, Wines BD, Nguyen THO, Mordant FL, Ellenberg P, Rowntree LC, Kedzierski L, Cheng AC, Doolan DL, Matthews G, Bond K, Hogarth PM, McQuilten Z, Subbarao K, Kedzierska K, Juno JA, Wheatley AK, Kent SJ, Williamson DA, Purcell DFJ, Anderson DA, Godfrey DI. A point-of-care lateral flow assay for neutralising antibodies against SARS-CoV-2. EBioMedicine. 2021. https://doi.org/10.1016/j.ebiom.2021.103729.

25. Kongsuphol P, Jia H, Cheng HL, Gu Y, Shunmuganathan BD, Chen MW, Lim SM, Ng SY, Tambyah PA, Nasir H, Gao X, Tay D, Kim S, Gupta R, Qian X, Kozma MM, Purushotorman K, McBee ME, MacAry PA, Sikes HD, Preiser PR. A rapid simple

point-of-care assay for the detection of SARS-CoV-2 neutralizing antibodies. Commun Med (Lond). 2021. https://doi.org/10.1038/s43856-021-00045-9.

26. Zettl F, Meister TL, Vollmer T, Fischer B, Steinmann J, Krawczyk A, V'kovski P, Todt D, Steinmann E, Pfaender S, Zimmer G. Rapid quantification of SARS-CoV-2-neutralizing antibodies using propagation-defective vesicular stomatitis virus pseudotypes. Vaccines (Basel). 2020; https://doi.org/10.3390/vaccines8030386

27. Khoury DS, Cromer D, Reynaldi A, Schlub TE, Wheatley AK, Juno JA, Subbarao K, Kent SJ, Triccas JA, Davenport MP. Neutralizing antibody levels are highly predictive of immune protection from symptomatic SARS-CoV-2 infection. Nat Med. 2021. https://doi.org/10.1038/s41591-021-01377-8.

28. Klüpfel J, Paßreiter S, Weidlein N, Knopp M, Ungerer M, Protzer U, Knolle P, Hayden O, Elsner M, Seidel M. Fully automated chemiluminescence microarray analysis platform for rapid and multiplexed SARS-CoV-2 serodiagnostics. Anal Chem. 2022. https://doi.org/10.1021/acs.analchem.1c04672.

29. Wunderlich A, Torggler C, Elsässer D, Lück C, Niessner R, Seidel M. Rapid quantification method for Legionella pneumophila in surface water. Anal Bioanal Chem. 2016. https://doi.org/10.1007/s00216-016-9362-x.

30. Meyer VK, Meloni D, Olivo F, Märtlbauer E, Dietrich R, Niessner R, Seidel M. Validation procedure for multiplex antibiotic immunoassays using flow-based chemiluminescence microarrays. Methods Mol Biol. 2017. https://doi.org/10.1007/978-1-4939-6584-7_13.

31. Meyer VK, Chatelle CV, Weber W, Niessner R, Seidel M. Flow-based regenerable chemiluminescence receptor assay for the detection of tetracyclines. Anal Bioanal Chem. 2020. https://doi.org/10.1007/s00216-019-02368-y.

32. Szkola A, Linares EM, Worbs S, Dorner BG, Dietrich R, Märtlbauer E, Niessner R, Seidel M. Rapid and simultaneous detection of ricin, staphylococcal enterotoxin B and saxitoxin by chemiluminescence-based microarray immunoassay. Analyst. 2014. https://doi.org/10.1039/c4an00345d.

33. Szkola A, Campbell K, Elliott CT, Niessner R, Seidel M. Automated, high performance, flow-through chemiluminescence microarray for the multiplexed detection of phycotoxins. Anal Chim Acta. 2013. https://doi.org/10.1016/j.aca.2013.05.028.

34. Wutz K, Meyer VK, Wacheck S, Krol P, Gareis M, Nölting C, Struck F, Soutschek E, Böcher O, Niessner R, Seidel M. New route for fast detection of antibodies against zoonotic pathogens in sera of slaughtered pigs by means of flow-through chemiluminescence immunochips. Anal Chem. 2013. https://doi.org/10.1021/ac400781t.

35. Meyer VK, Kober C, Niessner R, Seidel M. Regeneration of recombinant antigen microarrays for the automated monitoring of antibodies against zoonotic pathogens in swine sera. Sensors (Basel). 2015. https://doi.org/10.3390/s150202614.

36. Göpfert L, Elsner M, Seidel M. Isothermal haRPA detection of blaCTX-M in bacterial isolates from water samples and comparison with qPCR. Anal Methods. 2021. https://doi.org/10.1039/d0ay02000a.

37. Kunze A, Dilcher M, Abd El Wahed A, Hufert F, Niessner R, Seidel M. On-chip isothermal nucleic acid amplification on flow-based chemiluminescence microarray analysis platform for the detection of viruses and bacteria. Anal Chem. 2016; https://doi.org/10.1021/acs.analchem.5b03540

38. Yakimchuk K. Protein receptor-ligand interaction/binding assays. Mater Methods. 2011; https://doi.org/10.13070/mm.en.1.199

39. Yi C, Sun X, Ye J, Ding L, Liu M, Yang Z, Lu X, Zhang Y, Ma L, Gu W, Qu A, Xu J, Shi Z, Ling Z, Sun B. Key residues of the receptor binding motif in the spike protein of SARS-CoV-2 that interact with ACE2 and neutralizing antibodies. Cell Mol Immunol. 2020. https://doi.org/10.1038/s41423-020-0458-z.

40. Syedbasha M, Linnik J, Santer D, O'Shea D, Barakat K, Joyce M, Khanna N, Tyrrell DL, Houghton M, Egli A. An ELISA based binding and competition method to rapidly determine ligand-receptor interactions. JoVE (Journal of Visualized Experiments). 2016. https://doi.org/10.3791/53575.

41. Eble JA. Titration ELISA as a method to determine the dissociation constant of receptor ligand interaction. J Vis Exp. 2018. https://doi.org/10.3791/57334.

42. Weng Z, Zhao Q. Utilizing ELISA to monitor protein-protein interaction. Methods Mol Biol. 2015. https://doi.org/10.1007/978-1-4939-2425-7_21.

43. Pollard TD. A guide to simple and informative binding assays. Mol Biol Cell. 2010. https://doi.org/10.1091/mbc.E10-08-0683.

44. Bojadzic D, Alcazar O, Buchwald P. Methylene blue inhibits the SARS-CoV-2 spike-ACE2 protein-protein interaction-a mechanism that can contribute to its antiviral activity against COVID-19. Front Pharmacol. 2020. https://doi.org/10.3389/fphar.2020.600372.

45. Klüpfel J, Koros RC, Dehne K, Ungerer M, Würstle S, Mautner J, Feuerherd M, Protzer U, Hayden O, Elsner M, Seidel M. Automated, flow-based chemiluminescence microarray immunoassay for the rapid multiplex detection of IgG antibodies to SARS-CoV-2 in human serum and plasma (CoVRapid CL-MIA). Anal Bioanal Chem. 2021. https://doi.org/10.1007/s00216-021-03315-6.

46. Richardson JR, Götz R, Mayr V, Lohse MJ, Holthoff H-P, Ungerer M. SARS-CoV2 wild type and mutant specific humoral and T cell immunity is superior after vaccination than after natural infection. PLoS ONE. 2022. https://doi.org/10.1371/journal.pone.0266701.

47. Wolter A, Niessner R, Seidel M. Preparation and characterization of functional poly(ethylene glycol) surfaces for the use of antibody microarrays. Anal Chem. 2007. https://doi.org/10.1021/ac070243a.

48. Bemetz J, Kober C, Meyer VK, Niessner R, Seidel M. Succinylated Jeffamine ED-2003 coated polycarbonate chips for low-cost analytical microarrays. Anal Bioanal Chem. 2019. https://doi.org/10.1007/s00216-019-01594-8.

49. Cheng C-C, Platen L, Christa C, Tellenbach M, Kappler V, Bester R, Liao B-H, Holzmann-Littig C, Werz M, Schönhals E, Platen E, Eggerer P, Tréguer L, Küchle C, Schmaderer C, Heemann U, Renders L, Protzer U, Braunisch MC. Improved SARS-CoV-2 neutralization of delta and omicron BA.1 variants of concern after fourth vaccination in hemodialysis patients. Vaccines (Basel). 2022; https://doi.org/10.3390/vaccines10081328

50. Li X, Pang L, Yin Y, Zhang Y, Xu S, Xu D, Shen T. Patient and clinical factors at admission affect the levels of neutralizing antibodies six months after recovering from COVID-19. Viruses. 2022. https://doi.org/10.3390/v14010080.

51. Martin Knopp. MCR-analyser. 2022. https://github.com/mknopp/mcr-analyser. Accessed 3 Oct 2022.

52. National Institute for Biological Standards and Control. First WHO International Standard for anti-SARS-CoV-2 immunoglobulin (human), NIBSC code: 20/136, Instructions for use. 2020. https://www.nibsc.org/documents/ifu/20-136.pdf. Accessed 20 Sept 2022.

53. Bentley EM, Atkinson E, Rigsby P, Elsley W, Bernasconi V, Kristiansen P, Harvala H, Turtle LCW, Dobson S, Wendel S, Anderson R, Kempster S, Duran J, Padley D, Almond N, Rose NJ, Page M, Mattiuzzo Giada. Establishment of the 2nd WHO International Standard for anti-SARS-CoV-2 immunoglobulin and reference panel for antibodies to SARS-CoV-2 variants of concern. WHO Expert Committee on Biological Standardization. 2022

Publisher's note Springer Nature remains neutral with regard to jurisdictional claims in published maps and institutional affiliations.

Automated detection of neutralizing SARS-CoV-2 antibodies in minutes using a competitive chemiluminescence immunoassay

Julia Klüpfel[1‡], Sandra Paßreiter[1‡], Melina Rumpf[1], Catharina Christa[2], Hans-Peter Holthoff[3], Martin Ungerer[3], Martin Lohse[3], Percy Knolle[4], Ulrike Protzer[2,5], Martin Elsner[1], Michael Seidel[1]*

[1]Institute of Water Chemistry, Chair of Analytical Chemistry and Water Chemistry, Technical University of Munich, Lichtenbergstr. 4, 85748 Garching, Germany

[2]Institute of Virology, Technical University of Munich / Helmholtz Zentrum München, Trogerstr. 30, 81675 München

[3]ISAR Bioscience GmbH, Semmelweisstr. 5, 82152 Planegg

[4]Institute of Molecular Immunology/ Experimental Oncology, Technical University of Munich, Ismaningerstr. 22, 81675 München

[5]German Center for Infection Research (DZIF), 81675 München

‡ These authors contributed equally.

*Corresponding author: michael.seidel@mytum.de, tel: +49-89-289-54506

Content:

S1. Stopped-flow assay for total IgG measurement on the MCR-R

The total IgG antibody test was carried out in a stopped-flow manner, details on volumes and flow velocities can be found in Table S1. After injection of the sample into the device, the sample was pushed over the chip slowly in increments of 80 µL. After each increment, the flow was stopped for 5 s to allow for the sample to interact with the immobilized proteins. A total volume of 400 µL was transported over the chip consisting of 225 µL sample followed by an additional 175 µL to flush sample residues that might have resided in the tubing over the chip. Subsequently, flushing of the chip with running buffer was done, followed by the slow transport of the detection antibody, peroxidase-labelled anti human IgG antibody, over the chip. After another flushing step, the CL reaction was started by filling the chip with hydrogen peroxide and luminol with an immediate image recording by the CCD camera, followed by final flushing steps.

Table S1 Main assay steps for total anti-SARS-CoV-2 IgG assay on the MCR-R with details of used volumes and flow rates.

Step	Volume	Flow rate	Comment
Flushing of chip	2500 µL	500 µL s^{-1}	
Manual sample injection	225 µL	-	Manually via adapter
Sample transport	400 µL	10 µL s^{-1}	
	(5 increments, 5 s pause)		
Flushing	200 µL	10 µL s^{-1}	
	2000 µL	500 µL s^{-1}	
Injection of HRP-labelled	115 µL	50 µL s^{-1}	
anti IgG antibody	800 µL	10 µL s^{-1}	
Flushing	2000 µL	500 µL s^{-1}	
CL reagents injection	400 µL	150 µL s^{-1}	
Image acquisition	-	-	60 s exposure
Cleaning of sample input	2000 µL	-	Manually via adapter
Flushing of whole system	7500 µL	250 µL s^{-1}	

S2. Comparison of different chip materials and immobilization principles for use on the MCR-R

Previously, the MCR series had been used with polycarbonate and glass microarray chips for various applications [1–5] but no direct comparison of different chip types in one assay on the same platform had been done before. Therefore, we tested three different materials and two different activation strategies, namely glass chips, PC sheet chips with a thickness of 1 mm, and PC foil chips with a thickness of 0.25 mm. Glass chips were activated with DSC (whole surface activation) as well as with EDC/s-NHS (spot activation only), while for PC only EDC/s-NHS activation was feasible as PC does not tolerate the solvents necessary for DSC activation. Details on the experimental implementation can be found in the Materials and Methods section. The differences between the activation strategies on the molecular level are depicted in Figure S1.
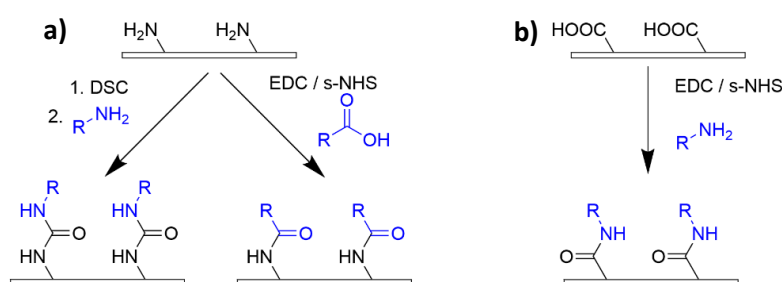

Figure S1 Activation strategies used for **a)** glass and **b)** PC microarray chips.

All chip types were then used for measurements of samples from SARS-CoV-2 naive, vaccinated and reconvalescent persons as shown in Figure S2. The measurements were done on the MCR-R as described previously [6].
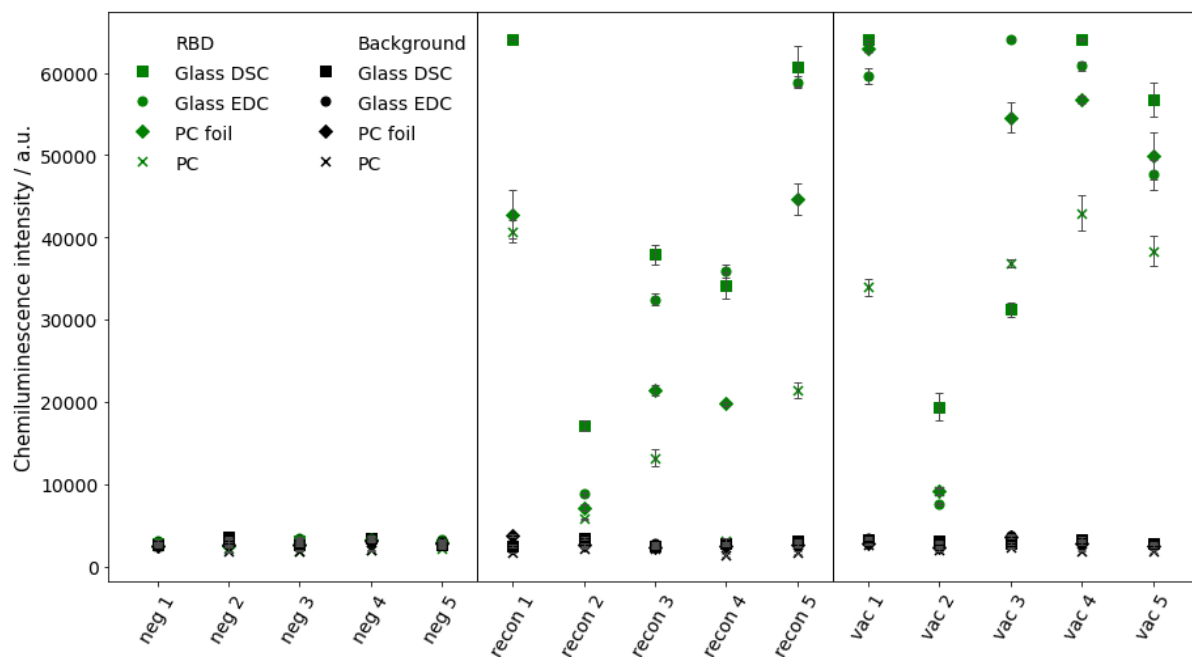

Figure S2 Comparison of measurement results for total antibody detection to SARS-CoV-2 RBD with positive (vaccinated/reconvalescent) and negative samples. RBD is immobilized on glass carrier, PC foils, and PC sheets (error bars show standard deviations of spot replicates on one chip, n = 5).

While the background values as well as the results for negative samples are comparable on all tested chip types, it is clearly visible that for most of the positive samples the highest intensities were measured on glass chips, followed by the two types of polycarbonate chips. Regarding the different activation methods on glass, the DSC activation overall gave slightly higher values compared to the EDC/s-NHS activation with very few exceptions as for example in sample vac 3, which can be attributed to a defect in this single chip. Therefore, DSC activation is considered the optimal activation method for protein immobilization on glass chips as here the protein itself is not compromised by possible crosslinking during the spotting process in contrast to the EDC/s-NHS strategy.

In PC chips, the EDC/s-NHS is used to activate the carboxy groups on the chip surface and let it react with amine groups on the proteins. This procedure generally led to lower intensities compared to glass chips, possibly due to a lower density of functional groups on the surface as during the carboxy coupling of Jeffamine double-substituted polymer that cannot be bound to the surface might result. Additionally, the screen-printing process might be less efficient than the melting process used for the coating of glass chips. Nevertheless, the PC foil chips often came close to the glass chip signals, while the thicker PC sheet chips generally showed a lower performance. A possible reason is the more even surface of foil chips after coating due to the better heat distribution during the incubation after screen printing.

As was detailed in the experimental section and previous publications [6], PC chips have significant advantages with regard to work expenditure and production time. On the other hand, an advantage of DSC-activated glass chips is the possibility to store activated chips at 4 °C for several weeks, while the spotting solutions can also be used for prolonged time as no activating reagents are added. In contrast, in EDC/s-NHS activation, spotting must be done within a few hours after preparation of the spotting solutions to prevent activity loss of the s-NHS ester intermediate. Performance-wise, glass

chips showed superior performance for the total SARS-CoV-2 antibody assay as shown here. But as especially PC foil chips showed relatively comparable results for some samples, chip material evaluations should be repeated whenever new immunoassays are developed.

S3. ACE2-RBD interaction measurements with immobilized RBD

While generally, we used immobilized ACE2 for interaction measurements, the immobilization of RBD is also possible. This principle would have the advantage of immobilizing different RBD variants on the same chip giving additional information within one measurement. To test the behavior of different variants in interaction measurements, wildtype RBD as well as delta RBD were immobilized in tenfold dilutions over a broad concentration range from 800 µg mL^1 (1:2 dilution) to 8 µg mL^{-1} (1:200 dilution). This wide concentration range was chosen to make differences between the different mutants more apparent. Different concentrations of biotinylated ACE2 were added in a range from 0 to 50 µg mL^{-1}, again resulting in sigmoidal binding curves as shown in Figure 4. For the highest dilution (1:200) only a relatively low signal is obtained at the highest tested ACE2 concentrations, but for 1:20 and 1:2 dilutions stronger signals are obtained already at lower ACE2 concentrations. Especially for the 1:20 dilutions a notable difference between wt RBD and delta RBD is noticeable with delta giving significantly higher signals and at the same time lower EC50 (12.1 µg mL^{-1} compared to 23.9 µg mL^{-1}), possibly indicating a higher affinity of delta RBD to ACE2 compared to wt RBD as one would expect and as has been shown in affinity studies before [7, 8]. Still, more thorough studies on the binding of different RBD variants to ACE2 will be done on the MCR-R in the future to complement these preliminary findings.

Despite these promising results with immobilized RBD, it was decided to conduct the neutralization measurements with immobilized ACE2 and a biotinylated RBD concentration of 5 µg/mL as that assay format showed significantly lower EC50 values, while the relatively high amounts of biotinylated ACE2 that would have been necessary for the alternate assay were considered at the present status of the assay development too cost intensive and, additionally, the measurement of neutralizing antibodies was less reliable (results not shown). This difference might be attributed to sterical reasons, and it may be a consequence of the different principle of the neutralization assay that is not based on RBD-antibody binding in the liquid phase and thus reduction of the available RBD amount but rather on competition on the chip surface. The optimization of this assay towards lower ACE2 amounts and its use in neutralization measurements will be objective of future research.
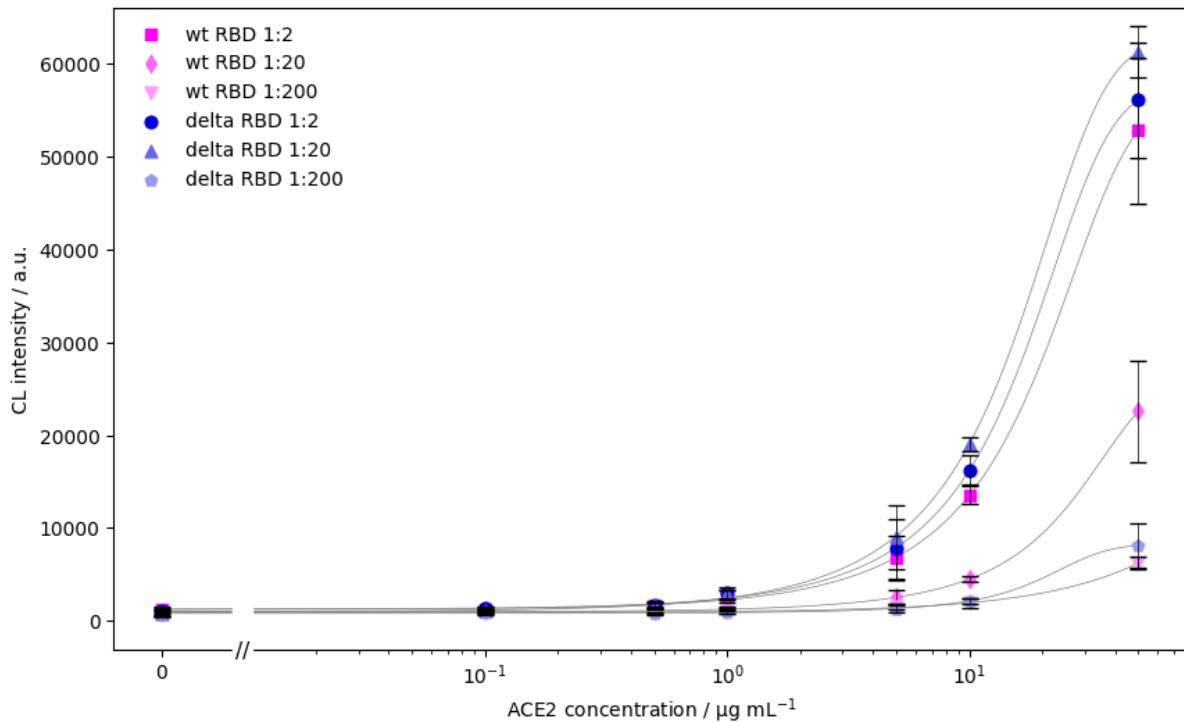
Figure S3 Comparison of different immobilized RBD mutants and concentrations for determination of ACE2-RBD binding (CL signals are background-corrected, error bars show standard deviations of triplicate measurements, curves were fitted using 4-parameter logistic fit, linear axis scaling is used left of the axis break to include 0 µg mL^{-1}).

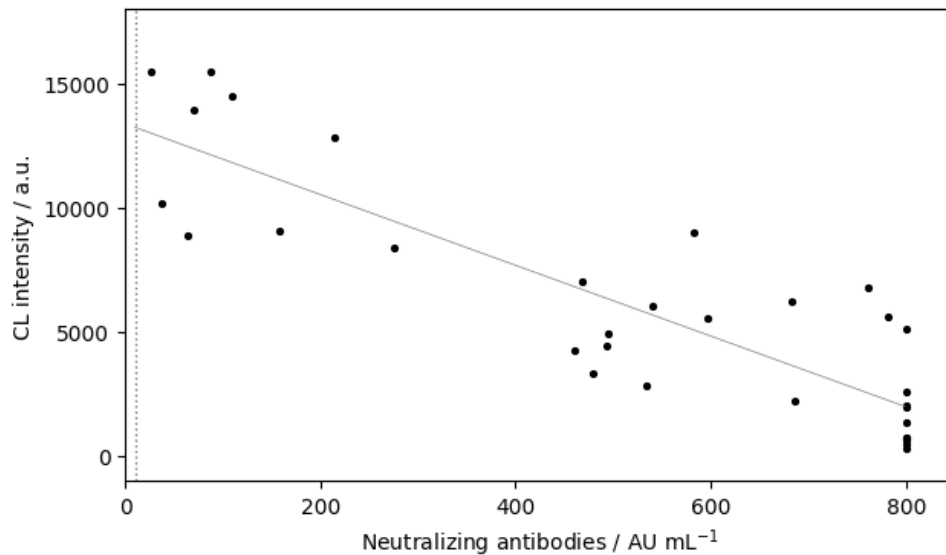## S4. Comparison measurements with commercial surrogate neutralization assay

Figure S4 Correlation between neutralizing antibody measurements of 33 seropositive samples in AU mL^{-1} (measured by YHLO iFlash neutralization assay) and CL signal obtained in MCR-R neutralization assay (CL signals are background-corrected, dotted line shows threshold value for positive samples (10 AU mL^{-1}), 800 AU mL^{-1} represents upper limit of quantification of YHLO assay, gray line shows linear fit of data).

References

1. Kunze A, Dilcher M, Abd El Wahed A, Hufert F, Niessner R, Seidel M. On-Chip Isothermal Nucleic Acid Amplification on Flow-Based Chemiluminescence Microarray Analysis Platform for the Detection of Viruses and Bacteria. Anal Chem. 2016; https://doi.org/10.1021/acs.analchem.5b03540

2. Seidel M, Niessner R. Chemiluminescence microarrays in analytical chemistry: a critical review. Anal Bioanal Chem. 2014; https://doi.org/10.1007/s00216-014-7968-4

3. Wolter A, Niessner R, Seidel M. Preparation and characterization of functional poly(ethylene glycol) surfaces for the use of antibody microarrays. Anal Chem. 2007; https://doi.org/10.1021/ac070243a

4. Kober C, Niessner R, Seidel M. Quantification of viable and non-viable Legionella spp. by heterogeneous asymmetric recombinase polymerase amplification (haRPA) on a flow-based chemiluminescence microarray. Biosens Bioelectron. 2018; https://doi.org/10.1016/j.bios.2017.08.053

5. Wutz K, Meyer VK, Wacheck S, Krol P, Gareis M, Nölting C, Struck F, Soutschek E, Böcher O, Niessner R, Seidel M. New route for fast detection of antibodies against zoonotic pathogens in sera of slaughtered pigs by means of flow-through chemiluminescence immunochips. Anal Chem. 2013; https://doi.org/10.1021/ac400781t

6. Klüpfel J, Paßreiter S, Weidlein N, Knopp M, Ungerer M, Protzer U, Knolle P, Hayden O, Elsner M, Seidel M. Fully Automated Chemiluminescence Microarray Analysis Platform for Rapid and Multiplexed SARS-CoV-2 Serodiagnostics. Anal Chem. 2022; https://doi.org/10.1021/acs.analchem.1c04672

7. Wu L, Zhou L, Mo M, Liu T, Wu C, Gong C, Lu K, Gong L, Zhu W, Xu Z. SARS-CoV-2 Omicron RBD shows weaker binding affinity than the currently dominant Delta variant to human ACE2. Signal Transduct Target Ther. 2022; https://doi.org/10.1038/s41392-021-00863-2

8. Wang Y, Liu C, Zhang C, Wang Y, Hong Q, Xu S, Li Z, Yang Y, Huang Z, Cong Y. Structural basis for SARS-CoV-2 Delta variant recognition of ACE2 receptor and broadly neutralizing antibodies. Nat Commun. 2022; https://doi.org/10.1038/s41467-022-28528-w

5 Summary & Outlook

In the beginning of this PhD thesis, SARS-CoV-2 had just started to emerge within Europe and the world. At that time, no medication or vaccination was available, nor was it known whether seroconversion after an infection would prevent reinfection. Additionally, it was yet unforeseen what mutations of the virus would occur over time and how they would influence disease severity and immune reaction.

Therefore, this work started at the perfect time for providing important information in the new field of SARS-CoV-2 serodiagnostics and was able to live up to the expectations over the course of three years. Many other research groups and diagnostic companies worldwide put enormous resources into the development of antibody tests using established diagnostic ELISA platforms for time-consuming high-throughput antibody tests for the conduction in specialized laboratories. Other groups focused on LFAs for the POC market that were rapid and easy to conduct but often had to fight matrix influences and therefore decreased specificity and sensitivity while additionally in large part not enabling any quantitative analysis. None of these two main test principles could fulfil all main requirements of the diagnostic sector, further fueling research groups to invest in novel approaches, resulting in several thousand publications on SARS-CoV-2 antibody tests over the course of three years.

What was needed to follow the dynamic pandemic situation were flexible tests that could easily be adjusted to any new research questions or changes in the virus and its behavior, optimally within few weeks. Quantitative tests were preferred as they could give an estimate of correlates of protection in contrast to qualitative tests that were often faster but provided less depth of information. Nevertheless, rapid test results generally were desired as they enabled versatile application fields and great opportunities for rapid optimization studies. But even more important was the availability of tests answering several questions at once, for example by testing for antibodies to different SARS-CoV-2 proteins simultaneously, by considering different SARS-CoV-2 mutants at once or by analyzing different antibody classes. Analytical platforms were required to offer many different test types so that the same equipment and training was usable for all diagnostic questions of interest. Fulfilling all these requirements was something that most analytical platforms and developed antibody tests were not able to do. Thus, an evident need for a test system combining as many of these requirements as possible emerged.

Therefore, three years after the beginning of this dissertation, it can be concluded that although little was known about serological testing in humans within the IWC at the beginning,

very significant results could be achieved that can compete with or even outperform other tests. Necessary prerequisites to enable these achievements were the availability of a suitable analysis platform for flow-based CL-MIAs, the MCR system, as well as the availability of high-quality recombinant SARS-CoV-2 antigens from eukaryotic sources produced by ISAR Bioscience GmbH.

Starting from these preconditions, a versatile antibody testing system for SARS-CoV-2 was developed. Using the principle of a flow-based, indirect, non-competitive CL-MIA, antibodies to different relevant antigens from the novel virus could be detected with extraordinary sensitivity and specificity in under 10 min. The microarray chips were proven to be optimally suited for analyses in blood although it represents a very demanding matrix. It was even possible to present different chip materials and covalent immobilization strategies that were all applicable for recombinant native antigens. The very short assay time, enabled by the flow-based principle that was possible owing to the MCR technology, made the assay faster than the great majority of all presented antibody assays over the time of the pandemic, as can be seen when comparing to the examples presented in Chapter 2.3.2. Apart from the analysis time, also the obtained sensitivity and specificity for the novel antibody assay compared favorable with assays in literature and also commercial antibody assays, showing that a competitive analysis tool was developed within very short time although all basic requirements and optimization steps for the development of antibody assays and the work with human blood, also from the viewpoint of laboratory safety, had to be acquired from scratch.

What already points towards the future developments that will emanate from the results of this dissertation, is the great versatility and adaptability of the assay. This was proven over the pandemic years by rapidly reacting to any new requirements developing from the course of the pandemic. Therefore, a successful test for the detection of different antibody classes (IgM and IgG) was developed, the first prototypic antibody assay was improved to manage with even less analysis time and sample volume, production capacities were upscaled and an even more complex matrix - whole blood - was proven to be applicable, opening the way for POC applications of the test portfolio.

As a final chapter of this dissertation, the reaction to another new demand during the pandemic was reported: the analysis of neutralizing antibodies. Although the test principle necessary therefore differed severely from the previously used assay principles - as it was a competitive assay relying on a very short static incubation of sample in the microarray chip and subsequent flow-based detection in contrast to the previous non-competitive flow-based assays - it could be developed within few months and gave remarkable results, even in comparison with other neutralization tests that were in part applied in routine serodiagnostics. Moreover, the new test was significantly faster than any other neutralization test reported during the three years of the pandemic, showing the versatile possibilities of microarray immunoassays on a well-researched

platform.

These rapid adjustments to any new requirements make the MCR platform an optimal instrument in the POC diagnostic market. Since commonly used platforms often are slow and require extensive financial and manpower effort to be adapted to new challenges, flexible platforms are needed not only in SARS-CoV-2 serology but also for other existing diseases and pandemics to come. Moreover, versatile, easily adaptable platforms are of high interest for the research market. Commercial platforms often are extremely expensive and come with pre-defined assays and without the opportunity to include new analysis targets. The development and inclusion of novel assays to answer research questions often is not offered by the platform providers or is very time and cost intensive. Here, an assay development service would be required, rapidly answering pressing research questions for research groups that lack the experience to develop serological assays by themselves if they are not commercially available.

Although this application field for custom-made serological assays on the MCR platform has not been part of the results presented within this work, first promising results have been gained already. The requirement was to develop an assay for the measurement of SARS-CoV-2 antibody avidity in ongoing follow-up work subsequent to this thesis. An avidity assay was developed within weeks and tested for a cohort of 20 patients with four samples of each patient that had been taken at different timepoints after vaccination or infection. The preliminary results compared very favorably with a commercial avidity assay while also giving additional information that could not be gained using the commercial assay, as several virus variants could be considered simultaneously.

Concluding, this dissertation paved the way for a novel field of analysis provided by the analysis platform MCR. This work is the basis for various future applications in serological diagnostics, as it was shown that detection of different antibody classes as well as the detection of the antibodies' activity by neutralizing protein-protein interaction is possible in a highly reliable manner. Additionally, it was proven that extension of the assay to additional antigens can easily be done. While in this work only results for SARS-CoV-2 were presented, additional results for other infections were obtained already, including endemic coronaviruses and influenza. Furthermore, measurements for various SARS-CoV-2 variants were done and proven successful. The microarray is well suited for the detection of immune response patterns for up to 20 different antigens at once. Therefore, in the future serodiagnostic tests showing the immune response to numerous pathogens simultaneously will be feasible, for example to do a complete vaccination status checkup within a few minutes and to then decide over the necessity of booster vaccinations. Even more, also diagnostics of acute infections can be thought for diseases where IgM is formed relatively early. Due to the flexibility of the microarray principle, adaptations can be made rapidly, broadening the application space for serological microarray immunoassays on the MCR.

A further possible extension of the test principles presented in this thesis is the detection of antigen-specific T cells. If it is not only possible to detect the humoral immunity by measuring antibodies formed after infection or vaccination but also to evaluate cellular immunity by measuring T cells, a profound statement on the immune status can be made, even a long time after the last immunization, when possibly no antibodies can be detected anymore but still T cells are present.

This dissertation has, therefore, pioneered a solid bioanalytical foundation for future wide-ranging immunological assessments for different diseases of interest. The results are promising for future new assay types as well as for a possible commercial application of the SARS-CoV-2 antibody assays presented herein that are well suited for the POC determination of antibodies in medical practices, hospitals or pharmacies. This work is a proof of how far one can come within the short time frame of three years and very low manpower, even when not being experienced in the field of serological diagnostics beforehand. Despite these odds, significant results were obtained that can live up to other research results as well as commercial platforms and will hopefully be further extended in the upcoming years, contributing to shaping the field of serodiagnostics and possibly even adding to preventing or efficiently fighting future disease outbreaks worldwide.

6 Bibliography

[1] Huremović, D. In *Psychiatry of Pandemics*; Huremović, D., Ed.; Springer International Publishing: Cham, 2019; pp 7–35.

[2] Johns Hopkins Center for Health Security, Event 201. `https://www.centerforhealthsecurity.org/our-work/exercises/event201/`.

[3] Zhou, P.; Yang, X.-L.; Wang, X.-G.; Hu, B.; Zhang, L.; Zhang, W.; Si, H.-R.; Zhu, Y.; Li, B.; Huang, C.-L. et al. *Nature* **2020**, *579*, 270–273.

[4] WHO, Coronavirus disease (COVID-19) pandemic. 30.08.2022; `https://www.who.int/europe/emergencies/situations/covid-19`.

[5] European Union External Action, *EEAS Blog* **23.03.2020**, *2020*.

[6] Coronaviridae Study Group of the International Committee on Taxonomy of Viruses, *Nature Microbiology* **2020**, *5*, 536–544.

[7] Lu, R.; Zhao, X.; Li, J.; Niu, P.; Yang, B.; Wu, H.; Wang, W.; Song, H.; Huang, B.; Zhu, N. et al. *The Lancet* **2020**, *395*, 565–574.

[8] Harrison, A. G.; Lin, T.; Wang, P. *Trends in Immunology* **2020**, *41*, 1100–1115.

[9] Khailany, R. A.; Safdar, M.; Ozaslan, M. *Gene Reports* **2020**, *19*, 100682.

[10] Cubuk, J.; Alston, J. J.; Incicco, J. J.; Singh, S.; Stuchell-Brereton, M. D.; Ward, M. D.; Zimmerman, M. I.; Vithani, N.; Griffith, D.; Wagoner, J. A. et al. *Nature Communications* **2021**, *12*, 1936.

[11] *Created with BioRender.com*

[12] Jackson, C. B.; Farzan, M.; Chen, B.; Choe, H. *Nature Reviews. Molecular Cell Biology* **2022**, *23*, 3–20.

[13] Hoffmann, M.; Kleine-Weber, H.; Schroeder, S.; Krüger, N.; Herrler, T.; Erichsen, S.; Schiergens, T. S.; Herrler, G.; Wu, N.-H.; Nitsche, A. et al. *Cell* **2020**, *181*, 271–280.e8.

[14] Peacock, T. P.; Goldhill, D. H.; Zhou, J.; Baillon, L.; Frise, R.; Swann, O. C.; Kugath-asan, R.; Penn, R.; Brown, J. C.; Sanchez-David, R. Y. et al. *Nature Microbiology* **2021**, *6*, 899–909.

[15] Fuentes-Prior, P. *The Journal of Biological Chemistry* **2021**, *296*, 100135.

[16] Trougakos, I. P.; Stamatelopoulos, K.; Terpos, E.; Tsitsilonis, O. E.; Aivalioti, E.; Paraske-vis, D.; Kastritis, E.; Pavlakis, G. N.; Dimopoulos, M. A. *Journal of Biomedical Science* **2021**, *28*, 9.

[17] Malone, B.; Urakova, N.; Snijder, E. J.; Campbell, E. A. *Nature Reviews. Molecular Cell Biology* **2022**, *23*, 21–39.

[18] Abu-Farha, M.; Thanaraj, T. A.; Qaddoumi, M. G.; Hashem, A.; Abubaker, J.; Al-Mulla, F. *International Journal of Molecular Sciences* **2020**, *21*.

[19] Qin, Z.; Sun, Y.; Zhang, J.; Zhou, L.; Chen, Y.; Huang, C. *Molecular Medicine Reports* **2022**, *26*.

[20] Sun, C.; Xie, C.; Bu, G.-L.; Zhong, L.-Y.; Zeng, M.-S. *Signal Transduction and Targeted Therapy* **2022**, *7*, 202.

[21] Hirabara, S. M.; Serdan, T. D. A.; Gorjao, R.; Masi, L. N.; Pithon-Curi, T. C.; Co-vas, D. T.; Curi, R.; Durigon, E. L. *Frontiers in Cellular and Infection Microbiology* **2021**, *11*, 781429.

[22] Chen, C.; Nadeau, S.; Yared, M.; Voinov, P.; Xie, N.; Roemer, C.; Stadler, T. *Bioinfor-matics (Oxford, England)* **2021**,

[23] Lorente-González, M.; Suarez-Ortiz, M.; Landete, P. *Open Respiratory Archives* **2022**, *4*, 100169.

[24] Diamond, M. S.; Kanneganti, T.-D. *Nature Immunology* **2022**, *23*, 165–176.

[25] Wu, Z.; McGoogan, J. M. *JAMA* **2020**,

[26] Song, P.; Li, W.; Xie, J.; Hou, Y.; You, C. *Clinica Chimica Acta* **2020**, *509*, 280–287.

[27] Beigel, J. H.; Tomashek, K. M.; Dodd, L. E.; Mehta, A. K.; Zingman, B. S.; Kalil, A. C.; Hohmann, E.; Chu, H. Y.; Luetkemeyer, A.; Kline, S. et al. *The New England Journal of Medicine* **2020**, *383*, 1813–1826.

[28] Ghazy, R. M.; Ashmawy, R.; Hamdy, N. A.; Elhadi, Y. A. M.; Reyad, O. A.; El-malawany, D.; Almaghraby, A.; Shaaban, R.; Taha, S. H. N. *Vaccines* **2022**, *10*.

[29] Wise, J. *BMJ (Clinical Research ed.)* **2022**, *376*, o309.

[30] Connors, M.; Graham, B. S.; Lane, H. C.; Fauci, A. S. *Annals of Internal Medicine* **2021**, *174*, 687–690.

[31] Taquet, M.; Dercon, Q.; Harrison, P. J. *Brain, Behavior, and Immunity* **2022**, *103*, 154–162.

[32] Zeng, B.; Le Gao,; Zhou, Q.; Yu, K.; Sun, F. *BMC Medicine* **2022**, *20*, 200.

[33] Tuekprakhon, A.; Nutalai, R.; Dijokaite-Guraliuc, A.; Zhou, D.; Ginn, H. M.; Selvaraj, M.; Liu, C.; Mentzer, A. J.; Supasa, P.; Duyvesteyn, H. M. E. et al. *Cell* **2022**, *185*, 2422–2433.e13.

[34] Khoury, D. S.; Docken, S. S.; Subbarao, K.; Kent, S. J.; Davenport, M. P.; Cromer, D. *medRxiv* **2022**,

[35] Janeway, C. A.; Travers, P.; Walport, M.; Shlomchik, M. J. *Immunobiology 5: The immune system in health and disease*, 5th ed.; Garland Pub: New York, 2001.

[36] Schmalstieg, F. C.; Goldman, A. S. *Journal of Medical Biography* **2008**, *16*, 96–103.

[37] Ehrlich, P. *Proceedings of the Royal Society of London* **1900**, *66*, 424–448.

[38] Metchnikoff, E. *Archiv für pathologische Anatomie und Physiologie und für klinische Medicin* **1884**, *96*, 177–195.

[39] Carlberg, C.; Velleuer, E. *Molecular Immunology*; Springer International Publishing: Cham, 2022.

[40] Marshall, J. S.; Warrington, R.; Watson, W.; Kim, H. L. *Allergy, Asthma, and Clinical Immunology* **2018**, *14*, 49.

[41] Kumar, V.; Abbas, A. K.; Fausto, N. *Robbins and Cotran Pathologic Basis of Disease*, 7th ed.; Elsevier Saunders: Philadelphia, Pa., 2005.

[42] Coico, R. *Immunology: A Short Course*, 7th ed.; John Wiley & Sons Incorporated: New York, 2014.

[43] Takeda, K.; Akira, S. *International Immunology* **2005**, *17*, 1–14.

[44] Anaya, J. M., Levy, R. A., Rojas-Villarraga, A., Shoenfeld, Y., Cervera, R., Eds. *Autoimmunity: From bench to bedside*; Colección Textos; Editorial Universidad del Rosario: Bogotá, 2013.

[45] Parkin, J.; Cohen, B. *The Lancet* **2001**, *357*, 1777–1789.

[46] Sarma, J. V.; Ward, P. A. *Cell and Tissue Research* **2011**, *343*, 227–235.

[47] Alberts, B.; Johnson, A.; Lewis, J.; Raff, M.; Roberts, K.; Walter, P. *Molecular Biology of the Cell*, 4th ed.; Garland Science: New York, 2002.

[48] Ni, K.; O'Neill, H. C. *Immunology and Cell Biology* **1997**, *75*, 223–230.

[49] Gutcher, I.; Becher, B. *Journal of Clinical Investigation* **2007**, *117*, 1119–1127.

[50] Cox, M. A.; Kahan, S. M.; Zajac, A. J. *Virology* **2013**, *435*, 157–169.

[51] Lieberman, J. *Nature Reviews. Immunology* **2003**, *3*, 361–370.

[52] Burleson, G. R.; Burleson, S. C.; Burleson, F. G. In *Comparative Biology of the Normal Lung*; Parent, R. A., Ed.; Elsevier Reference Monographs: s.l., 2015; pp 581–600.

[53] Murphy, K. M. *Janeway's Immunobiology*, 8th ed.; Taylor & Francis distributor: New York and London, 2011.

[54] Sam-Yellowe, T. Y. *Immunology: Overview and Laboratory Manual*, 1st ed.; Springer eBook Collection; Springer International Publishing and Imprint Springer: Cham, 2021.

[55] LeBien, T. W.; Tedder, T. F. *Blood* **2008**, *112*, 1570–1580.

[56] Pieper, K.; Grimbacher, B.; Eibel, H. *The Journal of Allergy and Clinical Immunology* **2013**, *131*, 959–971.

[57] Mårtensson, I.-L.; Almqvist, N.; Grimsholm, O.; Bernardi, A. I. *FEBS Letters* **2010**, *584*, 2572–2579.

[58] Schroeder, H. W.; Radbruch, A.; Berek, C. In *Clinical Immunology*; Rich, R. R., Fleisher, T. A., Shearer, W. T., Schroeder, H. W., Frew, A. J., Weyand, C., Eds.; Elsevier: St. Louis, MO, 2019; pp 107–118.e1.

[59] van Regenmortel, M. H.; Azimzadeh, A. *Journal of Immunoassay* **2000**, *21*, 211–234.

[60] Frasca, V. *Journal of Applied Bioanalysis* **2016**, *2*, 90–102.

[61] Siegenthaler, W., Blum, H. E., Eds. *Klinische Pathophysiologie*, 9th ed.; Georg Thieme Verlag: Stuttgart and New York, 2006.

[62] Krotkiewski, H.; Grönberg, G.; Krotkiewska, B.; Nilsson, B.; Svensson, S. *Journal of Biological Chemistry* **1990**, *265*, 20195–20201.

[63] Harris, L. J.; Larson, S. B.; Hasel, K. W.; McPherson, A. *Biochemistry* **1997**, *36*, 1581–1597.

[64] Perkins, S. J.; Nealis, A. S.; Sutton, B. J.; Feinstein, A. *Journal of Molecular Biology* **1991**, *221*, 1345–1366.

[65] Jmol: an open-source Java viewer for chemical structures in 3D. `http://www.jmol.org/`.

[66] Vainionpää, R.; Leinikki, P. In *Encyclopedia of Virology*; Mahy, B. W. J., Ed.; Elsevier: Amsterdam, 2008; pp 29–37.

[67] Trevethan, R. *Frontiers in Public Health* **2017**, *5*, 307.

[68] Hirst, G. K. *The Journal of Experimental Medicine* **1942**, *75*, 49–64.

[69] Albrecht, P.; Klutch, M. *Journal of Clinical Microbiology* **1981**, *13*, 870–876.

[70] Ogundiji, O. T.; Okonko, I. O.; Adu, F. D. *Journal of Immunoassay & Immunochemistry* **2013**, *34*, 208–217.

[71] Lennette, E. H.; Schmidt, N. J.; Magoffin, R. L. *Journal of immunology* **1967**, *99*, 785–793.

[72] Townsend, A.; Rijal, P.; Xiao, J.; Tan, T. K.; Huang, K.-Y. A.; Schimanski, L.; Huo, J.; Gupta, N.; Rahikainen, R.; Matthews, P. C. et al. *Nature Communications* **2021**, *12*, 1951.

[73] Kirchenbaum, G. A.; Sautto, G. A.; Richardson, R. A.; Ecker, J. W.; Ross, T. M. *Journal of Virology* **2021**, *95*, e0237920.

[74] Ertesvåg, N. U.; Xiao, J.; Zhou, F.; Ljostveit, S.; Sandnes, H.; Lartey, S.; Sævik, M.; Hansen, L.; Madsen, A.; Mohn, K. G. I. et al. *Communications Medicine* **2022**, *2*, 36.

[75] Neill, M. H. *Public Health Reports (1896-1970)* **1918**, *33*, 1387.

[76] Wadsworth, A.; Harris, N. M.; Gilbert, R. *American Journal of Public Health and the Nation's Health* **1934**, *24*, 727–731.

[77] Muschel, L. H.; Lowe, K. M. *The Journal of Laboratory and Clinical Medicine* **1955**, *46*, 147–154.

[78] Dreguss, M.; Farkas, E. *Archiv für die gesamte Virusforschung* **1948**, *4*, 47–54.

[79] Stoker, M. G.; Page, Z.; Marmion, B. P. *Bulletin of the World Health Organization* **1955**, *13*, 807–827.

[80] Adone, R.; Sali, M.; Francia, M.; Iatarola, M.; Donatiello, A.; Fasanella, A. *Frontiers in Microbiology* **2016**, *7*, 19.

[81] Zohar, T.; Loos, C.; Fischinger, S.; Atyeo, C.; Wang, C.; Slein, M. D.; Burke, J.; Yu, J.; Feldman, J.; Hauser, B. M. et al. *Cell* **2020**, *183*, 1508–1519.e12.

[82] Darwish, I. A. *International Journal of Biomedical Science* **2006**, *2*, 217–235.

[83] Yalow, R. S.; Berson, S. A. *Journal of Clinical Investigation* **1960**, *39*, 1157–1175.

[84] van Weemen, B. K.; Schuurs, A. *FEBS Letters* **1971**, *15*, 232–236.

[85] Engvall, E.; Perlmann, P. *Immunochemistry* **1971**, *8*, 871–874.

[86] Hosseini, S.; Vázquez-Villegas, P.; Rito-Palomares, M.; Martinez-Chapa, S. O. *Enzyme-Linked Immunosorbent Assay (ELISA)*; Springer Singapore: Singapore, 2018.

[87] Krähling, V.; Halwe, S.; Rohde, C.; Becker, D.; Berghöfer, S.; Dahlke, C.; Eickmann, M.; Ercanoglu, M. S.; Gieselmann, L.; Herwig, A. et al. *Journal of Immunological Methods* **2021**, *490*, 112958.

[88] Luo, S.; Xu, J.; Cho, C. Y.; Zhu, S.; Whittaker, K. C.; Wang, X.; Feng, J.; Wang, M.; Xie, S.; Fang, J. et al. *Laboratory Medicine* **2022**, *53*, 225–234.

[89] Chen, S.; Lu, D.; Zhang, M.; Che, J.; Yin, Z.; Zhang, S.; Zhang, W.; Bo, X.; Ding, Y.; Wang, S. *European Journal of Clinical Microbiology & Infectious Diseases* **2005**, *24*, 549–553.

[90] Zhao, L.; Sun, L.; Chu, X. *TrAC Trends in Analytical Chemistry* **2009**, *28*, 404–415.

[91] Radi, R. *Proceedings of the National Academy of Sciences of the United States of America* **2018**, *115*, 5839–5848.

[92] Roda, A.; Pasini, P.; Mirasoli, M.; Michelini, E.; Guardigli, M. *Trends in Biotechnology* **2004**, *22*, 295–303.

[93] Töpfer, G. In *Lexikon der Medizinischen Laboratoriumsdiagnostik*; Gressner, A. M., Arndt, T., Eds.; Springer Reference Medizin; Springer: Berlin and Heidelberg, 2019; pp 761–762.

[94] Ryu, W.-S. In *Molecular Virology of Human Pathogenic Viruses*; Ryu, W.-S., Ed.; Academic Press is an imprint of Elsevier: Amsterdam, 2017; pp 47–62.

[95] Simonetti, F. R.; Dewar, R.; Maldarelli, F. *Mandell, Douglas, and Bennett's Principles and Practice of Infectious Diseases*; Elsevier, 2015; pp 1503–1525.e7.

[96] Sarkari, B.; Ashrafmansouri, M.; Hatam, G.; Habibi, P.; Abdolahi Khabisi, S. *Interdisciplinary Perspectives on Infectious Diseases* **2014**, *2014*, 505134.

[97] Edouard, S.; Colson, P.; Melenotte, C.; Di Pinto, F.; Thomas, L.; La Scola, B.; Million, M.; Tissot-Dupont, H.; Gautret, P.; Stein, A. et al. *European Journal of Clinical Microbiology & Infectious Diseases* **2021**, *40*, 361–371.

[98] Nguyen, D.; Skelly, D.; Goonawardane, N. *Viruses* **2021**, *13*.

[99] Meyer, B.; Drosten, C.; Müller, M. A. *Virus Research* **2014**, *194*, 175–183.

[100] Hayden, O.; Luppa, P. B.; Min, J. *Analytical and Bioanalytical Chemistry* **2022**, *414*, 3161–3163.

[101] Koczula, K. M.; Gallotta, A. *Essays in Biochemistry* **2016**, *60*, 111–120.

[102] Xu, Y.; Liu, Y.; Wu, Y.; Xia, X.; Liao, Y.; Li, Q. *Analytical Chemistry* **2014**, *86*, 5611–5614.

[103] Yen, C.-W.; de Puig, H.; Tam, J. O.; Gómez-Márquez, J.; Bosch, I.; Hamad-Schifferli, K.; Gehrke, L. *Lab on a Chip* **2015**, *15*, 1638–1641.

[104] Fung, K.-K.; Chan, C. P.-Y.; Renneberg, R. *Analytica Chimica Acta* **2009**, *634*, 89–95.

[105] Fang, C.; Chen, Z.; Li, L.; Xia, J. *Journal of Pharmaceutical and Biomedical Analysis* **2011**, *56*, 1035–1040.

[106] McCance, K.; Wise, H.; Simpson, J.; Batchelor, B.; Hale, H.; McDonald, L.; Zorzoli, A.; Furrie, E.; Chopra, C.; Muecksch, F. et al. *PLOS ONE* **2022**, *17*, e0266086.

[107] Owen, S. I.; Williams, C. T.; Garrod, G.; Fraser, A. J.; Menzies, S.; Baldwin, L.; Brown, L.; Byrne, R. L.; Collins, A. M.; Cubas-Atienzar, A. I. et al. *The Journal of Infection* **2022**, *84*, 355–360.

[108] Conklin, S. E.; Martin, K.; Manabe, Y. C.; Schmidt, H. A.; Miller, J.; Keruly, M.; Klock, E.; Kirby, C. S.; Baker, O. R.; Fernandez, R. E. et al. *Journal of Clinical Microbiology* **2021**, *59*.

[109] Lake, D. F.; Roeder, A. J.; Kaleta, E.; Jasbi, P.; Pfeffer, K.; Koelbela, C.; Periasamy, S.; Kuzmina, N.; Bukreyev, A.; Grys, T. E. et al. *Journal of Clinical Virology* **2021**, *145*, 105024.

[110] Kharlamova, N.; Dunn, N.; Bedri, S. K.; Jerling, S.; Almgren, M.; Faustini, F.; Gunnarsson, I.; Rönnelid, J.; Pullerits, R.; Gjertsson, I. et al. *Frontiers in Immunology* **2021**, *12*, 666114.

[111] Seidel, M.; Niessner, R. *Analytical and Bioanalytical Chemistry* **2014**, *406*, 5589–5612.

[112] Hedde, P. N.; Abram, T. J.; Jain, A.; Nakajima, R.; Ramiro de Assis, R.; Pearce, T.; Jasinskas, A.; Toosky, M. N.; Khan, S.; Felgner, P. L. et al. *Lab on a Chip* **2020**, *20*, 3302–3309.

[113] Savvateeva, E.; Filippova, M.; Valuev-Elliston, V.; Nuralieva, N.; Yukina, M.; Troshina, E.; Baklaushev, V.; Ivanov, A.; Gryadunov, D. *Viruses* **2021**, *13*.

[114] Güven, E.; Duus, K.; Lydolph, M. C.; Jørgensen, C. S.; Laursen, I.; Houen, G. *Journal of Immunological Methods* **2014**, *403*, 26–36.

[115] Frutiger, A.; Tanno, A.; Hwu, S.; Tiefenauer, R. F.; Vörös, J.; Nakatsuka, N. *Chemical Reviews* **2021**, *121*, 8095–8160.

[116] Martinsky, T. In *A Beginner's Guide to Microarrays*; Blalock, E. M., Ed.; Springer eBook Collection; Springer: Boston, MA, 2003; pp 93–122.

[117] Wolter, A.; Niessner, R.; Seidel, M. *Analytical Chemistry* **2007**, *79*, 4529–4537.

[118] Lenigk, R.; Carles, M.; Ip, N. Y.; Sucher, N. J. *Langmuir* **2001**, *17*, 2497–2501.

[119] Angenendt, P.; Glökler, J.; Sobek, J.; Lehrach, H.; Cahill, D. J. *Journal of Chromatography A* **2003**, *1009*, 97–104.

[120] Bemetz, J.; Kober, C.; Meyer, V. K.; Niessner, R.; Seidel, M. *Analytical and Bioanalytical Chemistry* **2019**, *411*, 1943–1955.

[121] Henderson, J. R.; Taylor, R. M. *Proceedings of the Society for Experimental Biology and Medicine* **1959**, *101*, 257–259.

[122] Russell, P. K.; Nisalak, A. *The Journal of Immunology* **1967**, *99*, 291–296.

[123] Russell, P. K.; Nisalak, A.; Sukhavachana, P.; Vivona, S. *The Journal of Immunology* **1967**, *99*, 285–290.

[124] Gauger, P. C.; Vincent, A. L. *Methods in Molecular Biology* **2014**, *1161*, 313–324.

[125] Padoan, A.; Cosma, C.; Bonfante, F.; Della Rocca, F.; Barbaro, F.; Santarossa, C.; Dall'Olmo, L.; Pagliari, M.; Bortolami, A.; Cattelan, A. et al. *Clinica Chimica Acta* **2021**, *523*, 446–453.

[126] Whiteman, M. C.; Bogardus, L.; Giacone, D. G.; Rubinstein, L. J.; Antonello, J. M.; Sun, D.; Daijogo, S.; Gurney, K. B. *The American Journal of Tropical Medicine and Hygiene* **2018**, *99*, 1430–1439.

[127] Padoan, A.; Bonfante, F.; Pagliari, M.; Bortolami, A.; Negrini, D.; Zuin, S.; Bozzato, D.; Cosma, C.; Sciacovelli, L.; Plebani, M. *EBioMedicine* **2020**, *62*, 103101.

[128] Thomas, S. J.; Nisalak, A.; Anderson, K. B.; Libraty, D. H.; Kalayanarooj, S.; Vaughn, D. W.; Putnak, R.; Gibbons, R. V.; Jarman, R.; Endy, T. P. *The American Journal of Tropical Medicine and Hygiene* **2009**, *81*, 825–833.

[129] Roehrig, J. T.; Hombach, J.; Barrett, A. D. T. *Viral Immunology* **2008**, *21*, 123–132.

[130] Wallerström, S.; Lagerqvist, N.; Temperton, N. J.; Cassmer, M.; Moreno, A.; Karlsson, M.; Leijon, M.; Lundkvist, A.; Falk, K. I. *Infection Ecology & Epidemiology* **2014**, *4*.

[131] Nie, J.; Li, Q.; Wu, J.; Zhao, C.; Hao, H.; Liu, H.; Zhang, L.; Nie, L.; Qin, H.; Wang, M. et al. *Emerging Microbes & Infections* **2020**, *9*, 680–686.

[132] Tsai, W.-Y.; Ching, L. L.; Hsieh, S.-C.; Melish, M. E.; Nerurkar, V. R.; Wang, W.-K. *Emerging Microbes & Infections* **2021**, *10*, 894–904.

[133] Muhamuda, K.; Madhusudana, S. N.; Ravi, V. *International Journal of Infectious Diseases* **2007**, *11*, 441–445.

[134] Cao, Y.; Li, K.; Xing, X.; Zhu, G.; Fu, Y.; Bao, H.; Bai, X.; Sun, P.; Li, P.; Zhang, J. et al. *Journal of Clinical Microbiology* **2022**, *60*, e0214221.

[135] Huang, L.; Lu, Y.; Wei, Y.; Guo, L.; Liu, C. *Journal of Virological Methods* **2011**, *171*, 26–33.

[136] Münstermann, D.; Meyer-Schlinkmann Kristin, *Forum Sanitas* **2020**, 41–42.

[137] EUROIMMUN Medizinische Labordiagnostika AG, EUROLabWorkstation ELISA. 2022; `https://www.euroimmun.de/documents/Automation/ELISA/EUROLabWorkstation_ELISA/YG_0800_I_DE_D.pdf`.

[138] Hörber, S.; Soldo, J.; Relker, L.; Jürgens, S.; Guther, J.; Peter, S.; Lehmann, R.; Peter, A. *Clinical Chemistry and Laboratory Medicine* **2020**, *58*, 2113–2120.

[139] Kittel, M.; Muth, M. C.; Zahn, I.; Roth, H.-J.; Thiaucourt, M.; Gerhards, C.; Haselmann, V.; Neumaier, M.; Findeisen, P. *International Journal of Infectious Diseases* **2021**, *103*, 590–596.

[140] Jahrsdörfer, B.; Kroschel, J.; Ludwig, C.; Corman, V. M.; Schwarz, T.; Körper, S.; Rojewski, M.; Lotfi, R.; Weinstock, C.; Drosten, C. et al. *The Journal of Infectious Diseases* **2021**, *223*, 796–801.

[141] Byrum, J. R.; Waltari, E.; Janson, O.; Guo, S.-M.; Folkesson, J.; Chhun, B. B.; Vinden, J.; Ivanov, I. E.; Forst, M. L.; Li, H. et al. *medRxiv* **2021**,

[142] Gillot, C.; Douxfils, J.; Cadrobbi, J.; Laffineur, K.; Dogné, J.-M.; Elsen, M.; Eucher, C.; Melchionda, S.; Modaffarri, É.; Tré-Hardy, M. et al. *Journal of clinical medicine* **2020**, *9*, 3752.

[143] González-González, E.; Garcia-Ramirez, R.; Díaz-Armas, G. G.; Esparza, M.; Aguilar-Avelar, C.; Flores-Contreras, E. A.; Rodríguez-Sánchez, I. P.; Delgado-Balderas, J. R.; Soto-García, B.; Aráiz-Hernández, D. et al. *Sensors* **2021**, *21*.

[144] Doppler, C.; Feischl, M.; Ganhör, C.; Puh, S.; Müller, M.; Kotnik, M.; Mimler, T.; Sonnleitner, M.; Bernhard, D.; Wechselberger, C. *Analytical and Bioanalytical Chemistry* **2022**, *414*, 3291–3299.

[145] Wechselberger, C.; Süßner, S.; Doppler, S.; Bernhard, D. *Journal of Clinical Virology* **2020**, *131*, 104589.

[146] Dou, X.; Wang, E.; Hu, J.; Zong, Z.; Jiang, R.; Wang, M.; Kan, L.; Zhang, X. *Journal of Clinical Laboratory Analysis* **2021**, *35*, e23681.

[147] Shenzen YHLO Biotech Co. Ltd., iFlash-2019-nCoV NAb. 2020; `https://pdf.medicalexpo.com/pdf/shenzhen-yhlo-biotech-co-ltd/iflash-2019-ncov-nab/107786-233490.html`.

[148] Chen, H.; Yu, W.; Gao, X.; Jiang, W.; Li, X.; Liu, G.; Yang, Y. *Journal of Clinical Laboratory Analysis* **2022**, *36*, e24306.

[149] Saker, K.; Pozzetto, B.; Escuret, V.; Pitiot, V.; Massardier-Pilonchéry, A.; Mokdad, B.; Langlois-Jacques, C.; Rabilloud, M.; Alfaiate, D.; Guibert, N. et al. *Journal of Clinical Virology* **2022**, *152*, 105169.

[150] Becker, M.; Strengert, M.; Junker, D.; Kaiser, P. D.; Kerrinnes, T.; Traenkle, B.; Dinter, H.; Häring, J.; Ghozzi, S.; Zeck, A. et al. *Nature Communications* **2021**, *12*, 1152.

[151] Iriemenam, N. C.; Ige, F. A.; Greby, S. M.; Mpamugo, A.; Abubakar, A. G.; Dawurung, A. B.; Esiekpe, M. K.; Thomas, A. N.; Okoli, M. U.; Awala, S. S. et al. *PLOS ONE* **2022**, *17*, e0266184.

[152] Peng, R.; Pan, Y.; Li, Z.; Qin, Z.; Rini, J. M.; Liu, X. *Biosensors & Bioelectronics* **2022**, *197*, 113762.

[153] Yakoh, A.; Pimpitak, U.; Rengpipat, S.; Hirankarn, N.; Chailapakul, O.; Chaiyo, S. *Biosensors & Bioelectronics* **2021**, *176*, 112912.

[154] Basso, C. R.; Malossi, C. D.; Haisi, A.; de Albuquerque Pedrosa, V.; Barbosa, A. N.; Grotto, R. T.; Araujo Junior, J. P. *Analytical Methods* **2021**, *13*, 3297–3306.

[155] Djaileb, A.; Charron, B.; Jodaylami, M. H.; Thibault, V.; Coutu, J.; Stevenson, K.; Forest, S.; Live, L. S.; Boudreau, D.; Pelletier, J. N. et al. *A Rapid and Quantitative Serum Test for SARS-CoV-2 Antibodies with Portable Surface Plasmon Resonance Sensing*; 2020.

[156] Musicò, A.; Frigerio, R.; Mussida, A.; Barzon, L.; Sinigaglia, A.; Riccetti, S.; Gobbi, F.; Piubelli, C.; Bergamaschi, G.; Chiari, M. et al. *Vaccines* **2021**, *9*.

[157] Wang, H.; Wu, X.; Zhang, X.; Hou, X.; Liang, T.; Wang, D.; Teng, F.; Dai, J.; Duan, H.; Guo, S. et al. *ACS Central Science* **2020**, *6*, 2238–2249.

[158] Jiang, H.-w.; Li, Y.; Zhang, H.-n.; Wang, W.; Yang, X.; Qi, H.; Li, H.; Men, D.; Zhou, J.; Tao, S.-c. *Nature Communications* **2020**, *11*, 3581.

[159] de Assis, R. R.; Jain, A.; Nakajima, R.; Jasinskas, A.; Felgner, J.; Obiero, J. M.; Norris, P. J.; Stone, M.; Simmons, G.; Bagri, A. et al. *Nature Communications* **2021**, *12*, 6.

[160] Weller, M. G.; Schuetz, A. J.; Winklmair, M.; Niessner, R. *Analytica Chimica Acta* **1999**, *393*, 29–41.

[161] Knecht, B. G.; Strasser, A.; Dietrich, R.; Märtlbauer, E.; Niessner, R.; Weller, M. G. *Analytical Chemistry* **2004**, *76*, 646–654.

[162] Langer, V.; Hartmann, G.; Niessner, R.; Seidel, M. *Journal of Aerosol Science* **2012**, *48*, 46–55.

[163] Kober, C.; Niessner, R.; Seidel, M. *Biosensors & Bioelectronics* **2018**, *100*, 49–55.

[164] Kunze, A.; Dilcher, M.; Abd El Wahed, A.; Hufert, F.; Niessner, R.; Seidel, M. *Analytical Chemistry* **2016**, *88*, 898–905.

[165] Meyer, V. K.; Chatelle, C. V.; Weber, W.; Niessner, R.; Seidel, M. *Analytical and Bioanalytical Chemistry* **2020**, *412*, 3467–3476.

[166] Wutz, K.; Meyer, V. K.; Wacheck, S.; Krol, P.; Gareis, M.; Nölting, C.; Struck, F.; Soutschek, E.; Böcher, O.; Niessner, R. et al. *Analytical Chemistry* **2013**, *85*, 5279–5285.

7 Appendix

7.1 Reprint permissions

7.1.1 Publication 1

Automated, flow-based chemiluminescence microarray immunoassay for the rapid multiplex detection of IgG antibodies to SARS-CoV-2 in human serum and plasma (CoVRapid CL-MIA)

Julia Klüpfel, Rosa Carolina Koros, Kerstin Dehne, Martin Ungerer, Silvia Würstle, Josef Mautner, Martin Feuerherd, Ulrike Protzer, Oliver Hayden, Martin Elsner, Michael Seidel*

[*] Corresponding author, e-mail: michael.seidel@mytum.de

The article was reprinted without changes.

7.1.2 Publication 2

Fully Automated Chemiluminescence Microarray Analysis Platform for Rapid and Multiplexed SARS-CoV-2 Serodiagnostics

Julia Klüpfel, Sandra Paßreiter, Nina Weidlein, Martin Knopp, Martin Ungerer, Ulrike Protzer, Percy Knolle, Oliver Hayden, Martin Elsner, Michael Seidel*

[*] Corresponding author, e-mail: michael.seidel@mytum.de

The article was reprinted without changes.

7.1.3 Publication 3

Automated detection of neutralizing SARS-CoV-2 antibodies in minutes using a competitive chemiluminescence immunoassay

Julia Klüpfel[‡], Sandra Paßreiter[‡], Melina Rumpf, Catharina Christa, Hans-Peter Holthoff, Martin Ungerer, Martin Lohse, Percy Knolle, Ulrike Protzer, Martin Elsner, Michael Seidel*

[‡] These authors contributed equally

[*] Corresponding author, e-mail: michael.seidel@mytum.de

The article was reprinted without changes.

7.2 List of Publications

7.2.1 Journal Contributions

[4] *Automated detection of neutralizing SARS-CoV-2 antibodies in minutes using a competitive chemiluminescence immunoassay*
Julia Klüpfel[‡], Sandra Paßreiter[‡], Melina Rumpf, Catharina Christa, Hans-Peter Holthoff, Martin Ungerer, Martin Lohse, Percy Knolle, Ulrike Protzer, Martin Elsner, Michael Seidel
Analytical and Bioanalytical Chemistry **415**, 391 - 404 (2023).
[‡] These authors contributed equally.

[3] *Fully Automated Chemiluminescence Microarray Analysis Platform for Rapid and Multiplexed SARS-CoV-2 Serodiagnostics*
Julia Klüpfel, Sandra Paßreiter, Nina Weidlein, Martin Knopp, Martin Ungerer, Ulrike Protzer, Percy Knolle, Oliver Hayden, Martin Elsner, Michael Seidel
Analytical Chemistry **94 (6)**, 2855 - 2864 (2022).

[2] *Automated, flow-based chemiluminescence microarray immunoassay for the rapid multiplex detection of IgG antibodies to SARS-CoV-2 in human serum and plasma (CoVRapid CL-MIA)*
Julia Klüpfel, Rosa Carolina Koros, Kerstin Dehne, Martin Ungerer, Silvia Würstle, Josef Mautner, Martin Feuerherd, Ulrike Protzer, Oliver Hayden, Martin Elsner, Michael Seidel
Analytical and Bioanalytical Chemistry **413**, 5619 - 5632 (2021).

[1] *Macroporous epoxy-based monoliths for rapid quantification of Pseudomonas aeruginosa by adsorption elution method optimized for qPCR*
Lisa Göpfert[‡], **Julia Klüpfel**[‡], Charlotte Heinritz, Martin Elsner, Michael Seidel
Analytical and Bioanalytical Chemistry **412**, 8185 - 8195 (2020).
[‡] These authors contributed equally.

7.2.2 Conference & Seminar Contributions

Conference Papers

[2] *Detektion von Antikörpern gegen SARS-CoV-2 und ihrem Neutralisationspotential mittels Microarray-Immunoassays*
Julia Klüpfel, Martin Ungerer, Ulrike Protzer, Oliver Hayden, Martin Elsner, Michael Seidel
15. Dresdner Sensor-Symposium 2021 **3 (Biomedizinische Sensorik)**, 51 - 56 (2021).

[1] *Schnelle Anreicherung und kulturunabhängige Detektion von Pseudomonas aeruginosa in Trinkwasser*
Julia Klüpfel, Lisa Göpfert, Michael Seidel
Vom Wasser **119 (2)**, 40 - 42 (2021).

Oral Presentations

[6] *Use of recombinant proteins for the detection of SARS-CoV-2 antibodies in an automated, flow-based chemiluminescence microarray immunoassay*
Advanced Mass Spectrometry Seminar 2022 (Bavarian Biomolecular Mass Spectrometry Center/online)

[5] *Detektion von Antikörpern gegen SARS-CoV-2 und ihrem Neutralisationspotential mittels Microarray-Immunoassays*
Dresdner Sensor Symposium 2021 (DECHEMA/online)

[4] *Rapid detection of (neutralizing) SARS-CoV-2 antibodies by chemiluminescence microarray immunoassay*
Medical Biodefense Conference 2021 (Bundeswehr Institute of Microbiology/Munich)

[3] *From idea to application: development of flow-based chemiluminescence microarray immunoassays for point-of-care serodiagnostics*
EBS Digital Seminar Series 2021 (Technical University of Denmark/online)

[2] *Schnelle Anreicherung und kulturunabhängige Detektion von Pseudomonas aeruginosa in Trinkwasser*
Wassertagung 2021 (GDCh/online)

[1] *CoVRapid: Automated, flow-based chemiluminescence microarray immunoassay for the rapid multiplex detection of IgG antibodies to SARS-CoV-2 in human serum and plasma*
European Biosensor Symposium 2021 (TH Wildau/online)

Poster Presentations

[1] *Development of serological point-of-care microarray immunoassays for the detection of antibodies to SARS-CoV-2*
Analytica Conference 2022 (Munich)

7.3 Eidesstattliche Erklärung

Ich erkläre an Eides statt, dass ich die bei der TUM School of Natural Sciences zur Promotionsprüfung vorgelegte Arbeit mit dem Titel:

Development of Rapid Automated Chemiluminescence Microarray Immunoassays for SARS-CoV-2 Serological Assessments

an der TUM School of Natural Sciences, Lehrstuhl für Analytische Chemie und Wasserchemie, Gruppe für Bioanalytik und Mikroanalytische Systeme unter der Anleitung und Betreuung durch Priv.-Doz. Dr. Michael Seidel ohne sonstige Hilfe erstellt und bei der Abfassung nur die gemäß §6 Abs. 6 und 7 Satz 2 angebotenen Hilfsmittel benutzt habe.

- ☑ Ich habe keine Organisation eingeschaltet, die gegen Entgelt Betreuerinnen und Betreuer für die Anfertigung von Dissertationen sucht, oder die mir obliegenden Pflichten hinsichtlich der Prüfungsleistungen für mich ganz oder teilweise erledigt.

- ☑ Ich habe die Dissertation in dieser oder ähnlicher Form in keinem anderen Prüfungsverfahren als Prüfungsleistung vorgelegt.

- ☑ Ich habe den angestrebten Doktorgrad noch nicht erworben und bin nicht in einem früheren Promotionsverfahren für den angestrebten Doktorgrad endgültig gescheitert.

Die öffentlich zugängliche Promotionsordnung der TUM ist mir bekannt, insbesondere habe ich die Bedeutung von §28 (Nichtigkeit der Promotion) und §29 (Entzug des Doktorgrades) zur Kenntnis genommen. Ich bin mir der Konsequenzen einer falschen Eidesstattlichen Erklärung bewusst.

Mit der Aufnahme meiner personenbezogenen Daten in die Alumni-Datei bei der TUM bin ich

- ☑ einverstanden.

München, 13.01.2023

——————————————   ——————————————

       Ort, Datum   Unterschrift